GMe

Gesellschaft für Mikroelektronik

The Society for Microelectronics

Annual Report

1997

Vienna, April 1998

GMe

Gesellschaft für Mikroelektronik

The Society for Microelectronics

Annual Report

1997

Gesellschaft für Mikroelektronik
c/o Technische Universität Wien
Institut für Allgemeine Elektrotechnik und Elektronik
Gußhausstraße 27-29/359, A-1040 Wien

Vienna, April 1998

Editor: Karl Riedling

Layout: Claudia Ritter
Karl Riedling

© 1998 Gesellschaft für Mikroelektronik (GMe)
c/o Technische Universität Wien
Institut für Allgemeine Elektrotechnik und Elektronik
Gußhausstraße 27-29/359, A-1040 Wien

The Society for Microelectronics (GMe — Gesellschaft für Mikroelektronik)

E. Gornik, K. Riedling

**Gesellschaft für Mikroelektronik,
c/o Institut für Allgemeine Elektrotechnik und Elektronik, TU Wien
Gußhausstraße 27 – 29, A-1040 Wien**

1. Goals of the Society for Microelectronics

The Society for Microelectronics (GMe) was founded in 1985 with the aim to "*support microelectronics technology and its applications*" in Austria. The GMe defines its tasks as follows:

- Support of university-based "high-tech" research in the areas of microelectronics, semiconductor technology, sensors, and opto-electronics;
- Construction and operation of research facilities;
- Support and consulting for industry, in particular, for small and medium enterprises, within the area of microelectronics.

The central task of the GMe is to provide an internationally competitive *infra-structure* in the area of microelectronics technology. The GMe allocates funds to maintain research projects in the fields of semiconductor technology, sensors, opto-electronics, and ASIC design. Thus the infra-structure support generates a base for research projects that are funded by other funding agencies.

2. Activities of the Society

The present focal point activities of the GMe are:

- Construction and operation of university-based laboratories for microelectronics technology;
- Design of application specific integrated circuits (ASICs) — UNICHIP and TMOe.

2.1 Microelectronics Technology — Cleanrooms Vienna and Linz

The main task of the GMe in the area of microelectronics technology is the operation of cleanroom laboratories in Vienna and Linz. In 1992, the GMe coordinated the construction of the Microstructure Center (MISZ — Mikrostrukturzentrum) in Vienna; the funds were supplied by the Austrian Federal Ministry of Science and Research. The MISZ Vienna finished construction by the end of 1993 and went into operation in June 1994. The GMe now finances a significant part of the operation costs for the cleanroom laboratories in Vienna and Linz.

The following university institutes receive support within this focal point activity:

- TU Wien:
  - Institut für Festkörperelektronik
  - Institut für Allgemeine Elektrotechnik und Elektronik
- Johannes Kepler Universität Linz:
  - Institut für Halbleiterphysik
  - Institut für Experimentalphysik
  - Institut für Mikroelektronik

2.2 Application Specific Integrated Circuits (ASICs) — UNICHIP and TMOe

These activities of the GMe are closely linked to the requirements of the Austrian industry: Based on groups at the Technical Universities in Graz and Vienna ("UNICHIP"), and using equipment and software that were purchased from GMe funding, two major actions have been pursued now for more than a decade: (1) ASIC projects for partners in the Austrian industry, ranging from feasibility studies to the design of ASICs that are commercially produced; and (2) the education and training of engineers in the area of ASIC design. Due to its close links to industrial requirements, UNICHIP played a leading role in Austria. The UNICHIP groups also have a long-standing tradition in European cooperation; many years before Austria joined the EU, they participated in the "EUROCHIP" European project; currently, they are involved in the "EUROPRACTICE" program.

During 1996, the UNICHIP activities were merged into an Austria-wide activity that comprises all university-based competence centers for ASIC design, the *Technologieverbund Mikroelektronik Österreich* (TMOe). The TMOe receives separate funding from various federal and regional sources; the GMe acts as a mediator between the two federal ministries that provide basic funds, and the TMOe. The TMOe includes the following university institutes:

- TU Wien:
  - Institut für Allgemeine Elektrotechnik und Elektronik (*)
  - Institut für Computertechnik
  - Institut für Technische Informatik
- TU Graz:
  - Institut für Angewandte Informationsverarbeitung und Kommunikationstechnologie
  - Institut für Elektronik (*)
- Johannes Kepler Universität Linz:
  - Institut für Systemwissenschaften

Since only the original UNICHIP institutes marked with "*" in the list above got direct funding from the GMe, the other institutes included in the TMOe activity are out of the main scope of this report.

2.3 Microsensors and Other Projects

Microsensors are the most important among the remaining individual projects that received some GMe support. Projects carried out at the following institutions obtained GMe funding in 1997:

- TU Wien:
  - Institut für Allgemeine Elektrotechnik und Elektronik
  - Institut für Analytische Chemie
- Montanuniversität Leoben:
  - Institut für Physik

3. Other Activities of the Society

One of the declared tasks of the GMe is to provide information on current Austrian academic activities in the field of microelectronics to industry, in particular to Austrian small- and medium enterprises (SMEs). This will improve the transfer of "know-how" between Austrian universities and industry. As an example, the GMe supplied editorial articles to an Austrian publishing house that targets its magazines on the management and technical staff of Austrian industrial enterprises. The articles presented some of those projects supported by the GMe that had a direct impact on Austrian industry.

To enhance the distribution of the results of the research work done with GMe support, the GMe has put the contents of its previous annual reports — 1995 and 1996 — on its Web server; this will also happen for this report. Although we did not explicitly advertise on a larger scale the existence of this server and its contents, it has apparently been fairly well accepted by the international community. Access statistics in operation since November 1997 show an average access count of 3 per day; however, an amazingly large percentage of these accesses — close to 50 per cent — originates from net domains outside Austria. About one quarter of the visitors of the GMe's web site visited it more than once. The GMe Web server is available under the URL:

http://www.iaee.tuwien.ac.at/gme/

Finally, the GMe prepared and carried out the biennial seminar "*Grundlagen und Technologie elektronischer Bauelemente*" in Großarl, Salzburg, which took place in March 1997. The seminar has first been held in 1977; since 1987, the GMe contributes financial support, and since 1993, the Society acts as its main organizer. The 11th Großarl seminar presented seven main lectures given by international experts, and 20 short contributions, which resulted from work supported by the GMe. The program of this seminar is included in the appendix of this report. Currently, the GMe considers a major restructuring of the seminar that should address the Austrian and foreign industry to a greater degree, in conjunction with changing its venue. The next seminar is due in the spring of 1999; the first preparations are already on their way.

Contents

The Society for Microelectronics (GMe — Gesellschaft für Mikroelektronik)...... 3

Microelectronics Technology — Cleanroom Vienna............ 9

Cleanroom Vienna.. 11

Electron-Beam Lithography for Novel Devices 45

Novel Single-Mode Emission Laser Diodes Based on Surface-Mode Coupling 51

Magnetotransport in GaAs-AlGaAs Nanostructures 61

Development of THz-Devices 71

Microelectronics Technology — Cleanroom Linz 83

Microstructure Research: Cleanroom Linz 85

ZnSe/ZnCdSe Quantum Wires on Patterned Substrates 105

$Si/Si_{1-x-y}Ge_xC_y$ Heterostructures 111

UNICHIP 129

UNICHIP Vienna — ASIC Design with Austrian Universities.......................... 131

UNICHIP Graz — Design of Integrated Circuits 139

Microsensors and Other Projects 145

High Precision Depth Profiles with SIMS... 147

Integrated Sensor-Microflow-Systems.. 153

Scanning Force Microscopy Investigations of Thermally Grown Oxides on Polysilicon 163

Preparation of Nano-Structures for Space Applications 171

New Diode-Pumped Femtosecond Lasers 177

Appendix.. 187

Basics and Technology of Electronic Devices — Seminar Program 189

The Society's Managing Committee and Address... 193

Microelectronics Technology — Cleanroom Vienna

Cleanroom Vienna

G. Strasser

Institute of Solid State Electronics &
Center of Microstructure Research (MISZ), Techn. Univ. Vienna
A-1040 Vienna, Austria

In this report we describe the main activities in the cleanroom of the MISZ. Not included into this paper are activities directly sponsored by the same society (GMe) which, thus, have their own reports. Since 1995, in the cleanroom of the MISZ state of the art growth of III-V compounds as well as the production of patterned masks used in lithography is done on a regular basis. One of the main research areas of our institute is the preparation and characterization of III-V devices. Therefore the Institute of Solid State Electronics maintains several collaborations with national and international research institutions and companies by providing them with epitaxial layers (III-V-compounds). A second main research topic is the production of micron and sub-micron devices down to nanometer scale. Patterned masks for optical lithography are also provided to different institutions.

1. Introduction

Since 1995, the cleanroom of the MISZ is operated and maintenanced on a regular basis. Main research areas are the state of the art growth of III-V compounds and the processing of these layers resulting in transport and optical devices. Processing steps as lithography, structuring (different etching techniques), planarization and metallization of the different layers and, finally assembling of the different optoelectronic devices are performed on a routine basis. Production of patterned masks is part of the cleanroom facility as well as the deposition of dielectric materials by chemical vapor deposition (PE-CVD). Supplementary to the normal operation and maintenance of the cleanroom and the cleanroom equipment, additional equipment has been installed. Testing of the cleanroom quality and adjustment of parameters (laminar air flow, filters, cooling, humidity…) is done continuously.

During 1997, new equipment was installed in the cleanroom of the MISZ. In detail, an electrochemical CV profiler to measure doping versus thickness profiles was installed and supplied with an additional photovoltaic spectrometer to determine Aluminum concentrations of AlGaAs layers. A UHV system to outgas Knudsen cells and fire pBN-crucibles is under construction. A second spinner including hot plates was installed to spin on photosensitive polyimide. This enables us to produce mesas down to 1 μm with standard optical lithography.

The cleanroom is a necessary tool to manufacture state of the art devices. In the following we will describe all projects within the Institute of Solid State Electronics performed in this cleanroom.

2. Research Activities

2.1 Experimental Investigation on Grating Coupled Twinguide Semiconductor Lasers

(W. Schrenk, N. Finger, A. Köck, M. Haider, M. Socher, E. Gornik)

The demand on semiconductor lasers with determined emission wavelength and/or continuous tunable emission wavelength caused different sophisticated laser concepts. The concept to be investigated is a grating coupled twinguide laser. The two waveguides are the active laser waveguide and a passive waveguide on top of a conventional Fabry-Perot laser structure. The two waveguides with different optical properties are coupled via a grating contradirectional only for one determined wavelength. This mechanism acts as a strong wavelength filter in the laser cavity. Therefore the emission wavelength should not drift dramatically with temperature as typical for Fabry-Perot lasers.

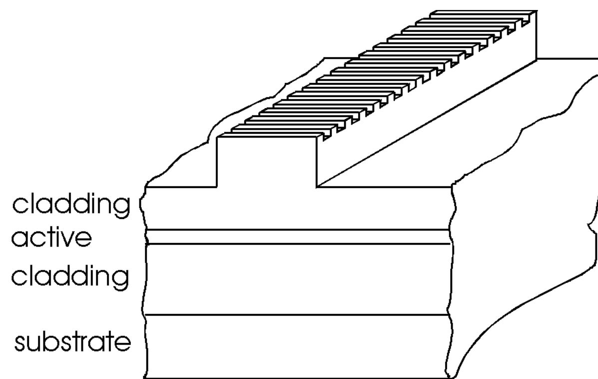

Fig. 1: Ridge with grating (schematic).

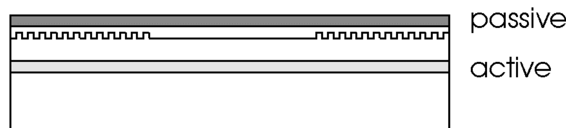

Fig. 2: Schematic view of a ring laser.

Thus, narrow ridge lasers with gratings on the top of the ridge are needed. This problem is solved for ridge widths down to about 1 µm and grating periods of several 100 nm. The second step is to add the passive waveguide on a special laser structure with a thin top cladding and to investigate the filter characteristic of the grating coupled waveguides in respect to the theory. This can be done by a test structure with short grating length. Consequently, a ring laser allows the demonstration of the wavelength selection. It should be possible to reduce the mirror-reflectance of the cleaved or etched mirrors to show laser operation based only on feedback via the passive surface waveguide. The technology for etched laser mirrors is also present. The emission wavelength should be tunable by changing the optical properties of the passive waveguide e.g. via the thickness of the passive waveguide. By adding some asymmetry it should also be possible to force light circulation in only one direction in the ring laser. After showing the coupling

mechanism with the ring laser the laser concept must be designed for good efficiency. This would probably be no ring laser but a laser with a grating extended over the full laser length and emission at one antireflection coated laser facet while the other facet could be a metallized mirror.

2.2 Fabrication of Vertical-Cavity Surface Emitting Laserdiodes

(T. Maier, W. Smola, G. Strasser, E. Gornik)

With the insertion of a carbon doping source in our MBE system at the beginning of the year we began to grow our first laser structures. To facilitate the characterization of the optical and electrical properties of our samples we used a high-quality GaAs/AlGaAs-DH laser structure received from an external source as a laboratory standard. This structure was grown five times, both LED and broad-area laserdiodes were fabricated, and compared to the standard-devices. The increasing cleanness of the MBE system and optimization of the doping levels brought a continuous improvement. Sample #4 was the first to show laser operation, sample #5 displayed thresholds and efficiencies that were at least equal to our standard sample (Fig. 3).

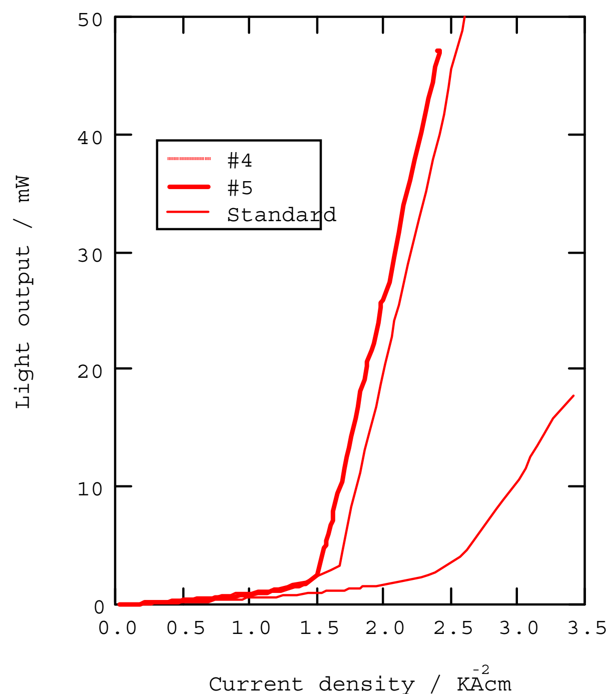

Fig. 3: LI- characteristics of our first broad-area laser diodes compared to a standard device.

The VCSEL structures were grown on n-doped substrates and comprised an n-doped AlGaAs/AlAs bragg-mirror and a DH-GaAs/AlGaAs diode as an active layer. The top mirror was deposited after MBE growth by PECVD and consisted of typically 11 pairs of SiO/SiN. This technique allows a much higher flexibility in the fabrication of the VCSELs compared to the usual all-epitaxial structures, especially the possibility of a post-growth tuning of the resonator to obtain perfect matching of the laser mode and the gain peak.

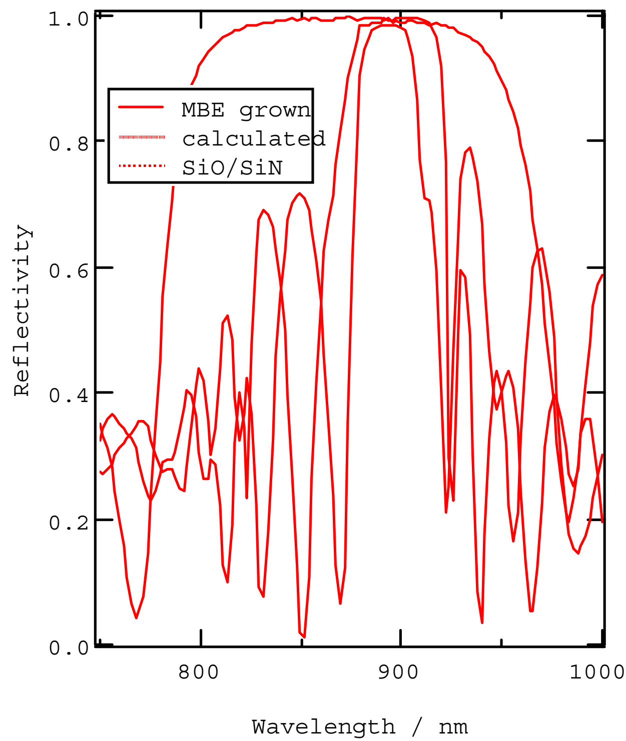

Fig. 4: Reflectivity of an MBE grown VCSEL-structure and that of the SiO/SiN top-mirror.

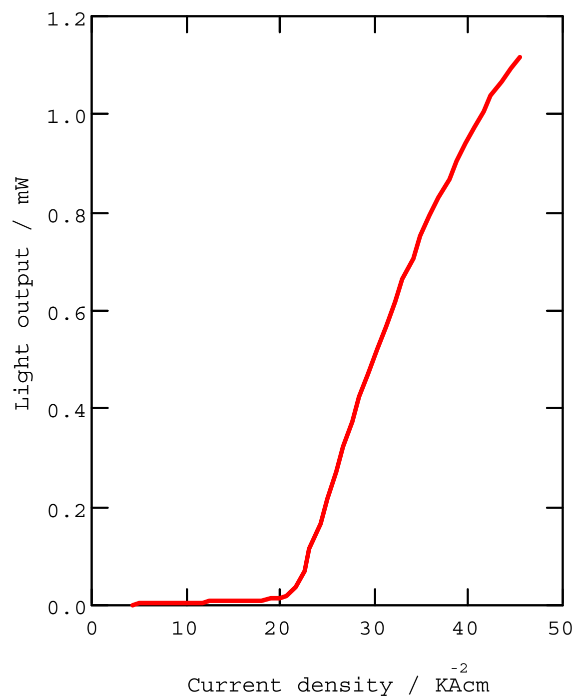

Fig. 5: LI-characteristic of a 7 µm diameter VCSEL with the mirrors shown in Fig. 4.

Figure 4 shows the measured reflectivity of a MBE grown structure together with a calculation. The good accordance underlines the high degree of thickness control during

MBE growth that has been achieved. Also shown is the measured reflectivity of a dielectric SiO/SiN top-mirror, reaching values of 99 %, thus fulfilling the demands for VCSEL mirrors.Figure 5 shows the LI-plot of a VCSEL with a 7 µm aperture, measured at a repetition rate of 10 KHz and a duty-cycle of 1 %. The lasing wavelength was 870 nm. The high threshold current densities of approximately 20 $KAcm^{-2}$ are probably due to a poor current spreading in the p-doped contact layers, resulting in a small mode-gain overlap. By optimizing the doping levels in these layers threshold is expected to be further reduced.

2.3 Single-Mode and Single-Beam Surface Emitting Laser Diodes in the Visible Regime

(P.O. Kellermann, A. Köck, N. Finger, E. Gornik)

The *surface-mode-emission* technique (SME) was successfully applied in the visible red wavelength regime to achieve a single-beam emission via the surface with low beam divergence (0.16° × 10°) as well as a single-mode emission in AC and in DC operation with a minimum spectral linewidth of 0.07 nm. The highest sidemode-suppression achieved in AC operation is 19 dB (Fig. 6). With the SME concept the characteristics of a horizontal cavity laser diode (wavelength, emission angle) can be adjusted by changing only the surface parameters (waveguide's optical thickness, grating period). An optimization of these red GaInP/AlGaInP SME laser diodes towards higher surface emitted power and higher sidemode suppression by contradirectional coupling between the surface- and the lasermode is planned. A diversification of the SME concept to the green regime is under progress, but at present the devices suffer from substantial heating.

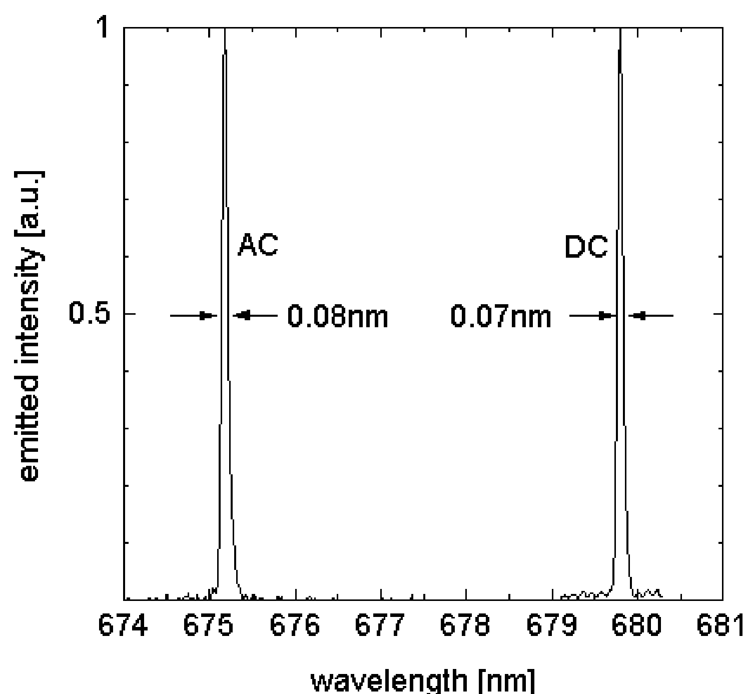

Fig. 6: Single-mode emission spectra of a red SME laser diode in AC operation on the left side and in DC operation on the right side.

The first application of a SME laser diode was realized in high resolution radiography using radiochromic film as dosimeter medium. The readout of the film implements radiochromic film dosimeter near the film's absorption maximum by using a SME laser diode (675 nm). At 675 nm the effective sensitivity of the film is approximately threefold higher than at 633 nm (helium-neon laser densitometer). Very good accuracy, high spatial resolution, and simple assembly of the readout system has been achieved. The beam profiles of the different collimator helmets of the Leksell Gamma Knife™ (Elekta Inc., Sweden) installed at the University of Vienna, Department of Neurosurgery, were determined experimentally. Shape and full width at half maximum of the profiles obviously correspond with the computer generated data of the dose planning system. The output factor of the collimators, essential for the application of well defined doses, was checked. The inquiries established an output factor of the 4 mm collimator that lies 9 % ± 1 % lower than the adjusted one.

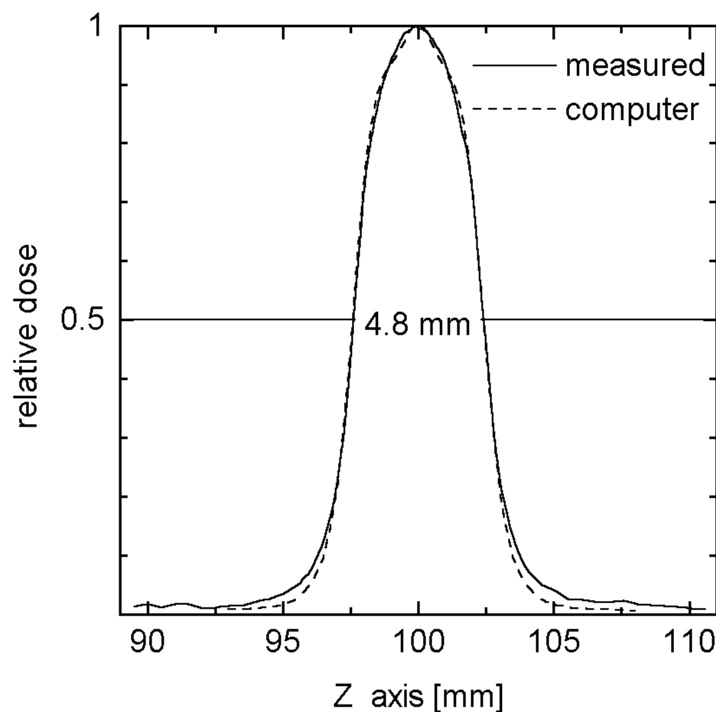

Fig. 7: Measured beam profile of the 4 mm collimator helmet of the Gamma Knife™ in comparison to the computer generated data.

2.4 Investigations on Surface Emitting LEDs by Surface Plasmons and Guided Waves

(S. Gianordoli, A. Köck, E. Gornik)

Excitation and light emission of surface plasmons (SP) represent a method to improve LED performance. To exploit the SP-technique the surface of the investigated LEDs was periodically structured and coated with different metal films. The dependence of the quantum efficiency (QE) and the radiation behavior on the thickness of different metal films (Au, Ag, Al) on cross and hexagonal gratings were investigated. The lowest beam divergence was obtained from a 40 nm thick Ag film on a hexagonal grating and is 17°.

The QE for this LED is only 0.22 % due to the reflection of the Au film back into the substrate. The QE without a metal film is 1.4 % to 1.44 %. In addition, photoresist (PR) was spin coated on the metal to stimulate also waveguide modes to increase the QE. The beam divergence broadened but the QE increased to a maximum of 1.37 % for a hexagonal grating with 10 nm thick Au and a 250 nm thick PR-film. In the slope of -30° to 30° the QE is 1 % higher than without metal and PR.

To cancel the decrease of the QE due to the metal backscattering a Bragg-mirror has to be integrated on the substrate side of the LEDs. Together with an optimization of the PR thickness the QE also can be increased.

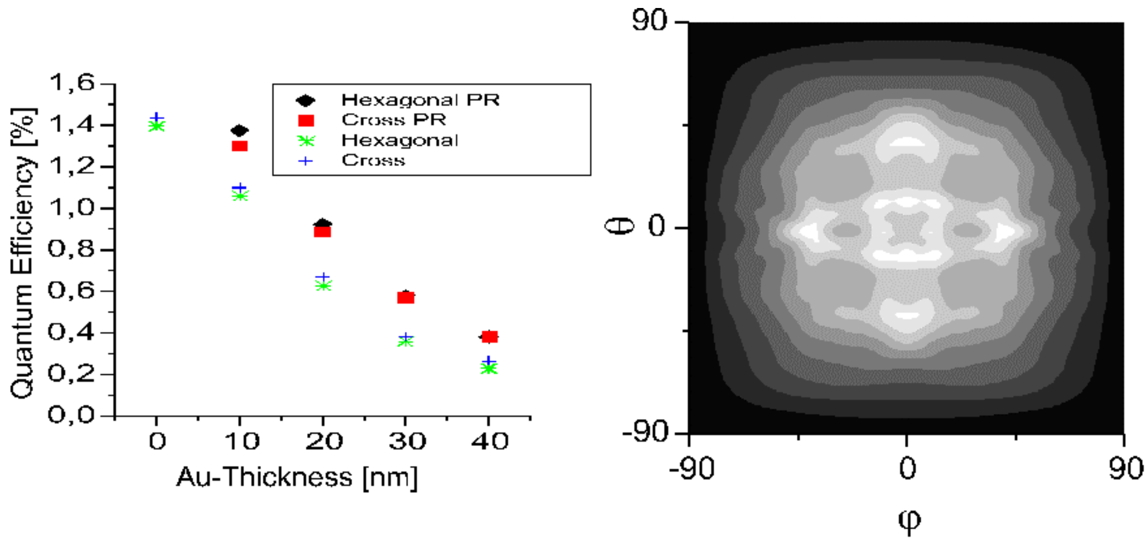

Fig. 8: Quantum efficiency as a function of gold thickness; the right side shows a far field pattern of the LED.

2.5 Time Resolved Temperature Mapping in Silicon-On-Insulator Smart Power Devices

(N. Seliger, D. Pogany, C. Fürböck, M. Stoisiek, P. Habas, E. Gornik)

Silicon-On-Insulator (SOI) by Direct Wafer Bonding has become an attractive technique for the fabrication of smart power devices. Self-heating effects in such structures are, however, more critical compared to bulk devices due to a reduced heat removal across the buried and trench oxides. We have developed an optical interferometer technique which allows measurements of the transient temperature variations inside and outside the SOI well of these devices. The temperature variation in the Si layer is monitored by the intensity change of an infrared laser beam (λ = 1.3 µm) which is focused on the device from the top side (Fig. 9a). A homogeneous temperature increase ΔT in the Si layer of the thickness L causes an increase in the optical thickness $\Delta L_{OPT} = \frac{dn}{dT} \cdot \Delta T \cdot L$ due to the thermooptical effect (dn/dT is the temperature coefficient of the refractive index). Light absorption in the highly doped substrate causes that only the temperature induced variation in the optical thickness of the SOI layer is detected via the reflectivity changes of the Fabry-Perot (F-P) resonator formed by SiO_2 passivation layer/Si layer/SiO_2 buried oxide/Si substrate (Fig. 9b).

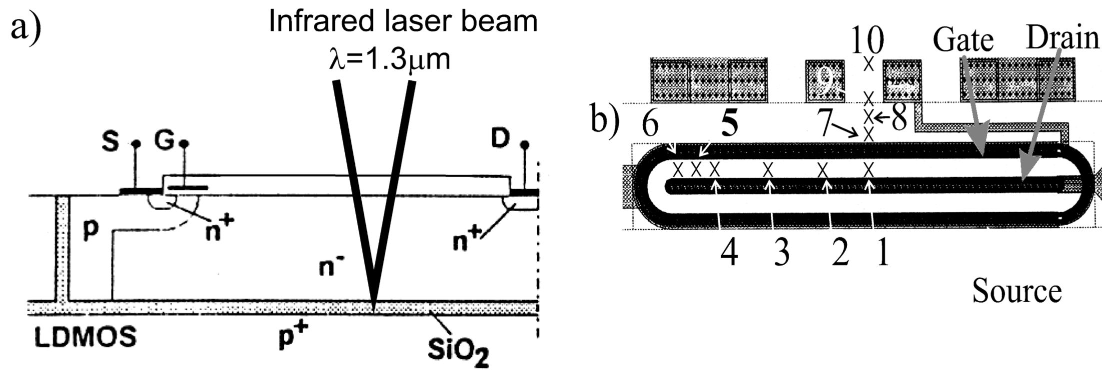

Fig. 9: a) Cross section of LDMOSFET with the laser beam indicated; b) Top view of the device with marked laser beam measurement positions.

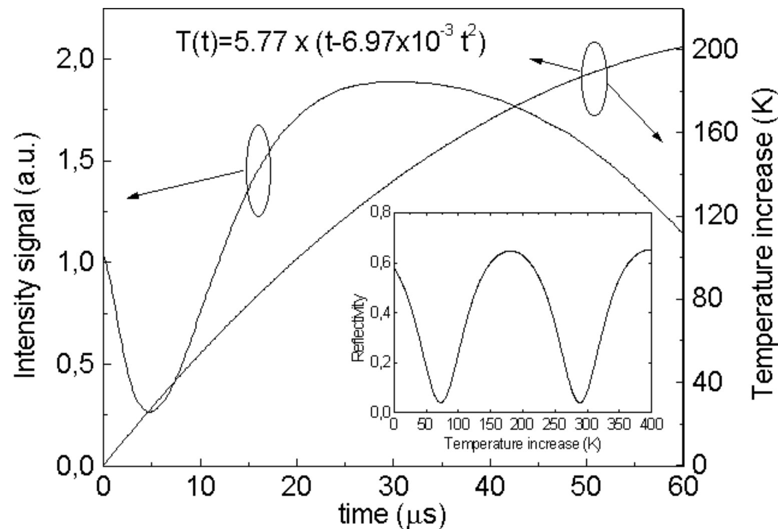

Fig. 10: Intensity signal measured on LDMOSFET and the corresponding temperature function evaluated from the experiment. The inset shows the calculated Fabry-Perot reflectivity as function of temperature for the SiO_2/Si/SiO_2-multilayer inherent in LDMOSFET.

Heating in the Si active layer is induced by applying short pulses of 20 μs to 100 μs from 0 to 12V to the gate under various drain-to-source biases. From the intensity signals (Fig. 10) measured on different positions we can obtain values for the temperature increase within the device and outside the device.

The temperature from experiment agrees well with results from simulation (Fig. 11).

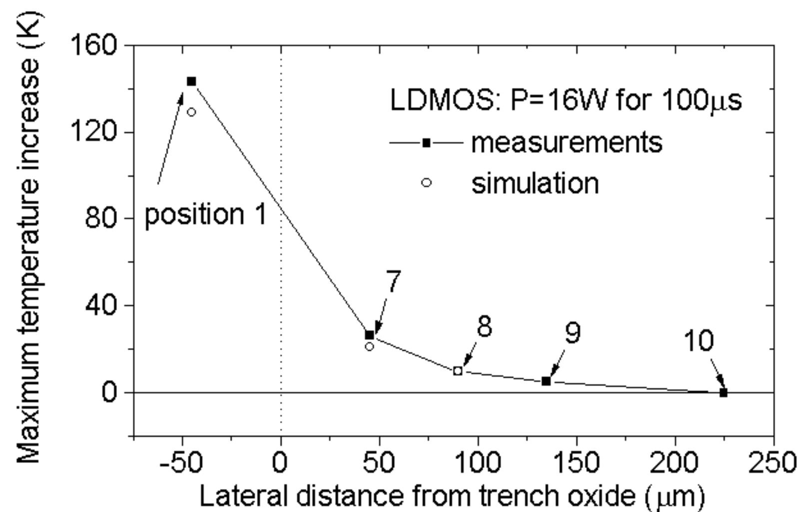

Fig. 11: Peak temperature measured and simulated at different lateral positions (see Fig. 9b) outside the well (Finite Element Simulation by ANSYS).

2.6 Internal Characterization of IGBTs Using the Backside Laser Prober Technique

(C. Fürböck, N. Seliger, R. Thalhammer, G. Wachutka, E. Gornik)

Insulated Gate Bipolar Transistors are MOS gated devices which have a high turn-off capability of large current densities in the case of short circuit. Laserprober experiments have been performed on 2nd generation SIEMENS IGBTs. To make the transistor accessible to the laserprober technique the collector metallization on the backside has to be prepared. To provide a vertical bipolar current flow, the IGBT has a thin p-doped layer on the backside (see Fig. 12).

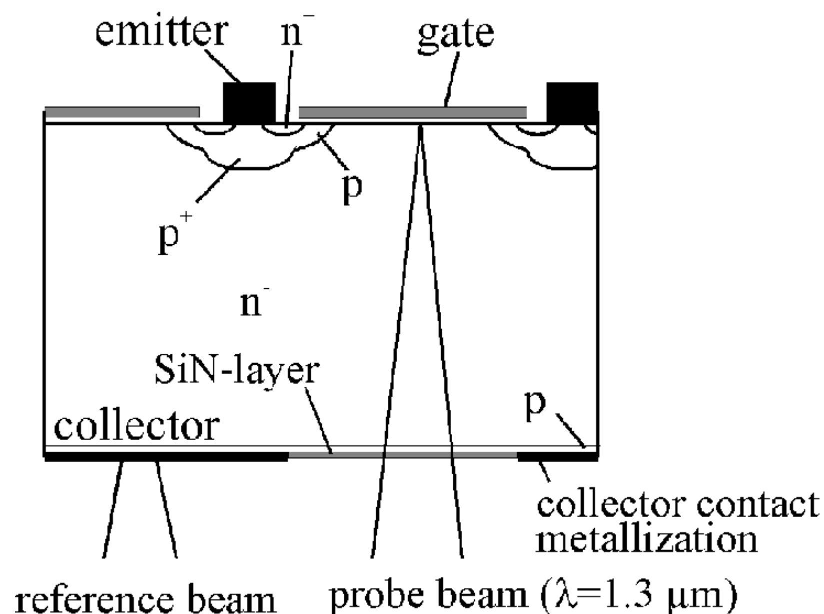

Fig. 12: Principle of backside laser-prober technique applied to the IGBT.

Because of this a mechanical removal of the collector metallization is not possible. A newly developed wet-etching technique provides the possibility to remove parts of the metallization film without etching the silicon. Windows of 70 µm and 90 µm in square are defined, and etched in a two-step process. To avoid multiple reflections within the substrate, an antireflection coating consisting of SiN is deposited in the window area.

In the experiments short circuit case 1 is investigated. A high collector-emitter voltage is applied to the device and the gate is switched to U_{GE} = 15 V for τ = 10 µs. To provide sufficient cooling between the pulses a pulse period of 95 ms is chosen. The voltage U_{CE} is varied from 50 to 300 V.

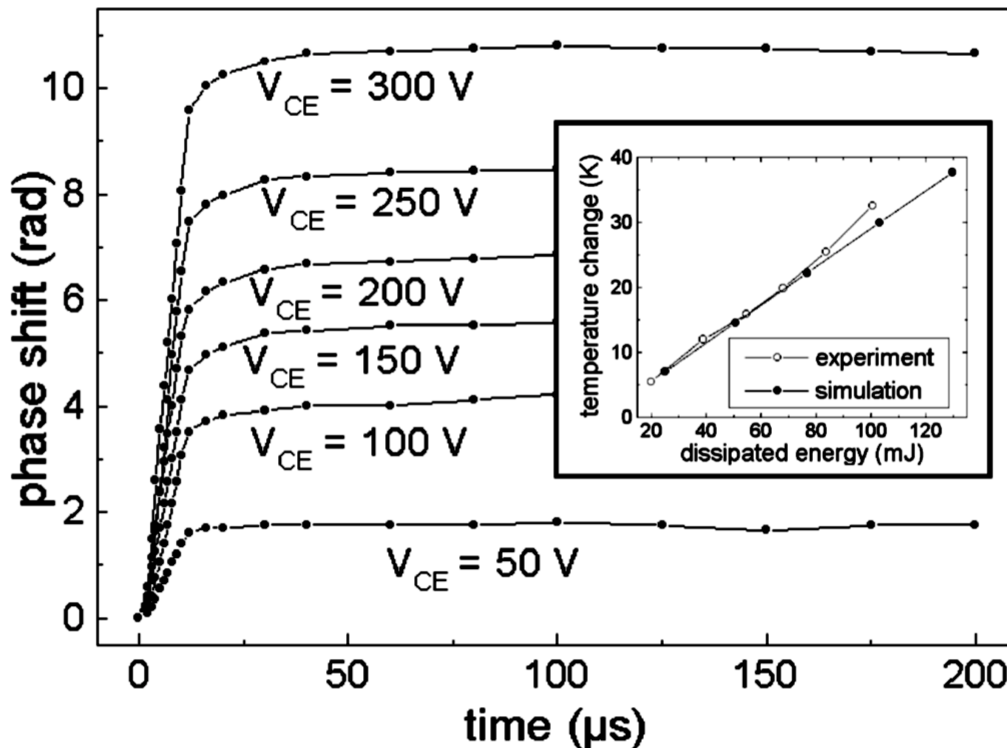

Fig. 13: Transient phase shift under short circuit operation with collector emitter voltages as parameter and a pulse duration of 10 µs. The inset shows the integral temperature change.

In collaboration with the Lehrstuhl für Technische Elektrophysik a simulation of the IGBTs has been performed. The effect of the window in the collector contact metallization on the device behavior was investigated. To distinguish between the signal contribution from the free-carrier and temperature modulation, we made measurements at a low collector-emitter voltage V_{CE}. The contribution from the free carrier concentration is in the range of a few mrad. Hence, it can be neglected at higher power dissipation conditions. Results for this second regime (short circuit operation under high emitter-collector voltage) are shown in Fig. 13. The phase shift is approximately proportional to the total heat dissipated inside the device. From the phase shift an integral temperature change is calculated using the temperature dependence of the refraction index dn/dT = $1{,}6\cdot10^{-4}$ K^{-1}. The results are compared with the values from DESSIS simulation, and good agreement has been found.

2.7 Optical Testing and Study of Thermal Effects in Semiconductor Devices

(D. Pogany, C. Fürböck, N. Seliger, E. Gornik, S. Kubicek, T. Lalinsky)

A noninvasive infrared laser interferometric technique is used to analyze 0.1 µm test technology NMOSFETs and 0.5 µm technology bipolar junction transistors and PMOS-FETs from the back side. The functional state and self-heating effect in the devices are probed by measurements of the optical phase changes caused by the free carrier and thermo-optical effects. The optical signal is studied as a function of bias conditions, device operation frequency and lateral distance from the device (Figs. 14 and 15).

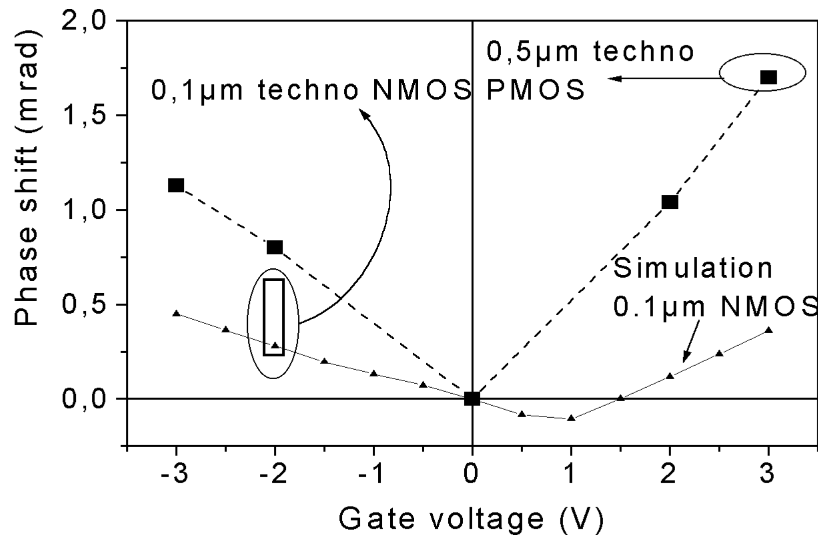

Fig. 14: Phase shift due to the free carrier effect as a function of the gate bias. The dashed line shows the simulation data.

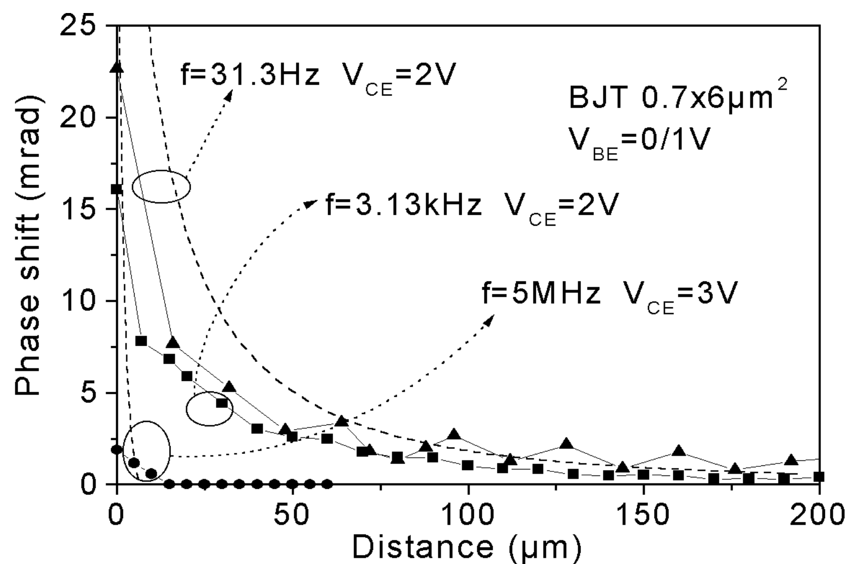

Fig. 15: Phase shift as a function of distance from the emitter of a bipolar transistor. The dashed lines are the simulation results.

Numerical simulation based on the optical characteristic matrix representation for a multilayer system is performed to calculate the free-carrier induced phase shift in MOS-FETs. The thermo-optical signal is modeled using a Fourier solution of the heat conduction equation and a simple geometric optic approach. The experiments are in good agreement with the simulations and shows the applicability of the laser method to test VLSI circuits.

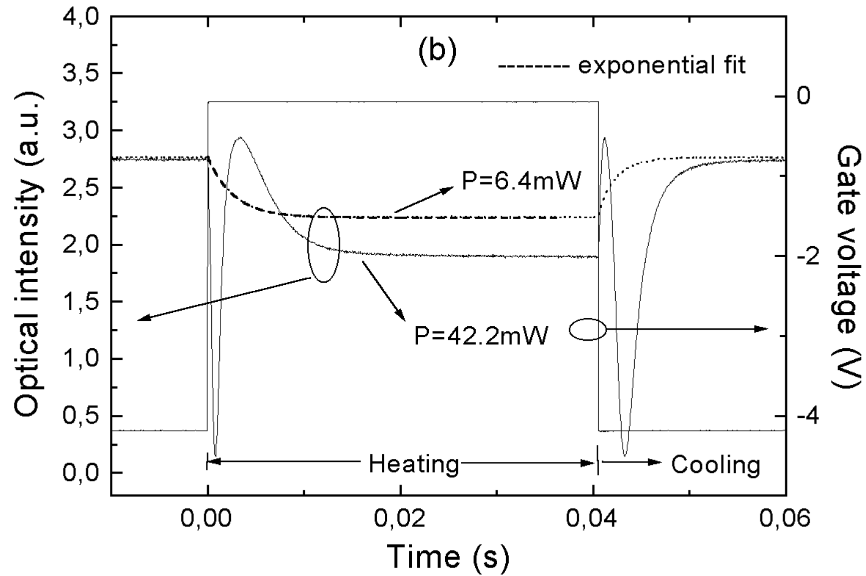

Fig. 16: Time dependencies of optical intensity for two power values. The laser beam is placed in the sensor active area.

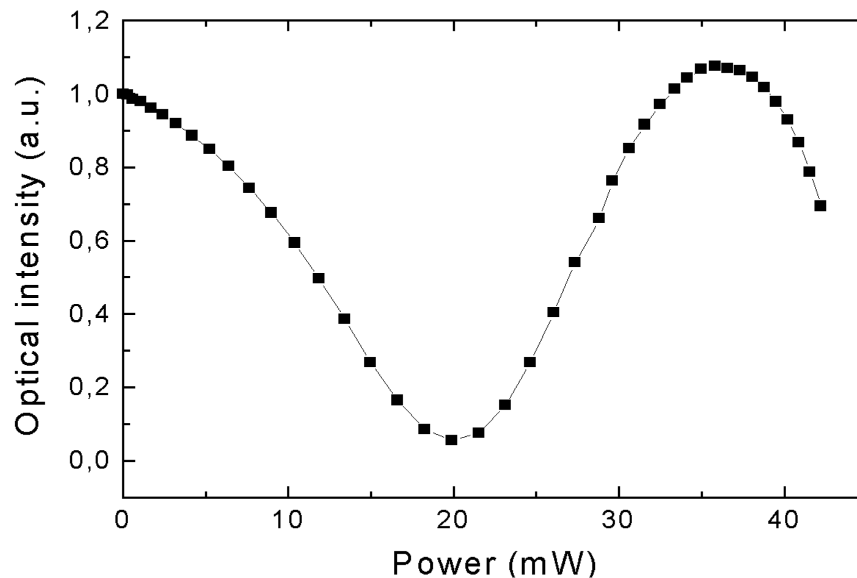

Fig. 17: Optical intensity as a function of dissipated power. The laser beam is positioned on the Schottky diode.

Thermal characteristics of GaAs power sensor microsystem consisting of two cantilever beams are studied by the infrared optical interferometer. Spatial temperature distribution on the cantilever, thermal time constant and power temperature characteristics of the sensor are obtained from time resolved measurements of thermally induced Fabry-Perot optical reflectivity changes (Figs. 16 and 17). A method based on mathematical analysis of the Fabry-Perot intensity peaks is developed to calculate the temperature as a function of time and power. The method is also used to calculate the temperature evolution in smart power devices prepared on silicon-on-insulator (SOI) substrates.

2.8 Low Temperature BEEM Studies on InAs/GaAs Heterostructures

(R. Heer, J. Smoliner, G. Ploner, G. Strasser)

Ballistic Electron Emission Microscopy (BEEM) has been used to perform low temperature studies on MBE grown InAs/GaAs heterostructures. BEEM is a three terminal technique where electrons tunnel between a STM tip (Scanning Tunneling Microscope) and a thin metal-film evaporated on a semiconductor such as Si or GaAs, schematically shown in Fig. 18. The third electrode on the backside of the sample is used to measure the amount of electrons which cross the metal film ballistically and penetrate into the semiconductor.

Originally, BEEM was applied to determine fundamental semiconductor properties such as metal-semiconductor barrier heights, band structure, and hot electron transport effects. Later, BEEM measurements were used to probe subsurface properties of the investigated samples and quantum confined states in a GaAs/AlGaAs double barrier were detected directly. Quantum wires and recently super lattices have also been studied by BEEM.

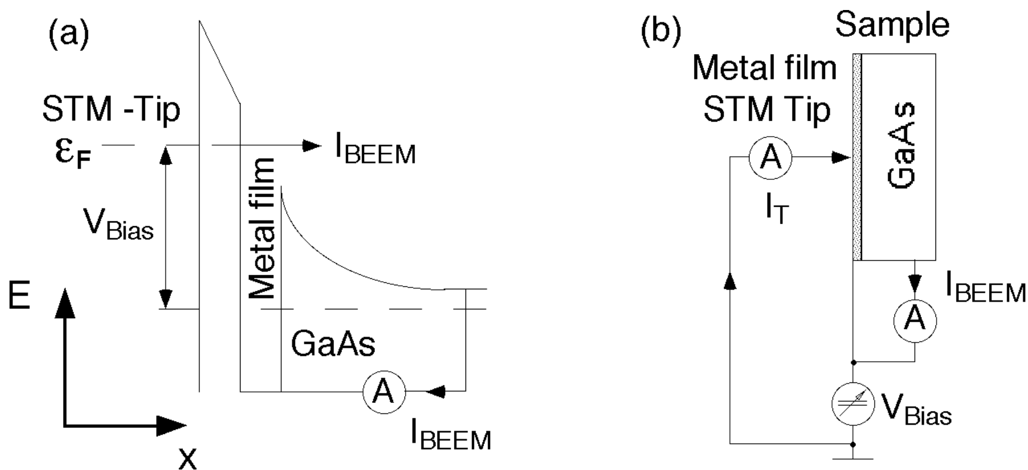

Fig. 18: Schematically set-up of a BEEM experiment, (a): Band diagram (b): Instrumentation.

BEEM offers the unique possibility of probing subsurface quantum states. Therefore it is important to raise the amount of those electrons which are able to penetrate into the sample, to improve the spectroscopic sensitivity of BEEM.

It is possible to increase the transmission coefficient through the base by more than a factor of 10. The commonly used thin metal film has to be replaced by a MBE grown

InAs layer. A passivated InAs cap layer leads to an attenuation length in the regime of 700Å – 900 Å. Compared to a vapor deposited Au film, with an attenuation length of 10 Å, one can see the power of this novel base electrode. In our experiments we could reach the transmission coefficient of 70 Å vapor deposited Au with an 3000 Å InAs cap layer.

Reducing the thickness of the InAs cap layer will lead to a much higher BEEM signal than by the usually used metal film as base electrode, and therefore open a wide spread field of BEEM spectroscopy in the deep subsurface region of samples.

2.9 Coherent Plasmons in n-Doped GaAs

(R. Kersting, R. Hoffmann, K. Unterrainer)

One of the most promising sources for pulsed few-cycle THz radiation are coherent plasmons in semiconductors. Due to the large dipole moment of the coherently oscillating charges intense far-infrared emission is expected.

A fundamentally new plasmon excitation is the coherent oscillation of extrinsic electrons in n-doped GaAs. Initially, the extrinsic electrons are confined between the substrate and the surface depletion region (Fig. 19). Femtosecond laser excitation of the GaAs leads to an ultrafast screening of the depletion field. The electrons respond to this field change which starts their coherent oscillation.

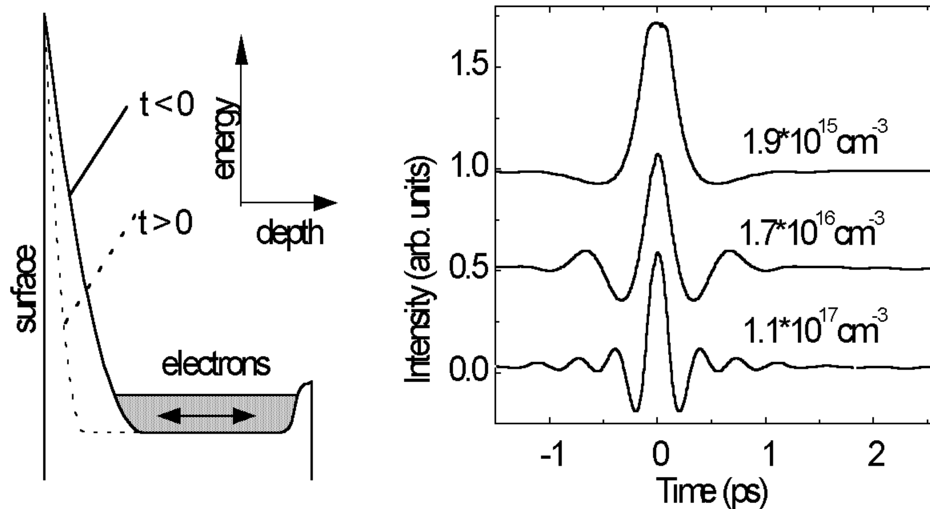

Fig. 19: Left side: Scheme of the excitation process of the coherent electron oscillations. The right side shows correlation data recorded at different doping densities.

Both the excitation and the damping process of the plasmons are investigated in time-resolved experiments on the emitted THz radiation. Figure 19 shows correlation data of the THz pulses. At low doping density an overdamped emission is observed since the oscillation is slower than the damping. According to $\omega_p \propto \sqrt{n}$ the plasma frequency increases with the electron concentration, which leads to well pronounced oscillations at higher doping densities. Since the signals show no dependence on excitation density we conclude that the emission results exclusively from the coherent oscillation of the extrinsic electrons.

In all experiments we observe temporally and spatially coherent THz radiation with intensities of up to 100 nW. However, the pulses are damped out after few oscillations. Temperature dependent measurements show that the damping is due to phonon scattering.

2.10 Transient Quantum Coherence of Intersubband Transitions

(R. Kersting, J.N. Heyman, E. Thaller, K. Unterrainer)

Recent technological innovations tend to use quantum coherence phenomena for novel ultrafast devices. One of the most attractive material systems are semiconductor heterostructures due to their huge oscillator strengths and sharp transition linewidths. In our experiments we use electro-magnetic THz pulses to drive electronic intersubband transitions in modulation doped GaAs quantum wells (QWs). The temporal quantum coherence gets directly visible by the time-dependent polarization of the electrons which follows the THz excitation.

The inset of Fig. 20 shows a scheme of the intersubband states in a modulation doped QW. Electrons which are initially located at the lower quantum level are excited by an ultrashort pulse with a center frequency of about 1.5 THz. This THz beam is transmitted through the sample and time-resolved by mixing it with a half-cycle THz pulse and detecting the superposition.

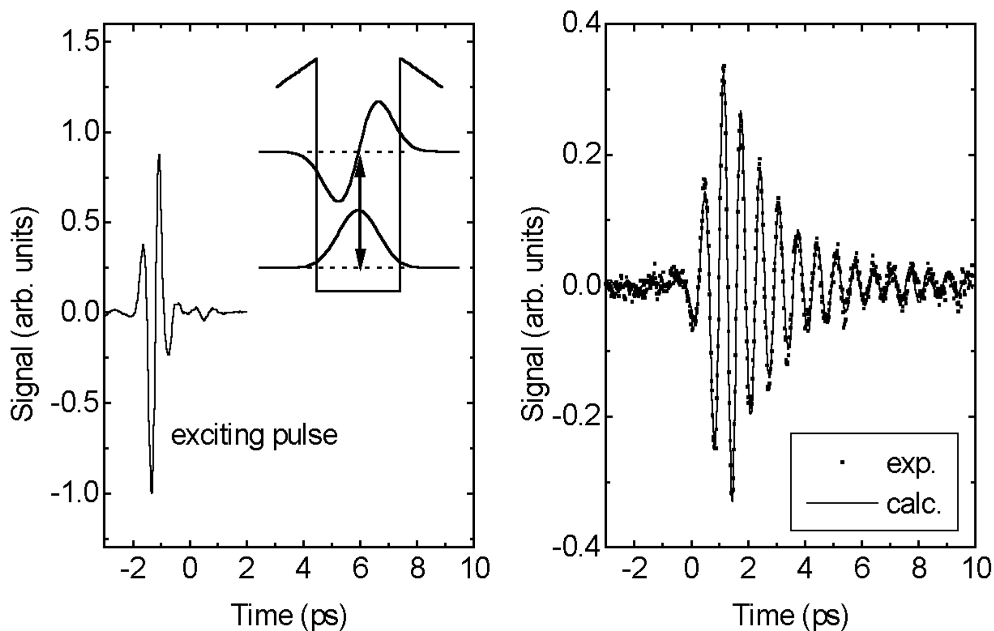

Fig. 20: Left side: The inset is a scheme of the confined electron states (e1, e2) within the QW. The data show the THz pulse exciting the intersubband transition. Right side: Transient response of the electrons when driven by the THz pulse.

Driving the electrons with the few-cycle THz pulse leads to a transient polarization which counteracts the field of the exciting pulse. Modulating the gate bias of the structure and thus the population of the QWs makes the response of the electrons directly visible. The oscillating signal results from the coherent superposition of the states in the first and second subband. During the first ps the exciting THz pulse leads to an increas-

ing amplitude of the electron oscillation. After the driving pulse decayed the amplitude decreases and shows the free induction decay of the collective mode. The solid line is the result of a two-level model calculation. The good agreement enables us to determine the dielectric function of the isolated electron gas in the quantum system.

2.11 Far-Infrared Emission from Parabolic Quantum Wells in Magnetic Fields

(R. Zobl, M. Fuchshuber, K. Unterrainer, E. Gornik)

In recent years various types of semiconductor quantum structures have been studied for emission in the THz range. Here the concept of a parabolic potential well and its plasmonic type of FIR emission is studied under lateral current injection. The most interesting feature of parabolically confined potentials is that they absorb and emit radiation only at the bare harmonic oscillator frequency ω_0, independent of the number of electrons in the well. This is in accordance with Kohn's theorem which states that cyclotron resonance absorption is unaffected by electron-electron interaction.

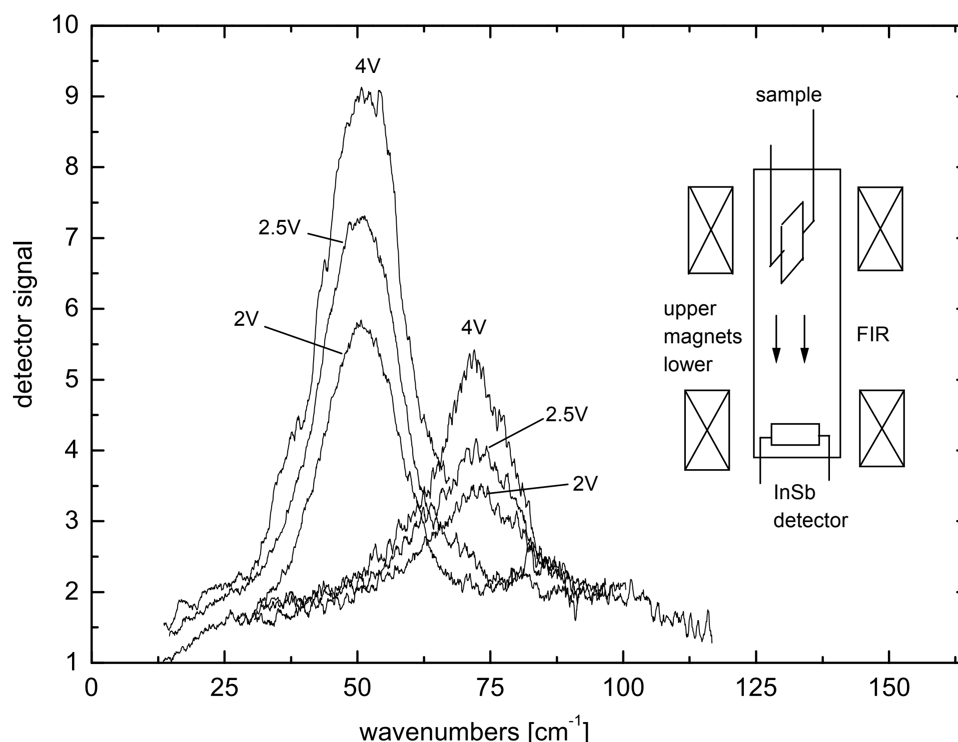

Fig. 21: FIR emission of a parabolic quantum well at 0 T and 4 T. The magnetic field shifts the center frequency by about 20 cm^{-1}. The sample has two top contact pads and a grating coupler.

To investigate the effect of a magnetic field on the FIR emission of the PQW magnetic fields up to 5 T were applied. For a magnetic field direction perpendicular to the layers no CR emission can be observed while the normal intersubband emission almost immediately vanishes even at low magnetic fields. If the magnetic field is applied parallel to the well but perpendicular to the direction of current flow (Fig. 21) CR emission again is not seen whereas a frequency shift of the intersubband radiation is observed starting at

magnetic field strengths above 2 T. The shift is attributed to the formation of a strong electric field perpendicular to the well via Hall effect. At 4 T the center frequency of the FIR emission has moved from 50 cm^{-1} to 70 cm^{-1} accompanied by a decrease in signal intensity of 50 %. The shifted center frequency position still is independent from the laterally applied electric field and the current flow.

2.12 Growth and Characterization of GaAs/AlGaAs Mid-Infrared Emitters

(L. Hvozdara, S. Gianordoli, W. Bichl, G. Strasser, P. Kruck, M. Helm, E. Gornik)

Environmental monitoring, medicine, optical communication and many other areas of technology create a field of application for both, coherent and non-coherent emitters for wavelengths from three to 15 microns.

In the structure depicted in Fig. 22 the intersubband radiative transition (3–2) can be achieved. The energy spacing between levels two and three can be tailored so that the corresponding emitted photon belongs to the mid-infrared band. For the achievement of lasing action there must be a population inversion between the level three and the level two established. An LO-phonon transition between level two and level one secures quick emptying of level two and in this way the condition $t_{(3-2)} > t_{(2-1)}$ for population inversion is satisfied.

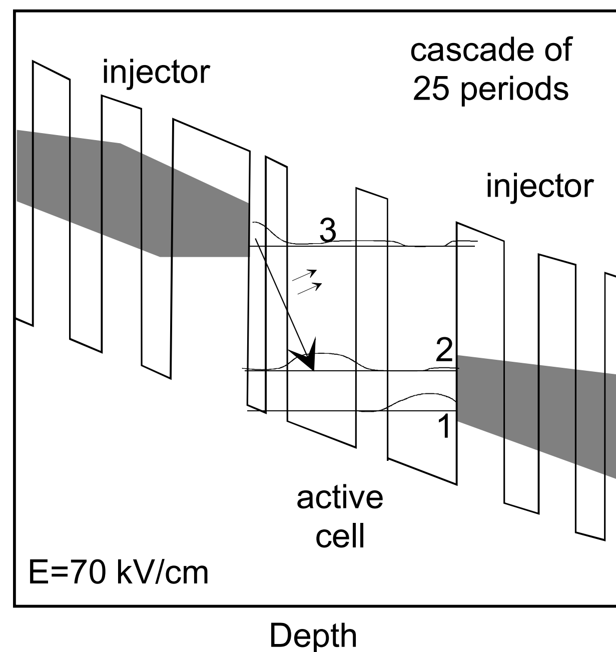

Fig. 22: Calculation of the biased structure. Transition 3–2 is radiative.

I-V characteristics and the photovoltage spectra (Fig. 23) are recorded and the correlation between the self-consistent calculation and the experimental results is found excellent. First attempts to design a laser structure encountered problems with the trade-off between the electrical and the optical properties of the cladding layers.

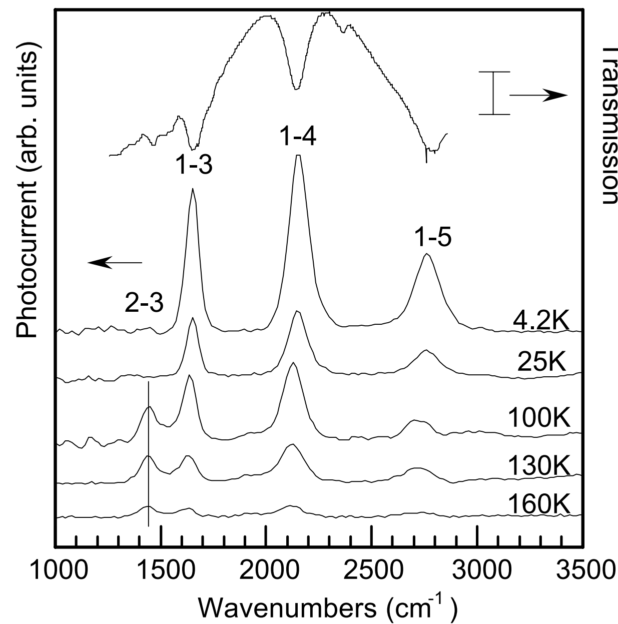

Fig. 23: Typical transmission and photovoltage spectra.

2.13 Ballistic Electron Spectroscopy of Semiconductor Quantum Heterostructures

(C. Rauch, G. Strasser, M. Kast, C. Pacher, W. Boxleitner, E. Gornik)

The technique of hot electron spectroscopy is used to measure the transmission properties of resonant tunneling diodes and semiconductor superlattices at different electric fields.

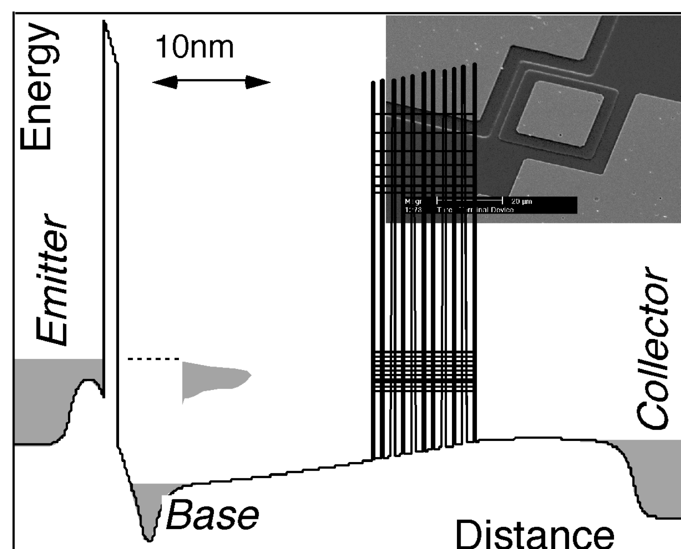

Fig. 24: Conduction band diagram of a hot electron transistor. The inset shows an SEM picture of the device.

A three terminal is used to generate an energy tunable electron beam by a tunneling barrier that passes the superlattice after traversing a thin highly doped n-GaAs base layer and an undoped drift region. The measured collector current reflects the probability of an injected electron to be transmitted through the superlattice. The transmittance of the superlattice can be measured directly at given superlattice bias conditions by varying the injected current independently from the superlattice bias voltage. When a uniform electric field is applied to the superlattice, the quasi-continuous minibands break up into a ladder of discrete Wannier-Stark states. This localization of the electron wave function has direct consequences on the ballistic electron transport. The structures were grown by molecular beam epitaxy on semi-insulating GaAs substrate, the devices were fabricated using standard lithography. An SEM picture and the conduction band diagram of the device is shown in Fig. 24.

Fig. 25 shows the miniband transmission versus applied electric field at 4.2 K. For negative collector bias (decelerating field) the measured current is proportional to the coherent current since electrons that are scattered within the miniband are accelerated back to the base. In case of positive collector bias we measure the coherent current and the additional field induced incoherent current due to Esaki-Tsu like band transport. Since the coherent current is considered to be symmetric for both bias directions, we are able to distinguish between the coherent and incoherent contribution of the collector current.

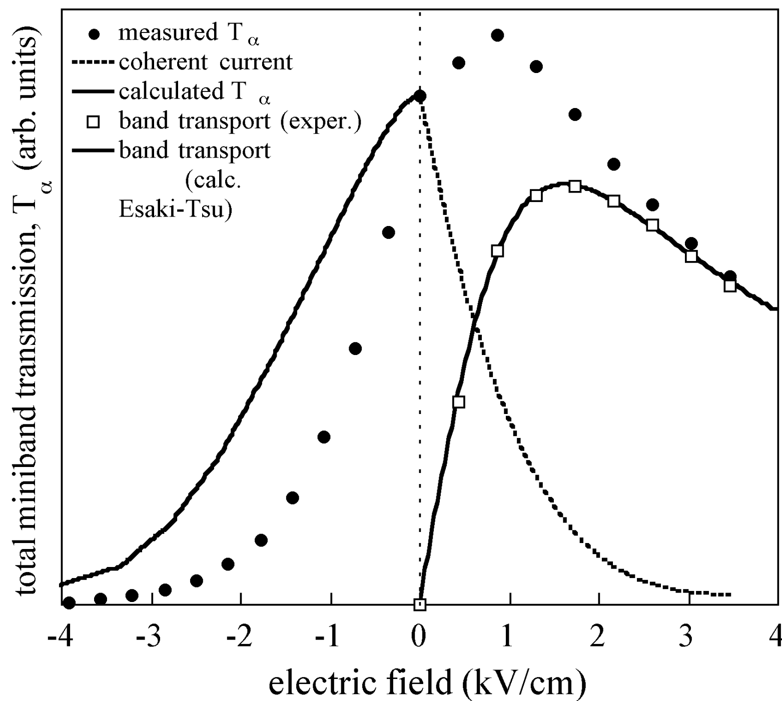

Fig. 25: Miniband transmission versus electric field. Coherent (dashed line) and incoherent current (squares) is present.

These experiments demonstrate for the first time the transition from coherent transport to band like scattering induced transport in a superlattice miniband. Furthermore we have determined the scattering time and the coherence length (l_{coh} = 80 nm) of the electrons in these superlattices.

By making the length of the superlattice close to the mean free path we believe to match the conditions for Bloch oscillations. The realization of a THz laser based on Bloch oscillation is subject of further experiments.

Project Information

Project Manager

Dr. Gottfried STRASSER

Institut für Festkörperelektronik, Technische Universität Wien

Project Group

Last Name	First Name	Status	Remarks
Almeder	Christian	student	
Andok	Robert	student	
Bichl	Herbert	student	
Boxleitner	Winfried	Post Doc	
Bratschitsch	Rudolf	student	
Eder	Claudia	dissertation	50% GMe
Finger	Norman	dissertation	
Fuchshuber	Michael	student	
Fürböck	Christoph	dissertation	
Gianordoli	Stefan	dissertation	
Golshani	Alireza	dissertation	
Gornik	Erich	Full Prof.	
Habas	Predrag	Post Doc	
Haider	Manfred	student	
Hainberger	Rainer	dissertation	
Hauser	Markus	Post Doc	
Heer	Rudolf	dissertation	
Hirner	Heimo	student	
Hobler	Gerhard	Assistant Prof.	
Hoffmann	Rainer	student	
Hvozdara	Lubos	dissertation	
Kast	Michael	student	
Kellermann	Peer Oliver	dissertation	
Kersting	Roland	Post Doc	
Köck	Anton	Assistant Prof.	
Kröll	Peter	technician	
Lampacher	Peter	student	

Last Name	First Name	Status	Remarks
Langmann	Gottfried	technician	
Liu	Jian	student	
Maier	Thomas	dissertation	
Pacher	Christoph	student	
Patz	Sybille	student	
Ploner	Guido	dissertation	
Pogany	Dionyz	guest scientist	
Prinzinger	Johannes	technician	
Rauch	Christoph	dissertation	
Schenold	Helmut	technician	
Schrenk	Werner	dissertation	
Seliger	Norbert	dissertation	
Smola	Winfried	student	
Smoliner	Jürgen	Assistant Prof.	
Socher	Michael	student	
Strasser	Gottfried	Assistant Prof.	
Thaller	Edwin	student	
Unterrainer	Karl	Assistant Prof.	
Zobl	Reinhard	dissertation	100% GMe
Zotl	Ernst	dissertation	

Publications in Reviewed Journals

1. M. Helm, W. Hilber, W.Heiss, B.N. Murdin, G. Strasser, E. Gornik, C.J.G.M. Langerak, C.R. Pidgeon: “Energy relaxation of electrons in GaAs/AlGaAs quantum wells and superlattices”, Proc. ITQW ‘97, Tainan, Taiwan, 15-18.12.97 (to be published)
2. P. Kruck, M. Helm, G. Strasser, L. Hvozdara, E. Gornik: “Quantum Cascade Electroluminescence in the GaAs/AlGaAs material system”, Proc. ITQW ‘97, Tainan, Taiwan, 15-18.12.97 (to be published)
3. G. Strasser, S. Gianordoli, L. Hvozdara, H. Bichl, K. Unterrainer, E. Gornik, P. Kruck, M. Helm, J.N. Heyman: “GaAs/AlGaAs intersubband mid-infrared emitter”, Proc. MRS Fall Meeting 1997, Boston, USA, 1-5.12.97
4. G. Strasser, C. Rauch, K. Kempa, E. Gornik: “Ballistic electron transport in semiconductor superlattices”, Proc. ISCS24, San Diego (1997), to be published
5. L. Hvozdara, J.N. Heyman, G. Strasser, K. Unterrainer, P. Kruck, M. Helm, E. Gornik: “Characterization of GaAs/AlGaAs mid-infrared emitters”, Proc. ISCS24, San Diego (1997), to be published
6. B.N. Murdin, N. Nasser, C.J.G.M. Langerak, W.Heiss, M. Helm, G. Strasser, E. Gornik, S.-C. Lee, I. Galbraith, C.R. Pidgeon: “Intersubband dynamics below the

optical energy for single and coupled quantum well systems", Phys. stat. sol. (b) 204, 208 (1997)

7. C. Rauch, G. Strasser, K. Unterrainer, W. Boxleitner, E. Gornik: "Quenching of miniband transport in biased undoped superlattices", Phys. stat. sol. (b) 204, 393 (1997)
8. R. Kersting, K. Unterrainer, G. Strasser, E. Gornik: "Coherent few-cycle THz emission from plasmons in bulk GaAs", Phys. stat. sol. (b) 204, 67 (1997)
9. J. Smoliner, C. Eder, G. Strasser, E. Gornik: "Ballistic electron emission microscopy on quantum wires", Phys. Stat. Sol. (b) 204, 386 (1997)
10. G. Strasser, C. Rauch, E. Gornik: "Current Transport in Multiple Superlattice Structures", Proc. MSS8, Santa Barbara (1997), to be published in Physica B
11. P. Kruck, G. Strasser, M. Helm, L. Hvozdara, E. Gornik: "Quantum Cascade Electroluminescence in GaAs/AlGaAs Structures", Proc. MSS8, Santa Barbara (1997), to be published in Physica B
12. C. Eder, J. Smoliner, R. Heer, G. Strasser, E. Gornik: "Probing of Superlattice Minibands by Ballistic Electron Emission Microscopy", Proc. MSS8, Santa Barbara (1997), to be published in Physica B
13. C. Rauch, G. Strasser, K. Unterrainer, W. Boxleitner, E. Gornik, K. Kempa: "Ballistic Electron Spectroscopy of Vertical Biased Superlattices", Proc. MSS8, Santa Barbara (1997), to be published in Physica B
14. G. Strasser, P. Kruck, M. Helm, J.N. Heyman, L. Hvozdara, E. Gornik: "Mid-infrared electroluminescence in GaAs/AlGaAs structures", Appl. Phys. Lett. 71 (20), 2892 (1997)
15. G. Ploner, J. Smoliner, G. Strasser, M. Hauser, E. Gornik: "Energy levels in quantum wires studied by magnetophonon effect", accepted at Phys. Rev. B. (1997)
16. C. Rauch, G. Strasser, K. Unterrainer, and E. Gornik: "Ballistic electron spectroscopy of semiconductor heterostructures", Basics of semiconductor device technology (1997) ISBN: 3-901578-02-1
17. C. Rauch, G. Strasser, K. Unterrainer, L. Hvozdara, W. Boxleitner, E. Gornik, B. Brill, and U. Meirav: "Hot electron spectroscopy of undoped GaAs/GaAlAs superlattices", Superlattices and Microstructures, Vol. 22 (2), 143 (1997)
18. G. Ploner, J. Smoliner, G. Strasser and E. Gornik: "Transport characterization of quantum wires by magnetophonon and magnetic depopulation experiments", Superlattices and Microstructures, Vol. 22 (2), 249 (1997)
19. C. Rauch, G. Strasser, K. Unterrainer, B. Brill, E. Gornik: "Ballistic Electron Spectroscopy of Vertical Superlattice Minibands", Appl. Phys. Lett. 70 (5), 649 (1997)
20. B.N. Murdin, W.Heiss, C.J.G.M. Langerak, S.-C. Lee, I. Galbraith, G. Strasser, E. Gornik, M. Helm, C.R. Pidgeon: "Direct observation of the LO phonon bottleneck in wide GaAs/AlGaAs quantum wells", Phys. Rev. B 55 (8), 5171 (1997)
21. R. Kersting, K. Unterrainer, G. Strasser, H.F. Kauffmann, E. Gornik: "Few-cycle THz emission from cold plasma oscillations", Phys. Rev. Lett. 79 (16), 3038 (1997)

22. P.O. Kellermann, A. Golshani, A. Köck, E. Gornik, H.-P. Gauggel, R. Winterhoff, M.H. Pilkuhn: “Single-mode and single-beam surface emission from visible red GaInP/AlGaInP laser diodes”, Applied Physics Letters Vol. 70 (18), 5.5.1997, USA

23. R. Kersting, K. Unterrainer, G. Strasser, and E. Gornik: “Coherent few-cycle THz emission of cold plasmas”, Proceedings of the Quantum Electronics and Laser Science Conf. QELS ‘97,’98, (1997)

24. A. Golshani, P.O. Kellermann, A. Köck, E. Gornik, L. Korte: “Five-wavelength surface emitting laser diode array based on postgrowth adjustment of emission wavelength”, Applied Physics Letters Vol. 71 (6), 11.8.1997, USA

25. C. Fürböck, R. Thalhammer, N. Seliger, D. Pogany, G. Deboy, G. Wachuta, E. Gornik: “Lokale Temperaturbestimmungen in Insulated Gate Bipolar Transistoren (IGBTs) mittels Laserdiodentechnik”, ÖVE-Schriftenreihe Nr.14,pp.117-122,1997

26. E. Burian, D. Pogany, T. Lalinsý, N. Seliger and E. Gornik: “Thermal Simulation and Characterization of GaAs Micromachined Power Sensor Microsystems”, accepted for publication at Eurosensors XI, Warsaw (1997).

27. N. Seliger, D. Pogany, C. Fürböck, P. Habas, E. Gornik and M. Stoisiek: “A Laser Beam Method for Evaluation of Thermal Time Constant in Smart Power Devices”, Proc. of ESREF Conf., Microelectr. and Reliab., Vol. 37, No. 10/11, pp. 1727-1730 (1997)

28. N. Seliger, D. Pogany, C. Fürböck, P. Habas, E. Gornik and M. Stoisiek: “A Study of Temperature Distribution in SOI-Smart Power Devices in Transient Conditions by Optical Interferometry”, Proc. of ESSDERC, p. 512, Stuttgart (1997).

29. D. Pogany, C, Fürböck, N. Seliger, P. Habas, E. Gornik, S. Kubicek and S. Decoutere: “Optical testing of submicron-technology MOSFETs and bipolar transistors”, Proc. of ESSDERC, p. 372, Stuttgart (1997)

30. N. Seliger, C. Fürböck, P. Habas, D. Pogany, and E. Gornik: “Backside-Laserprober Technique for Characterization of Semiconductor Power Devices”, Proceedings of the Seminar “Basics and Technology of Electronic Devices”, Großarl, Austria, March 1997, pp. 143-147

31. N. Seliger, P. Habas, D. Pogany and E. Gornik: “Time-Resolved Analysis of Self-Heating in Power VDMOSFETs Using Backside Laserprobing”, Solid State Electronics, Vol.41, No.9, pp.1285-1292 (1997)

32. D. Pogany, N. Seliger, T. Lalinský, J. Kuzmík, P. Habas, P. Hrkút and E. Gornik: “Study of Thermal Effects in GaAs Micromachined Power Sensor Microsystems by an Optical Interferometer Technique”, accepted for publication in Microelectronics Journal, January 1997

33. R. Heer, C. Eder, J. Smoliner, E. Gornik: “A floating electrometer for scanning tunneling microscope applications in the femtoampere range”, Rev. Sci. Instruments 68, 4488 (1997)

34. J. Liu, E. Gornik, S. Xu and H. Zheng: “Sequential resonant tunneling through Landau levels in GaAs/AlAs superlattices”, Semicond.Sci. Technol. 12, 1422, (1997)

35. D. Pogany and G. Guillot: "Normal and anomalous behaviour of the RTS noise amplitude in forward biased InGaAs/InP photodiodes", Solid State Electronics 41, 547 (1997)

36. K. Unterrainer, B.J. Keay, M.C. Wanke, S.J. Allen, D. Leonard, G. Medeiros-Ribeiro, U. Bhattacharya, M.J.W. Rodwell: "Observation of Shapiro steps and direct evidence of Bloch oscillations in semiconductor superlattices", Inst. Phys. Conf.Ser. 155, 729 (1997)

37. P. Habas: "Analytical Model and Qualitative Analysis of the Interface-Trap Charge Pumping Characteristics of MOS Structure", Proc. of 21st Int. Conf. on Microelectronics (MIEL), Nils(YU), Sept. 1997

38. P. Habas, G. Groeseneken, G. Van den bosch: "Geometric Current Component in Charge-Pumping Measurements", Proc. of 21st Int. Conf. on Microelectronics (MIEL), Nils (YU), Sept. 1997

39. P. Habas, G. Groeseneken, G. Van den bosch, H.E. Maes, and E. Gornik: "Detailed Study of the Parasitic Geometric Current Component in Charge Pumping Measurements: Determination of Relevant Parameters", Proc. of Semiconductor Interface Specialists Conf., Charleston (USA), (1997)

40. P. Habas, I. De Wolf, G. Groeseneken, A. Stesmans and H.E. Maes: "Analysis of Charge Pumping Characteristics of Single Interface Traps", Proc. of Semiconductor Interface Specialists Conf., Charleston (USA) (1997)

41. R. Kersting, J.N. Heyman, G. Strasser, K. Unterrainer: "Coherent volume plasmons in n-doped GaAs", Phys.Rev.B. (submitted)

42. J.N. Heyman, R. Kersting, G. Strasser, K. Maranowski, A.C. Gossard, K. Unterrainer: "Thz time-domain spectroscopy of intersubband plasmons", Proceedings of the Fourth International Workshop on Intersubband Transitions in Quantum Wells, Tainan, Taiwan, December 15th-18th, 1997 (accepted)

43. J.N. Heyman, R. Kersting, K. Unterrainer: "Time-Domain Measurement of Intersubband Oscillations in a Quantum Well", Appl. Phys. Lett., 72, 644 (1998)

44. A. Köck, A. Golshani, R. Hainberger, E. Gornik, L. Korte: "Digital beamsteering from surface emitting laser diodes based on surface-mode emission", in "In-plane semiconductor lasers: from Ultraviolet to Mid-Infrared", Hong.K. Choi, Peter S. Zory, Editors Proc. SPIE 3001, in print (1997)

Presentations

1. C. Eder, R. Heer, J. Smoliner, G. Strasser, E. Gornik, G. Weimann, G. Böhm: "Sub surface characterization of GaAs/AlGaAs heterostructures by scanning tunneling microscopy", *ETH Zürich*, 3.11.1997

2. G. Strasser: "Quantum cascade electroluminescence in GaAs/AlGaAs Structures", *Workshop on Semiconductor Infrared Detectors and Emitters*, National Research Council Canada, Ottawa, 23-25.7.1997

3. J.Smoliner, C. Eder, G. Strasser, E. Gornik: "BEEM on quantum wires", *HCIS10 Conference*, Berlin, Germany, July 1997

4. R. Kersting, K. Unterrainer, G. Strasser, E. Gornik: "Coherent few-cycle THz emission of cold plasmons", *1997 Quantum Electronics and Laser Science Conf.*, 18.-23.5.1997, Baltimore, USA
5. G. Strasser, S. Gianordoli, L. Hvozdara, H. Bichl, K. Unterrainer, E. Gornik, P. Kruck, M. Helm, J.N. Heyman: "GaAs/AlGaAs intersubband mid-infrared emitter", *MRS (Material Research Society) Fall Meeting 1997*, Boston, USA, 1-5.12.97
6. L. Hvozdara, J.N. Heyman, G. Strasser, K. Unterrainer, P. Kruck, M. Helm, E. Gornik: "Characterization of GaAs/AlGaAs mid-infrared emitters", *24. International Symposium on Compound Semiconductors*, San Diego 7-11.9.97
7. R. Kersting, K. Unterrainer, G. Strasser, E. Gornik: "Coherent few-cycle THz emission from plasmons in bulk GaAs", *10th Int. Conf. on Hot Carriers in Semiconductors*, Berlin, Germany, 28.7-1.8.97
8. C. Rauch, G. Strasser, K. Unterrainer, W. Boxleitner, K. Kempa, E. Gornik: "Hot electron transport in semiconductor quantum heterostructures", *10th Int. Conf. on Hot Carriers in Semiconductors*, Berlin, Germany, 28.7-1.8.97
9. P. Kruck, G.Strasser, M. Helm, L. Hvozdara, E.Gornik: "Quantum Cascade Electroluminescence in GaAs/AlGaAs Structures", *8. Conf. on Mod. Semicond. Struct. (MSS8)* , Santa Barbara, USA 14-18.7.97
10. C.Eder, J.Smoliner, R.Heer, G.Strasser, E.Gornik: "Probing of Superlattice Minibands by Ballistic Electron Emission Microscopy", *8. Conf. on Mod. Semicond. Struct. (MSS8)* , Santa Barbara, USA 14-18.7.1997
11. C. Rauch, G. Strasser, K. Unterrainer, W. Boxleitner, E.Gornik, K. Kempa: "Ballistic Electron Spectroscopy of Vertical Biased Superlattices", *8. Conf. on Mod. Semicond. Struct. (MSS8)* , Santa Barbara, USA 14-18.7.1997
12. C. Rauch, G. Strasser, K. Unterrainer, and E. Gornik: "Ballistic electron spectroscopy of semiconductor heterostructures", *Basics of semiconductor device technology*, Großarl, Austria, 19.3 - 22.3. 1997
13. K. Kempa, P. Bakshi, G. Strasser, K. Unterrainer, C. Rauch, E. Gornik: "Double quantum well structure for coherent plasmon generation", *MRS March Meeting 1997*, Kansas City, USA
14. J. Smoliner, M. Hauser, C. Eder, G. Strasser, E. Gornik: "Quantum dot structures for STM tips", *PHASDOMS 97*, Aachen, Germany, 1997
15. G. Strasser: "Coherent and non-coherent electron transport in superlattice structures", *Department of Physics*, Boston College, Boston, USA, 4.12.97
16. L. Hvozdara, G. Strasser, P. Kruck, M. Helm, K. Unterrainer, E. Gornik: "Wachstum und Charakterisierung von Intersubband-Laser-Strukturen", *Österreichische Physikalische Gesellschaft*, 47. Jahrestagung, Wien, Austria (9/97)
17. R. Zobl, C. Rauch, L. Hvozdara, G. Strasser, K. Unterrainer, K. Maranowski, A.C. Gossard, E. Gornik: "Halbleiter-Quantenstrukturen als THz-Emitter", *Österreichische Physikalische Gesellschaft*, 47. Jahrestagung, Wien, Austria (9/97)
18. R. Kersting, J.N. Heyman, G. Strasser, H.F. Kauffmann, K. Unterrainer: "Kohärente THz-Emission von Plasmaoszillationen in Halbleitern", *Österreichische Physikalische Gesellschaft*, 47. Jahrestagung, Wien, Austria (9/97)

19. M. Hauser, E. Zottl, G. Strasser, E. Gornik: “Nanostrukturierte Schottkydioden für den THz Bereich”, Österreichische Physikalische Gesellschaft, 47. Jahrestagung, Wien, Austria (9/97)
20. G. Strasser, C. Rauch, L. Hvozdara, K. Unterrainer, E. Gornik: “Stromtransport in Übergittern verschiedener Periodizität”, *Österreichische Physikalische Gesellschaft*, 47. Jahrestagung, Wien, Austria (9/97)
21. G. Ploner, J. Smoliner, G. Strasser, M. Hauser, E. Gornik: “Charakterisierung von Quantendrähten mittels Magnetophonon Effekt*”, Österreichische Physikalische Gesellschaft*, 47. Jahrestagung, Wien, Austria (9/97)
22. C. Eder, J. Smoliner, R. Heer, G. Strasser, E. Gornik: “Untersuchung von Übergittern mittels Ballistic Electron Emission Microscopy*”, Österreichische Physikalische Gesellschaft*, 47. Jahrestagung, Wien, Austria (9/97)
23. C. Rauch, G. Strasser, K. Unterrainer, K. Kempa, E. Gornik: “Ballistic electron transport in biased semiconductor superlattices*”, Österreichische Physikalische Gesellschaft*, 47. Jahrestagung, Wien, Austria (9/97)
24. G. Strasser, C. Rauch, K. Kempa and E. Gornik: “Ballistic electron transport in semiconductor superlattices”, 24. International Symposium on Compound Semiconductors, San Diego 7-11.9.97
25. C. Eder, J. Smoliner, R. Heer, G. Strasser and E. Gornik: “Direct observation of superlattice minibands with ballistic electron emission microscopy”, 9th Int. Conf. on STM, Hamburg, Germany, 21. - 25.7.1997
26. G.Strasser, C. Rauch, E.Gornik: “Current Transport in Multiple Superlattice Structures”, 8. Conf. on Mod. Semicond. Struct. (MSS8) , Santa Barbara, USA 14-17.7.1997
27. J.Smoliner, C. Eder, G. Strasser, E.Gornik: “Ballistic electron emission microscopy on quantum wires”, Proc. HCIS10, Berlin, Germany 1997
28. K. Unterrainer, R. Kersting, J.N. Heyman, G. Strasser, K. D. Maranowski, A.C. Gossard: “Few-Cycle THz Emission from Intersubband Plasmon Oscillation in Parabolic Wells”, *8. Conf. on Mod. Semicond. Struct. (MSS8)* , Santa Barbara, USA, 14-18.7.1997
29. C. Rauch, G. Strasser, K. Unterrainer, E. Gornik: “Ballistic electron Devices”, *International workshop on periodic potentials*, Les Houches, France (1997)
30. P.O. Kellermann, N. Finger, A. Golshani, A. Köck, W. Schrenk, E. Gornik, H.-P. Gauggel, R. Winterhoff und M.H. Pilkuhn: “Monomodige oberflächenemittierende Laserdioden im sichtbaren Bereich” (Poster*), Jahrestagung Österreichische Physikalische Gesellschaft*, 22.-26.9.1997, Wien
31. A. Golshani, N. Finger, P.O. Kellermann, A. Köck, W. Schrenk, E. Gornik, L. Korte: “Oberflächenemittierendes monomodiges Halbleiterlaserarray basierend auf Oberflächenmodenkopplung”, *Jahrestagung Österreichische Physikalische Gesellschaft*, 22.-26.9.1997, Wien
32. A. Golshani, P.O. Kellermann, A. Köck, E. Gornik, L. Korte: “Five-wavelength surface emitting laser diode array based on postgrowth adjustment of Surface Mode

Emission", *IEEE/LEOS 1997 Summer Topicals*, 11.-15.8.1997, Montreal, Quebec, Canada

33. A. Golshani, P.O. Kellermann, A. Köck, E. Gornik, L. Korte: "12-Wavelength Array of Single Mode Surface Emitting Laser Diodes Based on Surface Mode Emission", *CLEO´97*, Optical Society of America: 1997 Conference on Lasers and Electro-Optics, 18.-23.5.1997, Baltimore USA
34. A. Köck, A. Golshani, R. Hainberger, P.O. Kellermann, E. Gornik, L. Korte: "Oberflächenemittierende Laserdioden für WDM-Anwendungen", *Fortbildungsseminar der Gesellschaft für Mikroelektronik GMe "Grundlagen und Technologie elektronischer Bauelemente",* 19.-22.3.1997, Großarl
35. E. Burian, D. Pogany, T. Lalinsý, N. Seliger and E. Gornik: "Thermal Simulation and Characterization of GaAs Micromachined Power Sensor Microsystems", Eurosensors XI, Warsaw (1997).
36. N. Seliger, D. Pogany, C. Fürböck, P. Habas, E. Gornik and M. Stoisiek: "A Laser Beam Method for Evaluation of Thermal Time Constant in Smart Power Devices", *Proc. of ESREF Conf.*, Microelectr. and Reliab., Vol. 37, No. 10/11, pp. 1727 (1997)
37. C. Fürböck, R. Thalhammer, N. Seliger, D. Pogany, G. Deboy, G. Wachuta, E. Gornik: "Lokale Temperaturbestimmungen in Insulated Gate Bipolar Transistoren (IGBTs) mittels Laserdiodentechnik", *Informationstagung Mikroelektronik* (1997)
38. N. Seliger, D. Pogany, C. Fürböck, P. Habas, E. Gornik and M. Stoisiek: "A Study of Temperature Distribution in SOI-Smart Power Devices in Transient Conditions by Optical Interferometry", *Proc. of ESSDERC*, p. 512, Stuttgart (1997).
39. D. Pogany, C, Fürböck, N. Seliger, P. Habas, E. Gornik, S. Kubicek and S. Decoutere: "Optical testing of submicron-technology MOSFETs and bipolar transistors", *Proc. of ESSDERC*, p. 372, Stuttgart (1997)
40. N. Seliger, C. Fürböck, P. Habas, D. Pogany, and E. Gornik: "Backside-Laserprober Technique for Characterisation of Semiconductor Power Devices", *Proceedings of the Seminar "Basics and Technology of Electronic Devices"*, Großarl, Austria, March 1997, pp. 143-147
41. N. Seliger: "Charakterisierung von Halbleiterbauelementen mittels Laserinterferometrie", Seminar am Lehrstuhl für Technische Elektrophysik, TU München, 10.11.1997.
42. N.Seliger, C. Fürböck, P. Habaš, D. Pogany, and E. Gornik: "Backside-Laserprober Technique for Characterisation of Semiconductor Power Devices", *Seminar "Basics and Technology of Electronic Devices",* Großarl, Austria, 1997.
43. N. Seliger, D. Pogany, C. Fürböck, E. Gornik, M. Stoisiek: "Zeitaufgelöste Messung der Temperaturverteilung und der Ladungsträgerdichten in Silicon-On-Insulator Leistungsbauelementen mittels Laserinterferometrie", *47. ÖPG Jahrestagung*, (1997)
44. C. Fürböck, R. Thalhammer, N. Seliger, G. Deboy, G. Wachuta und E. Gornik: "Lokale Temperaturbestimmung in IGBTs mittels Lasersondentechnik", *47. ÖPG Jahrestagung*, (1997)

45. K. Unterrainer, B.J. Keay, M.C. Wanke, S.J. Allen, D. Leonard, G. Medeiros-Ribeiro, U. Bhattacharya, M.J.W. Rodwell: “Observation of Shapiro steps and direct evidence of Bloch oscillations in semiconductor superlattices”, *Inst. Phys. Conf.Ser.* **155**, 729 (1997)
46. P. Habas: “Analytical Model and Qualitative Analysis of the Interface-Trap Charge Pumping Characteristics of MOS Structure”, *Proc. of 21st Int. Conf. on Microelectronics (MIEL)*, Nils(YU), Sept. 1997
47. P. Habas, G. Groeseneken, G. Van den Bosch: “Geometric Current Component in Charge-Pumping Measurements”, *Proc. of 21st Int. Conf. on Microelectronics (MIEL)*, Nils (YU), Sept. 1997
48. P. Habas, G. Groeseneken, G. Van den Bosch, H.E. Maes, and E. Gornik: “Detailed Study of the Parasitic Geometric Current Component in Charge Pumping Measurements: Determination of Relevant Parameters”, *Proc. of Semiconductor Interface Specialists Conf.*, Charleston (USA), (1997)
49. P. Habas, I. De Wolf, G. Groeseneken, A. Stesmans and H.E. Maes: “Analysis of Charge Pumping Characteristics of Single Interface Traps*”, Proc. of Semiconductor Interface Specialists Conf.*, Charleston (USA) (1997)
50. A. Golshani, E. Gornik and L. Korte: “Single Mode Surface Emitting Laser Diodes based on Surface Mode Emission”, June, at *Swiss Federal Institute of Technology (EPFL)*, Lausanne, Swiss (1997)
51. A. Golshani, E. Gornik and L. Korte: “Single Mode Surface Emitting Laser Diodes based on Surface Mode Emission”, *19. Aug; Harvard University*, Boston, USA (1997)
52. A. Golshani, E. Gornik and L. Korte: “Surface Mode Emission based Single Mode Surface Emitting Laser Diodes; Low Cost Alternatives for WDM-Systems”, 17. April*, University of British Columbia*, Vancouver, Canada (1997)
53. T. Maier, A. Golshani, P.O. Kellermann, N. Finger, A. Köck, E. Gornik: “Ein Array von Oberflächenmode-emittierenden Laserdioden mit unterschiedlichen Wellenlängen”, Informationstagung Mikroelektronik 1997, Wien (1997)
54. K. Unterrainer: “Inverse Bloch oscillator”, *Workshop on “Atoms and Electrons in Periodic and Quasiperiodic Potentials”,* Les Houches, 27-31 January 1997
55. K.Unterrainer, R. Kersting, J.N. Heyman, G. Strasser, K.D. Maranowski, A.C. Gossard: “Few-cycle THz emission from Intersubband plasmon oscillation in parabolic wells”, *8th Int. Conf. on Modulated Semiconductor Structures*, 14.-18.7.1997, Santa Barbara, USA
56. J.N. Heyman, R. Kersting, G. Strasser, K. Maranowski, A.C. Gossard, K. Unterrainer: “THz time-domain spectroscopy of intersubband plasmons”, *Proceedings of the Fourth International Workshop on Intersubband Transitions in Quantum Wells*, Tainan, Taiwan, December 15th-18th, 1997
57. R. Kersting: “Konjugierte Polymere: ultraschnelle Relaxations- und Transportprozesse”, 10. Jan. 1997, *Universität Dortmund*, Germany.

58. R. Kersting, K. Unterrainer, G. Strasser, and E. Gornik: “Coherent few-cycle THz emission of cold plasmons”, *Quantum Electronics and Laser Science Conference*, QELS´97, 21. May 1997, Baltimore, USA.
59. R. Kersting, K. Unterrainer, G. Strasser, and E. Gornik: “Coherent few-cycle THz emission from Plasmons in bulk GaAs”, *International Conference on Nonequilibrium Carrier Dynamics in Semiconductors*, 19. July 1997, Berlin, Germany.
60. R. Kersting: “Ultrafast dynamics of excitons in conjugated polymers”, *Femtochemistry 98*, 3. September 97, Lund, Sweden.
61. R. Kersting: “Plasma oscillations: emission and absoption of THz pulses”, 10. Sept. 1997, *Toshiba Cambridge Research Corporation*, Cambridge, UK.
62. E. Gornik, N. Seliger, C. Fürböck, D. Pogany: “Charakterisierung von Halbleiterbauelementen mittlels einer Lasersondentechnik”, *SIEMENS Villach*, 4.4.1997
63. E. Gornik, N. Seliger, C. Fürböck, D. Pogany , P. Habas: “Characterisation of Semiconductor Devices by a Backside-Laserprober Technique”, *IMEC*, Leuven, April 1997
64. D. Pogany, E. Gornik, N. Seliger, C. Fürböck: “Characterisation of Semiconductor Devices by a Backside-Laserprober Technique”, *CNET (France Telecom)*, Lyon, April 1997
65. E. Gornik, D. Pogany, N. Seliger, C. Fürböck: “Charakterisierung von Halbleiterbauelementen”, Austria Mikro Systeme (AMS), Unterpremstätten, 17.11.1997

Patents

1. M. Stoisiek, N. Seliger, E. Gornik, Meßgerät zur Temperaturmessung, Patent-anmeldung

Doctor’s Theses

1. W. Boxleitner, Bandstruktur und Ballistischer Transport in Halbleiter-Heterostrukturen, TU Wien, 1997
2. C. Eder, Rastertunnelmikroskopie an Halbleiter-Nanostrukturen, TU Wien, 1997
3. A. Golshani, Fabrication of Steerable Single Mode Surface Emitting Laser Diodes Based on Surface Mode Emission, TU Wien, 1997

Habilitations

1. G. Hobler, Physikalische Modellierung der Ionenimplantation in Silizium
2. A. Köck, Development of New Single Mode Surface Emitting Laser Diodes
3. J. Smoliner, Current transport in Nanostructures

Cooperations

1. Universität Graz, Institut für Experimentalphysik, Prof. F. Aussenegg
2. Universität Innsbruck, Inst. F. Experimentalphysik, Mag. Fischler, N. Hecker
3. Universität Linz, Prof. M. Helm
4. Siemens AG Villach/München: Dr. Prybil, Dr. Stecher, Dr. Kerber, Dr. Werner, Dr. B. Borchert , Dr. L. Korte, Prof. E. Wolfgang, Dr.M. Stoisiek, Dr. G. Deboy, Dr. G. Sölkner; Dr. S. Görlich
5. Plansee AG, Reutte, Dr. Willhartitz
6. Walter Schottky Institut, TU-München, Dr. W. Wegscheidler, Deutschland
7. Technische Universität Berlin, Dr. A. Wacker, Deutschland,
8. TU München, Lehrstuhl für Techn. Elektrophysik, Prof. G. Wachutka, Deutschland
9. Universität Bremen, Inst. für Festkörperphysik, Prof. Dr. D. Hommel,Deutschland
10. Universität Stuttgart, 4. Physikalisches Institut, Prof. Dr. M.H. Pilkuhn, Deutschland
11. RWTH Aachen, Inst. f. Halbleiterelektronik, Prof. H. Kurz, Deutschland
12. Mütek Infrared Laser Systems, Dr. H. Wachernig, Germany
13. Centre National de la Recherche Scientific, Laboratoire de Microstructures
14. et de Microelectronique, B.Etienne, Cedex, France
15. Thomson-CSF Laboratoire Central de Recherches, Orsay , Dr. Sirtori, Dr. Corbin,France
16. Universite Paris Sud, Prof. F. Julien, France
17. Interuniversity Microelectronics Center (IMEC), Leuven, Belgium
18. Ioffe Physico-Technical Institute, St. Petersburg, Prof. Y. Ivanov, Rußland
19. Norwegian University of Science and Technology, Prof. K. Fossheim, Norwegen
20. Sub-Micron Center, Weizmann Institute, Rehovot, Prof. M. Heiblum, Israel
21. Univ. of California, Lawrence Berkeley Laboratories, Prof. E. E. Haller , USA
22. University of California Santa Barbara, Free-Electron-Laser, Prof. J. Allen, USA
23. University of California Santa Barbara, Materials Department, Prof. A. Gossard, USA
24. Boston College, Dep. of Physics, Boston, Massachusetts, Prof. K.Kempa, USA
25. EPI MBE Components, St. Paul, Minnesota, USA
26. Pontificia Universidade Catolica de Rio de Janeiro, Prof. de Souza, Brazil
27. Herriot Watt University, Edinburgh, Prof. C. Pidgeon, GB
28. Univ. Nottingham, Prof. M. Chamberlain, GB
29. INFM-SNS Pisa, Prof. F. Beltram, Italy
30. Technische Universität Delft, Faculty of Applied Physics, Pof. Wenckebach,NL
31. University Neuchatel, Prof. J. Faist, Swiss

32. Orbisphere Semiconductor Lasers, Swiss
33. Department of Physics, Slovak Academy of sciences, Dr. Thurzo (Slovakia)
34. Department of Microelectronics, Faculty of electrical engineering and information technology STU, Prof. Csabay (Slovakia)
35. Institute National des Sciences Appliques de Lyon, Villeurbanne, France
36. Institute of Electrical Engineering, Slovak Academy of Sciences,
37. Bratislava, Slovakia

Epitaxial Layers:

TU Wien:
Institut für Angewandte u. Technische Physik
Prof. Ebel (AlGaAs layers)
Doz. Schattschneider (GaAs on SiO_2)
Doz. Pongratz (Heterostruktures, metallic superlattices)
Atominstitut der österreichischen Universitäten
Prof. Harald Weber
Institut für Analytische Chemie
Prof. Robert Kellner

Universität Wien:
Institut für Physikalische Chemie
Prof. Kauffmann (LTGaAs for high-speed spektroskopy)

Universität Innsbruck:
Institut für Experimentalphysik
Doz. Seidenbusch (Heterostruktures, detectors)

Universität Linz:
Institut für Halbleiterphysik
Prof. Günter Bauer
Doz. Manfred Helm

Universität Leoben
Institut für Physik
Prof. Kuchar (Heterostruktures, 2DEGs)

University of Surrey, UK
Physics Department
Dr. B.N.Murdin

Herriot Watt University, Edinburgh, UK
Prof. C. Pidgeon

Academy of Sciences, Poland
High Pressure Research Center
Prof. Treciakowski (QWs) und Prof. Suski (QW, 2DEGs)

Academy of Sciences, Slowakei
Institut of Physics
Dr. Bartos (DLTS, CV)

Technische Universität Bratislava, Slowakei
Mikroelektronik
Prof. Csabay

Boston College, Boston, Massachusetts, USA
Dep. of Physics
Prof. K.Kempa. Prof. P. Bakshi (FIR emitter)
Prof. D. Broido (SLs)

Georgia State University
Prof. U. Perera (FIR Detectors)

Electron-Beam Lithography for Novel Devices

E. Zotl, M. Hauser, G. Strasser, E. Gornik

Institute of Solid State Electronics &
Center of Microstructure Research (MISZ), Techn. Univ. Vienna
A-1040 Vienna, Austria

The goal of this project was the production of a planar Schottky diode with integrated bow-tie antennas. Due to the planar structure of this device it can be easily implemented into integrated circuits, making it attractive for use as a Terahertz detector. Because of the importance of the RC product for high frequency applications one has to minimize the size of the Schottky contact. This can be achieved by electron-beam lithography and a new combination of positive and negative lithography processes, which allows the production of contacts with typical diameters of 100 nm. Furthermore, a first electrical characterization was made.

1. Introduction

Metal-semiconductor junctions are known since the end of the last century [1]. Point-contact diodes have been used for detector- and mixer-applications in the millimeter region for decades. Their parameters strongly depend on the manufacturing process, which causes poor reproducibility.

With the development of new technologies like MBE (molecular beam epitaxy) or evaporation of metals it was possible to increase the quality of the Schottky contacts. Although point-contact diodes are used in various applications, it is desirable to develop planar Schottky-diodes with integrated receiving antennas which can easily be implemented into existing electronics.

If one wants to extend the range of operation of the Schottky diode into the THz range, some problems have to be considered:

- Parasitic capacitance of contact pads and antennas are large;
- Electron beam lithography has to be used instead of optical lithography to define small Schottky contacts ;
- The coupling of the signal to be measured into the planar structure is poor compared to the whisker antenna.

The parasitic capacitance can be reduced by integrating the contact pads into the antennas. By use of electron beam lithography defined airbridges it is possible to reduce the contact areas to dimensions of 100 x 100 nm.

2. Submicron Schottky Diodes

2.1 Fabrication

A new processing technology for the fabrication of planar terahertz diodes has been developed utilizing electron-beam lithography and trench isolation. The major processing steps are summarized in Fig. 1.

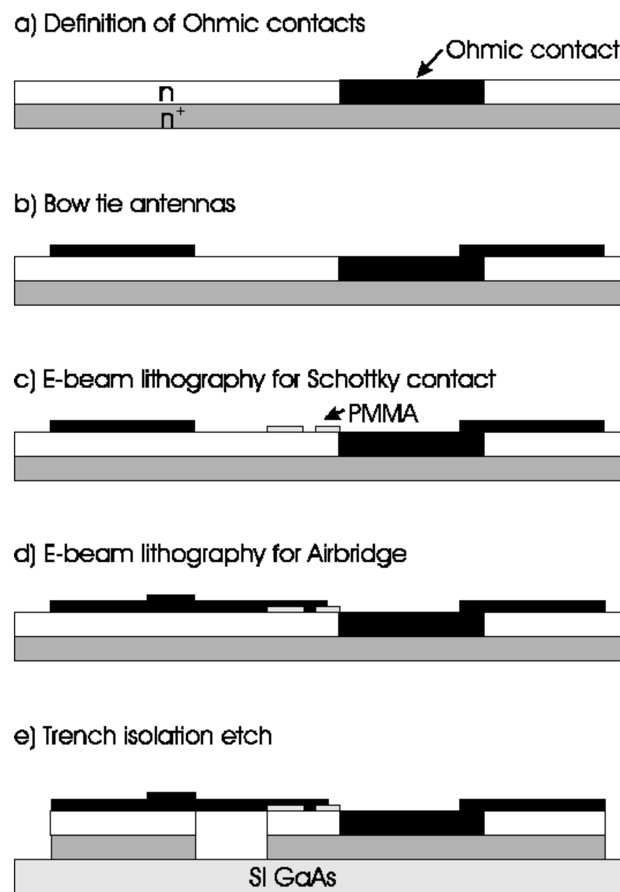

Fig. 1: Fabrication process of the submicron Schottky diode.

The first step was the evaporation of Ni/Ge/Au ohmic metal on the surface of the etched n+-layer surrounding the active area. The bow tie antennas were defined by conventional photolithography. In the next step, a narrow line (200 nm) was defined in the active region of the diode by electron beam lithography (EBL) in a positive process. After that it was necessary to irradiate the region surrounding the narrow line with an electron dose high enough to crosslink the macromolecules of the resist. This is needed for the isolation between the airbridge and the n-layer. Definition of the airbridge by EBL and evaporation of gold followed. The bow tie antennas were finally isolated by a deep trench etching down to the semi-insulating substrate. Scanning electron microscope pictures of the fabricated device and the Schottky contact are shown in Fig. 2 and Fig. 3.

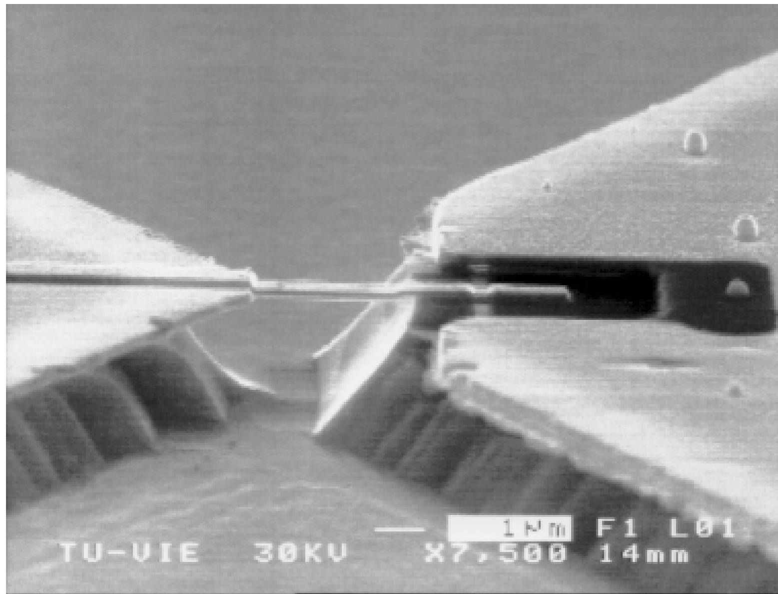

Fig. 2: SEM picture of the device including the airbridge and the Schottky contact.

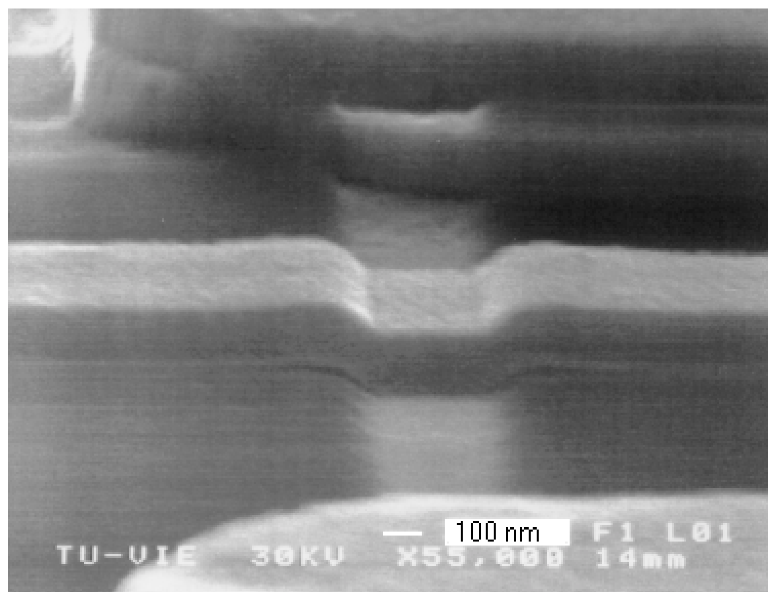

Fig. 3: SEM picture of the Schottky contact.

2.2 Measurements

The measurement of the I-V-curve (see Fig. 4) of the Schottky diode allowed the extraction of important parameters regarding the estimation of the working frequency of this device. The series resistance of the diode was found to be 150 Ohm.

The capacity of the Schottky contact can be calculated from the contact area and the width of the depletion region [2]. From a contact area of 200 nm x 250 nm follows a capacity of 1 fF, which results in a cut-off frequency of 11 THz.

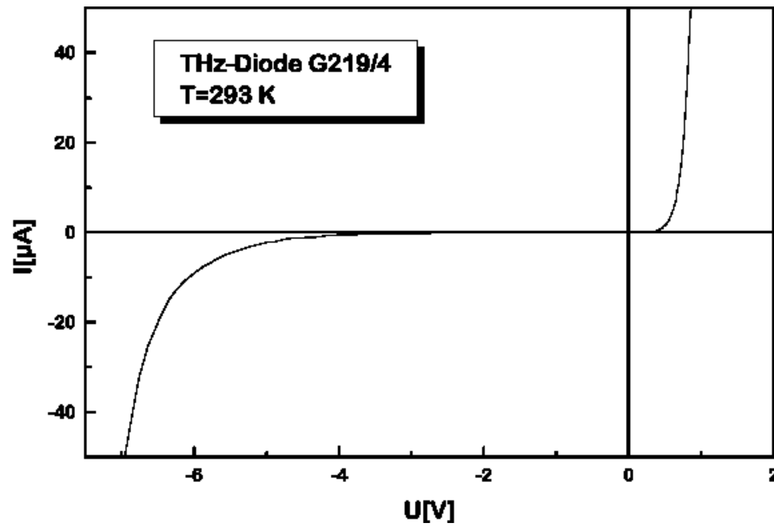

Fig. 4: I-V-curve of the Schottky diode.

3. Conclusion

A planar Schottky diode with integrated bow-tie antennas was fabricated. The process which was used for this device does not use ion implantation but etching techniques, simplifying the fabrication process drastically. First DC-measurements showed that it is possible to use this Schottky diode as a terahertz-detector. Measurements in the far infrared have to be done in the near future.

References

[1] F. Braun: "Über die Stromleitung durch Schwefelmetalle", *Ann. Phys. Chem.*, 153, 1874, pp. 556.

[2] J.T. Louhi: "Dynamic Shape of the Depletion Layer of a Submillimeter-Wave Schottky Varactor", *IEEE Trans. Microwave Theory Tech.*, 44, 1996, pp 2159

Project Information

Project Manager

Dr. Markus HAUSER

Institut für Festkörperelektronik, Technische Universität Wien

Project Group

Last Name	First Name	Status	Remarks
Kersting	Roland	postdoc	
Prinzinger	Johannes	technician	
Strasser	Gottfried	assistant professor	
Zotl	Ernst	student	

Publications in Reviewed Journals

1. G. Ploner, J. Smoliner, G. Strasser, M.Hauser, E. Gornik: "Energy levels in quantum wires studied by magnetophonon effect", accepted by *Phys. Rev. B*. (1997)

Presentations

1. J. Smoliner, M. Hauser, C. Eder, G. Strasser, E. Gornik: "Quantum dot structures for STM tips", PHASDOMS 97, Aachen, Germany, 1997
2. M. Hauser, E. Zottl, G. Strasser, E. Gornik: "Nanostrukturierte Schottkydioden für den THz Bereich", Österreichische Physikalische Gesellschaft, 47. Jahrestagung, Wien, Austria (9/97)
3. G. Ploner, J. Smoliner, G. Strasser, M. Hauser, E. Gornik: "Charakterisierung von Quantendrähten mittels Magnetophonon Effekt", Österreichische Physikalische Gesellschaft, 47. Jahrestagung, Wien, Austria (9/97)

Novel Single-Mode Emission Laser Diodes Based on Surface-Mode Coupling

N. Finger[1], A. Golshani, P.O. Kellermann, A. Köck, E. Gornik

Institute of Solid State Electronics &
Center of Microstructure Research (MISZ), Techn. Univ. Vienna
A-1040 Vienna, Austria

We present novel laser diode devices based on the surface-mode-emission (SME) concept. An array of single-mode and single-beam surface emitting laser diodes was realized. The emission wavelengths of the individual laser diodes were controlled by a postgrowth adjustment of the surface structure. The resulting average wavelength spacing is 1.1 nm with a deviation of 0.13 nm. The side mode suppression ratio (SMSR) was measured to be 20 dB in the best case. A beam-steering device based on a SME-laser diode is presented, which is capable of steering digitally a single, surface emitted beam with a divergence of 0.2° and a steering-range of 4.9°. The beam steering is achieved by a thermal mode-switching between two single-mode emission wavelengths. A single-mode visible red GaInP/AlGaInP laser diode with a side mode suppression of 19 dB was realized. A theory based on a Floquet-Bloch expansion was developed to investigate the underlying waveguide structures of SME laser diodes numerically.

1. Introduction

Semiconductor laser diodes have an important impact in the area of light wave transmission systems for optical telecommunication. In order to achieve high data transmission rates single-mode lasers are required to build up high-speed data highways using Wavelength-Division-Multiplexing (WDM). Various types of single-mode laser diodes like distributed-feedback (DFB) lasers, distributed-Bragg-reflector (DBR) lasers, coupled-cavity lasers and vertical-cavity-surface-emitting lasers (VCSELs) have been realized so far. Today most commonly DFB lasers are used for the purpose of optical telecommunication [1], [2].

Beam steering devices are expected to have many novel applications in future free-space optical communication systems like free-space communication between satellites, optical data storage and data reading and future optical computers [3], [4]. Incorporating the steering mechanism within the laser diode is the most efficient approach. Edge emitting [5], [6] as well as surface emitting [7], [8] laser diode beam steering devices have already been realized.

Semiconductor single-mode laser diodes in the visible regime are very suitable to be employed as light sources in the next generation optical disk drives because of their ability of reading and writing highly condensed optical information [9].

The surface-mode-emission (SME) concept, which was successfully applied to realize single-mode and single-beam surface emitting diode lasers [10], [11], was exploited to

---

[1] Electronic mail: nfinger@fkeserver.fke.tuwien.ac.at

realize a variety of optoelectronic devices: A novel device for WDM applications with postgrowth wavelength adjustment was realized. The SME technique was also used to make a laser diode beam-steering device. Furthermore, a single-mode and single-beam surface emitting visible red laser diode is presented. Hence the proposed flexibility of the SME-concept is proved. In order to improve the design of the SME-laser diodes a theory was developed to perform device simulation as far as the optical properties are concerned.

2. Experimental

2.1 Five-Wavelength Surface Emitting Laser Diode Array

We report on a five-wavelength surface emitting laser diode array achieved from monolithically integrated SME laser diodes [12]. The array consists of 15 laser diodes divided into five groups. The laser diodes of each group are assigned to emit the same wavelength. Each group emits at a different wavelength by a postgrowth-adjustment of the thickness of the surface waveguides. The emitted wavelengths vary from 867.92 nm to 872.67 nm and the average wavelength spacing is 1.1 nm with a wavelength deviation within the groups of 0.13 nm.

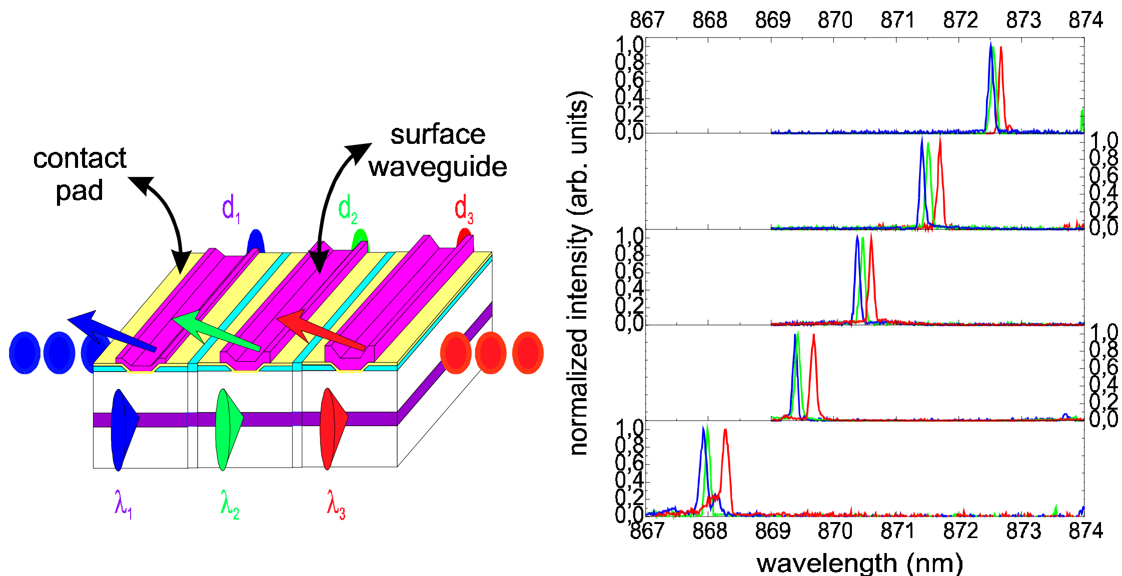

Fig. 1: Left: Schematic structure of the SME diode laser array. The thickness of the surface waveguide is slightly different on each laser diode group which leads to emission of different wavelengths. Right: Spectra of the array elements from first group (bottom layer) to fifth group (top layer). The waveguide thickness decreases from the first group to the fifth group.

The samples are MOCVD-grown GaAs/AlGaAs double heterostructure diode lasers consisting of an n-$Al_{0.35}Ga_{0.65}As$ cladding layer grown on an n-GaAs substrate followed by the GaAs active region (90 nm thick) and the 550 nm thick p-$Al_{0.3}Ga_{0.7}As$ top cladding layer. The crucial difference to conventional diode lasers is a surface-relief grating (period $\Lambda = 415$ nm, 100 nm deep) etched by ion-milling covered with a semitransparent

AuZnAu film (thickness 5/5/20 nm) and a spin coated photoresist layer (AZ6615; d ~ 300 nm) forming a surface waveguide (schematic drawing: see Fig. 1 left).

The single mode surface emission is a consequence of the excitation of the TE_0 surface-mode in the surface waveguide: The laser light in the active region couples via one grating vector $k_g = 2\pi/\Lambda$ to the TE_0 mode. The excited TE_0 surface mode either couples back into the laser structure, thus providing an active feedback resulting in single-mode operation, or decays via one grating vector into the air as the surface emission. By thinning the surface waveguide the dispersion relation of the TE_0 shifts, resulting in a shift of the emission wavelength towards longer wavelengths.

On the laser array the surface waveguide thicknesses of all laser diodes were thinned to ~ 255 nm by low power plasma ashering for single mode emission around 868 nm. Then the waveguide thicknesses of the distinct laser groups were adjusted by low power plasma ashering resulting in thickness differences of 2.2 nm between the groups.

Fig. 1 shows the measured emission spectra of the array. The samples were driven under pulsed conditions with the same current and duty cycle (pulse width = 0.5 µs; frequency = 30 kHz). The typical threshold current density is 1.8 ±6% kA/cm^2 over the array. Every laser diode shows single mode operation with a side mode suppression ratio (SMSR) of about 20 dB in the best case. The average full width at half maximum (FWHM) was measured to be 0.08 nm. The total emitted power of one individual laser is about 35 mW. About 20% of the power is emitted into a single surface beam with a FWHM of 0.12°. Single mode emission is achieved at a current of $1.1 \times I_{th}$ retaining up to $1.4 \times I_{th}$. The wavelength spacing between laser diode groups is 1.1 nm in average and the average deviation within each group is 0.13 nm.

2.2 Digital Beam Steering from SME Laser Diodes

We present a GaAs/AlGaAs laser diode beam steering device based on a single-mode SME-laser diode [13]. The temperature-dependence near room-temperature of the emitted wavelength of the SME laser diode was investigated: At temperatures below 285 K the mode near 871 nm is emitted. Heating the sample results in a red-shift with a rate of 0.07 nm/K, which is actually less then the rate of 0.09 nm/K for DFB lasers. After the temperature is raised to 286 K the mode near 878 nm is preferred. The emitted wavelength continues to shift towards longer wavelengths at the same rate as before. Thus a bistable operation of the laser diode can be achieved adjusting the temperature of the sample.

Since the angle of the surface emission $\alpha = \arcsin(n_{eff} \cdot 2\lambda/\Lambda)$ ($n_{eff} = 3.39$ is the effective refractive index of the laser structure and Λ is the grating period) depends on the wavelength λ, a switching between different wavelengths yields a switching between different angles. Driving the laser diode with short current-pulses (I = 270 mA, pulse width $D_p = 0.2$ µs) results in a single-mode and single-beam emission at $\lambda_1 = 874.13$ nm and $\alpha_1 = 58.5°$. Applying longer pulses (I = 215 mA, pulse width $D_p = 4$ µs) leads to a heating of the sample and results in an emission at $\lambda_2 = 874.13$ nm and $\alpha_2 = 63.4°$ (see Fig. 2). The beam divergence is in both cases 0.2°. Driving the laser diode with double pulse sequences yields the desired mode switching and the digital beam steering between α_1 and α_2 with a steering range of 4.9°. As the mode switching is based on thermal effects, the maximum frequency of applying double pulses is limited to 0.15 MHz.

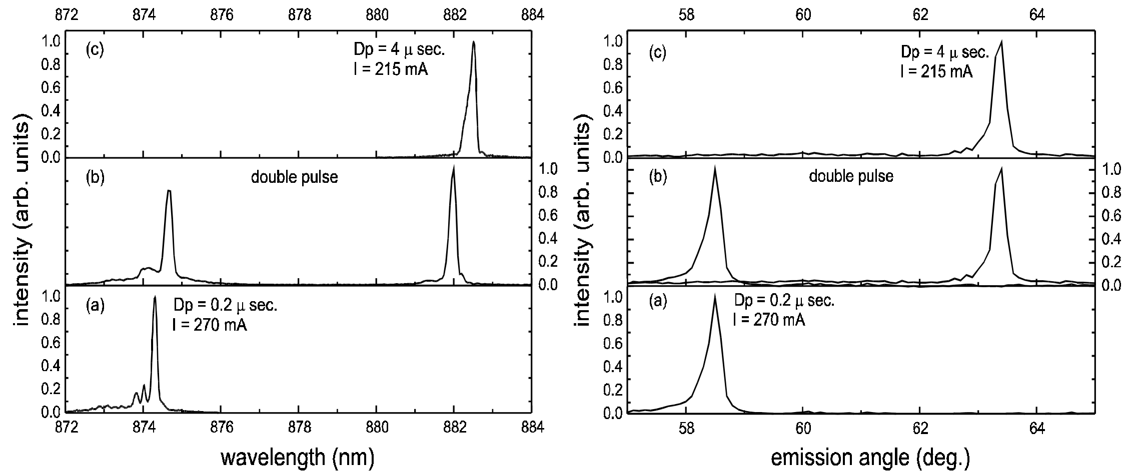

Fig. 2: Short-pulse operation of the device results in single-mode and single-beam operation at λ_1 = 874.13 nm and α_1 = 58.5° (a). Long-pulse operation yields emission at λ_2 = 874.13 nm and α_2 = 63.4° (c). Double pulses yield mode-switching and thus digital beam-steering (b).

2.3 SME Laser Diodes in the Visible Regime

The SME technique was successfully applied in the visible red wavelength regime to achieve single-mode emission in AC and in DC operation as well as single-beam emission via the surface [14]. The devices realized in this work are MOVPE-grown compressively strained double-quantum well GaInP/AlGaInP laser diodes. The asymmetric cladding layers (by the aspect of thickness and refractive index) are designed to shift the distribution of the optical field towards the surface to achieve a sufficient coupling between the laser light and the TE_0-surface mode. The first order grating for surface mode coupling (grating period = 328 nm, height = 100 nm) was etched into the top cladding layer (thickness 400 nm) using ion milling. The surface-waveguide structure is formed by a semitransparent AuZnAu film (5/5/20 nm thick) and a spin-coated photoresist (AZ6615) slab waveguide (schematic sample structure: see Fig. 3 left).

The SME laser diodes have threshold current densities between 1.4 kA/cm^2 for AC- and 1.9 kA/cm^2 for DC-operation. Single mode emission is achieved both in AC- and DC-operation with a side mode suppression of 19 dB in the best case. Fig. 3 shows single-mode emission spectra for AC- and DC-operation: The emitted wavelengths are λ = 675.17 nm (driving current $I = 1.2\times I_{th}$, f = 16.6 kHz, pulse width w_p = 4 μs) with a FWHM of 0.08 nm for AC- and λ = 679.79 nm (driving current $I = 1.1\times I_{th}$, FWHM = 0.07 nm) for DC-operation. The farfield of the single-beam surface emission has a beam divergence of 0.16° in the y-direction. Presently a power of 2 % (0.14 mW) of the whole light power (7 mW at $I = 1.7\times I_{th}$) is emitted via the surface.

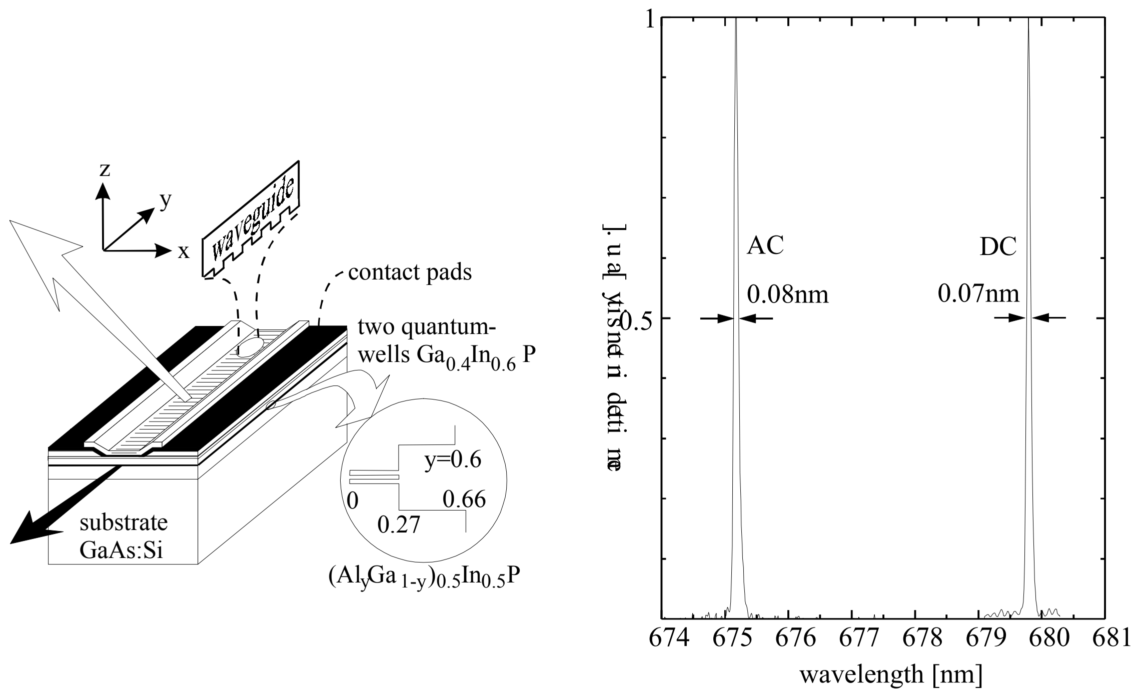

Fig. 3: Left: Schematic sample structure of the SME-laser diode. Right: Single-mode emission spectra for AC-operation ($I = 1.2\times I_{th}$, $f = 16.6$ kHz, $w_p = 4$ µs) and DC-operation ($I = 1.1\times I_{th}$).

3. Theory

In order to understand the coupling mechanisms within SME laser structures profoundly, the underlying waveguide structure (i.e. metallized surface-relief grating coupled waveguides) was investigated numerically. The analysis is based on a Floquet-Bloch expansion of the optical field [15]. Propagation constants and optical field distributions can now be calculated without a priori assumptions. In a further step coupling coefficients are extracted from the Floquet-modes providing the possibility of device-simulation using coupled mode theory. Longitudinal mode spectra and the radiation characteristics of SME lasers are calculated.

Fig. 4 shows the results for a SME laser structure based on a GaAs/AlGaAs-double-hetero-laser structure (sample W688): The tooth-shaped coupling-grating (period = 535 nm, height = 100 nm, duty cycle = 0.5), covered with a 30 nm thick Au-film, is followed by a SiO/SiN-surface waveguide (100 nm/425 nm thick). The cavity is taken to be 500 µm long with as cleaved facets. The longitudinal mode spectrum (threshold-gain vs. wavelength) and the radiation properties show a resonant behavior around 875 nm (TE_0 resonance). The plotted output powers via the facets, via the surface and into the substrate are normalized with respect to the power generated in the active region by stimulated emission. The total waveguide losses decrease in case of TE_0 resonance due to a reduction of the radiation losses into the substrate because a supermode of the twin-waveguide-system (laser-waveguide, surface-waveguide) is excited. On the contrary, the desired radiation losses via the surface increase due to an efficient coupling between the TE_0 surface-mode and the radiation field emitting into the air.

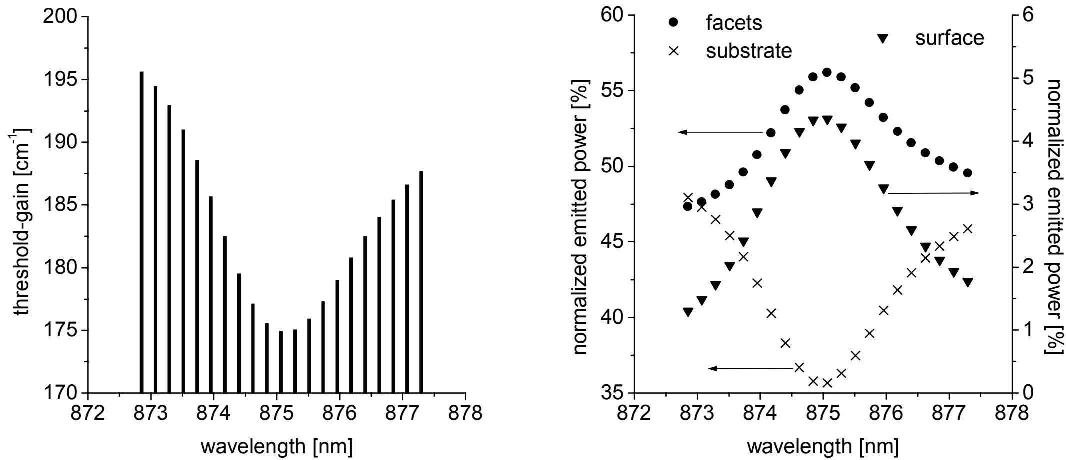

Fig. 4: Left: Calculated longitudinal mode spectrum. Right: Calculated output-powers, normalized with respect to the power generated by stimulated emission. The TE_0-resonance occurs at 875 nm.

4. Conclusion

Compared to DFB laser diodes the SME laser concept has various advantages. No regrowth processes are required and the device fabrication is simple and very flexible. Especially for WDM applications the possibility of post-growth wavelength adjustment makes the SME concept very suitable because monolithically integrated devices can be fabricated easily.

The major problem to be solved is the poor side mode suppression under high-injection conditions. To overcome this problem narrow index-guided laser structures have to be made to avoid the excitation of higher lateral modes. Recent calculations showed that a dramatic improvement of the wavelength-filter characteristics of the laser structure can be achieved by using contradirectional surface-mode-coupling instead of codirectional coupling. By changing the type of coupling the spectral linewidth of the surface-mode resonances can be decreased by one order of magnitude, which will result in a significant increase of the SMSR.

In the visible wavelength regime (especially for green and blue laser diodes) the SME concept has to be preferred rather than the DFB concept to achieve single-mode laser diodes. DFB laser diodes demand gratings with extremely small periods (100 nm and less), which would cause complicated and thus expensive device-processing (e-beam-lithography). SME lasers require longer grating-periods which can be processed easily using optical lithography.

Acknowledgments

This work was also sponsored by the Stiftung Volkswagen, Hannover, Germany.

References

[1] J. Buus: “Single Frequency Semiconductor Lasers”, Tutorial texts in optical engineering, Vol. TT5, *SPIE Optical Engineering Press* (1991)

[2] T. Ikegama: in “Optoelectronic Technology and Lightwave Communications Systems”, edited by C. Lin, *Van Nostrand Reinhold*, New York (1989)

[3] J.A. Neff: *Opt. Eng. 26*, 2 (1987)

[4] A. Hartmann, S. Redfield: *Opt. Eng. 28*, 315 (1989)

[5] D.R. Scifres, W. Streifer, R.D. Burnham: *Appl. Phys. Lett.* 33, 616 (1978)

[6] Y. Sun, C.G. Fanning, S.A. Biellak, A.E. Siegman: *IEEE Phot. Technol. Lett. 7(1),* 26 (1995)

[7] Y. Kan, Y. Honda, I. Suemune, M. Yamanishi: *Electron. Lett. 22*, 1311 (1986)

[8] N.W. Carlson et al.: *Appl. Phys. Lett. 53*, 2275 (1988)

[9] A.E. Bell: “Next-generation compact discs”, *Scientific American (International Edition)*, July 1996, vol.275, (no.1):28-32

[10] A. Golshani, A. Köck, S. Freisleben, C. Gmachl, E. Gornik, L. Korte, “Adjustable surface emission from AlGaAs/GaAs-laser diodes based on first-order-grating-coupled surface mode emission”, *Appl. Phys. Lett. 69 (16),* 2312 (1996)

[11] A. Köck, A. Golshani, R. Hainberger, E. Gornik, L. Korte, “Single-mode and single-beam emission from surface-emitting laser diodes based on surface mode emission”, *Appl. Phys. Lett. 69 (24)*, 3638 (1996)

[12] A. Golshani, P.O. Kellermann, A. Köck, E. Gornik, L. Korte: “Five-Wavelength Surface Emitting Laser Diode Array Based on Post Growth Adjustment of Emission Wavelength”, *Appl. Phys. Lett.*, 71, 762 (1997)

[13] A. Köck, A. Golshani, R. Hainberger, E. Gornik, L. Korte: “Digital beam-steering from surface emitting laser diodes based on surface mode emission”, *SPIE Proceedings Series,* 3001 “In-plain semiconductor lasers: from Ultraviolet to Mid-Infrared”, p.192, OE/LaSE’97, USA, *SPIE Optical Engineering Press* (1997)

[14] P.O. Kellermann, A. Golshani, A. Köck, E. Gornik, H.P. Gauggel, R. Winterhoff, J. Pilkuhn: “Single-Mode and Single-Beam Surface Emission from Visible Red GaInP/AlGaInP Laser Diodes”, *Appl. Phys. Lett. 70*, 2374 (1997)

[15] R.J. Noll, S.H. Macomber, “Analysis of Grating Surface Emitting Lasers*”, IEEE J. Quantum Electron. vol. QE-26*, pp.456-466, 1990

Project Information

Project Manager

Dr. Anton Köck

Institut für Festkörperelektronik, Technische Universität Wien

Project Group

Last Name	**First Name**	**Status**	Remarks
Finger	Norman	dissertation	
Golshani	Alireza	dissertation	
Gornik	Erich	Full Prof.	
Haider	Manfred	student	
Kellermann	Peer Oliver	dissertation	
Köck	Anton	Assistant Prof.	
Maier	Thomas	dissertation	
Schrenk	Werner	dissertation	
Smola	Winfried	student	
Socher	Michael	student	

Publications in Reviewed Journals

1. P.O. Kellermann, A. Golshani, A. Köck, E. Gornik, H.-P. Gauggel, R. Winterhoff, M.H. Pilkuhn: “Single-mode and single-beam surface emission from visible red GaInP/AlGaInP laser diodes”, Applied Physics Letters Vol. 70 (18), 5.5.1997, USA
2. A. Golshani, P.O. Kellermann, A. Köck, E. Gornik, L. Korte: “Five-wavelength surface emitting laser diode array based on postgrowth adjustment of emission wavelength”, Applied Physics Letters Vol. 71 (6), 11.8.1997, USA
3. A. Köck, A. Golshani, R. Hainberger, E. Gornik, L. Korte: “Digital beam steering from surface-emitting laser diodes based on surface mode emission”. (In-Plane Semiconductor Lasers: from Ultraviolet to Midinfrared, San Jose, CA, USA, 10-13 Feb. 1997). Proceedings of the SPIE - The International Society for Optical *Engineering,* 1997, vol.3001:192-8.

Presentations

1. P.O. Kellermann, N. Finger, A. Golshani, A. Köck, W. Schrenk, E. Gornik, H.P. Gauggel, R. Winterhoff, M.H. Pilkuhn: “Monomodige oberflächenemittierende

Laserdioden im sichtbaren Bereich" (Poster), Jahrestagung 1997 der Österreichischen Physikalischen Gesellschaft, 22.-26.9.1997, Wien

2. A. Golshani, N. Finger, P.O. Kellermann, A. Köck, W. Schrenk, E. Gornik, L. Korte: "Oberflächenemittierendes monomodiges Halbleiterlaserarray basierend auf Oberflächenmodenkopplung" (Poster), Jahrestagung 1997 der Österreichischen Physikalischen Gesellschaft, 22.-26.9.1997, Wien
3. A. Golshani, P.O. Kellermann, A. Köck, E. Gornik, L. Korte: "Five-wavelength surface emitting laser diode array based on postgrowth adjustment of Surface Mode Emission", IEEE/LEOS 1997 Summer Topicals, 11.-15.8.1997, Montreal, Canada
4. A. Golshani, P.O. Kellermann, A. Köck, E. Gornik, L. Korte: "12-Wavelength Array of Single Mode Surface Emitting Laser Diodes Based on Surface Mode Emission" (Poster), CLEO´97, Optical Society of America: 1997 Conference on Lasers and Electro-Optics, 18.-23.5.1997, Baltimore USA
5. A. Köck, A. Golshani, R. Hainberger, P.O. Kellermann, E. Gornik, L. Korte: "Oberflächenemittierende Laserdioden für WDM-Anwendungen" (Vortrag), Fortbildungsseminar der Gesellschaft für Mikroelektronik GMe "Grundlagen und Technologie elektronischer Bauelemente", 19.-22.3.1997, Großarl
6. A. Golshani, E. Gornik and L. Korte: "Single Mode Surface Emitting Laser Diodes based on Surface Mode Emission (SME)" Oral presentation, 20 June; at Swiss Federal Institute of Technology (EPFL) Lausanne, Switzerland (1997)
7. A. Golshani, E. Gornik and L. Korte: "Single Mode Surface Emitting Laser Diodes based on Surface Mode Emission (SME)" Oral presentation, 19. Aug; Harvard University, Boston, USA (1997)
8. A. Golshani, E. Gornik and L. Korte: "Surface Mode Emission based Single Mode Surface Emitting Laser Diodes; Low-Cost Alternatives for WDM-Systems" Oral presentation, 17. April; University of British Columbia, Vancouver, Canada (1997)
9. T. Maier, A. Golshani, P.O. Kellermann, N. Finger, A. Köck, E. Gornik: "Ein Array von Oberflächenmode-emittierenden Laserdioden mit unterschiedlichen Wellenlängen" (Poster), *Informationstagung Mikroelektronik 1997*, Wien (1997)

Doctor's Theses

1. A. Golshani, "Fabrication of Steerable Single Mode Surface Emitting Laser Diodes Based on Surface Mode Emission", TU Wien, 1997

Habilitations

1. A. Köck, "Development of New Single Mode Surface Emitting Laser Diodes", TU-Wien, 1997

Cooperations

1. Universität Stuttgart, 4. Physikalisches Institut, Prof. Dr. M.H. Pilkuhn, Deutschland
2. Universität Bremen, Inst. für Festkörperphysik, Prof. Dr. D. Hommel, Deutschland

3. Siemens AG, Dr. Bernd Borchert und Dr. Lutz Korte
4. Pontificia Universidade Catolica de Rio de Janeiro, Prof. de Souza, Brazil

Magnetotransport in GaAs-AlGaAs Nanostructures

G. Ploner, J. Smoliner, G. Strasser

Institute of Solid State Electronics &
Center of Microstructure Research (MISZ), Techn. Univ. Vienna
A-1040 Vienna, Austria

In this work, magnetophonon resonances in quantum wires were investigated. It was found that magnetophonon resonance measurements can be used as a tool for the characterization of the subband spectrum of quantum wires. The method proves to be particularly useful at low electron densities, when only few subbands are occupied and the standard magnetic depopulation characterization technique can no longer be used. By variation of the electron density in the wires through illumination with a red LED the 1D subband spacing, as determined from magnetophonon resonance measurements, is found to increase with decreasing electron density. In addition, subband energies determined by magnetophonon resonances were found to be systematically higher than the subband spacing obtained from magnetic depopulation measurements on the identical samples. We give an explanation of this observation which indicates that the combination of both transport characterization methods provides information on the actual shape of the underlying confinement potential.

1. Introduction

LO-phonon induced resonant scattering of electrons between Landau levels, also called the magnetophonon (MP) effect, has been widely used to obtain information on band structure parameters such as the effective mass and the electron-LO-phonon interaction in bulk and two-dimensional semiconductors. The magnetophonon effect has proved to be a useful magnetotransport tool for the determination of effective masses and is moreover particularly suitable to carry out investigations of the temperature dependence of m* in a temperature range which is commonly not accessible to other methods such as cyclotron resonance measurements.

In 2D systems such as quantum wells and single heterojunctions the magnetophonon effect has been used not only to measure effective masses of 2D electrons [1], but also to investigate the influence of various scattering mechanisms on the high temperature transport properties of these systems. Evidence has been found that interface phonons are especially effective in the MP resonant scattering in heterostructures and their frequency has been determined [2]. The self consistent consideration of all scattering mechanisms in the calculation of the high temperature magnetoresistance leads to the prediction of the collapse of MP oscillations at high magnetic fields, and excellent agreement between theory and experiment has been obtained [3], [4].

In quasi-one-dimensional electron gases (1DEGs) the investigation of magnetophonon resonances (MPR) is considered as an useful magnetotransport tool for the determination of the energy difference between adjacent 1D subbands arising from the lateral confinement. It can be shown that the lateral quantization leads to a shift of the magnetic field positions of the resonant extrema in the high temperature magnetoresistance. Un-

der certain premises this shift is proportional to the subband spacing E_0 and provides a particularly simple method to determine E_0. This is particularly useful in those cases where, due to a very low electron density or relatively high subband spacing, only a small number (less than, say, four) of subbands is occupied in the quantum wire. In these cases the standard magnetic depopulation (MD) method, commonly used to estimate the subband spacing, is no longer a suitable transport technique for the characterization of quantum wires. The MD method exploits the oscillatory structure in the low temperature magnetoresistance occurring when the magnetoelectric hybrid levels are successively shifted across the Fermi level by increasing the magnetic field. A small number of occupied subbands drastically reduces the oscillatory structure in $R_{xx}(B)$ and thus, the commonly used evaluation methods [5], [6] cannot be applied any more.

2. Experimental

The samples used in this work were conventional modulation doped heterostructures on which arrays of 40 quantum channels were fabricated by laser holography and wet chemical etching. The electron mobility and electron density of the unstructured samples are 1.6×10^6 cm^2/Vs and 1.1×10^{11} cm^{-2}, respectively, at 4.2 K. The measurements of the magnetoresistance were performed using a standard constant current procedure and a cryostat equipped with a variable temperature inset and a superconducting magnet which allowed magnetic field strengths up to 10 T. For measurements at variable electron densities, an array of wires has been fabricated which were completely depleted at 4.2 K due to the low carrier concentration of the underlying heterostructure. This allows to obtain the same set of wires at different electron densities if carriers are generated by illumination using a light emitting diode. After illumination, the samples were slowly heated to temperatures between 100 K and 160 K. When equilibrium, i.e. stable sample resistance, was reached the magnetoresistance was measured showing a distinct structure due to the magnetophonon effect. Subsequent to the high temperature measurement, the samples were cooled down slowly to T = 2 K and a magnetic depopulation (MD) measurement was performed to determine the electron density. Then the temperature cycle was repeated, while further gradual reduction of the carrier density was achieved by maintaining the sample at 180 K for several hours before the next MPR experiment at T near 100 K was performed.

3. Results

Typical data are shown in Fig. 1. As first striking feature, we find a strong dependence of the strength of the observed magnetophonon oscillations on the used sample structure and the preparation process. The effect is most pronounced in samples where the remote impurity scattering is reduced as far as possible by e.g. low doping and large spacer layers. We explain this observation by the fact that all kinds of additional scattering lead to a broadening of the density of states of magnetoelectric hybrid levels in the wires which smears out the MPR oscillations. Since the wet chemical etching, by which the confinement of the wires is achieved, induces additional sources of scattering such as a considerable surface roughness, it is clear that deeper etching on the purpose to get a stronger confinement will weaken or eventually destroy the magnetophonon effect in the wires. This is exactly what we observed. In Fig. 1, the oscillatory part of R_{xx}, normalized to the zero field resistance R_0, is shown for two samples which differ only by the depth

of the etch pits. When only slightly deeper etching is done, the amplitude of the resonances is reduced by almost an order of magnitude. Thus, to observe sufficiently pronounced MPRs we had to restrict ourselves to the case of relatively weak confinement, i.e. wires displaying subband energies in the range of 1 meV.

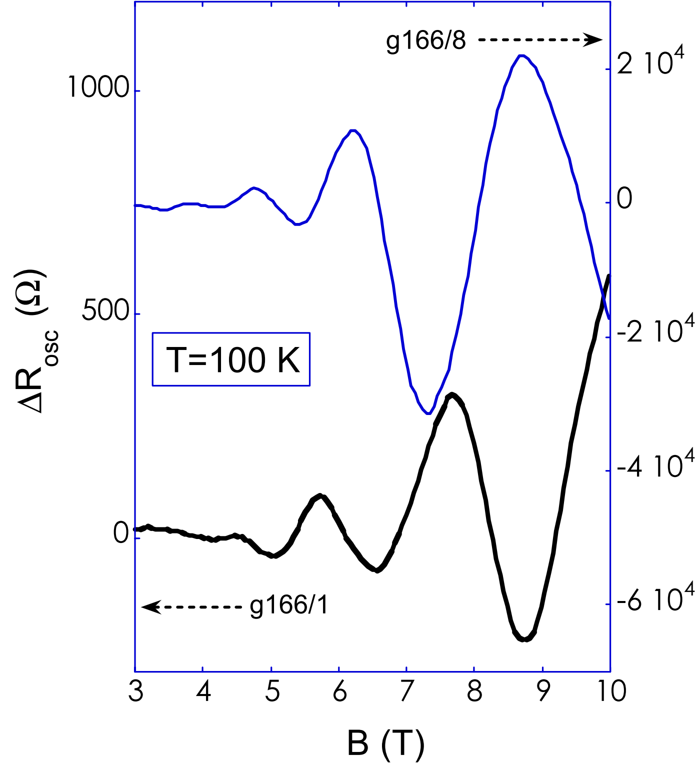

Fig. 1: Oscillatory part R_{osc} of the magnetoresistance at T = 100 K for two different samples, obtained after subtraction of the background resistance and normalization to the zero field resistance R_0. The two samples differ by the depth of the etch pits defining the lateral confinement. For g166/1 approximately 85 Å of the cap layer were removed, for g166/8 the etching depth is only 70 Å. Note the different scaling of the y-axes.

The main purpose of this work was to verify that the magnetophonon effect can be used to determine subband energies of quantum wires with small numbers of subbands occupied. We therefore compare the results of a high temperature measurement with those of a magnetic depopulation measurement performed at 2 K. Fig. 2 (a) shows a plot of the squared magnetic field positions of the resonant minima in the oscillatory part of R_{xx} measured at T = 100 K versus the inverse squared index N which is defined according to the generalized resonance condition (see e.g.[1]) $N\hbar\omega_{eff} = E_{LO}$, with E_{LO} = 36.6 meV being the LO phonon energy in bulk GaAs, $(\hbar\omega_{eff})^2 = (\hbar\omega_{cyclotron})^2 + E_0^2$ and E_0 the subband spacing of the 1D wires. As seen from Fig. 2 (a), the measured resonance positions lie clearly on a straight line and may therefore be analyzed in terms of the above resonance condition which can be rewritten in the following form :

$$B^2 = \left(\frac{m^*_{Pol}}{e\hbar}\right)^2 \frac{E_{LO}^2}{N^2} - \left(\frac{m^*_{Pol}}{e\hbar}\right)^2 E_o^2 \; .$$

According to this formula, the slope of the straight line is a measure of the polaron mass in the quantum wire, whereas its intersection with the B^2-axis gives the subband spacing E_0. It should be emphasized that this simple relationship is only valid if the confining potential can be approximated by a parabolic well. Another major approximation made is the assumption that the energy of the LO phonons is not influenced by the additional confining potential and can be taken to be the same as in bulk GaAs. With these assumptions we obtain from the data shown in Fig. 2 (a) a polaron mass of 0.069 m_e and a subband spacing of 1.6 ± 0.3 meV which is enhanced in comparison to the corresponding value obtained from a subsequent magnetic depopulation experiment (1.1 ± 0.3 meV). This enhancement was found in all investigated samples where a direct comparison was feasible and the subband spacings determined from MPR lie some 30% above those extracted from magnetic depopulation experiments.

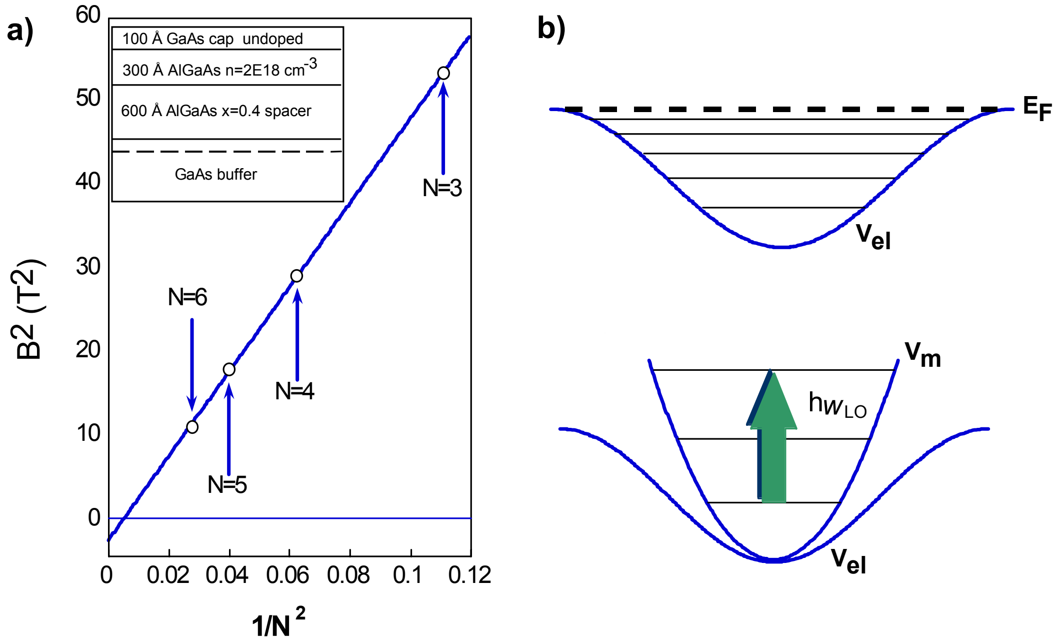

Fig. 2: (a) Plot of the squared magnetic field positions of the minima in R_{osc} versus the inverse squared index N explained in the text. The inset shows the sample structure. (b) Schematic potential forms used in the text to explain the difference in the subband spacing obtained by magnetophonon resonance and magnetic depopulation measurements.

Since temperature effects on the confining potential are small unless considerable recharging and reordering of electrically active impurities occurs [7], this difference can be explained by the following considerations (Fig. 2 (b)): The confinement in the investigated samples is obtained by very shallow etching leading to a relatively weak confining potential. From self consistent calculations reported earlier [8] it is known that the potential shape should be sinusoidal instead of simply parabolic. This in turn implies that the subbands near the upper edge of the confinement potential are closer to each other than they are at the bottom where the potential is parabolic to a good approxima-

tion. In MD experiments the subband spacing is estimated from the deviation of the low field minima in R_{xx} from the behavior observed in unstructured 2DEGs. In this case the value obtained for the subband spacing is determined by the depopulation of subbands lying near the upper edge of the confining potential which occurs at fairly low magnetic fields. MPR, on the other hand, are observed at the other end of the magnetic field scale where the magnetic confinement dominates the electrostatic one. Also electrons at the bottom of the confining potential can undergo resonant LO phonon scattering processes into empty states 36 meV higher in energy. Due to the increased density of states in high magnetic fields, a reduced number of subbands is occupied. They correspond to those states located deep in the confining potential where it is well described by a parabolic form. At high magnetic fields the deviation of V_{el} from the parabolic form is therefore negligible and the subband spacings determined from MPR correspond to those near the (parabolic) bottom of the confining potential which are larger than those estimated from MD experiments.

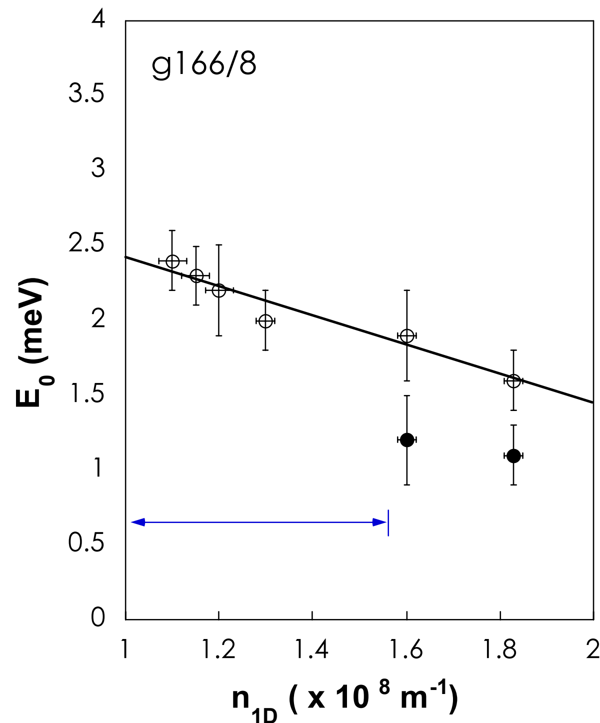

Fig. 3: Dependence of the subband spacing on the one dimensional carrier density in the wires determined by MPR experiments (open circles) and magnetic depopulation experiments (solid circles). The latter could be obtained only if sufficient numbers of subbands were occupied in the wires to apply standard evaluation methods. The straight line is the result of a linear fit to the values and is only a guide to the eye. The arrow indicates the regime, were MD measurements were not possible.

Using the procedure described in the experimental part of this paper the dependence of the subband spacing on the electron density in the quantum wires was investigated. The results of these measurements for sample g166/8 are displayed in Fig. 3. The E_0 values plotted in this figure are taken from MPR measurements at T = 100 K (open circles) as

well as MD experiments at T = 2K (solid circles). From the latter we could get this information only if a sufficient number of subbands was occupied to apply the evaluation method proposed by Berggren et al. [8]. The solid line drawn in Fig. 3 stems from a linear fit to the data and is only intended as a guideline to the eye.

The observed increase of the subband spacing with decreasing electron density has been predicted by self consistent calculations [9] and can be qualitatively explained as follows: The confining potential is formed by a periodic modulation of the donor distribution induced by the etching process. If the presence of conduction electrons in the so defined 1D channels is taken into account self consistently, the bare potential of this positive space charge is partially screened out. Therefore, the confinement will be the stronger the less electrons are present in the wire. Note that the same behavior of E_0 as a function of n_{1D} is also observed for various samples with different wafer structure, when the electron density is varied by alternative methods, e.g. by applying a back gate voltage.

4. Conclusion

In summary, we have used the magnetophonon effect to investigate the energy spectrum of quasi-one-dimensional electron systems. A systematic study of the dependence of the 1D sublevel spacing on the channel electron density was performed. By variation of the electron density in the wires through illumination with a red LED the 1D subband spacing, as determined from magnetophonon resonance measurements, is found to increase with decreasing electron density. Further, the subband spacing determined by MPR is found to be systematically higher than the subband spacing obtained from simultaneous magnetic depopulation measurements. It was further demonstrated that the combination of the two transport methods provides a particularly simple way to obtain direct information on the shape of the underlying electrostatic confinement potential in a way that MD measurements probe the subband spacing at the Fermi level and MPR measurements the subband spacing at the bottom of the confining potential.

Acknowledgments

The authors are indebted to Frank Stern for performing self-consistent calculations of confinement potentials and electron density distributions and for helpful discussions on the subject. Thanks are also due to J. C. Portal, Y. Levinson, J. Allen, P. Streda and W. Boxleitner for numerous discussions.

References

[1] D.C. Tsui, Th. Englert, A.Y. Cho, A.C. Gossard, *Phys. Rev. Lett*. 44, 341 (1980)

[2] M.A. Brummell, R.J. Nicholas, M.A. Hopkins, J.J. Harris, C.T. Foxon, *Phys. Rev. Lett* 58, 77 (1988)

[3] W. Xu, F.M. Peeters, J.T. Devreese, D.R. Leadley, R.J. Nicholas, *Int. J. Mod. Phys*. B 10, 169 (1996)

[4] D.R. Leadley, R.J. Nicholas, J. Singleton, W. Xu, F.M. Peeters, J.T. Devreese, J.A.A.J. Perenboom, L. van Bockstal, F. Herlach, J.J. Harris, C.T. Foxon, *Phys. Rev. Lett*. 73, 589 (1994)

[5] K.F. Berggren, D.J. Newson, *Semicond. Sci. Technol*. 1, 327 (1986)

[6] K.F. Berggren, G. Roos, H.van Houten, *Phys. Rev.* B 37, 10118 (1988)

[7] G. Berthold, J. Smoliner, C. Wirner, E. Gornik, G. Böhm, G. Weimann, M. Hauser,

[8] J. Smoliner, G. Berthold, F. Hirler and N. Reinacher, *Semicond. Sci. Technol*. 6, 642 (1991)

[9] J. Smoliner, G. Berthold, F. Hirler and N. Reinacher, *Semicond. Sci. Technol*. 6, 642 (1991)

Project Information

Project Manager

Dr. Jürgen SMOLINER

Institut für Festkörperelektronik, Technische Universität Wien

Project Group

Last Name	First Name	Status	Remarks
Eder	Claudia	dissertation	50 % GMe
Hirmer	Heimo	student	
Kröll	Peter	technician	
Ploner	Guido	dissertation	

Publications in Reviewed Journals

1. G. Ploner, J. Smoliner, G. Strasser and E .Gornik: “Transport Characterization of Quantum Wires by Magnetophonon and Magnetic Depopulation Experiments”, Proc. ICSMM9, Liege (1996) Superlatt. Microstruct. 22, 2 (1997)
2. G. Ploner, J. Smoliner, G.Strasser, M. Hauser and E. Gornik: “Energy levels in quantum wires studied by magnetophonon effect” to appear in Phys. Rev. B. (1998)
3. C. Eder, J. Smoliner, R. Heer, G. Strasser, E. Gornik: “Probing of Superlattice Minibands by Ballistic Electron Emission Microscopy”, Proc. MSS8, Santa Barbara (1997), to be published in Physica E (1998)
4. R. Heer, C. Eder, J. Smoliner, E. Gornik: “A floating electrometer for scanning tunneling microscope applications in the femtoampere range”, Rev. Sci. Instruments 68, 4488 (1997)
5. J. Smoliner, C. Eder, G. Strasser, E.Gornik: “BEEM on quantum wires”, Proc. HCIS10, Berlin (1997) Phys. Stat. Sol. 204, 386 (1997)

Presentations

1. C. Eder, J. Smoliner, R. Heer, G. Strasser, E. Gornik: “Probing of Superlattice Minibands by Ballistic Electron Emission Microscopy”, MSS8, Santa Barbara (1997)
2. J. Smoliner, C. Eder: “Ballistic electron emission microscopy using InAs tips.”, Int. Conf. STM97, Hamburg (1997)
3. J. Smoliner, M. Hauser, C. Eder, G. Strasser, E. Gornik: “Quantum dot structures for STM tips”, PHASDOMS 97, Aachen, Germany, 1997

4. C. Eder, J. Smoliner, R. Heer, G. Strasser, E. Gornik: “Probing of Superlattice Minibands by Ballistic Electron Emission Microscopy”, Int. Conf. STM97, Hamburg (1997) (Poster)
5. R. Heer, C. Eder, J. Smoliner, E. Gornik: “A high precision electrometer for scanning tunneling microscope applications in the femtoampere range”, Int. Conf. STM97, Hamburg (1997) (Poster)
6. J. Smoliner, C. Eder, G. Strasser, E. Gornik: “BEEM on quantum wires”, HCIS10, Berlin (1997)
7. G. Ploner, J. Smoliner, G. Strasser, M. Hauser, E. Gornik: “Charakterisierung von Quantendrähten mittels Magnetophonon Effekt”, Österreichische Physikalische Gesellschaft, 47. Jahrestagung, Wien, Austria (9/97)

Doctor’s Theses

1. C. Eder, Raster-Tunnelspektroskopie an niedrigdimensionalen Elektronensystemen (Nov. 1997)

Habilitations

1. J. Smoliner, Current transport in nanostructures, TU-Wien, Fakultät für Elektrotechnik, 16.04. 97

Development of THz-Devices

R. Zobl[1], D. Fuchshuber, R. Kersting, R. Hoffmann, C. Rauch, L. Hvozdara, G. Strasser, K. Unterrainer, E. Gornik

Institute of Solid State Electronics & Center of Microstructure Research (MISZ), Techn. Univ. Vienna A-1040 Vienna, Austria

THz emission from two different types of quantum well structures is reported. A novel combination of a stepped quantum well with a resonant injector and extractor is used to generate far infrared emission by excitation of instable plasma oscillations. The observed radiation is weak. Parabolically graded quantum wells were studied in two other sets of experiments. By putting the well in a 90° tilted position into a magnetic field a spectral shift of the emission by about 20 cm^{-1} is observed. Optical excitation of a similar parabolic well with ultrafast laser pulses enables one to investigate the dynamic response of the 2DEG in the well. The frequency of the emitted THz radiation at room temperature is around 50 cm^{-1}. A minimal increase of the frequency with excitation density is observed.

1. Introduction

Plasma effects are of special interest for FIR generation since the plasma frequency of free carriers in semiconductors usually is in the terahertz region. On one hand strong electroluminescence in the FIR region from a parabolic quantum well was recently demonstrated [1] whereas on the other hand the excitation of rising coherent oscillations in gaseous plasmas is a well known effect. In solids, however, these instable coherent modes are in strong competition with ordinary incoherent plasma oscillations and even more with thermal relaxation processes of the carriers so that the effect is not clearly identified in solids so far. To investigate various plasma effects two different sample types were prepared: a wide parabolic quantum well (PQW) and a stepped quantum well structure (G205). Time resolved experiments on parabolic quantum wells are explained in detail in section 6.

2. Plasma Oscillations

2.1 Parabolically Graded Quantum Well Potentials

One of the interesting features of parabolically confined potentials is that they absorb and emit radiation only at the bare harmonic oscillator frequency ω_0, independent of the number of electrons in the well This is in accordance with Kohn's theorem [2] which states that cyclotron resonance absorption is unaffected by electron-electron interaction. The similar property of the intersubband emission in parabolic quantum wells (PQW) is attributed to the formation of an electron slab in the well and a deformation of the self-

[1] rzobl@fkeserver.fke.tuwien.ac.at

consistent potential to rectangular shape, thus exactly canceling out the depolarization shift normally observed in 2D wells.

2.2 Theory of Plasma Instabilities

Monoenergetic current flow in collisionless gas plasmas excites oscillations. If the dispersion relation of these oscillations is complex, $\mathrm{Im}(\omega) > 0$ leads to exponentially growing plasma waves. A necessary condition for their self startup is a locally inversion of the carrier distribution in momentum space. This perturbation of the normal Maxwell-Boltzmann distribution must exhibit at least two maxima (Penrose criterion). Quantum mechanically the process is a particle-plasmon interaction [3]. Relaxation of single carriers by a direct transfer of energy into the plasma mode is only possible above a certain threshold so that high current injection is needed. This in turn leads to severe problems with heating and the effect can easily be wiped out by interaction with phonons. Careful sample design in form of small mesas is mandatory for this reason.

3. Sample Structures

Band structures of both samples are shown in Fig. 1 and Fig. 2 .

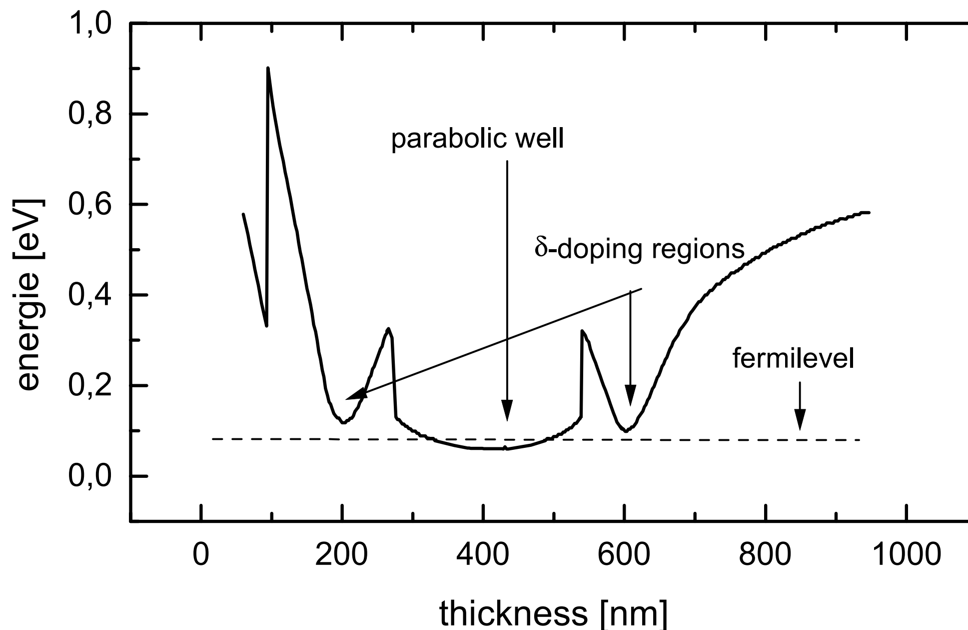

Fig. 1: Band structure of a wide parabolic quantum well (PQW).

The PQW consists of a single graded GaAs/AlGaAs quantum well grown on a semiinsulating substrate. On both sides of the well the barriers are modulation doped. The well is nominally 200 nm wide resulting in a bare oscillator frequency of 50 cm^{-1}. The sample has two annealed Au/Ge/Ni top contacts and a 20 µm period grating for outcoupling of the spontaneous terahertz emission. The net emissive area is 5x5 mm^2. Simple heating of the electron gas by lateral current injection is used to populate higher energy levels and to induce radiative downward transitions. There is no deformation of the potential shape through the lateral biasing.

To excite instable plasma modes in a 2DEG a stepped quantum well structure was fabricated. Electrons are injected selectively through a thin barrier into the upper miniband in the well. Due to the extension of this miniband in the wide area of the well the level spacing is small compared to the intermediate miniband in the narrow well region. The energy separation of the upper and the lowest miniband is matched to the LO phonon energy in GaAs. This in combination with a resonant extractor formed by two thin barriers leads to an effective depopulation of the intermediate levels while the upper and lower minibands are strongly populated by current injection and phonon assisted downward transitions, respectively. To minimize overheating effects the sample is designed as small mesas with annealed grating couplers on top which also act as top contacts. Between the grating metallization the highly doped regions are etched away to reduce self absorption.

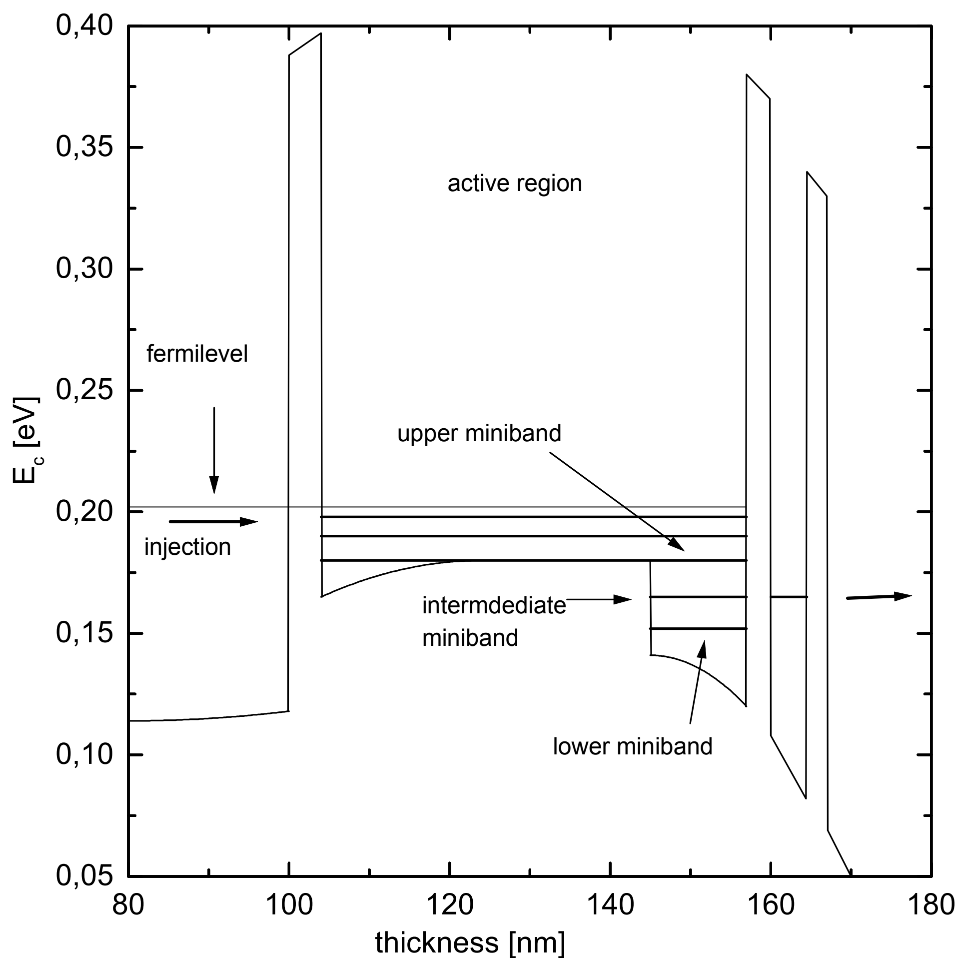

Fig. 2: Band structure of the stepped quantum well G205.

4. Measurements

All measurements were performed at 4,2 K in liquid helium. A triple set of photoconductive detectors is sitting in the center of a 7 T superconducting magnet at the lower end of the cryostat. One p-Ge broadband detector and two magnetically tunable fre-

quency selective detectors (GaAs, InSb) cover the spectral range from 30 cm^{-1} to 300 cm^{-1}. Radiation from the samples is guided to the detectors via a metallic light pipe.

For magnetic field dependent measurements the PQW was placed in the center of an upper magnet (up to 5 T). Two different sample orientations in the magnetic field were used as shown in Fig. 3 and Fig. 4 (see also Fig. 6).

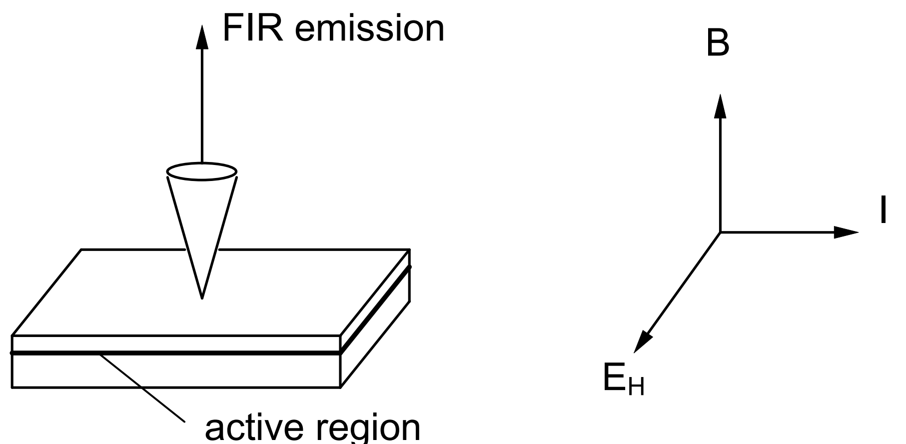

Fig. 3: Standard orientation of current flow I, magnetic field B and Hall field E_H for measurement of the parabolic quantum well in magnetic fields. Due to the sample geometry no Hall field is established in this arrangement. The grating on top of the sample is not shown.

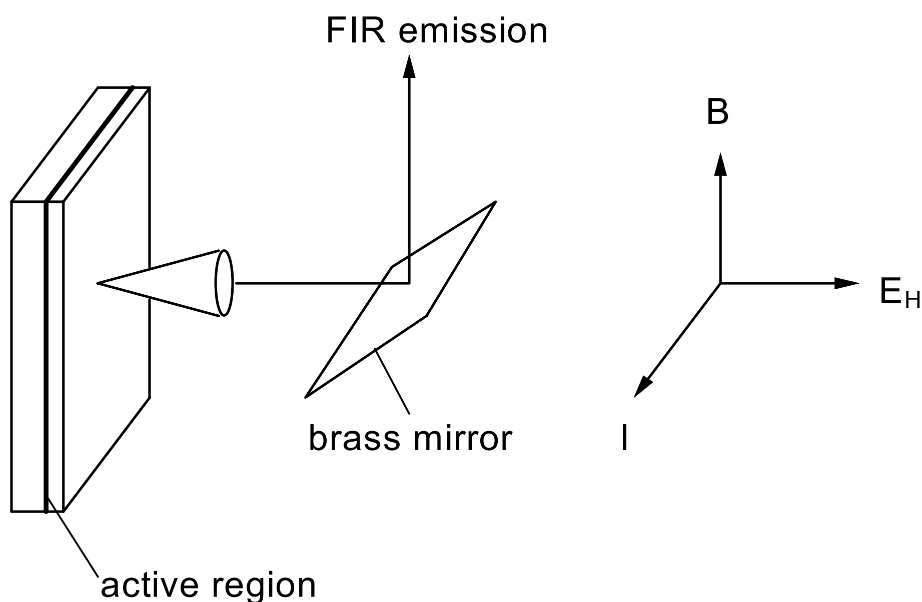

Fig. 4: Measurement of the PQW in a 90° tilted position. In this orientation the Hall field is strong. The outcoupling grating again is not shown.

On both sample types measurements were performed by applying pulses of several volts and several μs duration. A repetition rate of 23 kHz gave a duty cycle of 10 % to 20 %.

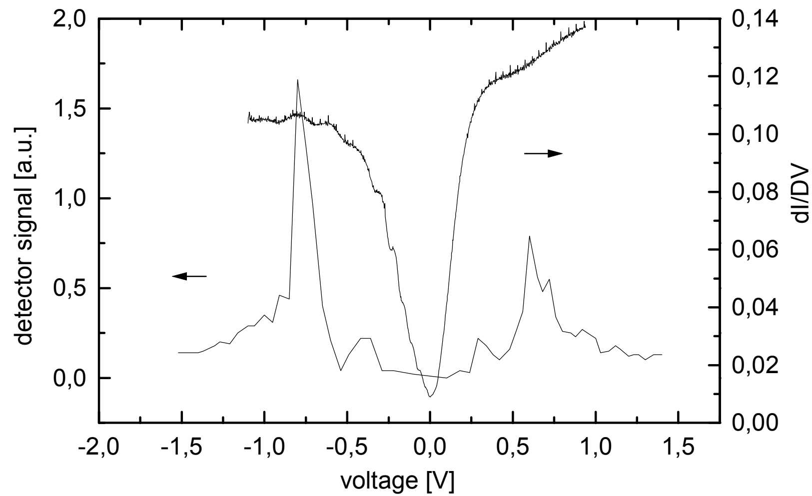

Fig. 5: Integral emission intensity of G205 with the GaAs detector. Also shown is the derivative of the I-V curve.

Figure 5 shows the measured broadband signal of sample G205 vs. applied voltage. Also shown is the derivative of the I-V. The change in the slope of the derivative coincides with two maxima in the emission, indicating the onset of a growing plasma mode in a narrow regime around 700 mV.

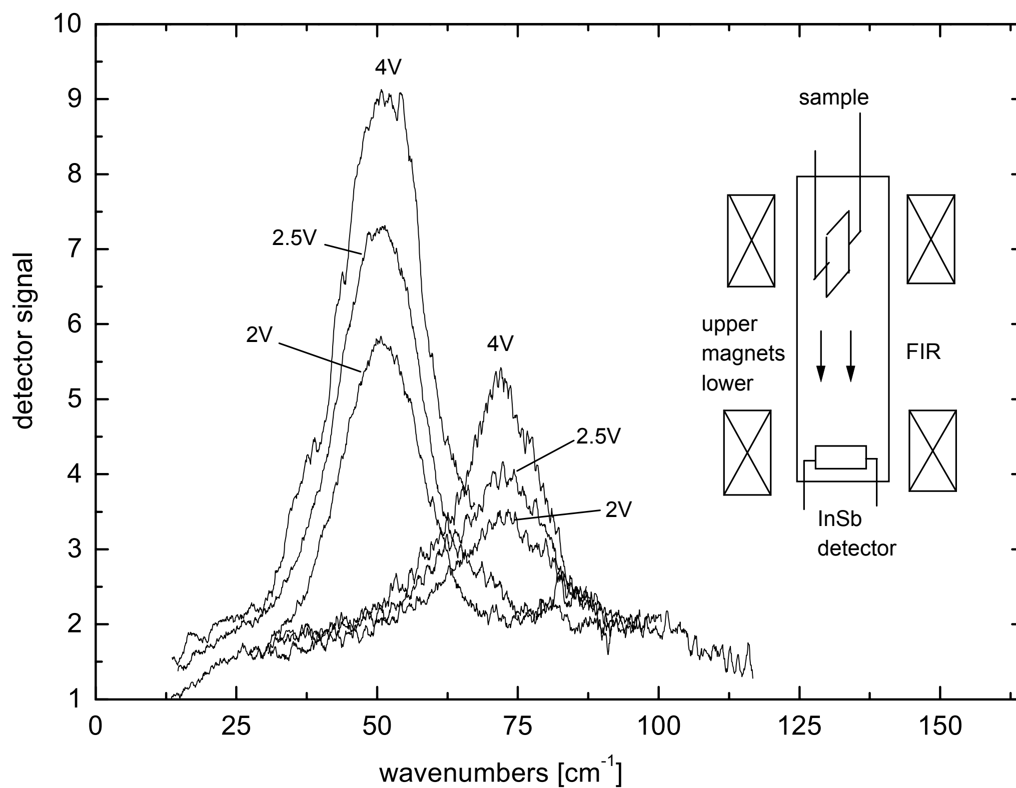

Fig. 6: Spectral shift of the Emission for a 90° tilted position of the PQW in the magnetic field.

To investigate the effect of a magnetic field on the FIR emission of the PQW magnetic fields up to 5 T were applied. For a magnetic field direction perpendicular to the layers no CR emission can be observed while the normal intersubband emission almost immediately vanishes even at low magnetic fields. If the magnetic field is applied parallel to the well but perpendicular to the direction of current flow (Fig. 6) CR emission again is not seen whereas a frequency shift of the intersubband radiation is observed starting at magnetic field strengths above 2 T. The shift is attributed to the formation of a strong electric field perpendicular to the well via Hall effect. At 4 T the center frequency of the FIR emission has moved from 50 cm^{-1} to 70 cm^{-1} accompanied by a decrease in signal intensity of 50 %. The shifted center frequency position is still independent from the laterally applied electric field and the current flow.

5. Conclusions for the Electroluminescence Experiments

For the sample G205 the formation of an instable plasma oscillation under vertical injection was demonstrated. The emitted FIR radiation was either too weak or outside the reach of the spectrally resolving detectors, a problem which can be overcome by simple increasing the number of emitters and switching to other detectors respectively. On the other hand the PQW shows a strong signal. So while the carrier distribution in a parabolic well cannot be inverted by itself a combination of the excellent oscillatory behavior of the PQW with resonant vertical injection through barriers seems promising. Adding a superlattice within the parabolic potential could create a gap between the energy levels of the well giving way to the formation of a growing plasma mode. However as the magnetic field measurements show, care must be taken that the symmetry of the structure is not affected for instance by the bias voltage which would lead to a breakdown of the Kohn theorem.

6. Few-Cycle THz Emission from Intersubband Plasmon Oscillation in Parabolic Wells

Few-cycle THz emission is observed from semiconductors excited by ultrafast laser pulses. The investigation of this THz emission is important for the understanding of the underlying carrier dynamics as well as for possible applications in spectroscopy and imaging. The emission is explained by coherent charge oscillations if the laser pulse generates a superposition within the subbands of a heterostructure, or by the instantaneous polarization and by the subsequent motion of photoexcited carriers in a depletion or in a built-in field of a semiconductor.

During the investigation of the ultrafast field screening on p-i-n structures in pump and probe experiments oscillations of the built-in field due to plasma oscillations of the photo generated carriers were observed [4]. We have performed THz emission experiments in such structures and have observed emission due to coherent plasma oscillations. In addition, we have also found that the screening of the surface field by the optical excited carriers induces plasma oscillations of cold electrons beyond the depletion zone of the n-doped epilayers. The plasma oscillations of cold electrons are characterized by a long damping time which leads to a very efficient emission process [5].

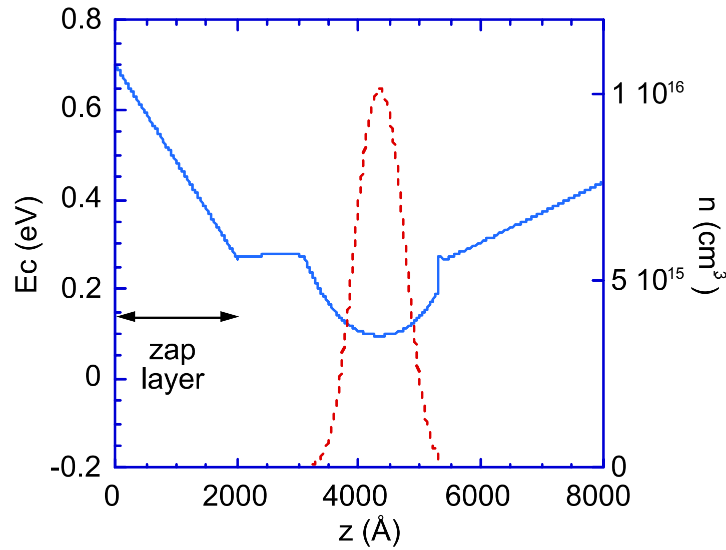

Fig. 7: Schematic band diagram of the parabolic well and of the top GaAs layer for photoexcitation.

In order to improve the THz emission and to investigate the dynamic response of a quasi two-dimensional electron gas we have designed a structure with a parabolic well just beyond the depletion zone of a n-doped GaAs cap layer (Fig. 7). From electrons in modulation doped wells we expect much longer damping times. According to Kohn's theorem the electrons in parabolically confined potentials will interact with light only at the bare harmonic oscillator frequency $\omega_0 = \sqrt{\frac{8\Delta}{L^2 m*}}$ (Δ is the depth of the parabolic potential, L the width, and m* the effective mass) independent of the carrier concentration in the well. The parabolic well was designed to be 2000 Å wide and to have a resonance frequency ω_0 of about 1.5 THz. The structure was modulation doped to give an electron concentration in the well of about $5 \cdot 10^{11}$ cm^{-2}. The design is similar to the one used in the previous explained electroluminescence setup. In experiments on a similar parabolic well where the electrons where heated by a lateral current spontaneous THz emission was observed at the expected resonance position [1].

The optical excited experiments were performed using a mode-locked Ti:Sapphire laser emitting 100 fs pulses at 800 nm. A 4.2 K bolometer is used to detect the THz radiation. Time resolution is achieved by focusing two delayed pulses on the samples and by recording the time integrated THz auto correlation signal as a function of the delay time.

We have observed coherent THz emission from the parabolic well sample at room temperature. The auto correlation signal and the Fourier transformed spectra are shown in Fig. 8 and Fig. 9 for different excitation densities. Clear oscillations are visible with a damping time corresponding to the DC mobility of the quasi two-dimensional channel. The observed frequency is around 1.5 THz. According to Kohn's theorem we do not expect a dependence of the emission frequency on the carrier excitation density. However, we observe a small increase of the frequency with excitation density which we suppose is due to filling of the parabolic well by photoexcited carriers.

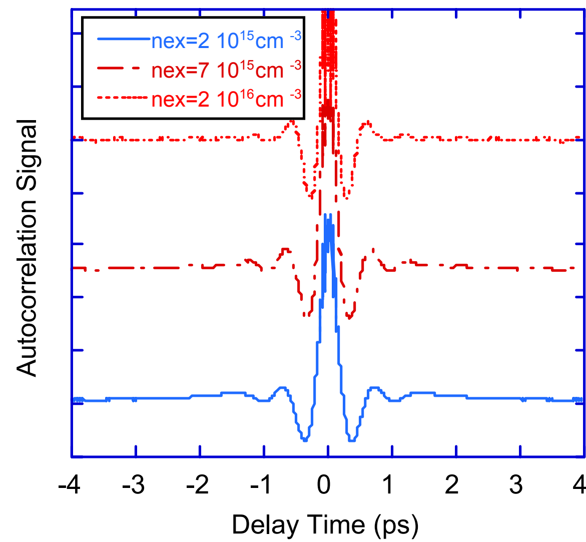

Fig. 8: Auto correlation of the THz emission from the parabolic well.

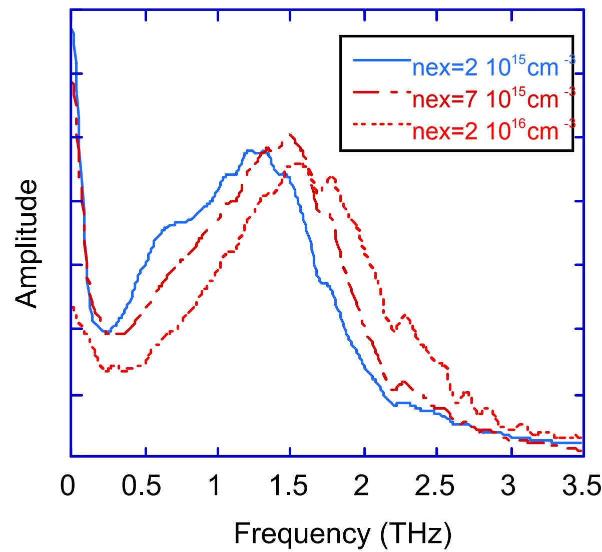

Fig. 9: Fourier transformed spectra of the optical excited THz emission from the parabolic well.

Acknowledgments

We acknowledge financial support by the Austrian Science Foundation (FWF, START Y47) and by the US Army Research Office.

References

[1] K. D. Maranowski, A. C. Gossard, K. Unterrainer, E. Gornik: "Far-infrared Emission from Parabolically Graded Quantum Wells", *Appl. Phys. Lett.,* Vol. 69, No. 23, 1996, p. 3522 – 3524.

[2] W. Kohn: “Cyclotron Resonance and de Haas-van Alphen Oscillations of an Interacting Electron Gas”, *Phys. Rev.,* Vol. 123, No. 4, 1961, p. 1242 – 1244.

[3] P. Bakshi, K. Kempa: “Current Driven Plasma Instabilities in Lower Dimensional Systems”, *Superlatt. Microstruct.*, Vol. 17, No. 4, 1995, p. 363 – 372.

[4] W. Shah, A. L. Smirl, W. F. Tseng: “Coherent Plasma Oscillations in Bulk Semiconductors”, *Phys. Rev. Lett.*, Vol. 74, No. 21, 1995, p. 4273 – 4276.

[5] R. Kersting, K. Unterrainer, G. Strasser, E. Gornik, H. F. Kauffmann: “Few -cycle THz emission from cold plasma oscillations”, *Phys. Rev. Lett.* , 79, 3038 (1997).

Project Information

Project Manager

Dr. Karl UNTERRAINER

Institut für Festkörperelektronik, Technische Universität Wien

Project Group

Last Name	First Name	Status	Remarks
Fuchshuber	David	student	
Gornik	Erich	university professor	
Hoffmann	Rainer	student	
Hvozdara	Lubos	dissertation	
Kersting	Roland	postdoc	
Rauch	Christoph	dissertation	
Strasser	Gottfried	assistant professor	
Unterrainer	Karl	assistant professor	
Zobl	Reinhard	dissertation	

Publications in Reviewed Journals

1. J.N. Heyman, R. Kersting, K. Unterrainer: "Time-Domain Measurement of Intersubband Oscillations in a Quantum Well", Appl. Phys. Lett., 72, p. 644 (1998).
2. R. Kersting, K. Unterrainer, G. Strasser, E. Gornik: "Coherent Few-Cycle THz Emission from Plasmons in Bulk GaAs", Journal physica status solidi (b), 204, 67 (1997).
3. R. Kersting, K. Unterrainer, G. Strasser, H.F. Kauffmann, E. Gornik: "Few-Cycle THz Emission from Cold Plasma Oscillations", Phys. Rev. Lett. , 79, 3038 (1997).
4. R. Kersting, K. Unterrainer, G. Strasser, H.F. Kauffmann, E. Gornik: "Coherent few-cycle THz emission of cold plasmons", Proceedings of the Quantum Electronics and Laser Science Conference, QELS97, 198 (1997).
5. K. Unterrainer, B.J. Keay, M.C. Wanke, S.J. Allen, D. Leonard, G. Meideiros-Ribeiro, U. Bhattacharya, M.J.W. Rodwell: "Observation of Shapiro steps and direct evidence of Bloch oscillations in semiconductor superlattices", Proceedings of 23rd International Symposium on Compound Semiconductors, St. Petersburg, Russia, 23-27 Sept. 1996; Edited by M.S. Shur, R.A. Suris, Bristol, UK, IOP Publishing, p. 729-34 (1997).

6. R. Kersting, J. N. Heyman, G. Strasser, K. Unterrainer: “Coherent volume plasmons in n-doped GaAs”, Phys. Rev. B. (submitted).
7. G. Strasser, S. Gianordoli, L. Hvozdara, H. Bichl, K. Unterrainer, E. Gornik, P. Kruck, M. Helm, J.N. Heyman: “GaAs/AlGaAs intersubband mid-infrared emitter”, Proc. MRS Fall Meeting 1997, Boston, USA, 1-5.12.97 (in print).
8. J.N. Heyman, R. Kersting, G. Strasser, K. Maranowski, A.C. Gossard, K. Unterrainer: “THz time-domain spectroscopy of intesubband plasmons”, Proceedings of the Fourth International Workshop on Intersubband Transitions in Quantum Wells, Tainan, Taiwan, December 15th-18th, 1997 (in print).
9. L. Hvozdara, J.N. Heyman, G. Strasser, K. Unterrainer, P. Kruck, M. Helm, E. Gornik: “Characterization of GaAs/AlGaAs mid-infrared emitters”, Conf. Proc. of the 24th Int. Symposium on Compound Semiconductors (in print).

Presentations

1. K. Unterrainer: “Inverse Bloch oscillator”, Workshop on “Atoms and Electrons in Periodic and Quasiperiodic Potentials”, Les Houches, 27-31 January 1997 (invited).
2. R. Kersting, K. Unterrainer, G. Strasser, E. Gornik: “Coherent few-cycle THz emission of cold plasmons”, 1997 Quantum Electronics and Laser Science Conference, 18.-23.5.1997, Baltimore, USA (invited)
3. J.N. Heyman, R. Kersting, G. Strasser, K. Maranowski, A.C. Gossard, K. Unterrainer: “THz time-domain spectroscopy of intesubband plasmons”, Fourth International Workshop on Intersubband Transitions in Quantum Wells, Tainan, Taiwan, December 15th-18th, 1997 (invited).
4. L. Hvozdara, J.N. Heyman, G. Strasser, K. Unterrainer, P. Kruck, M. Helm, E. Gornik: “Characterization of GaAs/AlGaAs mid-infrared emitters”, 24th Int. Symposium on Compound Semiconductors, 1.-5.9.1997, San Diego, USA.
5. R. Kersting, K. Unterrainer, G. Strasser, E. Gornik: “Coherent few-cycle THz emission from plasmons in bulk GaAs”, Int. Conf. on Nonequilibrium Carrier Dynamics in Semiconductors, 28.7.-1.8.1997, Berlin, Germany
6. K. Unterrainer, R. Kersting, J.N. Heyman, G. Strasser, K.D. Maranowski, A.C. Gossard: “Few-cycle THz emission from intersubband plasmon oscillation in parabolic wells”, 8th Int. Conf. on Modulated Semiconductor Structures, 14.-18.7.1997, Santa Barbara, USA.
7. R. Kersting: “Ultrafast dynamics of excitons in conjugated polymers”, Femtochemistry 97, 3. Sep. 1997, Lund, Sweden.
8. K. Unterrainer: “Anwendungen von IR-FEL-Strahlung in der nichtlinearen Spektroskopie von Halbleiterdetektoren”, FZ Rossendorf, Dresden, Deutschland, 17.4.1997
9. K. Unterrainer: “Time-resolved THz spectroscopy of Semiconductor Nanostructures”, LMU - Universität München, 26.6.1997
10. K. Unterrainer: “Few-cycle THz spectroscopy of semiconductor nanostructures”, Lucent, AT&T Bell Labs, Murray Hill, NJ, USA, 23.7.1997.

11. R. Kersting: “Konjugierte Polymere: ultraschnelle Relaxations- und Transportprozesse”, Univ. Dortmund, Deutschland, 10.1. 1997.
12. R. Kersting: “Plasma Oscillations: emission and absorption of THz pulses”, Toshiba Cambridge Research Corporation, Cambridge, UK, 10.9.1997.
13. R. Kersting, J.N. Heyman, G. Strasser, H.F. Kauffmann, K. Unterrainer: “Kohärente THz-Emission von Plasmaoszillationen in Halbleitern”, ÖPG Jahrestagung, Universität Wien, 22.-26.9.1997.
14. R. Zobl, C. Rauch, L. Hvozdara, G. Strasser, K. Unterrainer, K. Maranowski, A.C. Gossard, E. Gornik: “Halbleiter-Quantenstrukturen als THz-Emitter”, ÖPG Jahrestagung, Universität Wien, 22.-26.9.1997.

Cooperations

1. Boston College, Physics Department, Prof. Krisz Kempa
2. Macalester College, Physics Department, Prof. J.N. Heyman
3. Universität Wien, Physikalische Chemie, Prof. H.F. Kauffmann
4. University of California, Santa Barbara, Materials Department, Prof. A.C. Gossard

Microelectronics Technology — Cleanroom Linz

Microstructure Research: Cleanroom Linz

G. Bauer, H. Heinrich, H. Thim

Institut für Halbleiter- und Festkörperphysik and Institut für Mikroelektronik, Johannes Kepler Universität Linz, A-4040 Linz, Austria

The activities in the two cleanrooms of the Johannes Kepler Universität Linz are described which were supported in their operation through funds from the Gesellschaft für Mikroelektronik . The main activities are the molecular beam epitaxial growth of Si based heterostructures (Si/SiGe, Si/SiC and Si/SiGe/SiC, Si/SiGeC), the growth of magnetic heterostructures and superlattices like CdTe/CdMnTe, as well as of PbTe/EuTe and the MOCVD growth of GaAs based heterostructures like GaAs/GaInAs. The lateral patterning of Si/SiGe based heterostructures through holographic lithography as well as through electron beam lithography has been performed and the electronic properties of such structures were investigated by transport, magnetotransport as well as photoluminescence. A standard process module for Si-based heterostructure devices and for the implementation of modulation doped field effect transistors was developed consisting of either 5 or 6 lithographic masks. Furthermore, characterization techniques like UHV-STM AFM were used for studies of the surface morphology of heterostructures and reflectance difference spectroscopy has been implemented as an *in situ* control process in II-VI molecular beam epitaxy. In addition, experimental results with a 35 GHz Doppler radar unit are reported in this contribution. The measurement setup consists of a RF-front-end, signal conditioning, signal processing and a display unit. The sensitivity of the receiving part has been enhanced by matching a recently developed InGaAs-detector diode with the characteristic impedance of the microstrip transmission line.

1. Introduction

The GMe funding has made possible research work on various topics carried out by groups from three institutions in the two cleanrooms at the Institut für Halbleiterphysik and at the Institut für Mikroelektronik in Linz. In the following we give short presentations of the results achieved through support of various efforts carried out in these cleanrooms. This concerns the MBE and MOCVD growth of materials, the structural characterization of heterostructures and multilayers through several *in situ* as well as *ex situ* methods, the characterization of their electronic and optical properties, and finally the realization of standard process modules for Si based and GaAs based heterostructure devices and the development of high frequency emitters and detectors. Furthermore, research directed to the use of multiquantum well and superlattice structures for infrared detectors and emitters is reported. Detailed information is contained in the cited references, where also all contributors to the investigations are listed.

2. Experimental

2.1 Si-based Process Technologies

(F. Schäffler)

2.1.1 Si Molecular Beam Epitaxy

The activities regarding Si-based heterostructures rely strongly on the quality of the epi-layers, which are grown on-site in our Riber Si-MBE machine. It is located in the clean room of the Semiconductor Physics Group in Linz and utilizes the infrastructure there for substrate preparation and the initial mechanical characterization of the epi-layers by means of a step profiler.

Before introducing the 4” or 5” silicon substrates into the load-lock chamber of our MBE machine, they are chemically pre-cleaned. Since the wafers are usually production-quality substrates from a leading manufacturer, degreasing or other chemical treatments for a removal of organic contaminations are considered detrimental to the quality of the as-delivered substrate surfaces, and therefore avoided, unless a pre-structuring or dicing of the substrates has been performed before growth. Instead, the wafers are either pre-cleaned by a simple dip in diluted (typ. 5 %) HF, or they experience a modified RCA-cleaning procedure, which is very similar to the final treatment applied by the wafer manufacturers after polishing of the substrates. This process, which is named after its inventor, the RCA company, consists of a sequence of two etchants, namely SC1 ($NH_4OH/H_2O_2/H_2O$ 1:1:5) and SC2 ($HCL/H_2O_2/H_2O$ 1:1:5), which remove organic and metallic contaminations, respectively. Both SC1 and SC2 are kept in quartz tanks near the boiling point during the agitation period of typically 15 min. The wafers are thoroughly rinsed in DI water after either bath for as long as it takes to bring the DI water resistance to at least 15 MΩ. Combinations of the RCA clean with one or more HF dips (before and after SC1 and after SC2, or just after SC2) are frequently employed to remove the chemical oxide caused by both SC1 and SC2. The last step before mounting the substrates in the load-lock chamber is always dry blowing in an N_2 gas stream.

In 1997 we implemented the RCA cleaning procedure in a flow box next to our MBE machine. Heatable and temperature-controlled quartz tanks capable of adapting up to 6 4” or 5” Si substrates (i.e. the capacity of our load-lock chamber) were acquired from a commercial vendor. The HF tank was home-built and milled from one block of Teflon to avoid any source of contamination that could result from the gaps in a multi-part design. An N_2 bubble rinser connected to the DI water supply in our clean room and a N_2 blower for drying the wafers complement the cleaning facility.

Because of the decomposition of H_2O_2 in the RCA baths, and because of hydrocarbon contamination of the HF bath, all chemical agents used in this standard cleaning procedure can only be used once. To keep the cost for the required chemicals as low as possible we therefore reduced the tank volumes to the absolute minimum necessary to completely cover our maximum wafer size of 5”. Also, whenever possible (e.g. for calibration wafers or simple epi-tests) we skip the RCA procedure and employ just an HF dip for oxide removal immediately before introducing the wafers into the load-lock chamber. The disadvantage of the HF dip is the concomitant carbon contamination of the interface, which, although it is not electrically active in silicon, is not always acceptable, even if a Si buffer layer is introduced between the interface and the active heterolayers.

2.1.2 Standard Process Module for Si-based Devices

For an electrical characterization of Si-based heterostructures and for the implementation of modulation-doped field-effect transistors we developed a standard process module consisting of either 5 or 6 lithographic masks (diploma thesis Günther Steinbacher, 1997). Besides an array of field-effect transistors with variable gate length, the layout comprises gated Hall bars and various test structures for process characterization. For example, transmission lines allow to assess the Ohmic contacts, whereas Schottky diodes give access to the Schottky barrier heights an the doping profile near the epi surface.

The process module at this stage is based on the simple mesa technique usually employed for III-V devices, but employs as a Si-specific feature implanted Ohmic contacts. In addition, the process sequence is compatible with a SiO_2 or Si_3N_4 passivation layer, low-temperature deposition of which is planned to be installed in the near future.

The process sequence commences with reactive ion etching (RIE) of alignment marks, which are used for the subsequent lithographic layers. These marks are necessitated by the implanted contact areas, which cannot be used as marks because they become indistinguishable in the optical microscope of the mask aligner after recrystallization. The second lithographic layer defines the contact areas, which are implanted in-house with the photoresist as an implantation mask. After removal of the resist in an O_2 plasma and rapid thermal annealing (RTA) of the implanted areas, the same lithography mask is used a second time for lift-off definition of the metallic contact pads. The third lithographic mask defines, per lift-off, the Schottky gates of the transistors, the gated Hall bars and the test Schottky diodes. The fourth mask defines the mesa areas, i.e. it facilitates the lateral electrical separation of the devices and test elements. For this step a negative resist is employed in order to keep the polarity of all mask layers the same. The layout of the mesa-mask is such that the gates of the Hall bars operate as self-aligning mesa masks, i.e., the gate control of the Hall bars is not affected by misalignment. Mesa separation is then accomplished by RIE, with parameters that lead to relatively shallow mesa slopes. These are required by the fifth mask layer, which provides the gate contact pads via a lift-off procedure. To avoid shorts to the underlying active layers induced by ultrasonic contact bonding, the gate contact pads are located in the trenches between mesas, and hence require a connection to the gates on top of the mesas that has to climb up the slope. It is therefore essential to avoid too anisotropic etching of the mesas. The sixth, optional mask layer provides a back contact to the Schottky diodes, which is again located in the plane of the gate contacts. Alternatively, the Schottky diodes are fabricated in a planar fashion, with both contacts in the mesa plane.

The complete process module has been tested, and suitable process parameters for the respective steps have been assigned. Further improvements or fine tuning of these parameters are introduced as experience is gained with the process, or when required by special demands regarding the epi-layer design. For example, contact implantation has to be adapted to the depth of the 2D carrier gas underneath the surface, and it has been recognized that a double implantation, with a shallow projected range for maximum carrier concentration at or near the surface, and a deeper projected range near the 2D channel, is required for optimum contact performance.

The original layout of our process module is based on optical contact lithography. Hence the smallest reproducible structures are 1 μm wide (0.8 μm with some over-exposure). To allow submicron gates of the transistors, additional alignment marks are provided

that can be recognized in our e-beam writer. In such a hybrid process all but the gate process are implemented by optical lithography, whereas e-beam lithography and PMMA resist are used for the definition of the gate per lift-off process.

2.1.3 e-Beam Lithography

In 1997 our recently commissioned e-beam writer (Jeol 6400 SEM plus Raith Elphy driver) became operational with demonstrated minimum feature sizes < 100 nm both in additive and subtractive processes (diploma thesis Britta Fünfstück, 1997). The former are used for structuring of metal layers ("lift-off"), whereas the latter are utilized for pattern transfer into the heterostructures via RIE.

So far, our lift-off process is based on a single layer resist, which is only possible by careful determination of the exposure dose. Under optimum conditions, a negative slope of the resist edges develops through overexposure near the substrate by means of secondary electrons generated in the substrate. This procedure has been demonstrated to be working quite well in a situation where a single gate has to be written, which will be the case for implementing the hybrid process mentioned in the preceding subsection. For more complicated structures, or for double gates, where the proximity effect interferes with the required in-depth resist profiling via secondary electrons, more complicated procedures, such as two layer resists, may be required.

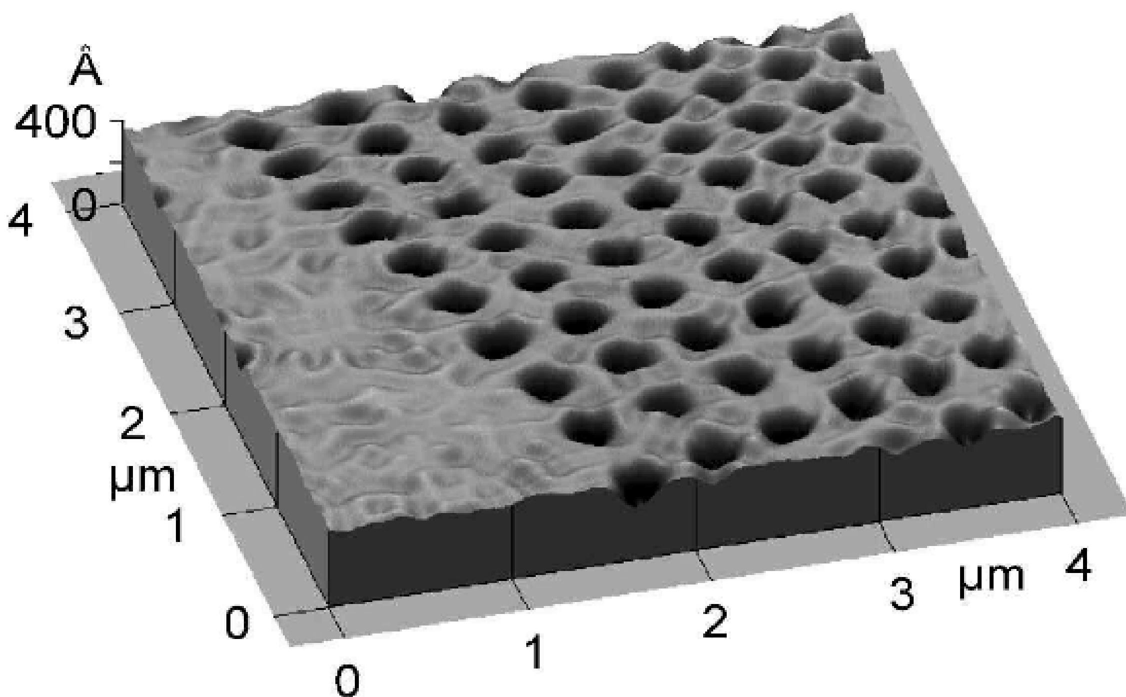

Fig. 1: Anti-dot superlattice defined by e-beam lithography and transferred by RIE into a modulation-doped Si/SiGe heterostructure.

Experiments revealed that structured PMMA is directly useable as a resist for RIE of Si-based heterostructures. By careful adjustment of the RIE parameters in a SF_6/CH_4 process, we were able to achieve comparable etching rates for Si and PMMA. This is for many purposes sufficient, since usually the RIE process is used for rather shallow trench or mesa etching, which need only be deep enough to interrupt the 2D channel of a highly

mobile carrier gas (typically less than 500 Å underneath the surface). As an example, Fig. 1 shows an anti-dot array produced this way with a period of 0.3 µm and an anti-dot diameter of about 150 nm. It was etched into one section of a Hall bar with six potential probes to the depth of the 2D electron gas of a modulation-doped Si/SiGe heterostructure grown in our Riber MBE apparatus. Despite non-optimized RIE parameters, which resulted in reduced carrier mobilities due to RIE damage, we observed a clear commensurability maximum in magnetoresistance measurements. We therefore believe that commensurability oscillations can be used as a sensitive probe for assessing, and optimizing, RIE process parameters with respect to minimum damage.

2.2 X-ray Diffraction and Reflectivity from Dry Etched SiGe Wires and Dots

(Y. Zhuang, A.A. Darhuber, J. Stangl, P. Mikulik and G. Bauer)

Si based heterostructures like Si/SiGe have found increasing interest especially because of their potential for application in high frequency circuits. In the SiGe material system the electronic properties depend strongly on the strain status of the layers, i.e. both the band gap as well as the band offsets differ significantly for fully strained or fully relaxed SiGe layers on Si. Any lateral structuring of Si/SiGe heterostructures induces a position dependent elastic relaxation of the misfit strain between the Si and SiGe layers. Therefore for a proper interpretation of optical and electronic properties of laterally patterned SiGe wires and dots, a knowledge of the strain status of the layers is required.

In the case of laterally periodic structures like arrays of wires and dots, the x-ray diffraction (XRD) peaks split into a series of satellites which can be investigated by a mapping of the two-dimensional intensity distribution in the reciprocal space. Information on the geometrical shape of the wire and dot structures is obtained from x-ray reflectivity measurements. Our experimental investigations have shown that strain relaxation in wires and dots is rather complex due to side wall related phenomena, as evidenced by a comparison with finite element calculations.

We have investigated series of dry-etched Si/SiGe quantum wires and dots which were fabricated from MBE grown 10 period Si/SiGe multiquantum well (MQW) structures with Ge contents about 20 %, SiGe layer thickness of about 30 Å and MQW periods of about 200 Å. The wires and dots were defined in the clean room Linz by holographic lithography using an Ar-ion laser set-up and were reactively ion-etched by using a mixture of CH_4 and SF_6 in an Oxford Plasmalab reactor. Apart from these about 200 nm wide structures, in collaboration with a group from the Nanoelectronics Research Center, Glasgow, also smaller dot structures which had been defined by e-beam lithography, were investigated as well.

With XRD reciprocal space maps of the wire and dot structures close to the (004) and (224) reciprocal lattice points were recorded as shown in Figs. 2 and 3 (10 period $Si/Si_{0.84}Ge_{0.16}$ MQW structure, d_{Si} = 214 Å, d_{SiGe} = 62 Å, lateral period: D = 440 nm, wire or dot width: 220 nm). The elastic relaxation is deduced from a shift of the diffraction pattern of the etched structures with respect to the substrate peak. The reduction of the in-plane compressive strain after the etching process manifests itself in a shift of the envelope of the wire and dot satellites. The elastic relaxation leads to a decrease of the measured average in-plane strain which is different for wire and dot structures. Due to the uniaxial compression exerted by the Si substrate along the wire axis, the average in-plane elastic relaxation in the wires turns out to be larger than that for the dots.

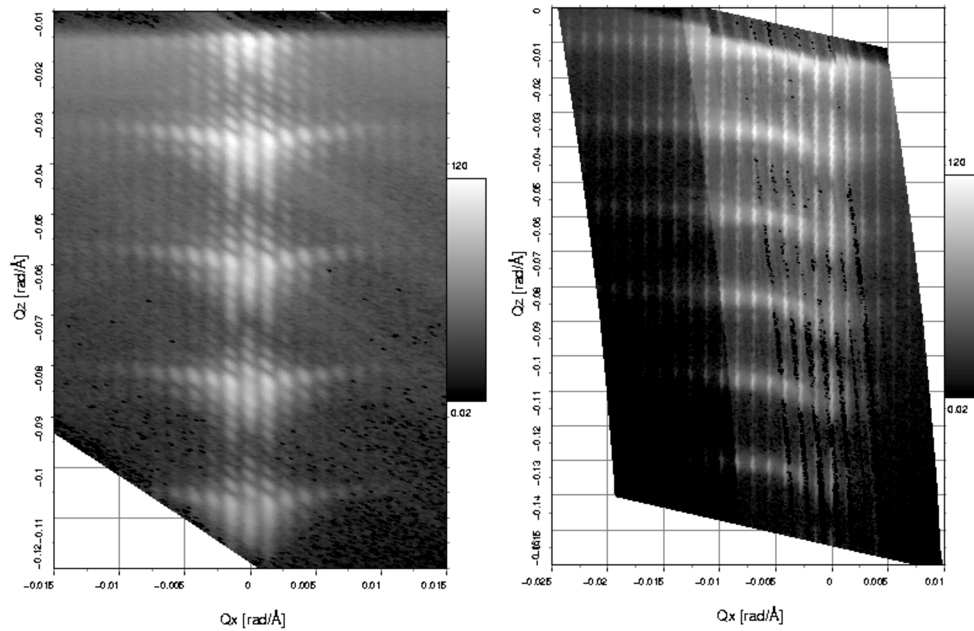

Fig. 2: X-ray diffraction ((004) and (224) reflections) from Si/SiGe reactive ion etched wires.

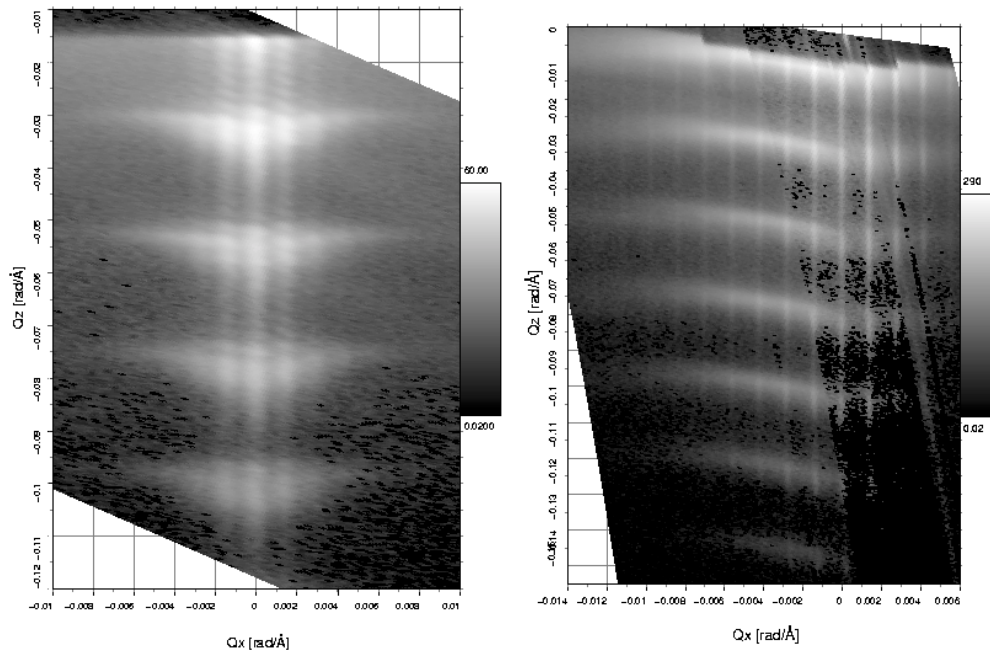

Fig. 3: x-ray diffraction ((004) and (224) reflections from Si/SiGe reactive ion etched dots

This relaxation is defined in relation to the bulk lattice constants of a corresponding SiGe mixed crystal with the same average lattice constant as the MQW structure.

The x-ray reflectivity measurements are sensitive to the grating shape as well as to the interface roughness of the Si/SiGe layers. In the reciprocal space maps recorded around

(000), the presence of even order truncation rods reflects side wall imperfections. Furthermore we have observed subsidiary diffuse maxima in between the high intensity wire satellites, which correspond to a period of about 1 µm. Since the Si/SiGe MQW's were grown on slightly miscut substrates, strain induced step bunching occurred during growth, which leads to terrace widths in the observed length scale. In collaboration with V. Holy, it has been shown that this step-bunching leads to the observed oblique roughness replication in Si/SiGe multilayers grown on miscut (001) Si substrates.

These investigations require in addition to the work done with laboratory x-ray sources experiments at synchrotron sources. We are grateful to DESY, HASYLAB, Hamburg, as well as to ESRF, Grenoble where x-ray diffraction and reflectivity work on these nanostructures has been performed. The MQW samples used for these investigations were grown by S. Zerlauth and F. Schäffler with the Si-Ge-C molecular beam epitaxy growth apparatus in the clean room of the semiconductor physics laboratory, Linz.

2.3 Quantum Well Infrared Detectors and Emitters for the Infrared

(M. Helm)

2.3.1 Infrared Detectors on the Basis of Si/SiGe Quantum Wells

The activities on the fabrication and characterization of infrared detectors on the basis of Si/SiGe quantum wells were continued. These detectors, with a spectral response between 4 and 10 µm, are highly sensitive and compatible with silicon technology. The fabrication in the clean room includes several steps of photolithography for the definition of etch and metallization areas, etching of the approximately 100 µm large detector mesas with reactive ion etching, as well as metallization for the formation of electrical contacts using electron beam evaporation. Finally, gold wires are bonded to the contact areas. The characteristics of the best detectors include a peak responsivity (at $\lambda = 5$ µm) of R = 75 mA/W and a detectivity D* of 2×10^{10}cm √Hz/W, both at a temperature of T = 77 K.

2.3.2 GaAs/AlGaAs Quantum Cascade Emitters

In collaboration with the Institute for Solid State Electronics at the TU Vienna activities were started to fabricate infrared sources on the basis of intersubband transitions in GaAs/AlGaAs quantum structures. The goal is the realization of a so called quantum cascade laser on the basis of GaAs, similar to the InP based laser, which has already been developed by other laboratories. The fabrication in the clean room again includes several photolithographical steps for the definition of etch and metallization areas, wet-chemical etching of the 100 µm large mesa structures, as well as metallization by e-beam evaporation for the forming of electrical contacts, and gold-wire bonding. Such structures already operate as infrared light emitting diodes, presently at a wavelength of around 7 µm. Eventually, stripe-shaped laser structures will be fabricated by using a suitable waveguide cladding and resonator. Their fabrication technology will require several steps more in the clean room.

2.3.3 Transport and Infrared Absorption in Semiconductor Superlattices

Transport and infrared absorption investigations were performed in GaAs/AlGaAs superlattices, aiming at the observation of a Wannier-Stark ladder and Bloch oscillations.

Standard mesa structures were fabricated using photolithography, wet-chemical etching, metallization, and bonding. The transport measurements show a negative differential resistance, in the infrared measurements the transition from minibands to a Wannier-Stark ladder could be demonstrated through a corresponding absorption line splitting.

2.4 Atomic Force and Scanning Tunneling Microscopy

(G. Springholz)

Atomic force microscopy (AFM) is extensively used for the characterization of the epitaxial layers grown in the three different molecular beam epitaxy systems at our institute. For the Si-Ge-C system, the main focus was on the characterization of the cross hatch surface pattern developed during strain relaxation of SiGe layers on Si substrates as a function of Ge content, rate of Ge increase in graded buffer layers and of growth conditions. A considerable part of these measurements were carried out in a research cooperation with the Daimler-Benz research laboratories in Ulm, Germany. For SiC layers, a distinct surface roughening was observed when the carbon content in the layer exceeds a certain critical value. Both observations have important implications for device applications. AFM was used also for defect characterization in strain relaxed SiGe layers where the defects are made visible by selective chemical etchants. For IV-VI semiconductor epitaxial layers, AFM is routinely able to resolve the atomic step structure on the surface and therefore the threading dislocation density in the layers can be directly determined by AFM measurements. AFM is here also used for determination of the size, density and size distribution of self-assembled PbSe quantum dots grown by MBE. Due to the high aspect ratio and highly faceted shape of these quantum dots, the true dot shape could be resolved only when using special ultra-sharp AFM tips. Similar measurements were also made on InAs dots on GaAs and for Ge dots on Si. Atomic force microscopy was also used as a metrology tool for determination of the critical dimensions of semiconductor nanostructures and for the development of sub-micron lithography and pattern transfer processes. We have also performed such measurements for industrial partners, in particular for Sony DAC, Salzburg, for characterization of process modifications in the production of compact discs.

For scanning tunneling microscopy (STM) under ultra-high vacuum conditions, we have designed and set up a new UHV vacuum chamber combined with a small UHV vacuum transfer chamber with which samples prepared by the molecular beam epitaxy systems can be transferred to the separate STM system all under ultra-high vacuum conditions in order to preserve the ultra clean surface structure present after epitaxial growth. With this new system we have investigated the growth mode transitions in strained-layer heteroepitaxy as well as the formation of subsurface defects such as interfacial misfit dislocations formed during lattice-mismatched epitaxial growth. In addition, we have also investigated the surface modifications due to buried 3D islands produced by strained-layer heteroepitaxy in the Stranski-Krastanow growth mode, which are of high interest for direct fabrication of quantum dots. Using spectroscopic techniques we found direct evidence for the electronic confinement in such structures by scanning tunneling microscopy.

As a final activity, we have also started a research activity on the development of submicron lithography based on mechanical modifications of thin photo resist layers by scanning force microscopy tips. As a first step we have successfully developed a spin

coating process for ultra-thin photo resist layers (thickness of 10 to 30 nm), which will be used as etch mask after modification by the AFM pattern generation.

2.5 Molecular Beam Epitaxy of IV-VI Heterostructures

(G. Springholz)

The activities on molecular beam epitaxy on IV-VI semiconductors were concentrated (a) on the direct synthesis of self-assembled quantum dots and (b) on the fabrication of Bragg mirrors for surface emitting lead-salt based optoelectronic devices for the 3 – 5 µm spectral region (mid infrared). Further work included the growth of short period magnetic semiconductor superlattices for the investigation of magnetic interlayer coupling and the preparation of various semiconductor heterostructures for surface studies by scanning tunneling microscopy.

The direct synthesis of self assembled quantum dots by molecular beam epitaxy is based on the general fact that for heteroepitaxy of highly strained layers, nano-scale three dimensional (3D) islands are spontaneously formed on the surface once a critical layer thickness is exceeded (Stranski-Krastanov growth mode). We have studied here a new materials system for the growth of self-assembled quantum dots, namely, heteroepitaxial growth of -5.4 % lattice-mismatched PbSe on PbTe (111), materials that have long been used for fabrication of efficient mid-infrared diode lasers. Epitaxial growth was studied using reflection high energy electron diffraction studies *in situ* during the deposition process and the evolution of surface morphology as a function of layer thickness determined by atomic force microscopy (AFM). We find that when a critical coverage of 1.5 monolayer is exceeded, first chains of PbSe islands are nucleated on the wetting layer, whereas homogenous nucleation sets in at a somewhat larger coverage. Both types of dots exhibit the same pyramidal shape that results from the formation of well defined (100) side facets. As compared to other materials systems (e.g. InAs/GaAs or SiGe/Si), the self-assembled PbSe quantum dots exhibit a remarkably narrow size distribution with relative variation of the dot heights of only ±10 %, which is more than a factor two smaller than for other materials. In addition, this small size variation is found to be independent of layer thickness. These facts indicate the presence of a highly effective mechanism for self-limitation of the island growth, which is obviously related to the highly faceted shape of the PbSe islands. Thus this materials system seems to be very promising for the investigation of zero dimensional quantum structures and for applications for mid-infrared light emitting devices.

With respect to the MIR Bragg mirrors, we have explored the possibilities to fabricate such mirrors by molecular beam epitaxy on the basis of IV-VI materials such that they can be used for IV-VI vertical cavity surface emitting lasers in the 3 – 5 µm region in order to achieve higher operation temperatures for the IV-VI diode lasers. As a starting point we have successfully designed and implemented the fabrication of a Bragg mirror stack consisting of 30 λ/4 layer pairs of $Pb_{1-x}Eu_xTe$ with alternating Eu content of 6 and 1 %, where the latter is realized as a short period PbTe/$Pb_{1-x}Eu_xTe$ superlattice. Thus, the whole structure consists of more the 1000 individual epitaxial layers and the total thickness is about 15 µm. The reflectivity of the Bragg mirror is tuned to the PbTe energy band gap at 77 K and optical measurements prove a more than 98% efficiency of the fabricated structures. For fabrication of a real laser structure, various wet chemical and plasma etching techniques for mesa definition, as well as the p-type doping of such mirrors was developed.

2.6 ZnSe/ZnCdSe Quantum Wire Structures Fabricated by MBE Growth on Patterned GaAs Substrates

(W. Heiss)

We have fabricated blue light emitting quantum wire structures by MBE growth of ZnCdSe/ZnSe quantum wells on patterned GaAs substrates. In particular, we structured (001)-oriented epi-ready GaAs substrates by laser holography using the 457.9 nm line of an Ar^+-ion laser. The period of the gratings were chosen to be between 600 nm and 800 nm. Wet chemical etching with a citric acid : H_2O_2 solution gave an etch rate of about 2 nm/s and resulted in U or V shaped grooves along the crystalline [1 -1 0] direction. Between the grooves, trapezoid-shaped stripes are formed with widths varying between 230 nm and 400 nm. The topology and surface quality of the achieved patterned substrates was checked by scanning electron microscopy and atomic force images. Prior to the growth, the substrates were cleaned and etched in hydrochloric acid for 30 s. This HCl etching procedure strongly improved the crystalline quality of the overgrown ZnSe layers.

On the patterned samples $Zn_{1-x}Cd_xSe$/ZnSe multilayer stacks were grown by MBE using elementary Zn, Cd and Se effusion cells. All samples were grown at a substrate temperature of 350 °C in an anion enriched growth regime. Prior to the growth the substrates were thermally cleaned in the UHV chamber at 650 °C until the characteristic reflection high energy electron diffraction (RHEED) pattern became visible. In the RHEED pattern, which exhibits a three dimensional spotty pattern, swallowtail features of the RHEED spots in [1 -1 0] direction reflected the geometry of the {1 1 1} sidewalls of the etched grooves. The growth rate of about 0.1 nm/s was monitored by laser interferometry and by observing the RHEED patterns.

2.7 II-VI Compound Heterostructures: Molecular Beam Epitaxy

(H. Sitter)

II-VI compound heterostructures based on ZnSe, ZnTe, CdSe, CdTe, MgSe, MgTe as well as ternary and quaternary compounds were grown on (001) GaAs as well as CdZnTe substrates. In particular, a computer based control system has been installed for choosing and controlling the growth parameters. *In situ* control is achieved through RHEED, laser interferometry in the visible spectral range, and *ex situ* control through scanning electron microscopy, transmission electron microscopy, photoluminescence reflectance difference spectroscopy, and x-ray diffraction.

In particular the studies on the doping limits of various II-VI compounds for p-type doping have been investigated. For that purpose two nitrogen plasma sources were developed and realized, one based on DC operation (discharge current) and the other on electron cyclotron resonance (ECR). The plasma parameters were characterized through optical spectroscopy.

Furthermore, RDS has been used for the first time as an *in situ* control method for the growth of II-VI epilayers in order to characterize surface processes which are related to doping. Using the linear electro-optical effect it turned out to be possible to optimize the doping process and to determine the doping concentration *in situ*. Using these *in situ* control methods further improvements in the realization of blue electro-luminescent II-VI heterostructure-diodes were achieved.

2.8 A Matched InGaAs Detector Diode for a Ka-Band Radar Front-End

(K. Lübke, G. Haider, C.G. Diskus, A. Stelzer, A.L. Springer, H.W. Thim)

2.8.1 Introduction

The demand for an increase in data transfer rate and sensor sensitivity raises the interest in devices for millimeter wave applications. The advantage of millimeter-wave sensors is their robustness against environmental factors like dust, water vapor, and noise.

In millimeter-wave systems suited for automotive applications Schottky-barrier diodes are used for detecting and mixing signals because of their high switching speed which results from the unipolar conduction mechanism. III-V semiconductors are the preferred materials because of their higher electron mobility. In this work the design and fabrication procedures of a GaAs FECTED oscillator and a zero bias $In_{0.38}Ga_{1-0.38}As$-Schottky detector diode for 35 GHz are described.

2.8.2 Experimental

The voltage sensitivity of a detector diode is a function of the reverse saturation current. For optimum sensitivity this current has to be in the range of 10^{-6} A. To achieve this value with GaAs technology at zero bias – which is desirable to keep the circuit as simple as possible – the barrier height must be tailored to 0.22 – 0.25 eV by incorporating indium. With increasing In content the energy gap of the semiconductor is lowered from 1.42 eV (GaAs) to 0.33 eV (InAs). With $In_{0.38}Ga_{0.62}As$ the desired barrier height of the Schottky contact can be adjusted. The diodes have been fabricated using epitaxial layers of GaAs and InGaAs grown by metal organic vapor deposition (MOCVD) on GaAs substrates. Ni/GeAu/Ni/Au films have been evaporated thermally respectively by e-beam and annealed to form ohmic contacts on n-type layers, Ti/Au and Cr/Au were evaporated and used for Schottky contacts. The ohmic contacts have been recessed by wet chemical etching and the connection to the Schottky contact on the top is led over a SiO_2 bridge. The etching of the SiO_2 has been performed in a reactive ion etching (RIE) reactor.

For reduced bandwidths the sensitivity can be further improved by matching the impedance of the diode to the characteristic impedance of the transmission line. The equivalent circuit of the diode has been deduced from network analyzer measurements. For the frequency range of 34 – 36 GHz a matching circuit consisting of a microstrip stub terminated by a radial stub has been designed and fabricated (Fig. 4).

The oscillator is a special planar Gunn diode (FECTED, Field Effect Controlled Transferred Electron Device) instead of a sophisticated transistor oscillator [1]. The device and the circuit have been fabricated on a 4 x 5 mm^2 GaAs chip with standard processing technologies. Further details of the FECTED have been published in [2].

The patterns for the contact pads, the interconnections and the matching network have been transferred to the substrate using both optical and e-beam lithography.

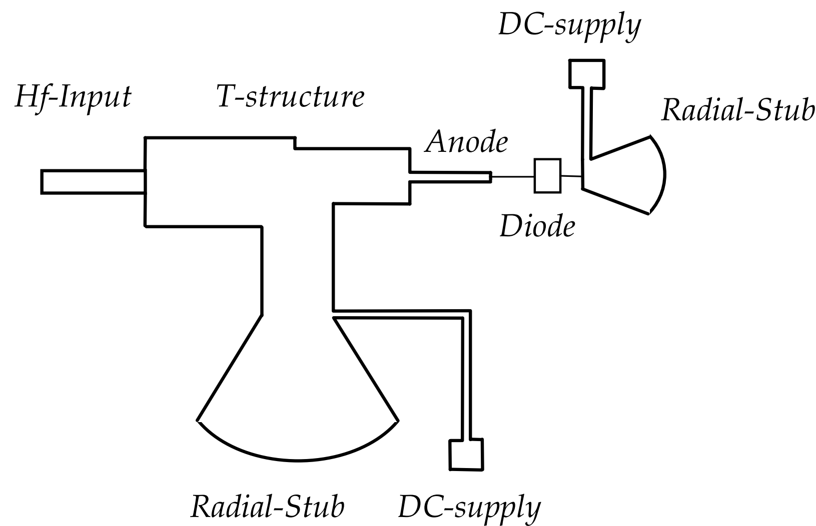

Fig. 4: Schematic illustration of the matching network for the detector diode.

A relatively inexpensive RT/duroid® 5880 (a trademark of Rogers Corp.) substrate material has been used for the fabrication of the antennas and the 10 dB directional coupler. Each antenna consists of 8 x 8 microstrip patches yielding a beamwidth of 8 degrees.

To guarantee a sufficiently high signal level at the A/D-converter an amplifier with automatic gain control (AGC) is provided. A band-pass filter enhances the quality of the signal by eliminating both noise and low frequency variations. The Doppler signal is converted with a resolution of 16 bit. The signal processing is performed on a DSP-board (Digital Signal Processor) equipped with a SHARC (Super Harvard Architecture Computer, Analog Devices Inc.) signal processor.

2.8.3 Conclusion

The speed sensor has been built and evaluated using an automatic test bench. An accuracy of 0.1 % has been achieved in the case of a corner reflector moving at constant speed. The maximum operational range exceeds 25 m.

2.8.4 Acknowledgments

The authors would like to thank M. Hinterreiter and J. Katzenmayer for fabricating and testing the devices. This work was supported by the Austrian Science Foundation (FWF) under Contract number P11424-ÖPY.

References

[1] C. G. Diskus, K. Lübke, A. L. Springer, H. W. Lettenmayr, H. W. Thim: “GaAs Field Effect Controlled Transferred Electron (FECTED) Oscillator MMIC”, WOCSDICE ’92

[2] K. Lübke, H. Scheiber and H. Thim: “A Voltage Tunable 35 GHz Monolithic GaAs FECTED oscillator”, *IEEE Microwave and Guided Wave Letters*, (1991) 1, n°2, pp. 35-37

Project Information

Project Manager

Univ.Ass. Dr. Gerhard BRUNTHALER

Institut für Halbleiter- und Festkörperphysik, Johannes Kepler Universität Linz

Project Group

Last Name	First Name	Status	Remarks
Bauer	Günther	Full professor	
Bonanni	Alberta	Ph.D. student	
Brunthaler	Gerhard	Univ. Assistent	
Diskus	Christian	Assistant professor	
Fünfstück	Britta	Diploma student	
Haider	Gerhard	Diploma student	
Heiss	Wolfgang	Univ. Assistent	
Helm	Manfred	Assistant professor	
Hilber	Wolfgang	Ph.D. student	
Hinterreiter	Marion	Technician	
Kainz	Ursula	Technician	
Katzenmayer	Hans	Technician	
Kocher	Gudrun	Diploma student	
Köck	Franz	Diploma student	
Kolmhofer	Gerald	Diploma student	
Kruck	Peter	Ph.D. student	
Lübke	Kurt	Univ. Assistent	
Mikulik	Petr	Postdoc	
Mühlberger	Michael	Diploma student	
Pinczolits	Michael	Ph.D. student	
Rabeder	Klaus	Technician	
Sandersfeld	Nils	Ph.D. student	
Sandner	Harald	Diploma student	
Schäffler	Friedrich	Associate professor	
Schelling	Christoph	Ph.D. student	
Schmid	Michael	Ph.D. student	
Schwarzl	Thomas	Diploma student	

Last Name	First Name	Status	Remarks
Seyringer	Heinz	Ph.D. student	
Sitter	Helmut	Assistant professor	
Springer	Andreas	Univ. Assistent	
Springholz	Gunther	Univ. Assistent	
Stangl	Julian	Ph.D. student	
Steinbacher	Günther	Diploma student	
Stelzer	Andreas	Ph.D. student	
Stifter	David	Ph.D. student	
Straub	Hubert	Ph.D. student	
Thim	Hartwig	Full professor	
Ueta	Yukio	Ph.D. student	
Wiesauer	Karin	Diploma student	
Wirtl	Elisabeth	Technician	
Wurm	Ernst	Technician	
Zerlauth	Stefan	Ph.D. student	
Zhuang	Yan	Ph.D. student	

Publications in Reviewed Journals

1. G. Brunthaler, T. Dietl, A. Prinz, G. Stöger, M. Sawicki, J. Jaroszynski, F. Schäffler, G. Bauer: “Magnetic field induced metal to insulator transition in Si/SiGe short period superlattices”, Proc. of 12th Int. Conf. on the Application of High Magnetic Fields in Semiconductor Physics, July 29 - August 2, 1996, eds. G. Landwehr, W. Ossau, World Scientific Publishing 1997, p. 995-968.
2. A.A. Darhuber, V. Holy, J. Stangl, G. Bauer, A. Krost, F. Heinrichsdorff, M. Grundmann, D. Bimberg, V.M. Ustinov, P.S. Kop’ev, A.O. Kosogov, P. Werner: “Lateral and vertical ordering in multilayered self-organized InGaAs quantum dots studied by high resolution x-ray diffraction”,Appl. Phys. Lett. 70, 955-957 (1997)
3. A.A. Darhuber, V. Holy, J. Stangl, G. Bauer, A. Krost, M. Grundmann, D. Bimberg, V.M. Ustinov, P.S. Kop’ev, P. Werner: “High-resolution x-ray diffraction and reflectivity studies of vertical and lateral ordering in multiple self-organized InGaAs quantum dots”,Jap. J. Appl. Phys. 36, 4084-4087 (1997)
4. A.A. Darhuber, J. Stangl, G. Bauer, P. Schittenhelm, G. Abstreiter: “X-ray diffraction and reflection from self-assembled Ge-dots”,Thin Solid Films 294, 269-299 (1997)
5. A.A. Darhuber, P. Schittenhelm, V. Holy, J. Stangl, G. Bauer, G. Abstreiter: “High resolution x-ray diffraction from multilayered self-assembled Ge-dots”,Phys. Rev. B55, 15652-15663 (1997)
6. A.A. Darhuber, J. Stangl, V. Holy, G. Bauer, A. Krost, M. Grundmann, D. Bimberg, V.M. Ustinov, P.S. Kop’ev, A.O. Kosogov, P. Werner: “Structural characterization

of self-assembled quantum dot structures by x-ray diffraction techniques",Thin Solid Films, 306, 198-204 (1997)

7. M. Helm: "Superlattice lasers go to longer wavelengths" Physics World 10, No. 7 (July 1997), p. 26-27
8. M. Helm, P. Kruck, T. Fromherz, A. Weichselbaum, M. Seto, G. Bauer, Z. Moussa, P. Boucaud, F. H. Julien, J.-M. Lourtioz, J. F. Nützel, G. Abstreiter: "Infrared studies of p-type Si/SiGe quantum wells: intersubband absorption, infrared detectors, and second-harmonic generation" Thin Solid Films 294, 330-335 (1997)
9. V. Holy, G. Bauer, J.-H. Li, F. Schäffler, H.-J. Herzog, K. Wolf, S. Jilka, H. Stanzl, W. Gebhardt: "Diffuse x-ray scattering from epitaxial thin layers", Surface Investigation 12, 329-344 (1997)
10. J.H. Li, V. Holy, G. Bauer, F. Schäffler: "Strain relaxation in high electron mobility Si1-xGex/Si structures", J. Appl. Phys. 82, 2881-2886 (1997)
11. C. Penn, S. Zerlauth, J. Stangl, G. Bauer, G. Brunthaler, F. Schäffler: "Influence of thermal annealing on the photoluminescence from preudomorphic Si1-yCy epilayers on Si", Appl. Phys. Lett. 71, 2172-2174 (1997)
12. F. Schäffler: "High-mobility Si and Ge structures", Semicond. Science and Technology, 12, 1515-1549 (1997)
13. G. Springholz: "Strain contrast in scanning tunneling microscopy imaging of subsurface dislocations in lattice-matched heteroepitaxy", Appl. Surf. Sci. 112, 12-22 (1997)
14. G. Strasser, P. Kruck, M. Helm, J. N. Heyman, L. Hvozdara, E. Gornik: "Mid-infrared electroluminescence in GaAs/AlGaAs structures" Appl. Phys. Lett. 71, 2892-2894 (1997).
15. A.Y. Ueta, G. Springholz, F. Schinagl, G. Marschner, G. Bauer: "Doping studies for molecular beam epitaxy of PbTe and Pb1-xEuxTe", Thin Solid Films, 306, 320-325 (1997)
16. S. Zerlauth, J. Stangl, A.A. Darhuber, V. Holy, G. Bauer, F. Schäffler: "MBE growth and structural characterization of Si1-yCy/Si1-xGex superlattices", Proc. 9th Int. Conf. on Molecular Beam Epitaxy, August 5-9, 1996, Pepperdine University, Malibu, California; J. Crystal Growth 175/176, 459-464 (1997)
17. S. Zerlauth, H. Seyringer, C. Penn, F. Schäffler: "Growth conditions for complete substitutional carbon incorporation into Si1-yCy layers grown by molecular beam epitaxy", Appl. Phys. Lett. 71, 3826-3828 (1997)
18. M. Berti, D.De Salvador, A.V. Drigo, R. Romanato, J. Stangl, S. Zerlauth, F. Schäffler, G. Bauer: "Lattice parameter in Si1-yCy epilayers: deviation from Vegard´s rule", Appl. Phys. Lett., accepted for publication
19. G. Brunthaler, T. Dietl, A. Prinz, M. Sawicki, J. Jaroszynski, P. Glod, F. Schäffler, G. Bauer, D.K. Maude, J.C. Portal: "Interaction effects at the magnetic-field induced metal-insulator transition in Si/SiGe superlattices", Solid State Commun., in print
20. A.A. Darhuber, V. Holy, P.Schittenhelm, J. Stangl, I. Kegel, Z. Kovats, T.H. Metzger, G. Bauer, G. Abstreiter, G. Grübel: "Structural characterization of self-

assembled Ge dot multilayers by x-ray diffraction and reflectivity methods", Physica E, in print

21. A.A. Darhuber, G. Bauer, P.D. Wang, C.M. Sotomayor Torres: "Shear strains in dry etched GaAs/AlAs wires studied by high resolution x-ray reciprocal space mapping", J. Appl. Phys., in print
22. V. Holy, A.A. Darhuber, J. Stangl, G. Bauer, J. Nützel, G. Abstreiter: "X-ray reflectivity investigations of the interface morphology in strained SiGe/Si multilayers", Semicond. Sci. Technol., submitted
23. V. Holy, A.A. Darhuber, J. Stangl, G. Bauer, J. Nützel, G. Abstreiter: "Oblique roughness replication in strained SiGe/Si multilayers", Phys. Rev. B, submitted
24. L. Hvozdara, J.N. Heyman, G. Strasser, K. Unterrainer, P. Kruck, M. Helm, E. Gornik: "Characterization of GaAs/AlGaAs mid-infrared emitters" Proc. 24th Int. Symp. on Compound Semiconductors (ISCS 24), in print (1997)
25. P. Kruck, A. Weichselbaum, M. Helm, T. Fromherz, G. Bauer, J. F. Nützel, G. Abstreiter: "Polarization dependent intersubband absorption and normal-incidence infrared detection in p-type Si/SiGe quantum wells" Superlattices and Microstructures, in print
26. P. Kruck, M. Helm, G. Bauer, J. F. Nützel, G. Abstreiter: "Normal-incidence p-type Si/SiGe mid-infrared detector with background-limited performance up to 85 K" Proc. Int. Conf. on Intersubband Transitions in Quantum Wells: Physics and Applications, Kluwer, Dordrecht, 1998, to be published
27. P. Kruck, M. Helm, G. Strasser, L. Hvozdara, E. Gornik: "Quantum cascade electroluminescence in the GaAs/AlGaAs material system", Proc. Int. Conf. on Intersubband Transitions in Quantum Wells: Physics and Applications, Kluwer, Dordrecht, 1998, to be published
28. P. Kruck, G. Strasser, M. Helm, L. Hvozdara, E. Gornik: "Quantum cascade electroluminescence in GaAs/AlGaAs structures", Proc. 8th Int. Conf. on II-VI Compounds, Grenoble 25-29. August 1997, France; Physica B, in print
29. J.H. Li, G. Springholz, H. Seyringer, V. Holy, F. Schäffler, G. Bauer: "Strain relaxation and surface morphology of compositionally graded Si/Si1-xGex buffers", Proc. Int. Conf. on SiGe Heterostructures, Barga 16.-20. Sept. 1997, Italy; J. Vac. Sci. Technol. (in press)
30. C. Penn, S. Zerlauth, J. Stangl, G. Bauer, G. Brunthaler, F. Schäffler: "Photoluminescence from pseudomorphic Si1-yCy layers on Si substrates", J. Vac. Sci. and Technol., submitted
31. F.Schäffler: "Si/Si1-xGex and Si/Si1-yCy Heterostructures: Materials for High-Speed Field-Effect Transistors", Thin Solid Films, in press
32. S. Senz, A. Plößl, U. Gösele, S. Zerlauth, J. Stangl, G. Bauer: "Growth of partially strain-relaxed Si1-yCy epilayers on (100) Si", Applied Phys. A, submitted
33. G. Springholz, Z. Shi and H. Zogg: "Molecular beam epitaxy of narrow gap IV-VI semiconductors", in: Heteroepitaxy: Thin Film Systems, ed. A. W. K. Liu and M. B. Santos (World Scientific Publishing Co., Singapore), in print.

34. J. Stangl, A.A. Darhuber, V. Holy, M.de Naurois, S. Ferreira, W. Faschinger, G. Bauer: “High resolution x-ray diffraction and x-ray reflectivity studies of short-period CdTe/MnTe superlattices”, J. Crystal Growth, in print

35. S. Zerlauth, C. Penn, H. Seyringer, J. Stangl, G. Brunthaler, G. Bauer, F. Schäffler: “Molecular beam epitaxial growth and photoluminescence investigatione of Si1-yCy layers”, Thin Solid Films, in print

36. S. Zerlauth, C. Penn, H. Seyringer, G. Brunthaler, G. Bauer, F. Schäffler: “Substitutional carbon incorporation into MBE-grown Si1-yCy layers”, Proc. Int. Conf. on SiGe Heterostructures, Barga, 16.-20. September 1997, Italy; J. Vac. Sci. and Technol., submitted

37. Y. Zhuang, S. Zerlauth, T. Grill, A.A. Darhuber, C. Penn, F. Schäffler, G. Bauer: “Characterization of reactive ion etched Si/SiGe nanostructures”, Beiträge der Informationstagung ME 97, ISBN 3-85133-010-2, 209-214 (1997)

38. A.A. Efanov, C.G. Diskus, A. Stelzer, H.W. Thim, K. Lübke, and A.L. Springer: “Development of a Low-Cost 35 GHz Radar Sensor”, Annales des Télécommunications / Annals of Telecommunications, Special Issue to the International Workshop on Millimeter Waves, Vol. 52, Nr. 3–4, March–April 1997, pp. 219–224. ISSN 0003-4347

Presentations

1. M. Helm: “Energy relaxation of electrons in GaAs/AlGaAs quantum wells and superlattices”, Int. Conference on “Intersubband Transitions in Quantum Wells: Physics and Devices”, Tainan, Taiwan, Dezember 1997.
2. M. Helm: “Normal-incidence p-type Si/SiGe infrared detectors”, Int. Conference on “Silicon Heterostructures: from Physics to Devices”, Il Ciocco, Barga, Italien, September 1997.
3. P. Kruck, T. Fromherz, M. Helm, G. Bauer, J. Nützel and G. Abstreiter: “Si/SiGe based quantum well infrared photodetectors: intersubband absorption and photoconductivity”, Workshop on Semiconductor Infrared Detectors and Emitters, NRC, Ottawa, Canada, July 23-25, 1997.
4. F. Schäffler: “Si/SiGe and Si/SiC Heterostructures: Materials for High-Speed Field-Effect Transistors”, 7th. Int. Symp. Silicon Molecular Beam Epitaxy, Banff, Canada, Juli 1997
5. G. Springholz: “Molecular Beam Epitaxy and Scanning Tunneling Microscopy of IV-VI Semiconductor Heterostructures”, 8th International Conference on Narrow Gap Semiconductors, Shanghai, China, April 1997
6. A.A. Darhuber: “X-ray diffraction and refelction from self assembled quantum dots” 3rd Autumn School on X-ray Scattering from Surfaces and Thin Layers, 1. – 4.10.1997, Smolenice, Slovakia
7. P. Kruck, G. Strasser, M. Helm, L. Hvozdara, E. Gornik: “Quantum cascade electroluminescence in GaAs/AlGaAs structures”, 8th Int. Conf. on Modulated Semiconductor Structures, Santa Barbara, CA, USA, July 1997.

8. P. Kruck, M. Helm, G. Strasser, L. Hvozdara, E. Gornik: “Quantum cascade electroluminescence in the GaAs/AlGaAs material system”, Int. Conference on “Intersubband Transitions in Quantum Wells: Physics and Devices”, Tainan, Taiwan, Dezember 1997
9. P. Kruck, M. Helm, G. Bauer, J. F. Nützel, G. Abstreiter: “Normal-incidence p-type Si/SiGe mid-infrared detector with background limited performance up to 85 K” Int. Conference on “Intersubband Transitions in Quantum Wells: Physics and Devices”, Tainan, Taiwan, Dezember 1997
10. J.H.Li, G.Springholz, H.Seyringer, V.Holy, F.Schäffler, and G.Bauer: “Strain relaxation and surface morphology of compositionally graded Si/Si1-xGex buffers” Int. Conference on “Silicon Heterostructures: from Physics to Devices”, Barga, Italien, September 1997
11. C.Penn, S.Zerlauth, J.Stangl, G.Bauer, and F.Schäffler: “Photoluminescence from pseudomorphic Si1-yCy layers on Si substrate Int. Conference on “Silicon Heterostructures: fromPhysics to Devices”, Barga, Italien, September 1997
12. S. Zerlauth, C. Penn, H. Seyringer, J. Stangl, G. Brunthaler, G. Bauer, and F. Schäffler: “Molecular beam epitaxial growth and photoluminescence investigations of SiGeC layers”, 7th. Int. Symp. on Silicon Molecular Beam Epitaxy, Banff, Canada, Juli 1997
13. S. Zerlauth, C. Penn, H. Seyringer, G. Brunthaler, G. Bauer, and F. Schäffler: “Substitutional carbon incorporation into MBE-grown Si1-yCy layers”, Int. Conference on “Silicon Heterostructures: from Physics to Devices”, Barga, Italien, September 1997
14. G. Springholz: “Strain effects in lattice-mismatched heteroepitaxial growth”, Gordon Research Conference on Epitaxial Thin Films, Plymouth, USA, July 1997
15. F. Köck, M. Pinczolits and G. Springholz: “UHV-STM investigations of subsurface defects in semiconductor heterostructures”, 9th Int. Conference on Scanning Tunneling Microscopy/Spectroscopy and Related Techniques Hamburg, Germany, July 1997
16. Y. Zhuang: “Diffraction and reflectivity studies on Si/SiGe reactive ion etched periodic wire and dot structures” 3rd Autumn School on X-ray Scattering from Surfaces and Thin Layers, 1.-4.10.1997, Smolenice, Slovakia
17. A.A. Efanov, K. Lübke, Ch. Diskus, A. Springer, A. Stelzer, H. W. Thim: “Development of a 35 GHz Radar Sensor”, Proceedings of the Seminar Basics and Technology of Electronic Devices, organized by the Society for Microelectronics (Gesellschaft für Mikroelektronik – GMe), 19th–22nd March 1997, Großarl / Pongau, pp. 11–16. ISBN 3-901578-02-1
18. K. Lübke, T. Hilgarth, C. Diskus, A. Stelzer, A. Springer, and H.W. Thim: “Zero-bias Detection with In0.38Ga0.62As Schottky Barrier Diodes”, Digest to the 21st Workshop on Compound Semiconductor Devices and Integrated Circuits (WOCSDICE ’97), May 25–28, 1997, Scheveningen, The Netherlands, pp. 114–115
19. L. Springer, C.G. Diskus, K. Lübke, A. Stelzer, H.W. Thim: “Transferred Electron Effect in AlGaAs/GaAs Multi-Quantum-Well Structures”, Digest to the 27th

European Solid State Device Research Conference (ESSDERC ‘97), 22. – 24. Sept. 1997, Stuttgart, Germany, pp. 296-299, ISBN 2-86332-221-4

20. A. Stelzer, C. Diskus, A. Efanov, K. Lübke, A. Springer und H. W. Thim: “Ein 35 GHz Low-Cost Radar Sensor”, Beiträge der Informationstagung Mikroelektronik, ME’97, Wien, Österreichischer Verband für Elektrotechnik, S. 135 – 140. ISBN 3-85133-010-2

Patents

1. H. Thim, K. Lübke: “Hot Electron Injection Field Effect Transistor (HEIFET)” Patentanmeldung beim Österreichischen Patentamt am 22. 05. 1997, Geschäftszahl A 868/97

Doctor’s Theses

1. Dipl.-Phys. Peter Kruck, “Infrared spectroscopy of semiconductor quantum well systems”, Linz, 1997
2. Dipl.-Phys. Hubert Straub, “Lateral patterning of II-VI compounds by holographic lithography and reactive ion etching”, Linz, 1997
3. M.Sc. Yukio Ueta, “MBE growth and characterization of PbTe/Pb1-xEuxTe epitaxial layers”, Linz, 1997
4. Dipl.-Ing. Stefan Zerlauth, “Molecular beam epitaxy of SiGeC”, Linz, 1997
5. Dipl.-Ing. Edwin Wirthl, “Auger Electron Spectroscopy on II-VI semiconductors”, Linz, 1997

Habilitations

1. C.G. Diskus, Halbleiterbauelemenete für die Mikrowellentechnik, Linz, 1997

Cooperations

1. Siemens München, Dr.Heide
2. Daimler Benz Reserach Laboratories Ulm, Dr. Presting, Dr. König
3. VOEST ALPINE, Linz, Dr.Angerer,
4. Siemens Villach,
5. AMS Unterpremstätten, Dr.Fromherz
6. KEBA, Linz, Ing.G.Krippner
7. Institut für Halbleiterphysik, Frankfurt/Oder
8. Sektion Physik, Ludwig-Maximilians Universität München
9. Physics Department, Cornell University
10. ETH, Zürich

11. ESRF Grenoble
12. DESY, Hasylab, Hamburg
13. FOM Institute Rijnhuizen, Niederlande
14. Walter Schottky Institut, TU München
15. IBM Research Center, Yorktown Heights
16. Institut für Festkörperelektronik, TU Wien
17. Philips Almelo, Niederlande
18. Heriot Watt University, Edinburgh, Scotland
19. University of Southampton, England
20. High Pressure Research Center, Warschau, Polen
21. Institue of Physics, Polish Academy of Sciences, Warschau
22. TU Berlin, Institut für Festkörperphysik
23. Universität Würzburg
24. Universität Bayreuth
25. Universität Bremen
26. Purdue University, Lafayette, IN, USA
27. MIT, Cambridge, MA, USA
28. NIST, Gaithersburg, MD, USA
29. Nanoelectronics Research Center, University of Glasgow, Scotland
30. University of Warwick, Coventry, England
31. North Carolina State University, NC, USA
32. IAF Freiburg
33. CENG Grenoble
34. Universität Paderborn
35. INSA, Lyon
36. Université de Montpellier
37. ELETTRA, Triest
38. Universiteit Instelling, Antwerpen, Niederlande
39. TASC Triest
40. ENEA, Roma
41. CNRSM-PASTIS, Brindisi
42. Akademie der Wissenschaften, Troitsk, Moskau
43. High Magnetic Field Lab., Grenoble

ZnSe/ZnCdSe Quantum Wires on Patterned Substrates

W. Heiß, D. Stifter, G. Prechtl, H. Sitter, W. Jantsch

Institut für Halbleiter- und Festkörperphysik,
Johannes Kepler Universität Linz, A-4040 Linz, Austria

Wide gap II-VI semiconductor compounds are important materials for the fabrication of blue light emitting laser diodes. In this contribution ZnSe/ZnCdSe is used to fabricate quantum well wires. This is achieved by MBE growth on nonplanar GaAs substrates, which are submicrometer gratings with U or V shaped grooves and trapezoidal shaped ridges. In these samples blue luminescence is observed up to room temperature. One dimensional confinement effects are observed by several experiments due to the lateral modulation of the electron gas in the quantum well.

1. Introduction

The first semiconductor lasers emitting green or blue light are based on wide gap II-VI compounds. In particular ternary ZnCdSe alloys have been used in the active zone of these laser structures [1], [2]. II-VI laser diodes are not available commercially, since the lifetimes of these devices are restricted to several hundred hours. To date, blue light emitting semiconductor lasers based on the GaN material system are more promising for industrial applications. Nevertheless, for several reasons, still lots of efforts are put in the development of laser diodes based on II-VI compound semiconductors.

For III-V semiconductor lasers emitting in the near infrared it was demonstrated already that devices realized from quantum well wire structures possess superior properties, like reduced threshold currents or narrowed emission bandwidths, compared to conventional quantum well lasers [3]. The aim of this work is to fabricate ZnSe/ZnCdSe quantum wire structures using the same technologies as used for the fabrication of laser diodes. ZnSe/ZnCdSe quantum wires showing lateral confinement effects have been achieved in the past by electron beam lithography and wet chemical etching or reactive ion etching. However, these technologies are not commonly used for laser fabrication. In this report we investigate the possibility to obtain II-VI quantum wire structures by MBE-growth on patterned GaAs substrates.

2. Sample Structures and Results

A cross section of a typical sample is sketched in Fig. 1. We use GaAs gratings with submicrometer periods having U-shaped or V-shaped grooves in a crystalline $[1\ \bar{1}\ 0]$ direction as substrates. On the substrates ZnSe/ZnCdSe multilayers are grown by molecular beam epitaxy. In particular, ZnSe buffer layers with various thicknesses are grown, followed by a ZnCdSe quantum well, 50 Å thick, and finally by a ZnSe capping layer. A quantum wire is formed due to the dependence of the growth rate on the crystalline orientation. Thus, the lateral width of the quantum wire is determined not only by

the period of the substrate, but also by the thickness of the buffer layer. Therefore, wire widths much smaller than the period of the substrate can be achieved.

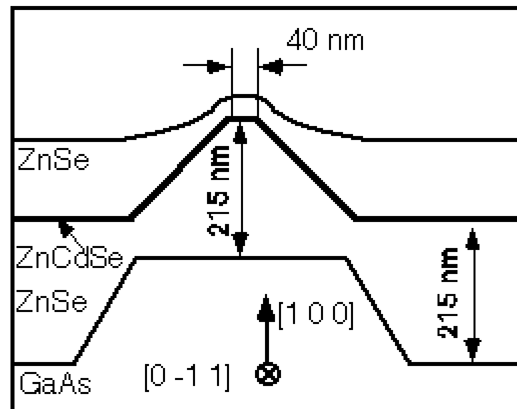

Fig. 1: Cross section of a typical ZnSe/ZnCdSe quantum well sample.

We have obtained ZnSe/ZnCdSe quantum wire structures, giving intense blue luminescence up to room temperature. TEM images have revealed that the quantum wires are formed on top of the GaAs ridges as sketched in Fig. 1. Depending on the sample structure, luminescence blue shifts up to 10 meV due to the lateral confinement are observed [4]. Furthermore, confinement induced optical anisotropies are observed for several samples [4]. The spatially resolved cathodoluminescence image in Fig. 2 shows clearly a stripe-like intensity distribution of the luminescence confirming the quantum wire nature of our obtained sample structures. Both X-ray investigations and photoluminescence experiments indicate a complex, lattice mismatch induced strain distribution in the quantum structures [5]. Finally, time resolved luminescence experiments reveal a modulation of the exciton-recombination time due to the lateral confinement. This fact opens us the possibility to design the exciton recombination time by nanostructurizing the quantum well samples. This can have important consequences for the improvement of blue light emitting II-VI laser diodes.

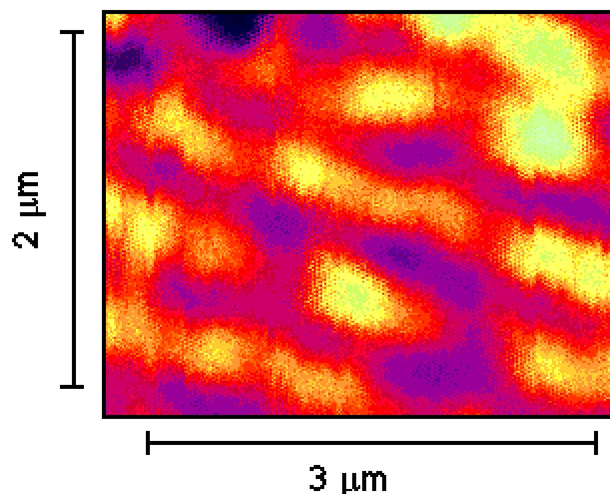

Fig. 2: Spatial resolved cathodoluminescence intensity.

3. Conclusion

We have fabricated blue light emitting ZnSe/ZnCdSe quantum wires by MBE growth on patterned GaAs substrates. The achieved structures have been investigated by transmission electron microscopy, X-ray measurements and spatial and temporal resolution in photoluminescence experiments. All performed experiments show confinement effects due to a lateral modulation of the two-dimensional electron gas in the quantum well.

Acknowledgments

This work was partially supported by the Austrian Science Foundation (FWF) under contract number P12100-PHY.

References

[1] M. A. Haase, J. Qiu, J. M. DePuydt, H. Cheng: “Blue-green laser diodes”, *Appl. Phys. Lett.*, Vol.59, 1272 –1274, 1991

[2] H. Jeon, J. Ding, W. Patterson, A. V. Nurmikko, W. Xie, D. C. Grillo, M. Kobayashi, R. L. Gunshor: “Blue-green injection laser diodes in (Zn,Cd)Se/ZnSe quantum wells”, *Appl. Phys. Lett.*, Vol. 67, 3619-3621, 1991

[3] S. Tiwari, J. M. Woodall: “Experimental comparison of strained quantum-wire and quantum-well laser characteristics”, *Appl. Phys. Lett.*, Vol. 64, 2211-2213, 1994

[4] W. Heiß, D. Stifter, G. Prechtl, A. Bonanni, H. Sitter, J. Liu, L. Toth, A. Barna: “Lateral confinement in ZnSe/ZnCdSe quantum wells grown on patterned substrates”, *Appl. Phys. Lett.*, Vol. 72, 1998, in print

[5] D. Stifter, W. Heiß, A. Bonanni, G. Prechtl, M. Schnid, K. Hingerl, H. Seyringer, H. Sitter, J. Liu, E. Gornik, L. Toth, A. Barna: “Molecular beam epitaxy of ZnSe/ZnCdSe wires on patterned GaAs substrates”, *J. of Crystal Growth*, 1998, in print

Project Information

Project Manager

Univ.-Prof. Dr. Wolfgang JANTSCH

Institut für Halbleiter und Festkörperphysik, Johannes Kepler Universität Linz

Project Group

Last Name	First Name	Status	Remarks
Heiß	Wolfgang	Assistant professor	
Jantsch	Wolfgang	University professor	
Prechtl	Gerhard	Student	
Sitter	Helmut	Associate professor	
Stifter	David	Dissertation	
Wirtl	Elisabeth	Technician	50% GMe funding

Publications in Reviewed Journals

1. D. Stifter, W. Heiß, A. Bonanni, G. Prechtl, M. Schnid, K. Hingerl, H. Seyringer, H. Sitter, J. Liu, E. Gornik, L. Toth, A. Barna: “Molecular beam epitaxy of ZnSe/ZnCdSe wires on patterned GaAs substrates”, J. of Crystal Growth, 1998, in print
2. W. Heiß, D. Stifter, G. Prechtl, A. Bonanni, H. Sitter, J. Liu, L. Toth, A. Barna: “Lateral confinement in ZnSe/ZnCdSe quantum wells grown on patterned substrates”, *Applied Physics Letters*, Vol. 72, 1998, in print

Presentations

1. D. Stifter, W. Heiß, A. Bonanni, G. Prechtl, M. Schmid, K. Hingerl, H. Seyringer, H. Sitter, J. Liu, E. Gornik, L. Toth, A. Barna: “Molecular beam epitaxy of ZnSe/ZnCdSe wires on patterned GaAs substrates”, *8th. Conference on II-VI compounds*, August 25-29 1997, Grenoble (France)

Doctor’s Theses

1. David Stifter: MBE von II-VI Vielschichtstrukturen, Universität Linz, 1998.

Cooperations

1. Research Institute for Technical Physics of the Hungarian Academy of Sciences, Budapest, Prof. L. Toth
2. Institut für Festkörperphysik, Universität Bremen, Prof. J. Gutowski
3. Institut für Experimentalphysik, Universität Magdeburg, Prof. J. Christen

$Si/Si_{1-x-y}Ge_xC_y$ Heterostructures

F. Schäffler and G. Bauer

Institut für Halbleiter- und Festkörperphysik, Abteilung für Halbleiterphysik,
Johannes Kepler Universität, A-4040 Linz, Austria

$Si/Si_{1-x-y}Ge_xC_y$ heterostructures are promising candidates for all-pseudomorphic n-type hetero-MOSFETs with enhanced electron mobilities that could become an alternative to n-channel Si/SiGe structures on virtual SiGe substrates. We report on the successful optimization of the growth parameters for this novel material combination, which allowed us to overcome problems reported in the literature concerning complete substitutional carbon incorporation into the intrinsically metastable $Si_{1-y}C_y$ layers. By concise characterization of the epi-layers with photoluminescence, x-ray diffraction and refraction, and atomic force microscopy, we could also establish a range of growth and annealing conditions that allows a low defect density and a smooth surface morphology. Thus we surpassed in several respects the state-of-the-art quality standards in this material system and achieved a sound material basis that will allow further assessment of this heterosystem regarding future high-performance device applications.

1. Introduction

It is the outstanding property of Si-based heterostructures to provide the application relevant combination of bandstructure engineering and the compatibility with silicon very-large-scale-integration (VLSI). In the past few years most of the basic properties regarding the lattice mismatched $Si/Si_{1-x}Ge_x$ material combination, and especially the effects of strain on the band offsets and bandgaps, have been investigated [1]. It has been found that the band offset at the interface between a pseudomorphic $Si_{1-x}Ge_x$ layer and a Si substrate occurs almost exclusively in the valence bands, whereas a tensilely strained Si layer is required for the implementation of useful conduction band offsets. By employing proper combinations of pseudomorphic and strain-relaxed epi-layers, both tensile and compressive strains can be custom designed, without sacrificing the important advantages of a Si substrate and the basic compatibility with Si technologies.

By exploiting *strain-engineering* as an additional degree of freedom, a wide variety of devices structures have been implemented in the Si/ $Si_{1-x}Ge_x$ material system, reaching from heterobipolar transistors (HBT) [2] over p- and n-type modulation-doped field effect transistors (MODFET) [3] to optical detectors in the near infrared, and even light emitters [4]. Nevertheless, so far only the pseudomorphic Si/SiGe HBT has reached production status, whereas other devices with demonstrated superior properties, such as the n-type MODFET, are still restricted to test devices on a laboratory level. The main reason for the much slower development of the MODFET lies in the necessity for strain relaxed $Si_{1-x}Ge_x$ buffer layers. These have successfully been implemented by several research groups [5], [6], [7], but defect and morphology control still require further refinement to make them suited for a production environment.

Ternary $Si_{1-x-y}Ge_xC_y$ alloys offer an alternative route to strain-engineering in silicon-based heterostructures, which finally may overcome the problems imposed by relaxed buffer layers: Due to the covalent radii of C and Ge, which are smaller and larger than that of Si, respectively, both compressively and tensilely strained pseudomorphic layers can be implemented by proper adjustment of x and y in the active layers of a heterostructure [8]. However, in contrast to the binary $Si_{1-x}Ge_x$ alloys, which are thermodynamically stable for all compositions x, carbon has almost negligible solid solubility in both Si and Ge, but instead exists in various SiC polytypes. Since strain engineering requires C concentrations of a few atomic percent to provide useful modifications of the band structure [9], non-equilibrium growth conditions at sufficiently low temperatures have to be established. This requires an optimization of the growth parameters to allow sufficiently high C incorporation without excessive degradation of the crystal quality through the undesirable generation of point defects. Also, the surface morphology has to be controlled in order to suppress strain-induced three-dimensional growth.

In the following we report on the recent progress that has been made in Linz regarding the growth and characterization of heterostructures containing ternary $Si_{1-x-y}Ge_xC_y$ alloys. The main emphasis in the report period has been put on optimizing the growth conditions to allow a complete substitutional carbon incorporation without sacrificing the structural, morphological, and optical qualities of these layer sequences. These investigations are the most essential prerequisite for any further assessment of the future role $Si_{1-x-y}Ge_xC_y$ alloys can play in the field of application-driven band structure engineering.

2. Experimental

2.1 Epitaxial Growth of $Si/Si_{1-y}C_y$ Heterostructures

(S. Zerlauth, M. Mühlberger, C. Penn, H. Seyringer, F. Schäffler)

In order to establish and optimize growth conditions for the substitutional incorporation of carbon in concentrations on the order of 1 – 3 at.% we designed and grew a series of six-period $Si/Si_{1-y}C_y$ superlattices (SLs) for subsequent characterization by x-ray rocking analyses, photoluminescence (PL), and atomic force microscopy (AFM). The aim of these investigations was to reach a high level of substitutional carbon (to be characterized by the x-ray strain measurements), a low level of electrically or optically active defects (to be characterized by PL measurements), and a smooth surface morphology (to be characterized by AFM experiments).

The two most important parameters for the growth of the thermodynamically metastable compounds, such as $Si_{1-y}C_y$ layers, are the growth temperature and the growth rate. Both affect the interplay between surface mobility of the impinging atoms and substitutional incorporation. Low growth temperatures and/or high growth rates always tend to suppress segregation or non-substitutional incorporation, but also lead to defective growth which finally yields an amorphous layer [10]. On the other hand, high growth temperatures and low growth rates move the system closer to thermal equilibrium, which reduces the defect density, but also leads to reduced carbon incorporation or, finally, to stochiometric β-SiC precipitation. Moreover, higher surface mobilities of the impinging atoms will favor three-dimensional (3D) growth, which is frequently observed in strained heterosystems that are allowed to minimize their surface free energy. Under

such conditions the reduction of the strain energy via 3D growth has to be larger than the added surface energy introduced by the 3D morphology [11].

In the experiments to be reported here, the growth rate was kept constant at MBE-typical values of around 1 Å/s, and only the growth temperature was varied systematically. To prevent artifacts that might have been introduced by long term fluctuations in the flux of our e-beam carbon source, the complete temperature range to be investigated was frozen into each of our SL samples. To achieve this, the samples were grown under constant Si and C fluxes each, whereas the substrate temperature was systematically increased by 50°C from $Si_{1-y}C_y$ layer to $Si_{1-y}C_y$ layer over the six periods. This way, each SL contained implicit information on the temperature-dependent incorporation of carbon in the temperature range between 400 and 650 °C. To deduce this information unambiguously, x-ray rocking curves of the SL samples were simulated dynamically with additional input from a set of reference spectra, which came from SLs that were grown at a constant temperature each [16].

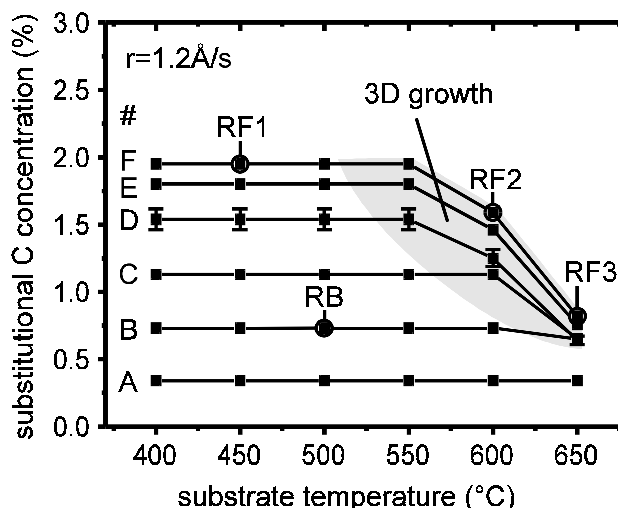

Fig. 1: Carbon incorporation as a function of growth temperature.

The results of these experiments are plotted in Fig. 1. The basic trend is a decrease of the percentage of substitutional carbon both with increasing y and with increasing temperature. In contrast to earlier results of other groups [13], however, we could demonstrate that with reasonably high growth rates (here 1.2 Å/s) complete substitutional carbon incorporation of up to about 2 % is possible at growth temperatures ≤ 500 °C. Even higher growth temperatures of up to 650 °C are allowed, as long as the desired carbon concentration remains below 1 %.

Beyond the limits established in Fig. 1, the amount of substitutionally incorporated carbon drops drastically with increasing growth temperature (hatched area in Fig. 1). By a combination of RHEED and AFM experiments we found that in this range surface roughness is also strongly increased, whereas the morphology remains basically smooth in the region of complete substitutional incorporation. Additional experiments are required (and planned) to figure out whether increased surface roughness causes the substitution incorporation of carbon to drop, or, vice versa, whether non-substitutional carbon triggers a transition to 3D growth.

Because of the large difference in the covalent radii of Si and C, it was not clear whether a linear interpolation between the lattice constants of Si and diamond (or of Si and SiC) is a good enough approximation even within the quite limited range of substitutional carbon concentrations accessible. Therefore, in cooperation with the group of A.V. Drigo in Padua, who performed resonant backscattering experiments at 5.72 MeV, we studied the variation of the lattice parameter of $Si_{1-y}C_y$ layers as a function of the substitutional carbon concentration y. In good agreement with theoretical predictions by Kelires [12], we found a pronounced deviation from Vegard's rule, which can be as large as 30 %. The reason for that behavior is attributed to the quite significant charge transfer from Si to C, which leads to a faster reduction of the lattice parameter with y than would be expected from a linear scaling of the average bond-length. These new results can be accounted for with a parabolic interpolation scheme, which has to be employed for an accurate determination of the substitutional carbon content via x-ray rocking analyses.

2.2 Assessment of $Si/Si_{1-y}C_y$ Layers by Photoluminescence

(C. Penn, S. Zerlauth, G. Bauer, F. Schäffler)

The unexpectedly large range of growth parameters that allows substitutional carbon incorporation (Fig. 1 above) makes it possible to grow at sufficiently high substrate temperatures to achieve $Si_{1-y}C_y$ layers of high crystal quality with substitutional carbon concentrations of up to at least 2 at. %. In fact, we were able to observe clear bandgap photoluminescence from $Si/Si_{1-y}C_y$ SLs within this composition range that allowed us the deduction of the strain-induced band gap narrowing in $Si_{1-y}C_y$ layers grown pseudomorphically on Si substrates (dashed line in Fig. 2).

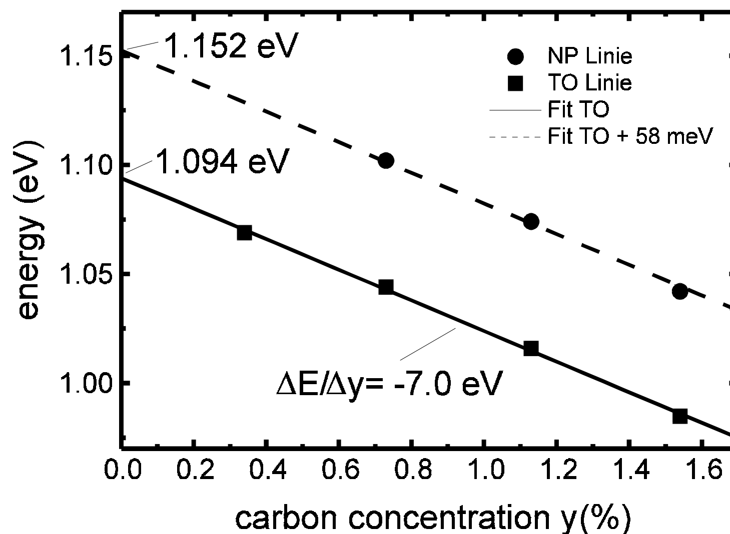

Fig. 2: Band gap variation with increasing substitutional carbon content as derived from photoluminescence measurements.

A linear band gap shrinkage with a slope of -70 meV per percent of substitutional carbon is observed, which leads to a useful band offset of 140 meV at y = 2 % in good agreement with results from other groups [9]. This band gap shrinkage, which is believed to be mainly accommodated by a conduction band offset [9], is almost entirely

due to the tensile in-plane strain in a pseudomorphic $Si_{1-y}C_y$ layer on a Si substrate, whereas a chemical contribution of the carbon atoms is rather small in the investigated concentration range. At higher concentrations (expected to be beyond 10 at.%) the band gap has to increase again, to finally approach the much larger band gaps of β-SiC (2.2 eV) or even diamond (5.5 eV). However, such large substitutional carbon concentrations are beyond the conceivable limits of metastable, pseudomorphic growth, which renders the question about the composition of the $Si_{1-y}C_y$ alloy with the minimum band gap interesting but of little practical relevance.

Photoluminescence spectroscopy is a versatile technique, which not only provides information on the band gaps and the band offsets, but is also a sensitive indicator of the overall crystal quality of the layers, since the density of non-radiative recombination centers has to be small enough to allow the observed phonon- or alloy-disorder-assisted radiative recombination. We have therefore investigated the changes in the PL spectra induced by thermal annealing of the samples, and also as a function of the sample temperature during the PL experiments to get insight into the thermal stability of these intrinsically metastable epi-layers and in the annealing behavior of growth defects.

Three types of samples were grown for these studies, namely $Si_{1-y}C_y$ single layers, $Si/Si_{1-y}C_y$ multiple quantum wells, and strain compensated $Si/Si_{1-y}C_y/Si_{1-x}Ge_x$ superlattices. In the first two types of samples the band offset is almost exclusively restricted to the conduction band, which is energetically lower in the tensilely strained $Si_{1-y}C_y$ layers due to a strain splitting of the six-fold degenerate, Si-like conduction band. The situation is analogous to strained Si grown on a relaxed $Si_{1-x}Ge_x$ buffer layer and is therefore of special interest for the implementation of n-type MODFETs. Band alignment in the $Si/Si_{1-y}C_y/Si_{1-x}Ge_x$ superlattices, which are interesting for infrared detector applications because of the inherent strain compensation, is more complex: Since the $Si_{1-x}Ge_x$ layers introduce an additional valence band offset, carrier confinement is indirect both in k-space and in real space, with electrons being located in the $Si_{1-y}C_y$ layers and holes in the $Si_{1-x}Ge_x$ layers.

At growth temperatures of around 500 °C the as-grown samples of all three types showed well behaved PL signals. There is presently only one other group worldwide that has published PL spectra of comparable quality measured on MBE layers [9]. As an example, Fig. 3 shows the spectrum of a ten-period $Si/Si_{0.989}C_{0.011}/Si_{0.9}Ge_{0.1}$ superlattice together with a schematic view of the strain-induced band alignment. Two distinct peaks are observed, which originate from band edge recombination in the vicinity of the $Si_{1-y}C_y/Si_{1-x}Ge_x$ interface, where the wave functions of electrons and holes have finite overlap. The peak at higher energies, labeled SiC-NP, results from the no-phonon transition, whereas the other peak is its TO phonon replica. A NP transition in an indirect gap material is only possible if symmetry breaking mechanisms are present, such as a heterointerface and/or the statistical fluctuations in a random alloy, which is both the case in our layers. The relative strength of the superlattice related peaks can by judged by comparison with the TO replicas originating from the Si layers and from the substrate. Obviously, the quantum wells very efficiently collect electron-hole pairs from the several μm deep excitation volume, and also maintain long enough lifetimes to allow the observation of radiative recombination. The strength of the bandgap PL signal is therefore an important indicator of the crystal quality, since an excessive amount of defects in the layers and at the heterointerfaces associated with non-radiative recombination would quench the PL signal altogether. This is indeed the case when growth temperatures below 450 °C are employed.

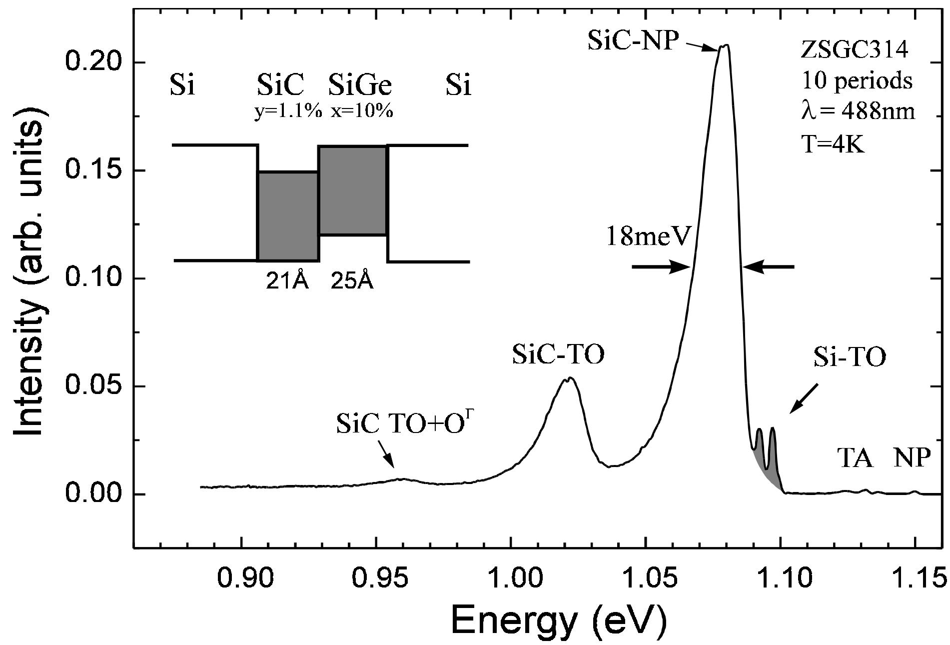

Fig. 3: PL spectrum of a ten-period $Si/Si_{0.989}C_{0.011}/Si_{0.9}Ge_{0.1}$ superlattice. The dominating signals are the no-phonon (NP) band edge recombination from the quantum well section and its TO-phonon replica. The shaded part of the spectrum is Si-related.

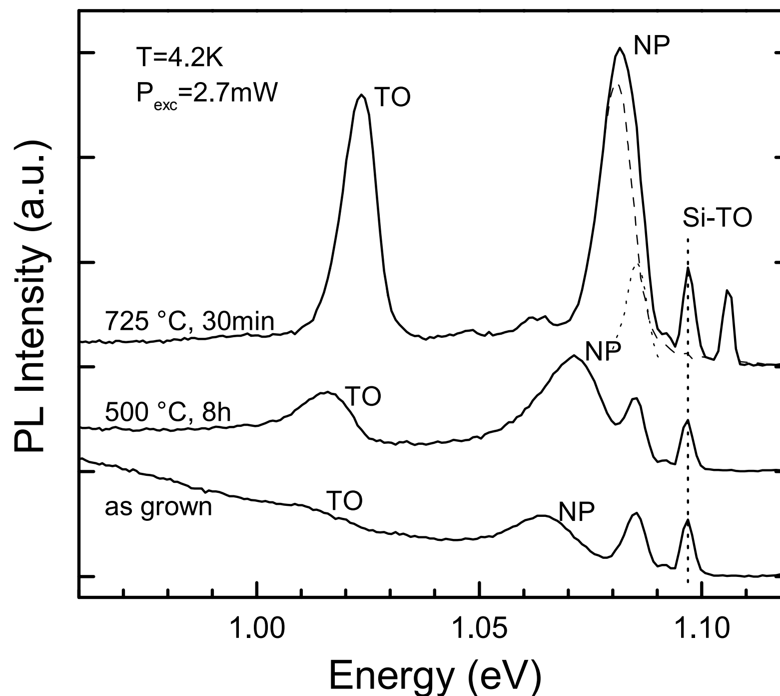

Fig. 4: Evolution of the PL signal of a single $Si_{1-y}C_y$ layer for increasing annealing temperatures. Note the blue shift and the line narrowing.

Compared with the well established quantum well luminescence from single $Si_{1-x}Ge_x$ layers [14], the PL signal in Fig. 3 is almost a factor of six broader. Since close to a factor of ten higher Ge concentrations are required to induce the same amount of strain that is provided by a given carbon concentration, the statistical fluctuations of both the well width and the well depth are much more pronounced in the case of a $Si_{1-y}C_y$ layer of comparable average strain. In addition, possible composition fluctuations from layer to layer may contribute to the line width from a superlattice. For the investigation of annealing effects we therefore mainly concentrated on single $Si_{1-y}C_y$ layers, which were grown thin enough to remain within the critical thickness limitations, but thick enough to suppress quantum confinement effects. Save for the exciton binding energy, this way the true band gap recombination is measured without any necessity for the correction of confinement energies. In addition, cross checks with the multiple quantum well samples confirmed that the annealing behavior is qualitatively the same.

Fig. 4 shows a series of PL measurements from a 100 nm thick $Si_{0.989}C_{0.011}$ layer which underwent annealing at successively higher temperatures in the range between 500 and 725 °C. There are three main effects associated with annealing: (i) The intensity of the band gap PL signal increases significantly within the range of annealing temperatures shown here. (ii) There is a noticeable *blue shift* of the PL lines amounting to about 15 meV. (iii) The line width after background subtraction becomes much narrower as the annealing temperature is increased. In fact, the linewidth of 8.4 meV in the topmost curve of Fig. 4 is the narrowest observed to date in any $Si_{1-y}C_y$ layer.

Most interesting, the pronounced changes of the PL signal are not associated with a change of the substitutional carbon concentration, as has been checked by x-ray rocking analyses. Only at higher annealing temperatures of >850 °C a loss of substitutional carbon is observed, whereas the PL intensity starts decaying already at about 750 °C.

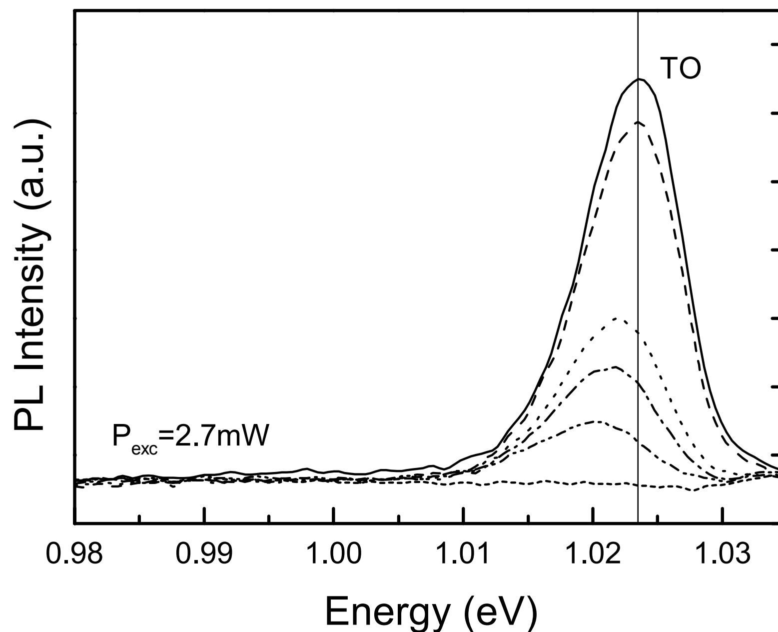

Fig. 5: Red shift of the PL signal with increasing measurement temperature. The TO-phonon replica is plotted here, because it is free of substrate-related signals.

Since changes of the *average* C concentration can be ruled out, and quantum confinement effects through possible short range diffusion of substitutional carbon can be neglected in the thick layers used here, the development of the PL signal has to have other reasons. To further elucidate these mechanisms, PL measurements of the samples with the highest PL intensity were recorded as a function of the measurement temperature. This is shown in Fig. 5, where the TO-replica of the band gap recombination, which is not affected by spurious signals from the Si substrate, is plotted for measurement temperatures in the range between 4.2 and 20 K. The most striking feature of these measurements, which was confirmed by experiments on the quantum well samples, is a *red shift* concomitant with a decay of the intensity as the temperature is increased.

A consistent interpretation of the annealing effects and of the red shift with higher measurement temperature can be derived, when assuming that the as-grown samples contain non-radiative recombination centers as well as non-statistical fluctuations of the local, substitutional carbon concentration. The latter may be associated with C_2 and C_3 molecules, which are observed in the mass spectrum of the carbon molecular beam, and which are tentatively not completely dissociated at the low growth temperatures employed. Based on these assumptions the following effects will occur during annealing:

(i) At low annealing temperatures (middle curve in Fig. 4, 500 °C for 8 h), non-radiative recombination centers associated with growth defects begin to disappear. This leads to an increase of the PL intensity, but only to a minor decrease of the line width.

(ii) At higher annealing temperatures (upper curve in Fig. 4, 725 °C 30 min) a redistribution of carbon on a local scale occurs, which leads to the dissolution of local carbon accumulations, introduced, e.g. by molecular forms of evaporated C. The overall effect is a more homogeneous, statistical distribution of carbon, which causes two effects: First, the PL signal experiences a blue shift, because homogenization of the carbon concentration smears out the local band gap minima in regions of originally enhanced concentration. Second, the line width becomes narrower as the statistical fluctuations become smaller. This interpretation is corroborated by the fact that the ratio between NP signal and TO-replica decreases, which means a reduction of the symmetry-breaking alloy fluctuations.

(iii) Although the fluctuations of the carbon concentration become more homogeneous upon annealing, the remaining alloy is still random. This explains the red shift with increasing measurement temperature, which results from carriers bound to alloy fluctuations, as has been observed in $Si_{1-x}Ge_x$ [15] and other random alloy material systems, too. With increasing temperature the electrons become mobile and establish an equilibrium distribution that preferentially fills the regions with the smallest band gaps. The many available reports in the literature allow the conclusion that a red-shift upon increasing the measurement temperature is a characteristic feature of strongly disturbed alloys with local carrier confinement, which certainly applies to the situation here, because of the large local strain induced by the unusually large difference of the covalent radii of Si and C.

(iv) The layers are thermally stable to beyond 850 °C, with no indications for a change of the average concentration of substitutional carbon. Thus noticeable diffusion of carbon or SiC precipitation requires higher temperatures and should not be a severe limitation for device processing.

2.3 Interface Morphology in SiGe/SiC/Si Superlattices

(J. Stangl, A.A. Darhuber, G. Bauer, S. Zerlauth, M. Mühlberger, F. Schäffler)

As has been mentioned above, too high growth temperatures can lead to a roughening of the $Si_{1-y}C_y$ layers at the growth front. This may be of crucial influence on the envisaged MODFET applications, because interface roughness scattering can be a mobility limiting mechanism. Now, roughness scattering in a $Si_{1-y}C_y$ channel MODFET would occur at the interface between the channel and the subsequently deposited Si spacer layer, and not on a free surface. Because the growth kinetics could modify that interface, it is important to employ a technique that is capable of probing a buried interface.

Sample No.	Periods	Layer 1	Layer 2	Layer 3	Remark
Z-SGC 312	10	$Si_{0.9}Ge_{0.1}$ 27Å	$Si_{0.988}C_{0.012}$ 23Å	Si 162Å	surfactant
Z-SGC 314	10	$Si_{0.989}C_{0.011}$ 21Å	$Si_{0.89}Ge_{0.11}$ 25Å	Si 150Å	
Z-SGC 315	10	$Si_{0.989}C_{0.011}$ 22Å	$Si_{0.89}Ge_{0.11}$ 25Å	Si 149Å	surfactant
Z-SGC 319	10	$Si_{0.91}Ge_{0.09}$ 31Å	$Si_{0.989}C_{0.011}$ 28Å	Si 191Å	
M-SGC 575	8	$Si_{0.79}Ge_{0.21}$ 25Å	$Si_{0.998}C_{0.002}$ 75Å	Si 191Å	
M-SGC 576	8	$Si_{0.78}Ge_{0.22}$ 25Å	$Si_{0.991}C_{0.009}$ 42Å	Si 191Å	
M-SGC 577	8	$Si_{0.775}Ge_{0.215}$ 25Å	-	Si 191Å	
M-SGC 580	8	$Si_{0.805}Ge_{0.195}$ 26Å	$Si_{0.996}C_{0.004}$ 74Å	Si 191Å	

Table I: Structural parameters of the investigated samples as obtained from x–ray diffraction and x–ray reflectivity measurements.

This rules out the commonly used and readily available surface sensitive techniques, such as atomic force microscopy or scanning tunneling microscopy. Transmission electron microscopy would be a useful approach, but it is restricted to very small sample areas per micrograph, and, in addition has an in-depth averaging problem that depends sensitively on the quality of sample.

X-ray reflectivity techniques, which are sensitive to changes in the average electron density and thus to chemical composition, can be used instead. In addition, these nondestructive techniques provide information on sample areas which are several mm^2 in size, and consequently considerably larger than those which are scanned with scanning probe techniques. However, x-ray reflectivity measurements are not useful for the determination of the strain status of the layers, which requires in addition x-ray diffraction techniques.

Apart from the above mentioned advantages, there are several disadvantages: x-ray reflectivity techniques require the use of synchrotron radiation for sufficient scattered intensity as well as the use of a quite elaborate data analysis. The scattered intensity is recorded in the vicinity of the origin of the reciprocal space (000), and information on interface roughness and its correlation properties are obtained from the analysis of diffusely scattered radiation which accompanies the coherently scattered one.

To investigate the interface morphology and its replication in Si/SiGe/SiC heterostructures, two series of superlattice (SL) samples have been grown by MBE. The first sample series consists of four 10–period $Si_{0.9}Ge_{0.1}/Si_{1-y}C_y/Si$ superlattices grown on (001) Si

substrates. The growth temperature of all samples was set to 500 °C to ensure fully substitutional incorporation of carbon; the flux rates were typically 1 Å/s. With this series the influence of the layer sequence (SiGe/SiC/Si or SiC/SiGe/Si) and the possible influence of a Sb surfactant was checked. All samples have a nominally 1000 Å thick Si cap on top, as they were also designed for PL–investigations of their neighboring confinement band structure.

The second sample series consisted of four superlattices, where the C content of the $Si_{1-y}C_y$ layers was varied, while the SiGe layer composition and thickness as well as the superlattice period were kept constant. The $Si_{1-y}C_y$ layer thickness was chosen accordingly to the C content in order to keep the superlattices strain symmetrized. The nominal growth parameters are listed in Table I.

All samples were characterized by (004) XRD rocking scans, and the miscut of the substrates was measured using triple axis diffractometry (TAD): The orientation of the lattice planes was measured for four different azimuths using the (004) Bragg reflection. The surface orientation was measured in the same azimuths by measuring the position of the specularly reflected beam at low incidence angles (typically 0.5°). By this method the miscut can be determined with a precision of about 0.01° in magnitude and 5° in azimuth.

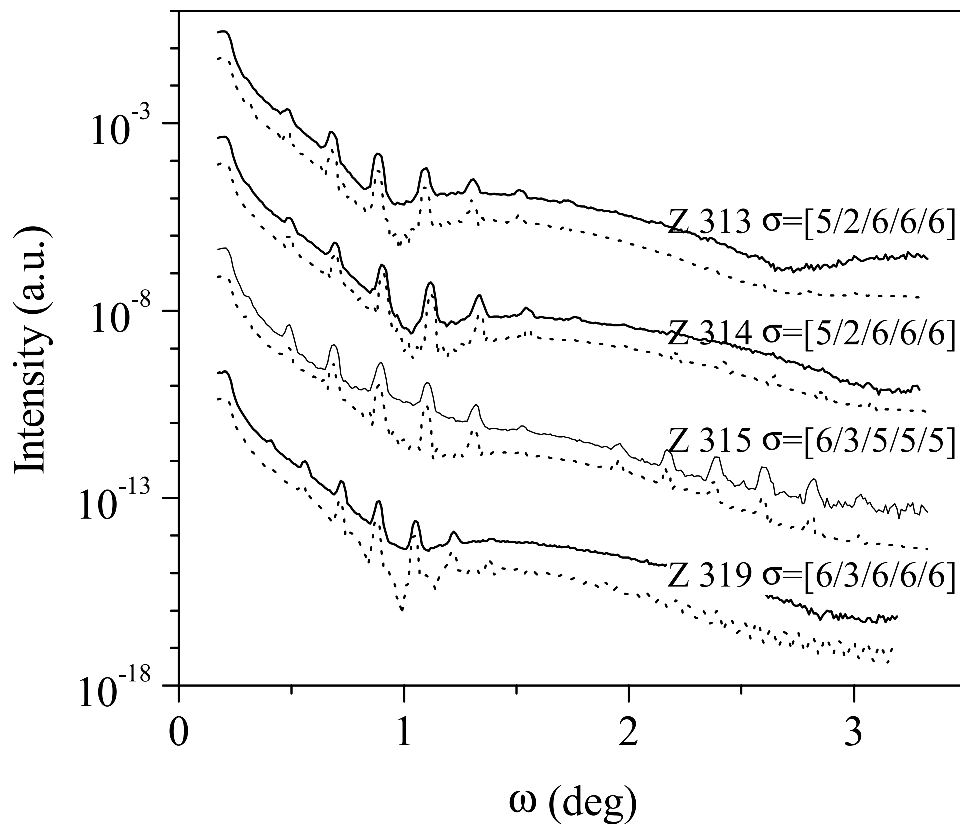

Fig. 6: Scans of the specularly scattered intensity (solid lines) of the first sample series, together with calculations (dotted lines). The corresponding r.m.s. interface roughness values are given in brackets.

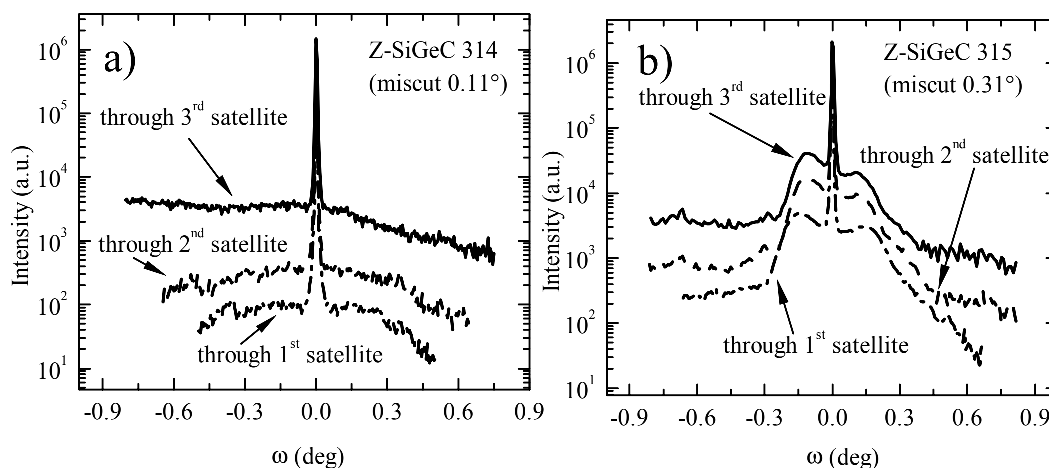

Fig. 7: ω–scans through satellite peaks of the specular curve for two samples.
a) for a sample with small miscut, no significant features are observed in the scans; b) for a sample with relatively large miscut, side maxima in the scans are clearly visible.

X–ray reflectivity measurements of the specularly as well as the diffusely scattered intensity were recorded at the Optics beamline (BM5) at the ESRF in Grenoble, France, at the beamlines D4 and RÖMO1 at HASYLAB, DESY, in Hamburg, Germany, and at a laboratory diffractometer in Brno, Czech Republic.

The specular scans of the first sample series (Z-SGC 312 … Z-SGC 319) is shown in Fig. 6, together with calculations using a Parrat-formalism. The resulting r.m.s. roughness values are listed in brackets in the figure. No significant influence of the layer sequence and of the surfactant on the r.m.s. roughness could be detected.

ω–scans of the diffusely scattered intensity revealed different interface morphologies of samples with relatively large miscut (e.g. sample Z-SGC 315 with a miscut of 0.31°) and those with a relatively small miscut (e.g. sample Z-SGC 314 with a miscut of 0.11°), see Fig. 7. For samples with low miscut, no specific structure in the ω–scans besides the sharp central peak of the specularly scattered beam could be observed (Fig. 7a). For samples with high miscut strong features in the ω–scans could be observed, depending on the azimuth of the measurement. If the scattering plane was perpendicular to the miscut steps of the surface, side maxima in the ω–scans were clearly observed (Fig. 7b). From calculations using distorted wave Born approximation, the corresponding length scale of the interface waviness was determined to be approx. 1.7 µm. If the scattering plane is parallel to the miscut steps, only one broad peak in the center of the scan is observed. Furthermore, the vertical correlation length, i.e. the typical decay length for the replication of interface features, is of the order of 2500 Å for the samples with higher miscut, but only 100 to 200Å for samples with small miscut. This clearly indicates that the miscut of the substrate has a significant influence on the growth of the heterostructures.

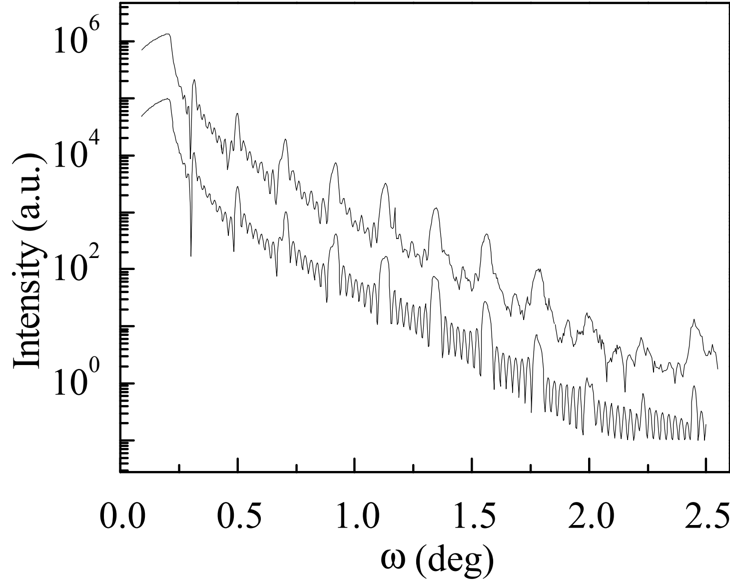

Fig. 8: Scan of the specularly scattered intensity of sample M-SGC 577, together with a simulation.

For the second sample series (M-SGC 575 … M-SGC 580) the interface roughness is slightly smaller: Simulations of the specularly reflected intensity yield an r.m.s. value of 4 Å (see Fig. 8). Virtually no vertical correlation of the interface morphology is observed in these samples, not even in the reference sample M-SGC 577 without SiC interlayers.

The vertical correlation lengths are lower than 100 Å, at least for lateral length scales over 4000Å, which are probed with our experimental setup. We ascribe this effect to the relatively low growth temperature of our samples of only 500 °C.

3. Conclusion

We have established MBE growth conditions for high-quality $Si/Si_{1-y}C_y$ and $Si/Si_{1-y}C_y/Si_{1-x}Ge_x$ samples with substitutional carbon concentrations of up to 2 %. Well-behaved PL signals from band edge recombination in the $Si_{1-y}C_y$ layers, and at the $Si_{1-y}C_y/Si_{1-x}Ge_x$ interface, respectively, have been observed. The quality of the layers improves significantly upon annealing at moderate temperatures of about 725 °C, without affecting the substitutional carbon concentration. At these temperatures annealing mainly reduces the defect density in the layers and leads to a more homogeneous distribution of substitutional carbon. The layers are thermally stable to beyond 850 °C, where we observe first indications for a reduction of the substitutional carbon content. By employing x-ray diffraction and refraction techniques, we were able to gain information on the roughness and replication of buried $Si/Si_{1-y}C_y$ interfaces, which is important for interface roughness scattering and almost impossible to gain by other techniques.

Successful growth of carbon-containing, Si-based heterostructures is an important prerequisite for a future implementation of n-type MODFETs with tensilely strained $Si_{1-y}C_y$ quantum wells. In a next step the established growth parameters for high-quality $Si_{1-y}C_y$ layers on Si will be used as a starting point for the implementation of modulation-doped

$Si_{1-y}C_y$ quantum wells. This will allow a direct comparison with the established Si-channel MODQWs on strain-relaxed SiGe buffer layers. It will be of special interest to assess the role of alloy scattering in the $Si_{1-y}C_y$ wells which directly competes with an elemental Si channel. From such experiments further insight both in the importance of alloy scattering and the future use of $Si_{1-y}C_y$ layers can be derived.

Acknowledgments

Close collaboration with Daimler-Benz-Research in Ulm, Germany and with the group of Prof. Drigo in Padua is gratefully acknowledged. The x–ray reflectivity measurements were recorded at the Optics beamline (BM5) at the ESRF in Grenoble, France, at the beamlines D4 and RÖMO1 at HASYLAB, DESY, in Hamburg, Germany, and at a laboratory diffractometer in Brno, Czech Republic. Financial support by the Fonds zur Förderung der wissenschaftlichen Forschung (FWF), and by the Oesterreichische Nationalbank are gratefully acknowledged. C. Penn was partly supported by a scholarship from the Österreichische Akademie der Wissenschaften.

References

[1] for an overview see e.g. E. Kasper and F. Schäffler: “Group IV Elements”, *Semiconductors and Semimetals*, Vol. 33, Academic Press, Boston 1991; chapter 4

[2] for an overview see e.g. A. Gruhle: “Heterobipolar Transistor”, *Springer Series in Electronics and Photonics*; Vol. 52; Springer, Berlin 1994, chapter 4

[3] for an overview see e.g. F. Schäffler: “High-Mobility Si and Ge Structures”, *Semicond. Sci. Technol.,* Vol. 12,; 1997; pp. 1515 – 1549

[4] for an overview see e.g. H. Presting, H. Kibbel, M. Jaros, R.M. Turton, U. Menczigar, G. Abstreiter, H.G. Grimmeiss: “Ultrathin SiGe Strained-Layer Superlattices - a Step towards Si Optoelectronics”, *Semicond. Sci. Technol.*, Vol. **7**, 1992; pp. 1127 –1148

[5] E.A. Fitzgerald, Y.-H. Xie, M.L. Green, D. Brasen, A.R. Kortan, J. Michel, Y.-J. Mii, B.E. Weir, *Appl. Phys. Lett.*; Vol. 59; 1991; 811 – 813

[6] F.K. LeGoues, B.S. Meyerson, J.F. Morar, *Appl. Phys. Lett.*;Vol 66; 1991; 2903 – 2905

[7] F. Schäffler, D. Többen, H.-J. Herzog, G. Abstreiter, B. Holländer, *Semiconductor Sci. Technol.*; Vol. 7; 1992; 260 – 265

[8] K. Eberl, S.S. Iyer, F.K. LeGoues, *Appl. Phys. Lett.*; Vol. 64; 1994; 739 – 741

[9] K. Brunner, K. Eberl, W. Winter, *Phys. Rev. Lett.*; Vol. 76; 1996; 303 – 305

[10] H. Jorke, H. Kibbel, F. Schäffler, H.-J. Herzog: “Low Temperature Kinetics of Si(100) MBE Growth”, *Thin Solid Films;* Vol. 183; 1989; 307 – 313

[11] This so called Stranski-Krastanov growth mode is now widely employed for the investigation of self-organization phenomena, which can be useful for the fabrication of zero-dimensional quantum dots.

[12] P.C. Kelires, *Phys. Rev. B*; Vol. 55; 1997; 8785

[13] H.J. Osten, M. Kim, K. Pressel, P. Zaumseil: "Substitutional vs. interstitial carbon incorporation", *J. Appl. Phys.*; Vol. 80; 1996; pp. 6711 – 6715

[14] F. Schäffler, M. Wachter, H.-J. Herzog, K. Thonke, R. Sauer, *J. Cryst. Growth,* Vol. 127; 1993; 411 – 415

[15] L.P. Tilly, P.M. Mooney, J.O. Chu, F.K. LeGoues, *Appl. Phys. Lett.*, Vol. 67; 1995; 2488 – 2490

[16] S. Zerlauth, H. Seyringer, C. Penn, F. Schäffler: "Growth Conditions for Complete Substitutional Carbon Incorporation int $Si_{1-y}C_y$ Layers", *Appl. Phys. Lett.*; Vol. 71; 1997; 3826 – 3828

Project Information

Project Manager

Univ.-Prof. Dr. Friedrich SCHÄFFLER

Institut für Halbleiter- und Festkörperphysik, Abt. für Halbleiterphysik, Johannes Kepler Universität Linz

Project Group

Last Name	First Name	Status	Remarks
Fünfstück	Britta	student	Diploma Thesis Jan. 98
Gann	Rudolf	student	
Mühlberger	Michael	student	
Penn	Christian	grad. student	GMe funded since Sep. 97
Sander	Harald	student	
Schäffler	Friedrich	Univ.-Prof.	
Seyringer	Heinz	grad. student	
Stangl	Julian	grad. student	
Steinbacher	Günther	student	Diploma Thesis Sept. 97
Zerlauth	Stefan	grad.student/post-doc	Ph.D. Thesis Oct. 97

Publications in Reviewed Journals

1. S. Zerlauth, J. Stangl, A.A. Darhuber, V. Holý, G. Bauer, and F. Schäffler: "MBE growth and structural characterization of Si1-yCy/Si1-xGex superlattices", J. Cryst. Growth, Vol. 175/176, 1997, 459 – 464
2. J.H. Li, V. Holý, G. Bauer and F. Schäffler: "Strain relaxation in high electron mobility Si1-xGex/Si structures", J.Appl. Phys., Vol. 82, 1997, 2881 – 2886
3. C. Penn, S. Zerlauth, J. Stangl, G. Bauer, G. Brunthaler, and F. Schäffler: "Influence of thermal annealing on the photoluminescence from pseudomorphic Si1-yCy epilayers on Si", Appl. Phys. Lett., Vol. 71, 1997, 2172 – 2174
4. F. Schäffler: "High mobility Si and Ge structures", Semicond. Sci. Technol., Vol. 12, 1997, 1515 – 1549
5. S. Zerlauth, H. Seyringer, C. Penn, and F. Schäffler: "Growth Conditions for Complete Substitutional Carbon Incorporation into Si1-yCy Layers Grown by Molecular Beam Epitaxy", Appl. Phys. Lett, Vol. 71, 1997, 3826 – 3828
6. F. Schäffler: "Si/Si1-xGex and Si/Si1-yCy Heterostructures: Materials for High-Speed Field-Effect Transistors", Thin Solid Films (in press)

7. S. Zerlauth, C. Penn, H. Seyringer, J. Stangl, G. Brunthaler, G. Bauer, and F. Schäffler: “Molecular Beam Epitaxial Growth and Photoluminescence Investigation of Si1-x-yGexCy Layers”, Thin Solid Films (in press)
8. S. Zerlauth, C. Penn, H. Seyringer, G. Brunthaler, G. Bauer, and F. Schäffler: “Substitutional Carbon Incorporation into MBE-Grown Si1-yCy Layers”, J. Vac. Sci. Technol. (in press)
9. C. Penn, S. Zerlauth, J. Stangl, G. Bauer, and F. Schäffler: “Photoluminescence from Pseudomorphic Si1-yCy Layers on Si Substrate”, J. Vac. Sci. Technol. (in press)
10. J.H. Li, G. Springholz, H. Seyringer, V. Holy, F. Schäffler, and G. Bauer: “Strain-Relaxation and Surface Morphology of Compositional Graded Si/Si1-xGex Buffers”, J. Vac. Sci. Technol. (in press)
11. M. Berti, D. De Salvador, A.V. Drigo, F. Romanato, J. Stangl, S. Zerlauth, F. Schäffler, and G. Bauer: “Lattice Parameter in Si1-yCy Epilayers: Deviation from Vegard’s Rule”, Appl. Phys. Lett. (accepted)

Presentations

1. F. Schäffler: “ Si/Si1-xGex and Si/Si1-yCy Heterostructures: Materials for High-Speed Field-Effect Transistors”, 7th Int. Symp. Si MBE, Banff, Canada, July 1997
2. S. Zerlauth, C. Penn, H. Seyringer, G. Brunthaler, G. Bauer, and F. Schäffler: “Substitutional Carbon Incorporation into MBE-Grown Si1-yCy Layers”, 7th Int. Symp. Si MBE, Banff, Canada, July 1997
3. S.Zerlauth, C. Penn, H. Seyringer, J. Stangl, G. Brunthaler, G. Bauer, and F. Schäffler: “Molecular Beam Epitaxial Growth and Photoluminescence Investigation of Si1-x-yGexCy Layers”, Silicon Heterostructures: Int. Conf. on From Physics to Devices, Barga, Italy, September 1997
4. C. Penn, S. Zerlauth, J. Stangl, G. Bauer, and F. Schäffler: “Photoluminescence from Pseudomorphic Si1-yCy Layers on Si Substrate”, Int. Conf. on Silicon Heterostructures: From Physics to Devices, Barga, Italy, September 1997
5. J.H. Li, G. Springholz, H. Seyringer, V. Holy, F. Schäffler, and G. Bauer: “Strain-Relaxation and Surface Morphology of Compositional Graded Si/Si1-xGex Buffers”, Int. Conf. on Silicon Heterostructures: From Physics to Devices, Barga, Italy, September 1997
6. F. Schäffler: “Silizium-basierende Heterostrukturen: Der Weg zu schnellen, Silizium-kompatiblen Bauelementen”, Informationstagung Mikroelektronik, Wien, October 1997

Ph.D. Theses

1. Stephan Zerlauth: “MBE-Wachstum und Charakterisierung von siliziumbasierenden Heterostrukturen”, Johannes Kepler Universität Linz, Oct.

Cooperations

1. Daimler-Benz AG, Forschungsinstitut Ulm (Dr. König)
2. Universita Degli Studi Di Padova (Prof. Drigo)
3. Walter-Schottky-Institut Munich (Prof. Abstreiter)
4. Institut für Werkstoffwissenschaften, Universität Erlangen (Prof. Strunk)
5. Imperial College London (Dr. McPhail)

UNICHIP

UNICHIP Vienna —
ASIC Design with Austrian Universities

N. Kerö, G.R. Cadek, W. Kausel, E. Kowarsch, P. Thorwartl

Institute for General Electrical Engineering and Electronics, Techn. Univ. Vienna, A-1040 Vienna, Austria

After giving a short overview of the main goals of the UNICHIP initiative and its development over the last years selected activities are presented which have been completed in the last year. Besides two research oriented projects in the area of user programmable logic devices the results of another two ASIC designs for Austrian SMEs are summarized. The report concludes with a description of a LEONARDO project dealing with continued education in Austrian electronic industry.

1. Introduction

The UNICHIP project was originally proposed in 1987 by the Institute of General EE and Electronics at the Vienna University of Technology. Since its very beginning this national activity was focused on three main topics in the area of the design of digital and analog integrated circuits. Firstly, undergraduate education had to be intensified by means of offering students unrestricted access to state-of-the-art hard- and software electronic design automation (EDA) together with the possibility to actually manufacture selected designs. Secondly, the effective accomplishment of research and advanced development projects should become feasible. Finally, the Austrian industry – mainly small and medium sized enterprises (SMEs) – need to be supported in using new technologies and design methodologies.

All of these aims required continuos investments in design hard- and software tools. Additionally a measurement lab had to be installed enabling the verification on both digital and analog behavior of integrated circuits which have been fabricated in the scope of UNICHIP.

The GMe has funded UNICHIP throughout the past years so we were able to set up and operate a ASIC design facility and thereby achieve every one goal of UNICHIP at least to a certain extent within the first years. The participation in the ESPRIT project *Teaching VLSI Design Skills* (EUROCHIP) and later on in EUROPRACTICE turned out to be a major breakthrough for UNICHIP. Both of these projects were launched by the European community to accomplish similar goals as UNICHIP but on a pan-European level. Several services are available such as very cheap access to both a variety of EDA tools and to IC prototype manufacturing facilities. Education and academic research word are showing great success and have been pushed to an advanced level comparable to other European universities. In the recent past the SME support activities — by far the most difficult task — have been successful.

2. An SCSI-2 Target Marco for FPGAs

In order to speed up the design process of complex digital systems it is common design practice to use macro blocks or modules wherever possible. As long as an FPGA family is selected as the target device these blocks tend to be highly technology dependent. Even worse, families from different FPGA vendors have varying module libraries, thus making it very difficult to migrate a design from one family to another.

Therefore, the aim of this project was to design a re-targetable SCSI-2 macro, to be included in any complex FPGA design. Besides its wide spread usage for the connection of mass storage devices the SCSI bus can handle the attachment of nearly any custom IO device to a standard PC. The necessity to either use (and program) a full fledged SCSI controller or to design one from scratch has been the limiting factor for such applications as shown in Fig. 1.

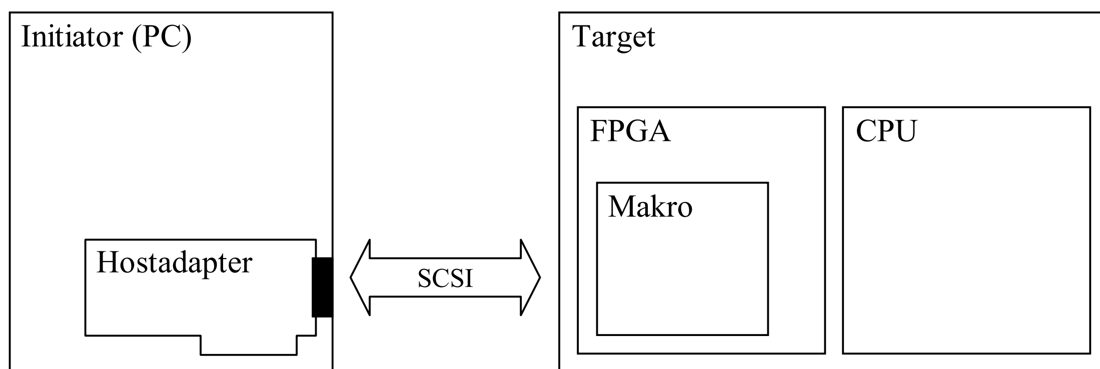

Fig. 1: Typical SCSI application.

The macro was designed not only by means of VHDL, but with a generic library for the design capture system ViewLogic®. This approach has been chosen because ViewLogic is supported by nearly every FPGA vendor.

The SCSI macro was successfully targeted both to XLINX® and ALTERA® devices. The complexity is roughly 2500 gates which equals 60 CLBs for the logic family XC-4000 from XILINX. A prototype implementation consisting of 4 devices has been tested without any problem with several host adapters.

3. CULT — Classification of User Programmable Logic Devices with Scaleable Test Structures

The purpose of this project was the search for a new means of classification for User Programmable Logic Devices (UPLD) together with their associated software needed for the design process. In the area of UPLDs are many different concepts and devices all of which are well promoted by their manufacturers as the optimum solution for any digital circuit. Thus an independent classification is of utmost important for the customer, who must select the right architecture for his design problem. All specifications in the official data sheets, like the number of gates or the maximum system frequency, must be corrected by the factor UGF (User Gullibility Factor), depending on the quality of the marketing division.

Existing benchmarks evaluate UPLDs by implementing a set of well defined complex test circuits. The selection of these circuits is a major influence on the results. This project uses very simple identical circuits, so that different UPLD can be compared with each other and also with an easily calculated near optimum result. The different test structures are optimized for measurement of interesting features like system frequency, propagation delay, and utilization of the device.

Entering a certain number of circuits for any different device type seems a rather dull task. A program was developed which can generate all the necessary files in most of the common formats like ViewLogic WIR Files, EDIF or VHDL. Another advantage of this method is the parameterization and scaleability of the benchmark. It is very important to use a well defined design flow to reproduce the results. The single steps of a the design flow are executed automatically with batch files or scripts. The results of the benchmarks are stored in a database.

With this method it is also possible to compare the computational power of different development platforms (PC, SUN). The concepts of this kind of test circuits were verified with all the actual device families from to different vendors (Altera, Xilinx). For the measurement of the propagation delay it is a good idea to use very simple combinatorial circuits like AND gates, exclusive OR gates or multiplexers.

There are three parameters to vary complexity of the test circuit:

- The number of product terms which means the kind of the gate;
- The number of the input pins;
- How often the structure is repeated.

The actual maximum propagation delay is measured with a static timing analyzer. If, with an increasing number of output pins, the delay time converges the devices can be called predictable. This is typical for CPLDs in contrast to FPGAs. A comparison of delay time with the number of input pins shows the granularity of the logic cell in a device and the number of logic levels to implement the gate.

On the other hand, for the measurement of the maximum clock frequency the simplest sequential circuit is a serial shift register with various numbers of flip-flops. The results show us the effects of utilization an the maximum possible system frequency. Typically this value is much smaller than the toggle frequency of the D-flip-flops which is the preferred value presented in the data sheets. This test stresses also the partitioning, place and route tools, adjacent flip-flops must be placed as close as possible to each other to achieve the maximum system frequency. This can easily be verified in a floor planner.

The third kind of benchmarks are barrel shifters, which are a combination of the preceding test structures of multiplexers with shift registers. When the number of input pins increases, also the number of logic levels for the combinatorial logic grows and the system frequency decreases rapidly. From these results you can determine the maximum number of logic levels for a given system frequency.

One goal of this work was the demonstration of usefulness of this kind of benchmarks and the development of a set of tools for their evaluation. This is the first type of UPLD benchmark which compares the results to a calculated optimum result derived from theoretical analysis instead of comparing with other UPLD structures.

4. IVASIC16 — A Binaural Audio Processor ASIC

In a previous project we designed a customized DSP called DAP (Digital Audio Processor) in cooperation with the Austrian company AKG for processing digital audio data to simulate a realistic and natural sound impression, which is achieved by special deep FIR algorithms. The audio processing system was developed by AKG for usage in a professional digital audio environment like recording studios. It comprises a microcontroller, fixed memory, a DAC, a fast static RAM, some glue logic, and finally the ASIC specially designed for this purpose.

We extended the idea of this audio processing system to applications in the area of consumer electronics. For this purpose we had to adapt the concept of the DAP in order to meet the special requirements of a high volume consumer market. We implemented all functions into one chip except for the digital-to-analog conversion and the storage of coefficient data. The goal of this work was to prove the capability of system integration to minimize the overall system cost. Beyond these more economical reasons we wanted to gain detailed experience in using logic synthesis through this industrial design task.

In order to obtain an easily transferable design we decided to use the hardware description language Verilog® for functional design input together with the logic synthesis tool SYNOPSYS®. Placement and routing were accomplished using the CADENCE® software. The design was initially started as a diploma thesis and later carried on as an industrial cooperation together with AKG.

We showed that using system integration offers a large number of benefits. The overall system cost may be reduced by a considerable amount. The usage of VERILOG based functional design entry combined with synthesis using SYNOPSYS showed not only good results but also a speed-up of the design entry task and the capability of fast switching from one ASIC technology to another. The whole design task took about six months. The design has been finished and prototypes have been tested successfully. Volume production is expected to be started within the next months.

5. Design of a DSP-Based Quad COMBO

Together with our partner company SEMCOTEC we developed a new DSP based four-channel (quad) Combo® device which in turn will be manufactured by National Semiconductor Corp. The main application area of such devices is the telecommunication industry because in digital telephony one Combo® is required for every single subscriber. Currently an advanced integrated circuit production technology permits the integration of the required A/D converter, D/A converter with all the associated filters not only for one subscriber channel but for several channels in a single chip. Devices like that are often referred to as Single/Multi-channel Combos (a combination of COderDECoder + Filter).

The first monolithic Combo devices have become feasible years ago when switched capacitor technology enabled the manufacturing of fully integrated high precision filters together with A/D and D/A converters on the same chip. Devices from this first Combo generation are often referred to as type one Combos and for many good reasons their usage has still not decreased, even today. A type one Combo together with a state of the art monolithic SLIC - or with a conventional transformer SLIC - builds a complete system which can operate a standard voice telephone with all its functionality like ringing,

dialing, on-hook/off-hook detection and so on from a standard PCM highway and a digital signaling data carrier. Many thousands of these so called line cards are present in typical digital exchange offices.

The targeted device is a simple, efficient, easy to use, multi-channel Combo. It has to be familiar to the system designers and system manufacturers all over the world who have gained a lot of experience with so called type-one Combos. Therefore all of the features which are not used in low end but high volume applications need not be present. Superior and highly repeatable transmission performance however will distinguish the new multi-channel Combo device from the older and newer analog competitors. By using a state of the art, sub-micron process allowing digital signal processing in combination with over sampling converter techniques most of the disadvantages of current analogue competitors can be avoided.

- Small chip area (first priority)
- Optimum yield (minimum matching requirements)
- Shortest possible testing times (design for testability)
- Minimum power consumption
- Repeatable transmission performance (digital filters, minimum analogue content)
- Modular design to allow reuse of parts in high-end and eight channel devices
- Small package (SO-40, PLCC-44)
- Customer diagnostics and production test modes

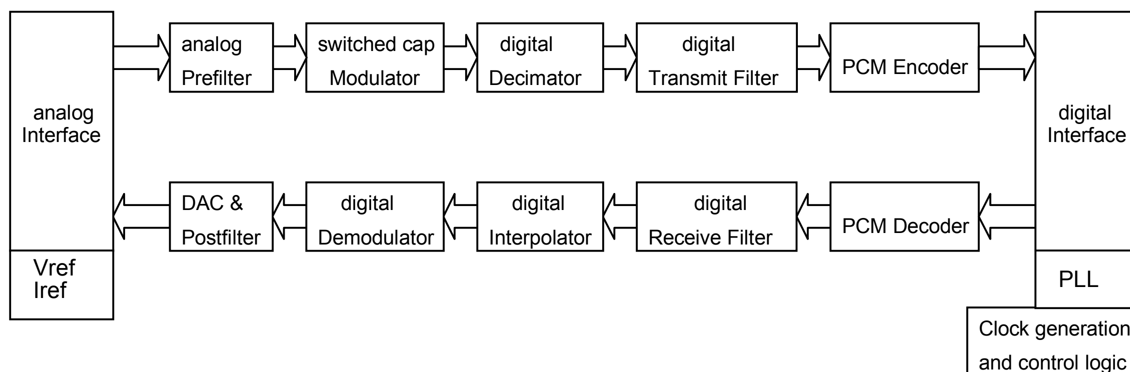

Fig. 2: Global Block Diagram.

The architectural design and the design of the digital blocks were done by the authors while the analog blocks were designed by design engineers from National Semiconductor. The digital design was described in VHDL and extensively simulated with respect to transmission characteristics. Finally, we used SYNOPSYS DesignCompiler for logic synthesis. It took about 15 months from the specification of the devices to the first silicon. The first prototypes were tested successfully. Only some minor design changes have to be applied to adjust the analog behavior. Currently the devices are qualified for production.

6. LEONARDO Transnational Training Institute

Being a member of the EUROFORM network the institute participates in the LEONARDO project “Transnational Training Institute”. The scope of work is the evaluation of the training methodologies employed in SMEs in the area of microelectronics. Together with 7 other partner institutions the efficiency of different approaches such as external or in-house training is analyzed. As a consequence of an overall comparison of the evaluation results in 6 countries the most effective means of training is selected in terms of increased ability to solve given design problems.

EUROFORM is an European network consisting of 60 partners. Within each country a node is responsible for the national coordination of all activities. These nodes are:

- France: University of Paris-Sud XI
- France: University of Bordeaux I
- Germany: University of Aachen
- Italy: University of Bologna
- Ireland: Trinity College of Dublin
- Portugal: INSEC
- Spain: University of Computer Science of Madrid

In Austria a cooperation with all institutions dealing with training on microelectronics was established. Together with the University Extension Center of the TU Wien and Danube (European Training, Research & Technology) a questionnaire was designed and sent to all known participants of recent training activities. Besides some general information of the structure of the enterprise the questions were focused of the respective activity and the method of distributing the knowledge of the training within the SME.

Finally the SMEs were asked to comment on the type of training they prefer and whether they would accept modern means of presentation (CD-ROM, Internet and the like) and the like.

First evaluations show a strong interest in external training courses with considerable emphasis on hand-on training using EDA-tools and workstations.

Acknowledgments

The Jubiläumsfonds der Österreichischen Nationalbank supported our activities within the project “ASIC-Design Station”, the BMwA, the Federal Ministry of Economical affairs, by funding the TMOe (Technologieverbund Mikroelektronik Österreich).

We wish to thank both institutions for their assistance.

Project Information

Project Manager

Dipl.-Ing. Nikolaus KERÖ

Vienna University of Technology, Institute for General Electrical Engineering and Electronics

Project Group

Last Name	First Name	Status	Remarks
Cadek	Gerhard	postdoc	
Kausel	Wilfried	dissertation	
Kowarsch	Eduard	student	50 % GMe funding
Nachtnebel	Herbert	dissertation	
Pommer	Heinrich	dissertation	
Thorwartl	Peter	dissertation	

Publications in Reviewed Journals

1. N. Kerö, S. Jankoviæ, W. Fallmann, V. Litovski: “A High Speed Serial Bus Controller ASIC”, MIEL´97, Proceedings of the MIEL ´97, pp. 737-742, Niš, 1997.
2. M. Stockinger, G. Brasseur, N. Kerö, T. Sauter: “An Integrated Current-Controlled Current Source with Programmable Gain for Charge Amplifier Applications”, In IEEE Conference on Instrumentation and Measurement Technology (IMTC/97), Ottawa, Canada, May 19-21, pp.1154-1159, 1997.

Presentations

1. M. Brüstle, G. Cadek, P. Thorwartl: “SCSI-2 Target Makro für FPGAs”, Austrochip´97, Universitätsverlag Rudolf Trauner, 1997.
2. R. Hawel, L. Matzinger: “Serielles Programmiergerät für Microchip-Controller”, Austrochip´97, Universitätsverlag Rudolf Trauner, 1997.
3. T. Sauter, N. Kerö: “Entwurf eines integrierten Analog-Interface-ICs für die Sprachdatenvermittlung”, Austrochip´97, pp. 344 – 350, Universitätsverlag Rudolf Trauner, 1997.
4. P. Söser, N. Kerö: “ASIC Entwicklung und Technologietransfer an österreichischen Universitäten”, pp. 22-25, Telematik, Jahrgang 3, 4/97.
5. M. Stockinger, T. Sauter, N. Kerö: “Das EKV-Modell für PSPICE”, Austrochip´97, pp. 351-357, Universitätsverlag Rudolf Trauner, 1997.

6. M. Stockinger, T. Sauter, N, Kerö: “Entwurf eines integrierten CMOS Temperatursensors mit offsetkompensiertem Meßverstärker”, Austrochip´97, pp. 183 – 188, Universitätsverlag Rudolf Trauner, 1997.
7. P. Thorwartl, N. Kerö: “CULT Skalierbare Benchmarks für programmierbare Logikbausteine”, Austrochip´97, pp. 247 – 253, Universitätsverlag Rudolf Trauner, 1997.
8. P. Thorwartl, J. Vogelhuber: “Ansteuerung von großflächigen, mehrfarbigen LED-Anzeigetafeln”, Austrochip´97, pp. 227 – 232 Universitätsverlag Rudolf Trauner, 1997.

Doctor’s Theses

1. Gerhard R. Cadek: Entwurf und Realisierung eines mehrkanaligen, digitalen, integrierten Schaltkreises zur Sprachkomprimierung mit neuartiger Architektur, Vienna University of Technology, 1997.

Cooperations

1. AKG Acoustics, Mr. Ernst Stöttinger
2. Semcotec, Mr. Manfred Raab
3. Frequentis Nachrichtentechnik, Mr. Heckmann
4. Institut für Computertechnik, TU Wien, Prof. D. Dietrich
5. Institut für Technische Informatik, Prof. Grünbacher
6. Institut für Elektronik, TU Graz, Prof. Leopold
7. Institut für Angewandte Informationsverarbeitung, Prof. Posch
8. Institut für Systemwissenschaften, Universität Linz, Prof. R. Hagelauer

UNICHIP Graz — Design of Integrated Circuits

P. Söser

**Department of Electronics,
Graz University of Technology, A-8010 Graz, Austria**

To satisfy the growing demand for engineers trained in the design of integrated circuits (ICs) the Department of Electronics offers several academic courses to cover this topic. In order to establish fundamental knowledge on design flow, verification, and test of ICs also some research projects are carried out at the Department. The main area in IC-design is the wide topic of mixed signal ASICs in CMOS or BiCMOS technology. In the following chapters there will be an introduction to the facilities and the courses at the Department of Electronics. Furthermore some IC projects of the year 1997 are presented.

1. Introduction

A main part of the 1997 activity at the Department of Electronics in UNICHIP was training the students in the field of IC-design. The Department offers 5 courses to cover the following topics:

- Basic IC-technology (fabrication, design-flow, silicon-technology)
- Fundamentals of MOS and bipolar transistors
- Use of CAD tools (analog and digital simulation, layout, standard-cell design etc.)
- Analog and digital circuit design
- Testing integrated circuits

In order to get a deeper understanding of the problems encountered with analog integrated circuit design a course at the Imperial College in London/Great Britain was attended by a member of the project team.

2. Academic Courses

The following table shows the titles and further information on all courses related to IC design offered at the Department of Electronics.

There were 16 theses worked on in 1997. Some of them where carried out in close cooperation with the three major enterprises in Austria dealing with IC design and manufacturing (AMS, Siemens-EZM and Philips Semiconductor Gratkorn).

title of the course	type	hours/term	participants/year
Integrierte Schaltungen 1	VO	30	80
Integrierte Schaltungen 2	VO	30	40
Integrierte Schaltungen 2	UE	30	40
Testen Integrierter Schaltungen	LU	45	28
Elektronikprojekt	PR	90	10

Table 1: Courses dealing with IC-design

3. Facilities

3.1 Hardware

We are using the following hardware components in our courses as well as for research projects:

- 11 SUN-SPARC Stations, 6 PCs
- Micromanipulation Tool with Laser-Cutter
- PC-based measurement environment and logic verifier for digital ICs

3.2 Software

We are using the following software-tools in our courses and for research projects:

- Mentor Graphics®: V8.5 Design Framework; GDT
- Analog Simulation: HSPICE (Meta Soft®); PSPICE (MicroSim®)
- XACT; Xilinx tools for FPGA-development using Mentor Graphics front-end
- HP-VEE; PC-based test-program-generation for IEEE-488 bus system

4. Experimental

In many courses there is a practical aspect, which leads to fabrication of chips by means of MPW-runs (Multi-Project-Wafer).

4.1 Student Projects

4.1.1 Testboard Development for Automated AD-Converter Characterization

Five testboards were successfully designed and used for various AD-Converters (types: 20 bit charge-balance; 12 bit successive approximation; sigma-delta and 8 bit flash) to automate the characterization by means of PC-based test programs, which were part of each project.

4.1.2 Characterization of a 1 GHz Mixer Chip

The design of a test environment and prototype testing for a mixer chip used in a GSM transceiver chipset was carried out in this project.

4.1.3 Design, Simulation and Layout of Source-Coupled-Logic Building Blocks

Source-coupled-logic building blocks (NAND, NOR, Latch etc.) were designed and compared to standard cells with respect to area as well as static and transient current consumption.

4.1.4 VHDL-Based Digital Circuit Design

The digital parts of a 20 bit AD-Converter and a quantization unit for periodic, digital signals were designed using VHDL and logic synthesis.

4.2 Research Projects

4.2.1 Evaluation of Former Projects

The engineering samples of two projects of 1996 (ENDOR [1], ENDEAVOR [2]) were tested and their correct functionality was evaluated.

4.2.2 Device Generators for Contacts and Cap-Arrays

Two generators were realized to expand the palette of device generators for Mentor Graphics® IC-Design framework used at our department. One is for shape- or path-based contacts and the other one is for binary weighted arrays of capacitors with minimum mismatch errors.

4.2.3 Automated Characterization of Operational Amplifiers by Means of Simulation

For details see [3].

4.2.4 Design, Simulation and Layout of the Analog Elements of a 12-Bit AD-Converter

For details see [4].

4.2.5 Realization Studies for the Monolithic Integration of a Velocity-of-Sound Encoder

To measure the velocity of sound in a fluid the time can be determined which an ultrasonic pulse needs to propagate over a known distance. In existing PCB systems this time is approximately 10 µs, and a resolution of 10 ps has to be achieved. Realization studies were carried out to integrate such a system on one chip.

5. Conclusion

The design of integrated circuits from the idea to the chip is the main goal for the project "UNICHIP-Graz, Entwurf integrierter Schaltungen". To train the students in this field there are some academic courses offered. There are also some research projects which are all together in the field of mixed-signal ASICs for sensor applications.

Acknowledgment

The "Steiermärkische Landesregierung, Abteilung für Wirtschaftsförderung" is funding this project by carrying a substantial part of the cost for personnel.

References

[1] W. Meusburger, R. Röhrer, H. Senn, P. Söser: "ENDOR - Ein ASIC für ein batteriebetriebenes Handdichtemeßgerät", *proceedings of "Austrochip '97"*, Linz 1997; ISBN: 3 85320 826 6; p. 297 – 300

[2] H. Leopold, W. Meusburger, R. Röhrer, H. Senn, P. Söser: "ASICs in electronic instrumentation", *proceedings of "Grundlagen und Technologie elektronischer Bauelemente";* Großarl 1997; ISBN: 3-901578-02-1; p. 99 – 105

[3] G. Schatzberger, A. Hopper, W. Meusburger, H. Senn, P. Söser: "Ein schneller 12-bit A/D-Umsetzer für niedrige Betriebsspannungen", *proceedings of "ME 97"*, Wien 1997; ISBN 3-85133-010-2; p. 163 – 168

[4] G. Schatzberger, H. Senn, P. Söser: "Automatisierte Charakterisierung von Operationsverstärkern mit Hilfe von Simulationswerkzeugen", *proceedings of "Austrochip '97"*, Linz 1997; ISBN: 3 85320 826 6; p. 337 – 343

Project Information

Project Manager

Dipl.-Ing. Dr. P. SÖSER

Institut für Elektronik, TU Graz

Project Group

Last Name	First Name	Status	Remarks
Leopold	Hans	professor	BMWV
Meusburger	Walter	assistant	BMWV
Röhrer	Robert	assistant professor	BMWV
Schatzberger [1]	Gregor	student	Inst. f. Elektronik
Senn	Helmuth	researcher	Inst. f. Elektronik
Söser	Peter	assistant	BMWV

The salaries for H. Senn and G. Schatzberger were refunded by Steiermärkische Landesregierung, Abteilung für Wirtschaftsförderung.

Publications in Reviewed Journals

1. H. Leopold, W. Meusburger, R. Röhrer, H. Senn, P. Söser: “ASICs in electronic instrumentation”; Proceedings of “Grundlagen und Technologie elektronischer Bauelemente”; Großarl 1997; ISBN: 3-901578-02-1; p. 99 – 105
2. G. Schatzberger, A. Hopper, W. Meusburger, H. Senn, P. Söser: “Ein genauer und schneller Komparator für den Einsatz in einem 12-Bit Analog/Digital-Umsetzer nach dem sukzessiven Approximationsverfahren”; Proceedings of “Austrochip ‘97”; Linz 1997; ISBN: 3-85320-826-6; p. 202 – 208
3. P. Söser, H. Senn, 6 Students: “Projekte der integrierten Schaltungstechnik im Lehrbetrieb”; Proceedings of “Austrochip ‘97”, Linz 1997; ISBN: 3-85320-826-6; p. 276 – 281
4. W. Meusburger, R. Röhrer, H. Senn, P. Söser: “ENDOR - Ein ASIC für ein batteriebetriebenes Handdichtemeßgerät”; Proceedings of “Austrochip ‘97”, Linz 1997; ISBN: 3-85320-826-6; p. 297 – 300
5. G. Schatzberger, H. Senn, P. Söser: “Automatisierte Charakterisierung von Operationsverstärkern mit Hilfe von Simulationswerkzeugen”; Proceedings of “Austrochip ‘97”, Linz 1997; ISBN: 3-85320-826-6; p. 337 – 343

[1] January to June 1997

6. G. Schatzberger, A. Hopper, W. Meusburger, H. Senn, P. Söser: “Ein schneller 12-bit A/D-Umsetzer für niedrige Betriebsspannungen”; Proceedings of ME 97, ÖVE-Schriftenreihe Nr. 14; Wien 1997; ISBN 3-85133-010-2; p. 163 – 168

Presentations

1. P. Söser: “ASICs in electronic instrumentation”; Seminar “Grundlagen und Technologie elektronischer Bauelemente”; Großarl 19.3.1997 – 22.3.1997
2. P. Söser: “Projekte der integrierten Schaltungstechnik im Lehrbetrieb”; Austrochip ’97, Linz 1997
3. W. Meusburger: “ENDOR - Ein ASIC für ein batteriebetriebenes Handdichtemeßgerät”; Austrochip ‘97, Linz 1997
4. G. Schatzberger: “Automatisierte Charakterisierung von Operationsverstärkern mit Hilfe von Simulationswerkzeugen”; Austrochip ‘97, Linz 1997
5. G. Schatzberger: “Ein schneller 12-bit A/D-Umsetzer für niedrige Betriebsspannungen”; ME 97, Wien 1997

Cooperations

1. Institut für Angewandte Informationsverarbeitung und Kommunikationstechnologie; TU Graz, Prof. Dr. R. Posch
2. Forschungsgesellschaft Joanneum, Institut für Sensorik, Graz
3. Labor für Meßtechnik, Dr. H. Stabinger, Graz
4. Fa. Anton Paar GmbH, Graz
5. AMS, Austria Mikrosysteme International AG; Unterpremstätten
6. Entwicklungszentrum für Mikroelektronik; Siemens, Villach
7. Fa. Philips Semiconductor (was MIKRON), Gratkorn

Microsensors and Other Projects

High Precision Depth Profiles with SIMS

H. Hutter, K. Piplits, M. Gritsch

Institute of Analytical Chemistry, Vienna University of Technology A-1060 Vienna, Austria

This contribution demonstrates applications of surface analysis techniques for the investigation and characterization of materials and production processes. SIMS depth profile measurements of erbium in silicon demonstrate that high precision measurements of low concentrations are necessary to assist implantation and simulation groups. Measurements of the internal structure of light-emitting diodes verify that the development of new microelectronic components is a great challenge for analytical chemistry.

1. Introduction

Surface analysis techniques play an important role in supporting material development and process optimization. One of the most common techniques is Secondary Ion Mass Spectrometry (SIMS). This is due to the high detection power of the method, the fact that all elements are detectable, and the possibility of registering two- and three dimensional distributions of trace elements.

To support various investigations in the field of microelectronics, the performance of analytical methods has to be increased. The actual questions of technology demand a permanent development of the precision of measurements, especially at very low concentrations. The supervision of the implantation process stability by measurements of depth profiles for erbium demonstrates the support of optimizing production processes.

2. Results

2.1 Erbium in Silicon

The 4f shell of rare earth elements is well shielded by the outer shell electrons. Therefore these elements exhibit sharp and almost atom-like spectra when incorporated as dopants in semiconductors and insulators. The emitted wavelengths practically coincide with those observed for isolated atoms and depend only little on the host material. Erbium implanted into Si produces rich spectra of sharp lines in photo- and also in electroluminescence in a narrow spectral region close to 1.54 µm. This wavelength stimulates interest in Si:Er as a candidate for light emitting devices for fiber optics communication systems and also for on-chip and inter-chip optical data transfer [1].

In this project an erbium containing silicon film on a waver was produced by an MBE process. The erbium concentration was verified by the used sources with different Er-content. The results of different sources and different parameters were determined. The concentrations of O and Er were determined by the use of standards. The C and B content were not quantified, because only the relative differences of the samples were rele-

vant. Fig. 1 gives an example of the measurements. In this example it is visible that the O concentration is not constant and there is a C contamination on the interfaces.

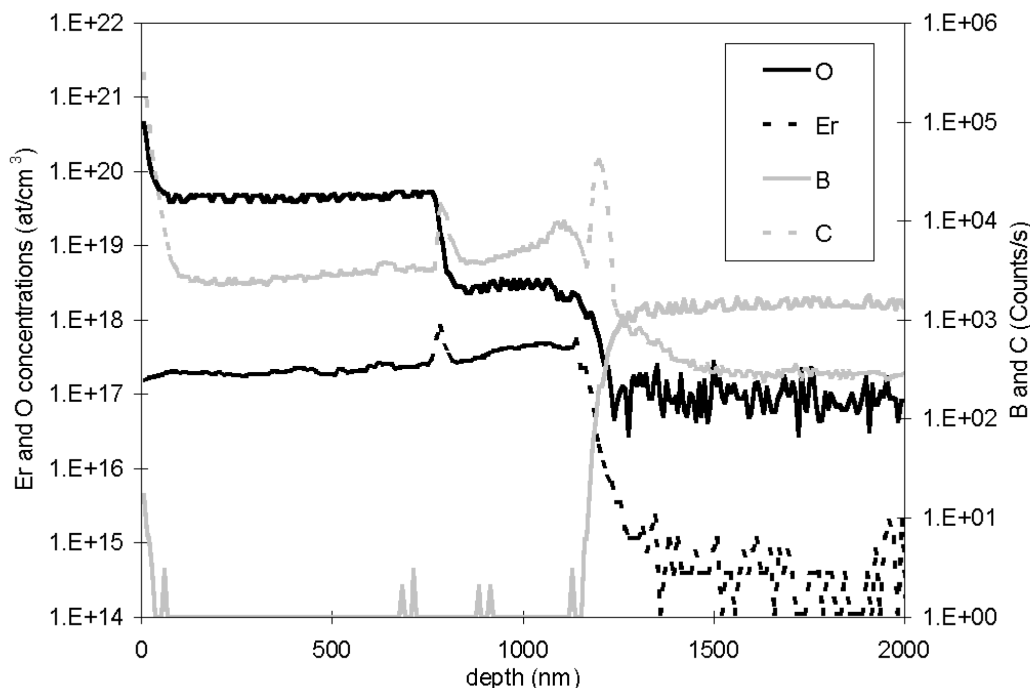

Fig. 1: SIMS depth profile of an erbium film on silicon. The elements Er and O were quantified by the use of standards, therefore the concentration is given in at/cm^3 (left axis). Because for the elements B and C no standards were available only the counts/s are indicated (right axis).

2.2 Blue Light-Emitting Electrochemical Cells

Light-emitting diodes based on conjugated polymers (PLEDs) can be realized with high efficiencies over the whole visible range. The most attractive application of PLEDs is their usage in self-emissive flat panel displays [2].

This part reports the investigations of blue light-emitting electrochemical cells (LEC) based on a ladder-type poly(paraphenylene) (m-LPPP). The turn-on voltage of these LECs occurs at 2.7 V and external efficiencies of around 0.3% and a brightness of around 250 cd/m^2 at 10 V were obtained with the LECs based on m-LPPP. The phase morphology of the LECs based on m-LPPP can be optimized in a way that LECs with a very fast pulse response in the range of 20 – 30 µs are obtained.

These LECs consist of three layers. The first is an ITO layer (thickness: ~200 nm) as transparent electrode on a glass substrate, the second consists of the conjugated polymer mixed with polyethylenoxide and $LiCF_3SO_3$ (ratio 20:10:3, thickness: ~100 nm). As top-electrode usually Al was evaporated on top of the blend film in high vacuum (thickness: ~200 nm).

The SIMS measurements should clarify if there is a separation of the Li^+ and the $CF_3SO_3^-$ ions during production and/or the use of the diodes. Ti was of special interest if an enrichment of the ions on the interfaces polymer-ITO and polymer-Al is observable.

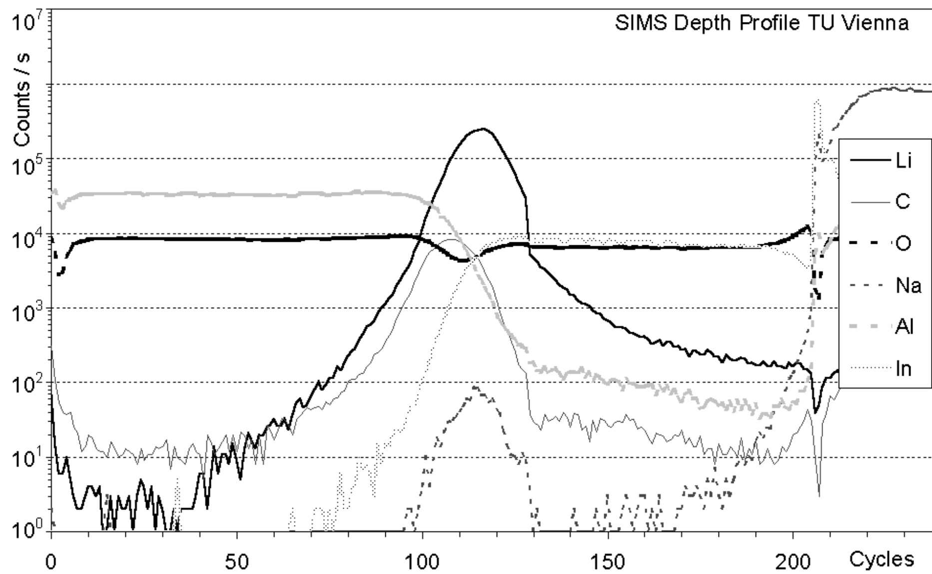

Fig. 2: SIMS depth profile of the LED. Primary ions: O_2^+. On the right side of the profile the insulating glass substrate is reached. The sample becomes charged at this depth. The Li^+ signal is shifted to the right side (relative to the C-peak). This indicates an enrichment of Li at the interface polymer–ITO.

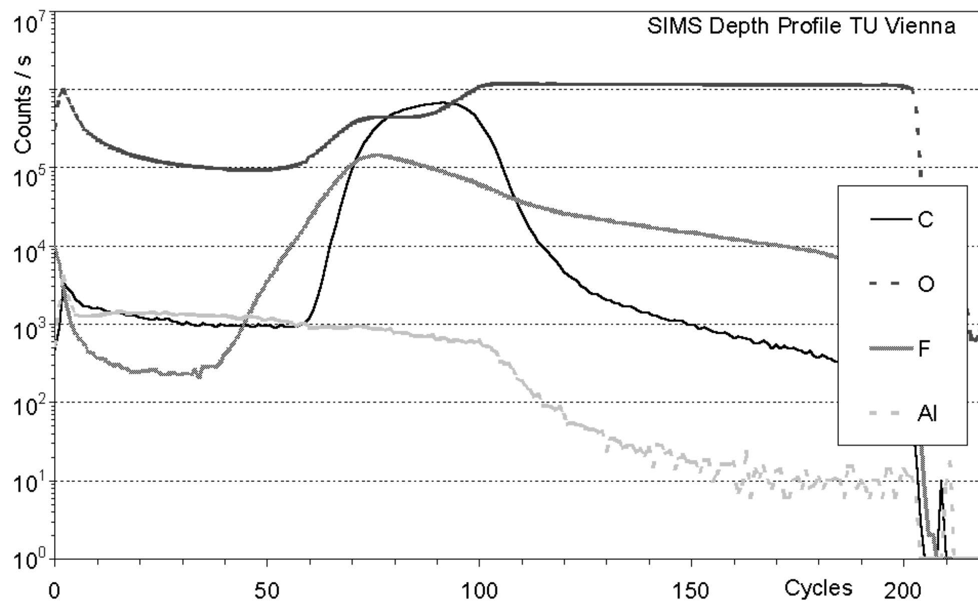

Fig. 3: SIMS depth profile of the LED. Primary ions: Cs^+. Due to the atomic-mixing effect the C peak appears wider under Cs bombardment compared to the oxygen profile. The F peak is shifted to the left side relative to the C peak. This indicates an enrichment of F at the interface polymer–Al.

Here only the results of the unused LECs are presented. Due to the different sensitivity of the ions it was necessary to measure the Li^+ distribution under oxygen bombardment (see Fig. 2) and the F^- and O^- ions under cesium bombardment (see Fig. 3). The detec-

tion of the S^- ion was not possible without the use of high mass resolution, because of the mass interference with O_2^-. The detection of C as an identifier of the polymer in both measurements allows to fit the depth profiles. This fit is presented in Fig. 4, by way of exception (for SIMS depth profiles) this diagram has a linear y-axis.

In Fig. 4 is clearly visible that there is a enrichment of the ions at the interfaces. This separation takes place already during the manufacturing of the LECs, not by contacting to the supplying voltage.

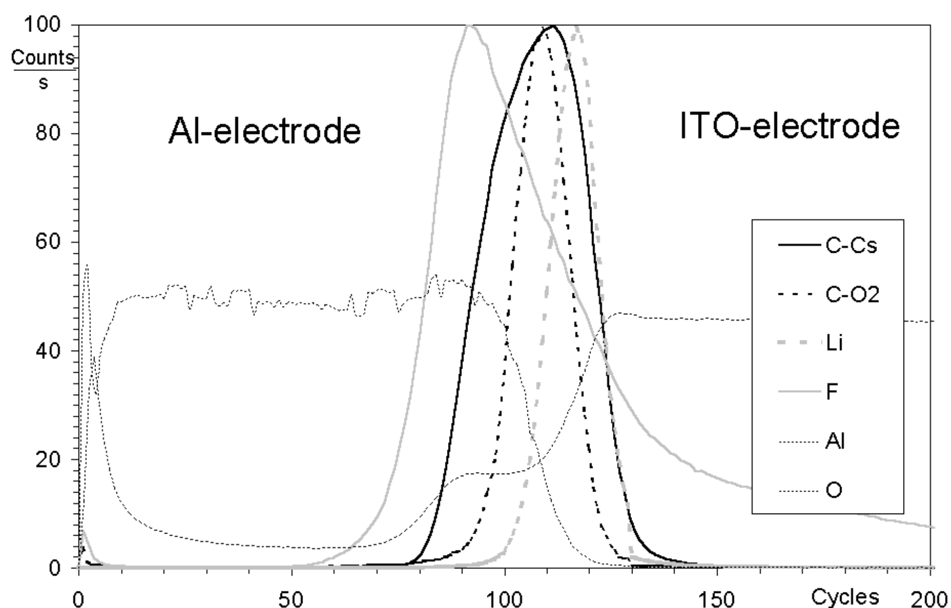

Fig. 4: Normalized intensities from the Cs^+- and O_2^+ measurements. The C peaks from both measurements are printed. For indication of the layers the Al^+ and O^- signal are given. The maximum of the F^- peak is at the interface polymer–Al, the maximum of the Li^- peak is at the interface polymer–ITO.

In this project furthermore the influence of different electrodes (Al and Au) was determined. Besides the change of the ions distribution during the use of the LECs were observed.

3. Conclusion

Microelectronics is a continual challenge for modern material analysis. In many cases improvements of well established analytical methods, like SIMS, are necessary to obtain precise measurement results of the concentration of dopands and trace elements. This knowledge makes the development of new processes and materials possible.

References

[1] W. Jantsch, L. Palmetshofer, “Erbium Related Centres in Silicon” *Grundlagen und Technologic elektronischer Bauelemente*, Großarl 1995, ISBN 3-901578-01-3

[2] G. Leising, S. Tasch, W. Graupner, "Fundamentals of Electroluminescence in Paraphenylene-Type Conjugated Polymers and Oligomers", *Handbook of Conducting Polymers* (T. Skotheim ed.), Marcel Dekker New York (1997)

Project Information

Project Manager

Dr. Herbert HUTTER

Institute for Analytical Chemistry, Vienna University of Technology

Project Group

Last Name	First Name	Status	Remarks
Gritsch	Martin	diploma thesis	
Piplits	Kurt	technician	partial GMe funding
Wolkenstein	Martin	dissertation	

Publications in Reviewed Journals

1. Ch. Brunner, H. Hutter, P. Wilhartitz, M. Grasserbauer: “Investigation of the Formation and Properties of Protective Oxide Layers on High Purity Chromium with SIMS Images Techniques”, Mikrochim. Acta 125, 69-72 (1997)
2. M. Wolkenstein, H. Hutter, M. Grasserbauer: “Comparison of Wavelet Filtering with Well-known Techniques for EPMA Image Denoising”, J. of Trace and Microprobe Techniques, 15(1), 33-49 (1997)
3. M. Griesser, H. Hutter, M. Grasserbauer, W. Kalss, R. Haubner, B. Lux: “SIMS-Analysis on B, N, and C Containing Layers”, Fresenius J. Anal. Chem. (1997) 358:293-296

Cooperations

1. Institut für Festkörperphysik, TU Graz, Prof. Leising
2. Institut für Halbleiterphysik, Uni Linz, Prof. Palmetshofer
3. Plansee AG, Dr. P. Wilhartitz

Integrated Sensor-Microflow-Systems

G. Urban, F. Kohl, A. Jachimowicz, J. Steurer, F. Keplinger, P. Svasek, E. Svasek

Institut für Allgemeine Elektrotechnik und Elektronik, TU Vienna A-1040 Wien, Austria

This report describes first experiences with a new high resolution, miniaturized optical pH sensor principle we developed and presents results obtained for a novel biosensor for liver enzymes assay and a wide range conductometric sensor. The integration of those sensors, among others, on a common carrier requires advanced integrated sensor-microflow-systems. This topic is addressed by an experimental study on different miniaturized fluidic mixer structures and the investigation of miniaturized flow sensors using a new signal conditioning device.

1. Introduction

Modern medical research and intensive care requires very complex biochemical analysis to be done e.g. at the patient's bedside. This task necessitates small sensors as well as cheap and handy equipment. Integrated sensor-microflow-systems address those technical needs. To build up effective integrated analysis systems there is a variety of essential prerequisites like miniaturized sensors, bioreactors, actuators, and valves. Beside these miniaturized components there must exist adequate techniques to interconnect these essential components.

2. Experimental

2.1 A Novel Thin Film Integrated Optics pH Sensing System

By combining an ultrathin photopatterned pH dependent swelling membrane with a replicated chirped grating coupler as a transducer an optical pH sensor was created.

The pH sensitive membrane is made from a poly(80 mol% Hydroxyethyl methacrylate – 20 mol% N,N' Dimethylaminopropyl methacrylate) copolymer. With a pK value of 7.5 the pendant amino groups become protonated. This leads to an increase of the osmotic pressure in the gel that increases the swelling and, due to the relative lower refractive index of water, the gel's refractive index decreases. A polymer solution, comprising benzoquinone as photoactive agent, is applied to the substrates by spin coating to produce layers of 100 nm thickness. Benzoquinone forms a charge transfer complex with the amino groups of the polymer which facilitates crosslinking upon UV exposure. This makes it possible to pattern this "negative working" membrane precursor with a mask aligner at one minute exposure time.

The replicated chirped grating couplers, which are contributed by the Paul Scherrer Institute Zurich, are made on polycarbonate with a TiO_2 waveguide and two chirped gratings. Since the grating periodicity continuously varies at chirped gratings, the coupling criterion is matched only on one point. In this way, changes in the refractive index are

related to moves of the emitted light point at the outcoupling grating. Such devices showed a resolution of 10^{-4} pH units and response times of less then one minute. Because of the relatively easy and potentially cheap manufacturing, their planarity, and sensitivity, they are attractive candidates for microphysiometry applications. Even quantification of single cell metabolic activity seems feasible.

2.2 Rapid Liver Enzyme Assay with Bioanalytical Microsystem

Assays of transaminases present in the serum play an important role in diagnosis and monitoring of the course of liver diseases or myocardial infarction. Elevated serum activity of GOT – *Glutamic Oxaloacetic Transaminase* – indicates severe damage to the cells of heart or liver. Especially in the early detection of myocardial infarction monitoring of GOT during the first 24 hours helps to gain an insight into the seriousness of the infarction. GPT – *Glutamic Pyruvic Transaminase* – is present in high concentrations only in the cytosol of hepatocytes. Therefore raised plasma activity of GPT indicates a severe liver disease like viral hepatitis or toxic liver necrosis causing disruption of cell membranes.

The realized amperometric assay detects the transaminase acivities by detecting the product glutamate by means of a thin film glutamate biosensor. Production and performance of the thin film biosensor array are described by Moser et al. [1]. The sensor array comprising two glutamate sensors and two blank sensors is 4x7 mm^2 wide and made by means of thin film technology. The transaminase activity assaying device comprises of the thin film biosensor array assembled on a microfluidics realized with the dry film photoresist technology (see 2.5). This integration not only minimizes the sample volume required but also increases the reliability of the analysis performed.

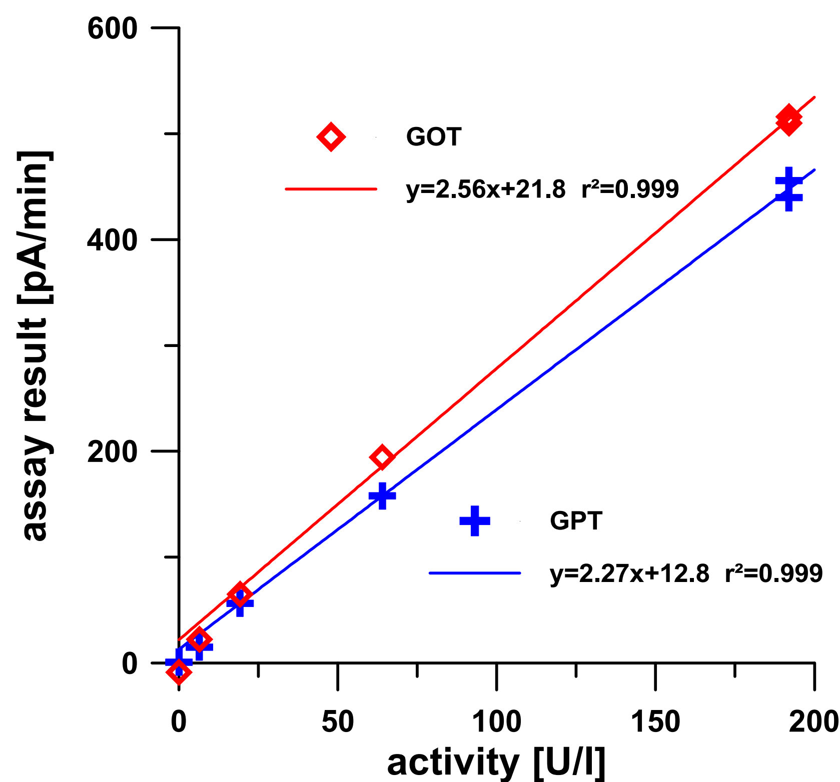

Fig. 1: Calibration graphs of GPT and GOT assays.

2.2.1 Experimental Results

The calibration graphs of the GOT and GPT assays are shown in Fig. 1. Increased activity of the enzyme in the range of 100 – 200 U/l indicates most of the liver diseases [1]. Compared to the traditional spectrophotometric techniques of transaminase acivity assays this novel analytical device offers serious advantages. Most important, readout can be obtained within a few minutes. Sample volume requirement is reduced, too. No NADH and no soluble enzymes are required in the assay and therefore the stability of the substrate solutions is enhanced. The small dimensions of the device, the stability of the reagents used, and the relatively simple measurement electronics should allow the development of a hand-held device for the point of care assay of GOT and GPT.

2.3 Miniaturized Planar Four Electrode Conductometric Sensors

Conductometric transducers covered with functional membranes will become important transducers in medical, biological, and environmental diagnostics. We studied planar devices featuring structure widths of 2 µm and 5 µm (Fig. 2) and two as well as four electrode arrangements. The results of impedance measurements obtained with these were compared with simulation results for the voltage-current relations. Measurements using two and four electrode techniques were carried out. The voltage applied at the current terminals of such transducers must not exceed 10 mV_{eff} to prevent electrochemical reactions, and the useful frequency ranges from 100 Hz to some 10 kHz.

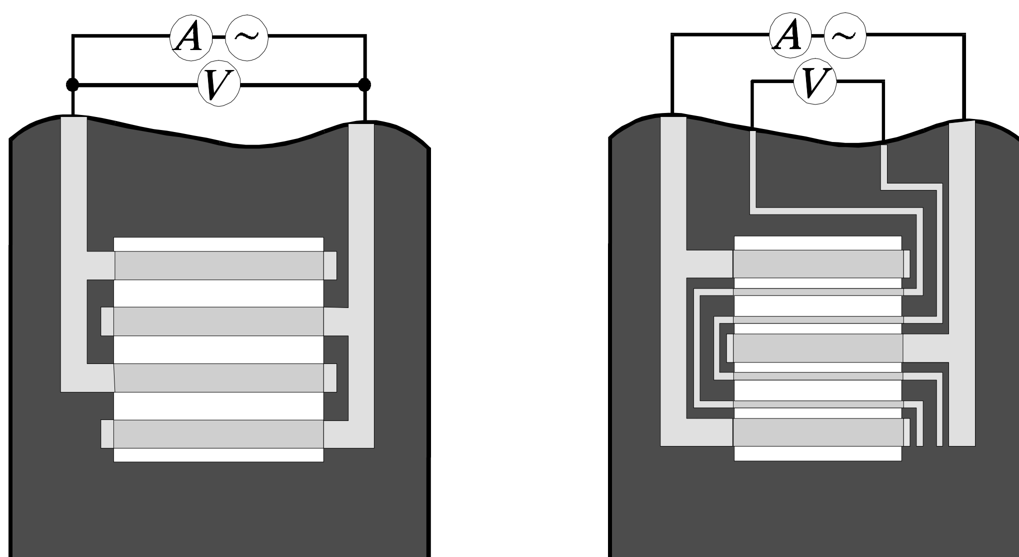

Fig. 2: Electrode structures used for the experiments and the simulations. Interdigital distances typical 2 to 5 µm, overall area 2 by 2 mm^2.

With shrinking structure widths the limited rate of charge transfer between the electrodes and the electrolyte becomes of main importance. For two-electrode impedance measurements they put severe limits on the measurable ion concentration ranges and the maximum operating frequency. By using four-electrode techniques one can extend the measuring range far beyond these limits if signals in the 1 µV range are acceptable.

For miniaturized structures the large relative width of the voltage measuring electrodes causes deviations near the surface from the ideal electric field configuration of four probe arrangements. Also the influence of the electrolyte layer thickness, which is determined by the dimensions of the miniaturized flow channel cross section, have to be taken into account. Because of the lateral channel dimensions and the periodicity of the electrode arrangement a two-dimensional model of the electrolyte cell geometry was chosen for all numerical simulations which were carried out using the ANSYS software packet.

2.3.1 Measurement Results

A comparison of measured and calculated admittance values shows good consistence of the concentration dependency, leading to a extremely wide useful measuring range of 0.001 mS/cm to 100 mS/cm (Fig. 3). As long as the electrolyte resistance doesn't dominate the over-all resistance the calculated admittance of the model is significantly higher than the measured quantity, indicating that the model assumes too high values for the charge transfer rates at the electrodes.

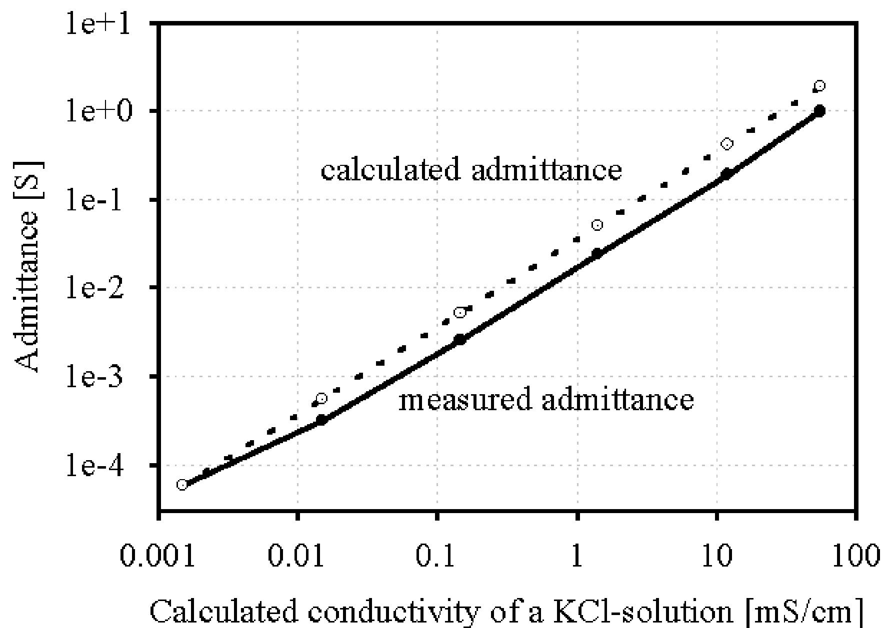

Fig. 3: Comparison between calculated and measured admittance of a four-electrode transducer.

2.4 Miniaturized Flow Transducers

Controlled intermixture of reagents or the addition of small amounts of drugs during infusion calls for miniaturized flow sensors. Hot film flow sensors based on thin-film amorphous germanium thermistors offer quick response, high sensitivity, recognition of flow direction, and a wide dynamic range. Integration of these thermistors on a micromachined thin membrane could further enhance their sensitivity and, as a benefit from miniaturization, give a faster response to flow changes. Flow direction could be recognized using two temperature sensors placed on the membrane symmetrically to a thin-film platinum resistor that sources the heat. Figure 4 shows a realized structure of a mi-

cromachined flow sensor which comprises two substrate thermistors that can be used to eliminate the influence on sensor performance of ambient temperature changes.

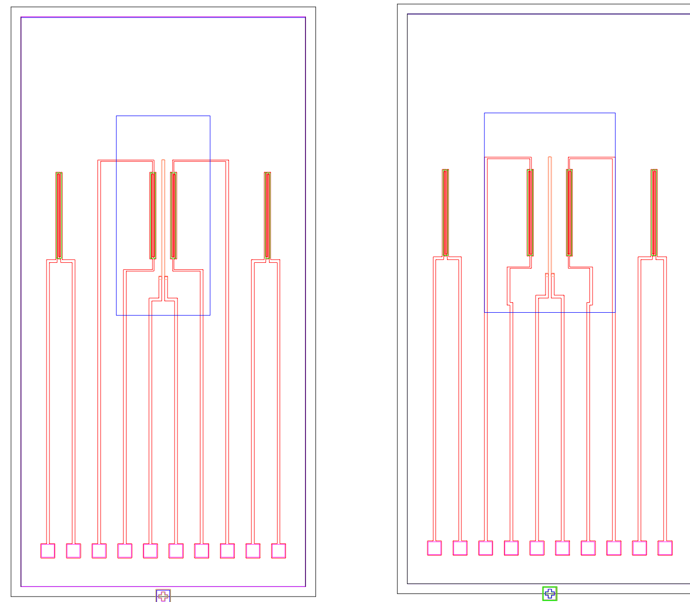

Fig. 4: Mask layouts of two different miniaturized flow sensor structures. The micromachined membrane area, defined by the smallest rectangles, bears two flow sensing thermistors and an intermediate metal film resistor. Two additional thermistors serve for substrate temperature monitoring.

2.4.1 Flow Measurement Results

A constant temperature difference between the ambient and the average temperature of the membrane thermistors was maintained by an electronic controller. The signal was derived from the temperature difference at the membrane thermistors sites. An investigation of the transducer mounted to a flow channel of 0,5 mm^2 cross sectional area delivered a useful measuring range from 200 µl/h to 200 ml/h for the volume flux of water. That measuring range should be sufficient for nearly all medical applications. The corresponding detection limit for the volume flux of air was 1,3 ml/h for the same arrangement. This are reasonable good results for a transducer optimized for short response time rather than maximum flow sensitivity.

The observed response time of 1 ms is in good agreement with the predictions of FE model calculations. The output power of the controller could be used as a measure for the magnitude of the flow velocity, too. But in this operation mode the recognition of the direction of flow is not possible. A linear response to the flow was obtained at full bandwidth by digitizing the sensor signals and using a look-up table transformation.

2.5 Dry Resist Miniaturized Mixing Devices

Three different types of miniaturized mixer structures have been fabricated by means of dry film photoresist technology [2]. Enhanced mixer performances using specially designed microstructures were compared with that of a smooth channel, which is 600 µm wide, 100 µm high and 170 mm long.

The second type of micro-mixer consists of a channel of the same dimensions but with additional diagonal grooves in the bottom. These grooves add a rotational movement to the stream.

The so-called Moebius principle has been applied for the third mixing device. The basic element of a Moebius mixer performs rotation, splitting the flow, separate rotation and recombination. Rotation is achieved by groups of fins at the bottom of the channel.

2.5.1 Measurement and Results

The mixing behavior was made visible using solutions of iodine-starch blue and Na thiosulfate, which decolorizes the first one by chemical reaction. Complete mixing takes a considerably long time in a smooth channel and therefore very low flow rates have to be used. Grooves improved the mixing performance roughly by an order of magnitude. The improved performance of the Moebius type of mixers is very impressive. Complete mixing occurs at considerably higher flow rates and takes much less time, while the internal volume is even lower.

type of mixer	internal volume	complete mixing at	mixing time
smooth channel	10.2 µl	≤ 0.12 µl/min	85 min
channel with 164 diagonal grooves	16.3 µl	≤ 1.3 µl/min	12.5 min
4-stage Moebius mixer	6.5 µl	≤ 285 µl/min	1.4 s

Table 1: Performances of different types of static mixers

3. Conclusion

Our recent developments of sensors extend the field of metabolics measurable by microsensors. The progress of cheap integration technologies enables complete integrated sensor-microflow systems to be built. We have shown that this concept works well by the new transaminase assay, which is based on a specific implementation of the integrated sensor-microflow-system concept.

Acknowledgments

Part of this work was supported by the Brite Euram program of the European Community, the companies AVL and Schlumberger Paris, and the Forschungsförderungsfonds der gewerblichen Wirtschaft.

References

[1] I. Moser, G. Jobst, E. Aschauer, P. Svasek, M. Varahram, G. Urban, V. Zanin, G. Tjoutrina, A. Zharikova, T. Berezov: "Miniaturized Thin Film Glutamate and Glutamine Biosensors", *Biosensors & Bioelectronics* 10, (1995) 527 – 532.

[2] P. Svasek, G. Jobst, G. Urban, E. Svasek: "Dry Film Resist Based Fluid Handling Components for µTAS", *Proc. 2nd Intern. Symposium on Micro Total Analysis Systems µTAS96*, Basel, Switzerland, 1996, 78 – 80.

Project Information

Project Manager

Univ. Doz. Dr. Gerald URBAN, Dr. Franz KOHL

Institut für Allgemeine Elektrotechnik und Elektronik, TU Wien

Project Group

Last Name	First Name	Status	Remarks
Biacovsky	Dalibor	dissertation	
Fasching	Rainer	dissertation	
Jachimowicz	Artur	assistant professor	1.1.1997 – 30.9.1997
Jobst	Gerhard	technician	
Keplinger	Franz	assistant professor	partially GMe funded
Kohl	Franz	assistant professor	
Moser	Isabella	post doc	1.1.1997 – 31.8.1997
Steurer	Johannes	assistant professor	partially GMe funded
Svasek	Peter	technician	
Svasek	Edeltraut	technician	
Urban	Gerald	associate professor	1.1.1997 – 31.3.1997
Vahraram	Mehdi	dissertation	

Books and Contributions to Books

1. E. Aschauer, G. Jobst, R. Fasching, M. Varahram, P. Svasek, I. Moser, G. Urban: “Miniaturisierte integrierte Biosensoren für Glukose- und Laktatmonitoring”, H. Ahlers ed., Multisensorik-Praxis, Springer Verlag 1997, 225 – 238
2. G. Urban: “Microelectronic Biosensors for Clinical Applications”, Handbook of Biosensors, Food, and the environment, CRC Press 1997, chapter 12, 257 – 279
3. G. Urban, G. Jobst: “Techniques for fabrication of implantable sensors”, Biosensors in the Body: Continuous in vivo Monitoring, John Wiley & Sons (Chichester, UK), 1997, 197 – 216
4. G. A. Urban, G. Jobst: “Biosensors with modified electrodes for in-vivo and ex-vivo applications”, Frontiers in Biosensorics II, (ed.: F.W.Scheller), Birkhäuser Verlag 1997, 161 – 173
5. G. A. Urban, G. Jobst: “Sensor Systems”, Topics in Current Chemistry ”Microsystem Technology in Chemistry and Life Sciences”, (ed. Manz, Becker), Springer Verlag 1998, 189 – 215

Publications in Reviewed Journals

1. G. Jobst, I. Moser, G. Urban: “Numerical simulation of multi-layered enzymatic sensors”, Biosensors & Bioelectronics 11, No 1-2 (1996) 111 – 117
2. E. Aschauer, R. Fasching, M. Varahram, G. Urban, G. Nicolussi, W. Husinsky, G.Friedbacher, M.Grasserbauer: “Surface modification of platinum thin film electrodes towards a defined roughness and microporosity”, Journal of Electroanalytical Chemistry 426, (1997) 157 – 165
3. Z. Trajanoski, P. Wach, G. Jobst, G. Urban, P. Kotanko, F. Skrabal: “Portable Device for Continuous Blood Sampling and Continuous Ex Vivo Blood Glucose Monitoring”, Biosensors & Bioelectronics, Vol 11, No. 3 (1996)
4. G. Jobst, M. Varahram, I. Moser, P. Svasek, E. Aschauer, Z. Trajanoski, P. Wach, P. Kotanko, F. Skrabal, G. Urban: “Thin-film Microbiosensors for Glucose-Lactate Monitoring”, Anal. Chem., Vol. 68, 18 (1996) 3173 – 3179.
5. R. Freaney, A. McShane, T.V. Keaveney, M. McKenna, K. Rabenstein, F. Scheller, D. Pfeiffer, G. Urban, I. Moser, G. Jobst, A. Manz, E. Verpoorte, M. Widmer, D. Diamond, M. Smyth, E. Dempsey: “Novel Instrumentation for Real-Time Monitoring using Miniaturised Flow Systems with Integrated Biosensors”, Annals of Clinical Biochemistry, 34 (1997), 1 – 12.
6. G.V. Tjoutrina, A.V. Zarikova, V.A. Zanin, T.B. Berezov, I. Moser, G. Jobst, E. Aschauer, P. Svasek, M. Varahram, G. Urban: “Miniaturized thin film biosensors sensitive to glutamate and glutamine”, Voprosy Meditsinskoi Khimii 43-1 (1997) 22 – 30
7. I. Moser, T. Schalkhammer, F. Pittner, G. Urban: “Surface Techniques for an Electrochemical DNA Biosensor”, Biosensors & Bioelectronics (1997), 12 , 729 – 737
8. I. Moser, G. Jobst, P. Svasek, E. Svasek, M. Varahram, G. Urban: “Rapid liver enzyme assay with miniaturized liquid handling system comprising thin film biosensor”, Sensors and Actuators (1997) 44/1-3, 377 – 380

Doctor’s Theses

1. A. Jachimowicz: “Miniaturisierte Kaliumsensoren in der Dünnschichttechnik”, TU Wien, 1997.

Cooperations

1. Institut für Mikrosystemtechnik, Albert-Ludwigs-Universtität Freiburg, Am Flugplatz 079, D-79104 Freiburg, Prof. Dr. G. Urban
2. AVL List Gmbh, Kleisstr. 48, 8010 Graz, Dr. Schindler
3. Schlumberger Paris, Dr. D. Dominguez

Scanning Force Microscopy Investigations of Thermally Grown Oxides on Polysilicon

F. Kuchar, A. Benkitsch

**Institut für Physik, Montanuniversität Leoben,
A-8700 Leoben, Austria**

The investigations concerned the topography of oxides on silicon and oxygen precipitates in the Si wafers which strongly influence the performance of the oxide layers. In the second case, the size and distribution of oxygen precipitates in Czochralski (CZ) silicon were investigated by Atomic Force Microscopy (AFM). In order to cover the range of interstitial oxygen provided by CZ silicon growth, three ranges of oxygen, 20 – 25, 25 – 30, and 30 – 35 ppma were chosen. The influence of the precipitation behavior on the device performance was determined by measuring the alignment accuracy and the device yield. It could be shown that device performance is not only influenced by the initial oxygen content but also by the size and distribution of oxygen precipitates.

1. Introduction

We have studied the topography at the transition from the gate oxide to the field oxide. Observed were influences of the nitride etching, thinning of the gate oxide near the bird's beak, remains of organic resist layers.

To meet the requirements of additional process module integration into deep sub-µm CMOS processes, the properties of the substrate become increasingly important. Therefore AFM investigations have been performed to investigate the size and distribution of oxygen precipitates which are known to directly influence the number of gate oxide defects in MOS transistors.

Since almost all silicon wafers used for the production of VLSI devices are grown by CZ silicon crystal technology, the wafers used for this study were taken from CZ grown ingots. During a CZ process silicon is molten in a quartz or fused silica (SiO_2) crucible. A seed crystal is brought into contact with the melt and then slowly withdrawn. Oxygen, an unintended dopant, enters the crystal via melt dissolution of the crucible. The oxygen rich silicon melt rises along the crucible wall, following the thermal convection flow pattern to the surface of the melt, and then to the melt center. There it is drawn towards the crystal by the forced convection induced by the crystal rotation [1].

Only a small fraction (< 5 %) of the dissolved oxygen is incorporated into the growing crystal, because most of the oxygen (> 95 %) evaporates from the free melt surface as silicon monoxide [2]. Therefore the oxygen content of CZ ingots usually ranges from 20 to 33 ppma (old ASTM, 1979).

During the diffusion steps of a CMOS process oxygen precipitates are formed, which causes two advantages. First, the mismatch of the Si and SiO_2 lattices and the increase in volume ($V_{Si} : V_{SiO2} = 1 : 2$) lead to the emission of dislocations, which getter unintentional contaminants and increase the capability of the wafer to withstand thermal

stress. Second, as these precipitates reduce the lifetime of minority carriers, they improve the junction breakdown characteristics [3].

There is a strong interrelationship between crystal growth conditions, grown-in defects, and their impact on device performance. The higher the cooling rate of the crystal, the higher the density of grown-in defects and the smaller their size [4]. Since defects of the lattice are nucleation sites for oxygen, the thermal history of the ingot has a strong influence on the precipitation behavior of the wafers.

2. Experimental

The radial distortion of 30 N-type wafers (14 – 24 Ohm*cm) with an oxygen content varying from 20 to 35 ppma O_i was measured by determining the current alignment mark position of each chip on the wafer by a laser interferometer after each diffusion step of the CMOS process. To estimate the width of the denuded zone as a function of the oxygen content, a simulation was performed [8].

Additionally one wafer per oxygen range was cleaved and etched with a 50% SECCO etching solution [5], [6] to determine the size and distribution of the oxygen precipitates by an UHV-AFM in contact mode. At the end of the CMOS process, the yield was determined and correlated with the radial distortion of the wafers.

3. Results

A strong correlation between oxygen content and radial distortion was found (see Fig. 1). But in contrary to what one might expect, the medium oxygen range showed the highest distortion values. Usually the lowest oxygen range should show the highest distortion due to the reduced ability to withstand thermal stress [7]. Further distortion during subsequent diffusion steps doesn't seem to be influenced by the initial oxygen content (see Fig. 2).

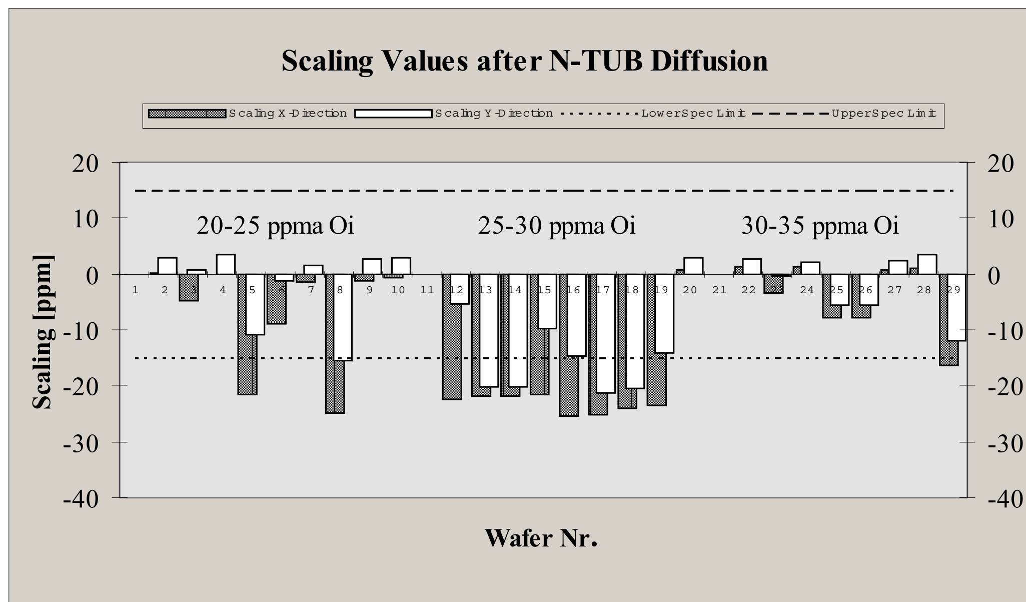

Fig. 1: Wafer scaling after N-TUB Diffusion.

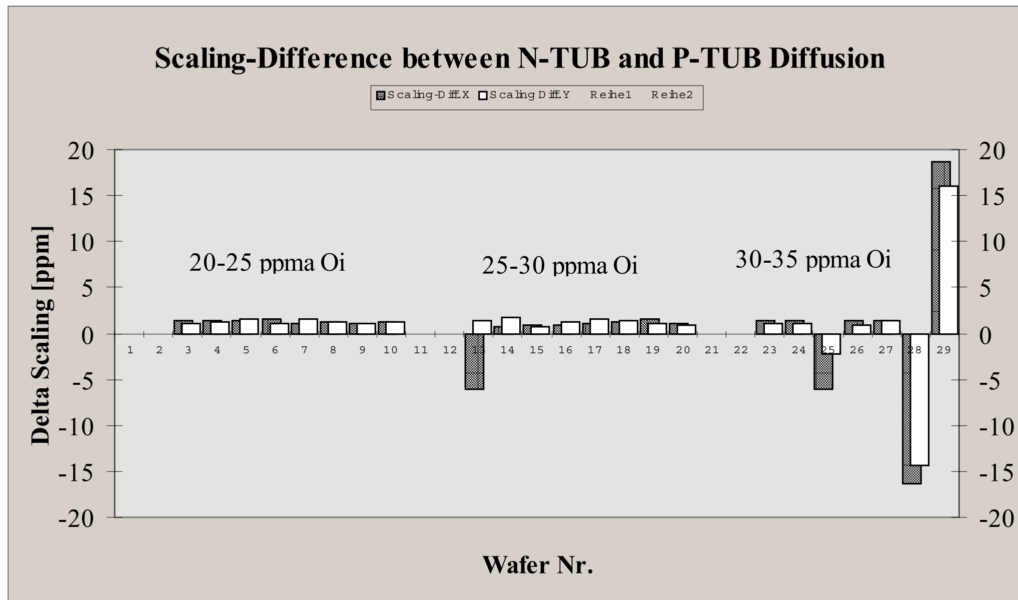

Fig. 2: Scaling difference between N-TUB and P-TUB Diffusion.

The precipitation simulation yielded a denuded zone of 20 µm for wafers with 35 and 70 µm for wafers with 20 ppma O_i, respectively [8], [9], [10].

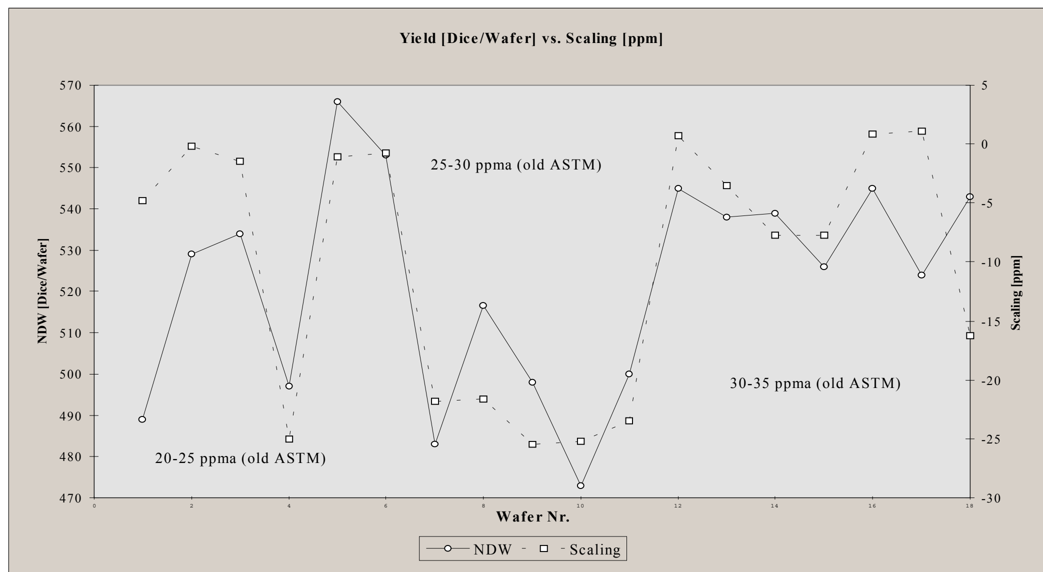

Fig. 3: Overall yield of the device.

The overall wafer yield also corresponds very well to the scaling values of the wafer (Fig. 3). Wafers showing high distortion exhibit few but big oxygen precipitates (Figs. 4 and 5), whereas wafers showing low distortion exhibit many small precipitates (Fig. 6).

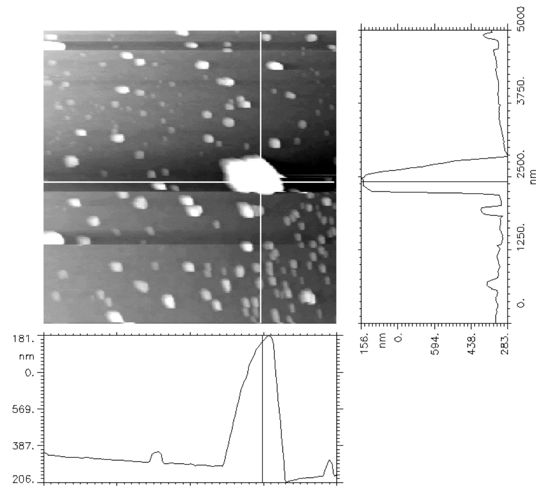

Fig. 4: Cross section of (100) wafer containing 25 – 30 ppma O_i.

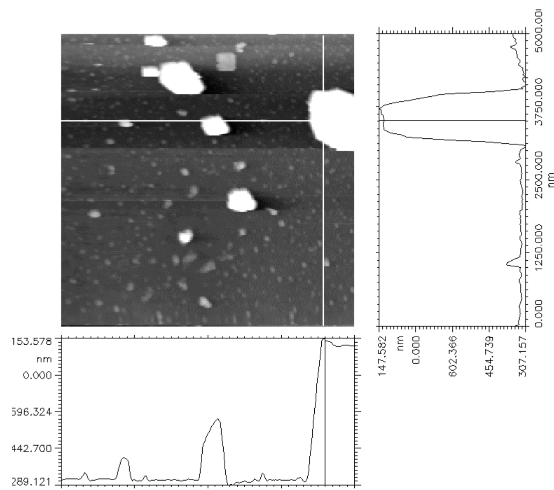

Fig. 5: Cross section of (100) wafer containing 20 – 25 ppma O_i.

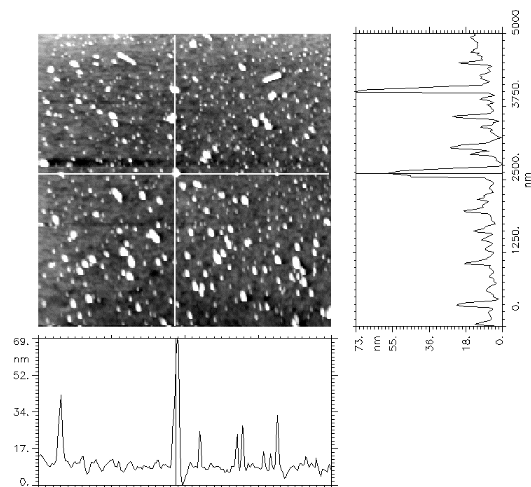

Fig. 6: Cross section of (100) wafer containing 30 – 35 ppma O_i.

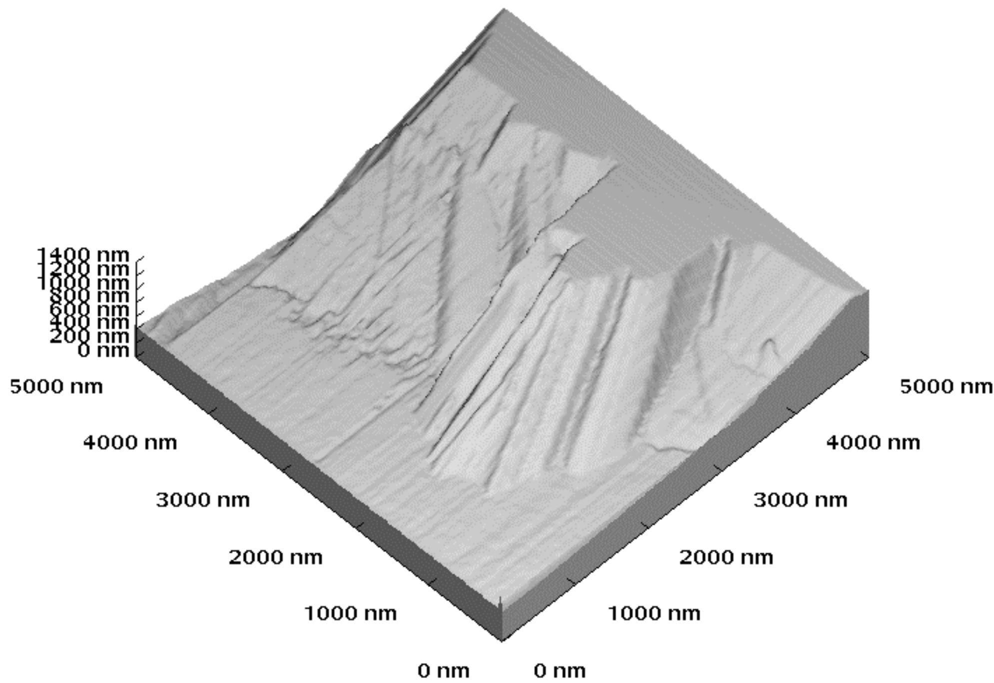

Fig. 7: Step on the cross section of the cleaved wafer (100).

The surface structure exhibits steps and other topographic features (see Fig. 7) due to interaction of the crack with reflected stress waves from the surface of the wafer [11]. These can cause local stress fields at the tip of the crack to be perturbed, thereby altering the trajectory of the crack by kinking it. Other causes of an uneven crack can be load variations as the crack advances. Due to the sufficiently low height of the steps found, no further preparation between cleaving and preferential etching was applied. Apart from that, additional techniques, like polishing, may cause other topographical effects.

4. Conclusion

The abnormal distortion of some wafers is due to heterogeneous precipitation of oxygen. This is indicated by the different sizes and distributions of the precipitates. Since all wafers were taken from one ingot the different thermal history of each wafer and hence the different densities of intrinsic point defects, which act as nucleation sites, can explain this behavior. In order to reduce the yield loss due to scaling, which reduces the alignment performance of lithography steps, one does not only have to take the oxygen content of the wafers into account but also their thermal history.

References

[1] F. Shimura: "Oxygen in Silicon, Semiconductors and Semimetals", Vol. 42, *Academic Press, Inc.*

[2] Kyong Min Kim: "Growing Improved Silicon Crystals for VLSI/ULSI Applications", *Solid State Technology* Vol. 39, No.11, November 1996.

[3] J. Borland, R. Singh: "Improved p-well CMOS latch-up immunity and device performance through intrinsic gettering techniques", *technical report*.

[4] G. Borionetti, P. Godio, M. Porrini, S. Ilic, *Electrochem. Soc. Proceedings* Volume 96-13, p.164

[5] F. Secco d'Aragona, J. *Elektrochem. Soc*. 119, 948 (1972)

[6] H. Rauh: "Wacker's Atlas for Characterization of Defects in Silicon", *Wacker-Chemitronic GmbH*, Burghausen, Germany

[7] F. Shimura: "Semiconductor Silicon Crystal Technology", *Academic Press*, Inc.

[8] M. Cornara: "Simulation of oxygen precipitation", *MEMC Electronic Materials*, Technical Report, February 199 7

[9] M. Pagani: "Oxygen in Silicon: Nucleation and Precipitation", *MEMC Electronic Materials*, Technical Report Nr.: GETP0170881104 SS

[10] M. Pagani: "Denuded Zone Formation", *MEMC Electronic Materials*, Technical Report Nr.: GETP0110881104 SS

[11] A.-B. Chen: "The Mechanical Properties of Semiconductors", *Semiconductors and Semimetals*, Vol. 37, Academic Press, Inc.

Project Information

Project Manager

Univ.-Prof. Dr. Friedemar KUCHAR

Institut für Physik, Montanuniversität Leoben

Project Group

Last Name	First Name	Status	Remarks
Benkitsch	Andreas	dissertation	also: process engineer (AMS)
Gold	Herbert	dissertation	
Kuchar	Friedemar	university professor	
Lutz	Josef	assistant professor	(until Sept 1997)

Publications in Reviewed Journals

1. A. Pleschinger, J. Lutz, F. Kuchar: "A study of polycrystalline and amorphous LPCVD-silicon films by atomic force microscopy", Surface and Interface Analysis, Vol. 25, 529 (1997)
2. A. Benkitsch, J. Lutz, F. Kuchar: "AFM Study of Oxygen Precipitates in Single Crystal Silicon", Proc. DRIP VII, Templin, 7-10 Sept, 1997 (in print)
3. K. Sorschag, H. Gold, J. Lutz, F. Kuchar, M. Pippan, H. Noll: "Topographical and structural investigations of phosphorous-doped silicon films", Appl.Phys. A, 1998 (in print)
4. H. Gold, J. Lutz, F. Kuchar, M. Pippan, H. Noll: "AFM investigations of the influence of the doping process on the structure of LPCVD-silicon films", Inst.Phys. Conf. Ser. 157, 607 (1997)
5. A. Pleschinger, J. Lutz, F. Kuchar, H. Noll, M. Pippan: "A structural and topographical study of LPCVD-polysilicon by scanning probe microscopy", J.Appl.Phys. Vol. 81 (10), 6749 – 53 (1997)

Presentations

1. H. Gold, J. Lutz, F. Kuchar: "Topographical and structural investigations of phosphorous doped silicon films", 9th International Conference on Scanning Tunneling Microscopy (Spectroscopy and Related Techniques, Hamburg, BRD, 20 – 25 July 1997
2. A. C. Benkitsch, J. Lutz, F. Kuchar: "AFM Study of Oxygen Precipitates in Single Crystal Silicon", DRIP VII-7th International Conferencce on "Defect Recognition and Image Processing in Semiconductors, Templin, BRD, 7 – 10 Sept 1997

3. H. Gold, J. Lutz, F. Kuchar: "AFM investigation of the influence of the doping process on the structure of LPCVD-silicon films P-doped silicon films", Microscopy of Semiconducting Materials X, Oxford, U.K., 7 – 10 April, 1997

Cooperations

1. Austria Mikro Systeme International AG, Unterpremstätten, Dr. H. Noll, Dr. M. Pippan

Preparation of Nano-Structures for Space Applications

G. Stangl, P. Hudek[1], I. Kostic[1], F. Rüdenauer[2], I. Rangelow[3], K. Riedling, W. Fallmann

Institut für Allgemeine Elektrotechnik und Elektronik,
TU Wien, A-1040 Vienna, Austria

Regular arrays of sub-0.5 µm tips are of increasing interest, for example, as field emitters, calibration structures, or, in our particular case, as collector surfaces for sub-µm dust particles in a space experiment. This contribution describes the preparation of 1 x 1 cm² arrays of micro-columns with a high aspect ratio (10:1) and a diameter in the sub-micrometer range (150 – 300 nm). The process is based upon a chemically amplified novolak resist (CAR), electron beam lithography, and ECR plasma etching.

1. Introduction

For a space mission of ESA, arrays of sub-µm structures are required as collectors for particles of cosmic dust with 50 – 500 nm diameter. The collected particles will be imaged and classified by atomic force microscopy techniques. It is important that the collector surfaces can collect small high-speed particles with high efficiency and without damage to the particles. They must absorb the kinetic energy of the incoming dust by inelastic processes to avoid reflection of the particles. This can, for example, be achieved by using an array of free-standing columns with a diameter of the order of 0.3 µm and a height in the µm range. An impinging particle may break a number of these columns, thereby incurring an inelastic energy loss that depends on the fracture stress and modulus of the column material and on the column geometry.

The properties of these "collector surfaces" can therefore be tailored to the particular requirements by a variation of the column material and dimensions. By ion etching photoresist column structures into a silicon substrate it is possible to produce arrays of free-standing cones whose fracture energy is considerably lower than that of the resist columns.

2. Experimental

One of the prerequisites for an optimized plasma etching transfer of the structures from the resist layer into an inorganic substrate (for example, silicon or SiO_2) is a uniformly structured, relatively thick resist layer with close to perpendicular sidewalls, as shown in Fig. 1.

[1] Academy of Science, SK-84237 Bratislava, Slovakia
[2] Österreichisches Forschungszentrum Seibersdorf, A-2444 Seibersdorf, Austria
[3] University of Kassel, D-34109 Kassel, B.R.D.

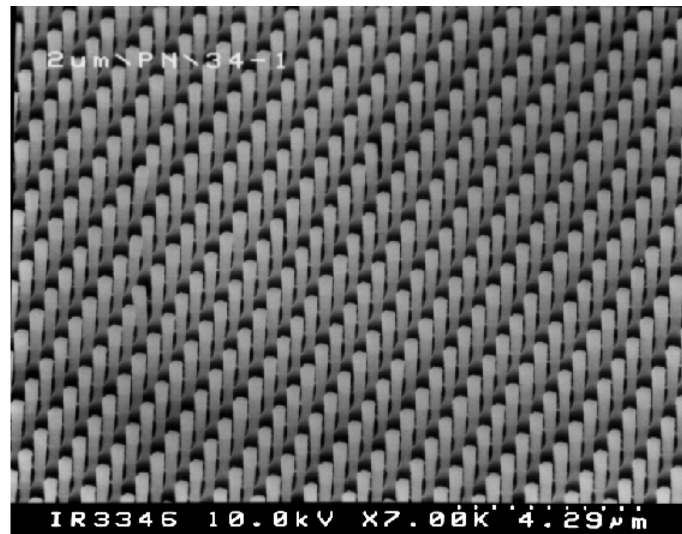

Fig. 1: Large field (1x1 cm²) array of high-aspect-ratio and high density resist pillars made by using e-beam lithography and chemically amplified resist.

This requires a careful optimization of the deposition, exposure, and of the pre- and post-exposure resist processing. In the experiments reported here, a single film of a three-component negative-toned Novolak CAR (Kalle Hoechst AZ PN 114) has been used [1]. Although the high sensitivity of this resist type makes it very attractive, particularly for electron beam exposure, it causes problems with the control and the uniformity of the critical dimensions. It also requires a precise compensation of proximity effects during electron beam exposure if the pattern dimensions decrease below 0.5 µm, and an optimized resist processing. The most critical factor in resist processing turned out to be the post-exposure delay, which must be less than a few minutes. Although a simulation of the exposure process is indispensable for controlling the proximity effects, the optimization of the entire process heavily depended on experimental work. This is true because the complexity of the three-component resist system and the lack of an exact model of the resist response prohibit a comprehensive simulation.

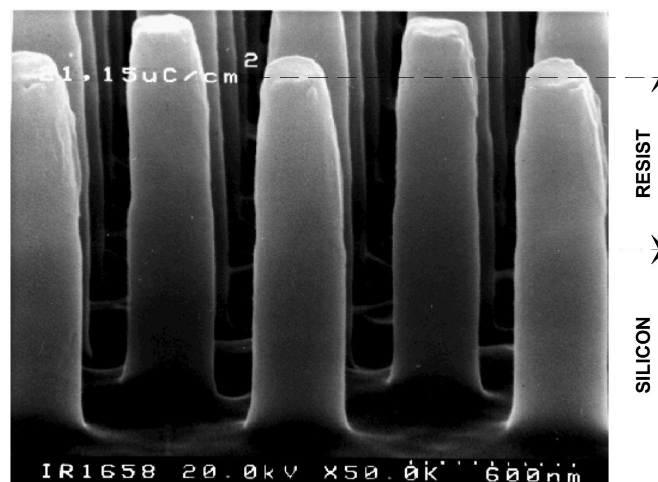

Fig. 2: Large field array of resist pillars transferred into silicon by dry plasma etching (ECR).

The resist column structures may either be directly used as catching structures for dust particles, or they may be transferred into the underlying silicon substrate by means of ECR dry etching (Fig. 2). A careful choice of the etching parameters can allow virtually any shape of the resulting silicon columns (Fig. 3), although the conical shape of Fig. 3(b) appears preferable for the particular purpose. The mechanical behavior and thus the dust collecting capabilities of the structures may also be modified by either removing the resist layer after the etching step or by leaving the mask layer on top of the silicon columns, as shown in Fig. 2.

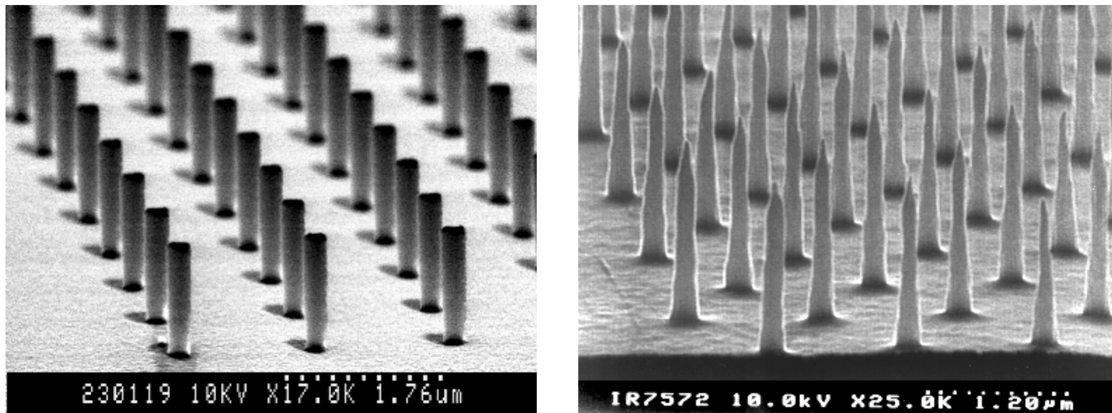

Fig. 3: Cylindrical pillars (a) and needles (b) prepared in silicon by ECR plasma etching.

3. Alternative approaches

Other large-area arrays of periodical structures may serve a similar purpose as the columns presented above. Using the same techniques, an array of dust collector boxes may be prepared (Fig. 4).

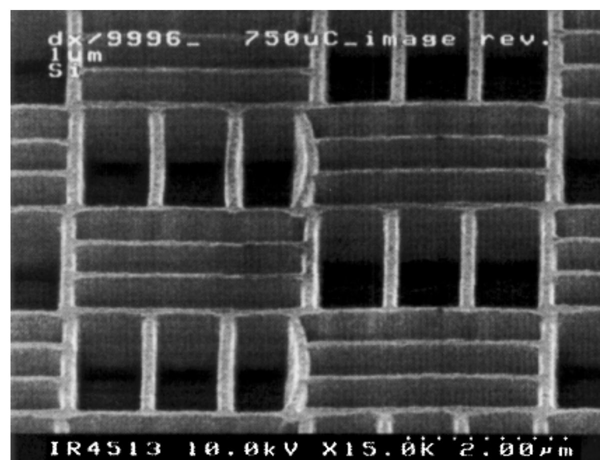

Fig. 4: Array of dust collector boxes prepared by e-beam lithography in chemically amplified resist.

Furthermore, dust collector structures may be “lined” with an energy absorbing sandwich structure consisting of alternate films of crystalline bacterial cell surface proteins (”S”-layers) [2] and evaporated or sputtered metals, e.g., titanium, niobium, or tantalum (Fig. 5(a)). A particle that impinges on such a damping multilayer will either break one or more of the metal films or inelastically deform the S-layer, which results in a smooth absorption of its energy and avoids the loss of particles by reflection (Fig. 5(b)).

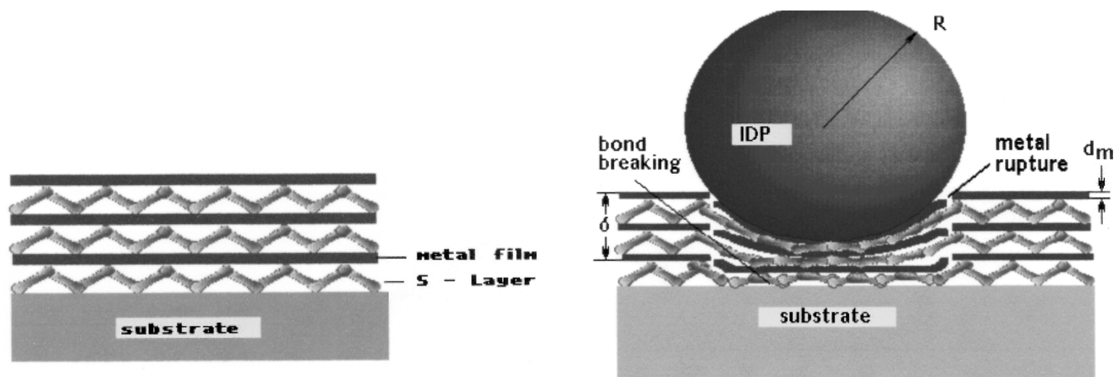

Fig. 5: Damping multilayer structure (a) and stopping of a particle (b).

4. Conclusion

The careful optimization of an electron-beam lithography based single-layer resist process permitted the high aspect ratio patterning of sub-0.5 µm structures in resist with a thickness of up to 5 µm, which is a requirement for a subsequent deep plasma etching. Since the limit for the etching depth in silicon is typically between 2 and 2.5 times the resist thickness, etching depths exceeding 5 µm appear easily feasible with the process presented [3].

Acknowledgments

In addition to the Society for Microelectronics, this work was supported by the Austrian East-West-Funds-Project (OWP-92), and the Erwin Schrödinger Gesellschaft, Institute of Lithographic Research.

References

[1] I. Rangelow, P. Hudek, I. Kostic, Z. Borkiwicz, G. Stangl: “Submicro- and nanometer e-beam lithography and reactive ion etching with single layer chemically amplified negative resist”, *Microelectronic Eng.* 23 (1994) 283.

[2] D. Pum, G. Stangl, C. Sponer, W. Fallmann, U.B. Sleytr: “Deep UV patterning of monolayers of crystalline S-layer protein on silicon surfaces”, *Biointerfaces* 8 (1997) 157 – 162.

[3] P. Hudek, W. Rangelow, I. Kostic, G. Stangl: “Submicro- and nanometer structure fabrication using direct electron-beam writing and reactive ion etching”, *Electron Technology* 28/4 (1996) 251 – 258.

Project Information

Project Manager

A.o.Univ.Prof. Dr. Karl RIEDLING

Institut für Allgemeine Elektrotechnik und Elektronik, TU Wien

Project Group

Last Name	First Name	Status	Remarks
Fallmann	Wolfgang	university professor	
Riedling	Karl	associate professor	
Stangl	Günther	technician	

Publications in Reviewed Journals

1. P. Hudek, G. Stangl, I. Kostic, F. Shi, F. Rüdenauer, M. Belov, I. Rangelow, W. Fallmann: "Fabrication of dust particles collector surfaces and their investigation with SPM", accepted for Proc. SPMM '97.
2. D. Pum, G. Stangl, C. Sponer, K. Riedling, P. Hudek, W. Fallmann, U.B. Sleytr: "Patterning of Monolayers of Crystalline S-layer Proteins on a Silicon Surface by Deep Ultraviolet Radiation", Microelectronic Engineering 35, 1997, 297 – 300.
3. G. Stangl, P. Hudek, I. Kostic, F. Rüdenauer, I. Rangelow, K. Riedling, W. Fallmann: "Micro-technology of densely spaced non-conventional patterns for space applications", accepted for Microelectronic Engineering.

Presentations

1. P. Hudek, G. Stangl, I. Kostic, F. Shi, F. Rüdenauer, M. Belov, I. Rangelow, W. Fallmann: "Fabrication of dust particles collector surfaces and their investigation with SPM", SPMM '97.
2. G. Stangl, P. Hudek, I. Kostic, F. Rüdenauer, I. Rangelow, K. Riedling, W. Fallmann: "Micro-technology of densely spaced non-conventional patterns for space applications", Micro- and Nanoengineering 97, Athens, 1997.

Cooperations

1. Academy of Sciences, Bratislava: Dr. P. Hudek
2. ÖFZS Seibersdorf: Prof. Dr. Rüdenauer
3. University of Kassel: Prof. Dr. Rangelow

4. Fraunhofer Institut für Mikrostrukturierung, Berlin
5. IMS — Ionen Mikrofabrikations Systeme GmbH, Vienna: Dr. H. Löschner
6. Technics-Plasma, Munich
7. Shipley
8. DuPont, Frankfurt
9. Kalle-Höchst, Frankfurt

New Diode-Pumped Femtosecond Lasers

E. Sorokin, I.T. Sorokina, A. Unterhuber, S. Naoumov, E. Wintner,
Institut für Allgemeine Elektrotechnik und Elektronik,
TU Wien, A-1040 Vienna, Austria

A.I. Zagumennyi, I.A. Shcherbakov,
General Physics Institute, Russian Academy of Sciences,
Moscow, Russia

V. Carozza, A. Toncelli, M. Tonelli,
Dipartamento di Fizica, University of Pisa,
Pisa, Italy

A. V. Shestakov,
POLUS Science-Technical Company, Moscow, Russia

Diode-pumped tunable (over 80 nm) cw operation achieving 30 mW of output power was demonstrated in a novel mixed garnet crystal Cr,Tm,Ho:YSGG:GSAG at room temperature. A comparison has been made with Cr,Tm,Ho:YAG and Tm,Ho:YLF. We also report the first demonstration of room-temperature continuous-wave laser action at 1.5 μm of Cr^{4+}:YAG directly pumped at 970 nm by a 2 W diode array.

1. Introduction

Compact all-solid-state tunable and mode-locked crystalline lasers, operating in the vicinity of the 2 μm region, attract a lot of interest for many applications in medicine, remote sensing, and laser radar measurement. The largest vibronic shift in rare-earth-doped active media and correspondingly large tunability range of more than 100 nm was demonstrated in Tm:YAG and Tm:YSGG [1]. The shortest published pulses (35 ps at 70 mW of average output power), generated in the 2 μm-region, have been obtained in actively mode-locked cw Tm:YAG lasers [2]. Tm-based lasers, however, are known to have higher threshold and be less stable in the cw regime as compared to Tm,Ho-systems [3], associated with the combined action of the thermo-lensing effect and a relatively small emission cross-section of Tm^{3+} ions. In this respect the Tm,Ho-doped crystals are generally more favorable for diode-pumping and cw mode-locking. However, the tunability of Ho ions is characterized by smaller tuning ranges and a more spiky tuning curve since the phonon-broadened fluorescence linewidth of individual Stark transitions is less than the separations of the Stark lines. Although the multiplicity of the Stark levels in the Ho and Tm ions is higher than in other rare-earth ions, their fluorescence spectrum is not smooth, being unfavorable for both tuning and mode-locking. That is why we looked for a suitable host crystal for Tm^{3+} and Ho^{3+} ions, allowing smooth and broad tunability, simultaneously allowing for efficient diode-pumping and mode-locking.

A few years ago, a new class of laser-active media has been developed, the crystals of solid solutions of scandium containing aluminum and gallium garnets $YSGG_xGSAG_{1-x}$ [4], which we call “mixed garnets”. The disordered nature of these crystals results in a strongly inhomogeneous broadening of both the fluorescence line (Fig. 1) and the ab-

sorption bands. This allowed in case of Nd-doped GSAG:GSGG garnets to broaden and smoothen the gain spectrum, and decrease the achievable mode-locked pulse duration by an order of magnitude [5,6].

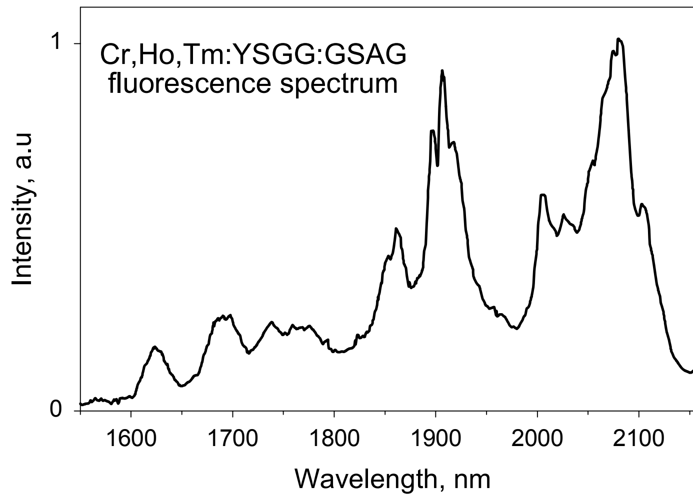

Fig. 1: Fluorescence spectrum of Cr,Tm,Ho:YSGG:GSAG.

We implemented the approach of solid solution crystals towards the development of Tm and Ho-doped active media, and grew high optical quality crystals of yttrium-gadolinium-scandium-gallium-aluminum garnet with the following composition: Cr,Tm,Ho:$YSGG_{0.5}GSAG_{0.5}$. The crystals were grown by Czochralski technique in a radio-frequency-heated iridium crucible, which was 60 mm in diameter and 60 mm high. The orientation of growth was <110>. The dopant concentrations in the crystal were c_1 (Cr^{3+}) = 2x10^{20} cm^{-3}, c_2 (Tm^{3+}) = 4x10^{20} cm^{-3}, c_3 (Ho^{3+}) = 0,5x10^{20} cm^{-3}. The boule was 140 mm long and 22 mm in diameter. Growth conditions were characterized by a pulling rate of 4 mm/h, a rotation rate of 20 r.p.m., and an atmosphere of nitrogen containing 2 % by volume of oxygen. The crystals were annealed at 1200 ° C for 10 h in the air. The lattice parameter of Cr,Tm,Ho:$(GSAG)_{0.5}(YSGG)_{0.5}$ is a = 12.4093 Å. The crystal has a density of 5.54 g/cm^3. The thermal conductivity of these crystals at a temperature of 300 K is about 5.9 W/(cmK), being slightly less than in Cr:Tm:Ho:YAG and Cr:Tm:Ho:YSAG laser crystals [7], but comparable with that of the crystal components (YSGG and GSAG).

Another alternative for diode pumped broad band IR lasers is the Cr^{4+}:YAG laser, first reported in [8], being a unique laser source, tunable over an attractive wavelength range for many applications of 1.34 – 1.6 μm [9]. Diode-pumping of Cr^{4+}-doped materials, however, remains a challenging task due to difficulties in growing of the crystals with high Cr^{4+} concentration. The diode-pumped operation of Cr^{4+}:forsterite and Cr^{4+}:$Co_{a2}GeO_4$ reported recently required the ideal beam of a MOPA source [10]. Hence, no results on direct diode-pumping of any Cr^{4+}-doped material with a conventional diode array are known to us at the moment.

Although only Cr^{4+} ions in tetrahedral sites are responsible for laser action [11], [12], growth of this material generates a large concentration of parasitic Cr^{4+} and Cr^{3+} ions in octahedral sites. In this work, the doping levels of Cr_2O_3 and charge-compensating MgO were optimized to achieve highest concentration of Cr^{4+} in tetrahedral sites with lowest

Cr_2O_3 level. For the final Cr^{4+}_{tetr} concentration of ~10^{18} cm^{-3} the starting Cr_2O_3 concentration was only $2x10^{19}$ cm^{-3}. To further increase the $Cr^{4+}_{tetr}/Cr^{4+}_{oct}$ ratio, we used annealing for 200 hours at 1250 – 1300 °C in oxygen atmosphere. This resulted in a reduced absolute laser threshold at high initial absorption coefficient (~3 – 3.5 cm^{-1}).

2. Experimental

2.1 Cr,Tm,Ho:YSGG:GSAG Lasers

In order to make a fair comparison of different crystals we used equal 2.5 mm thick Brewster-cut samples. For diode pumping the resonator was X-shaped with 20 – 40 cm arm lengths, and two curved (R = 75 mm) mirrors (Fig. 2). For mode-locking experiments the arm lengths were increased to 70 cm to match the fixed frequency of the acousto-optic modulator, and we took R = 100 mm mirrors. Output coupling was 0.6 % – 3 % . The laser was pumped at 782 nm by both, Ti:sapphire (up to 1.4 W) and a diode array (up to 0.9 W), but due to the unoptimized Tm^{3+} concentration only ~35 – 50% of pump power was absorbed. Tuning was performed by a 1.5 mm Lyot filter.

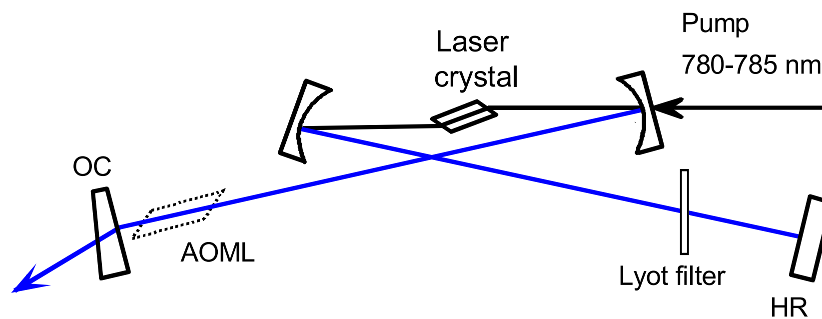

Fig. 2: Schematic diagram of a setup for both, diode and Ti:sapphire pumping of Tm,Ho lasers. OC: output coupler. HR : High reflector. AOML: acousto-optic mode-locker.

To characterize the cw performance of the newly developed Cr,Tm,Ho:YSGG:GSAG crystal we also tested other common 2-µm active media as Cr,Tm,Ho:YAG, Cr,Tm,Ho:YSGG, and Tm,Ho:YLF in the same cavity (see Table 1). As expected, Tm,Ho:YLF showed the lowest threshold and the highest efficiency, pumped by either source, but only 20 nm tuning range. In case of Cr,Tm,Ho:YAG lasing was achieved between 2085 and 2117 nm. The tuning curve, however, consisted of distinct lines, which could be identified as Stark lines in the fluorescence spectrum. Finally, Cr,Tm,Ho:YSGG:GSAG allowed to reach the goal of a wide unbroken tunability under both, Ti:sapphire- and diode-pumping (Fig. 3), which along with the good slope efficiency (14.3 %, comparable to Cr,Ho,Tm:YAG) certainly favor the new material.

	Cr,Tm,Ho:YSGG:GSAG		Cr,Tm,Ho:YAG		Tm,Ho:YLF	
Pumping:	Ti:Sapphire	Diode	Ti:Sapphire	Diode	Ti:Sapphire	Diode
Threshold						
OC = 0.6 %	78 mW	190 mW	71mW	180 mW	40 mW	120 mW
OC = 3 %	280 mW	460 mW	180 mW	400 mW	65mW	175 mW
Slope						
OC = 0,6 %	10 %	6,7 %	10 %	9 %	23 %	9,7 %
OC = 3 %	40 %	14,3 %	42 %	22 %	59 %	28,5 %

Table 1: Cw performance summary at room temperature.

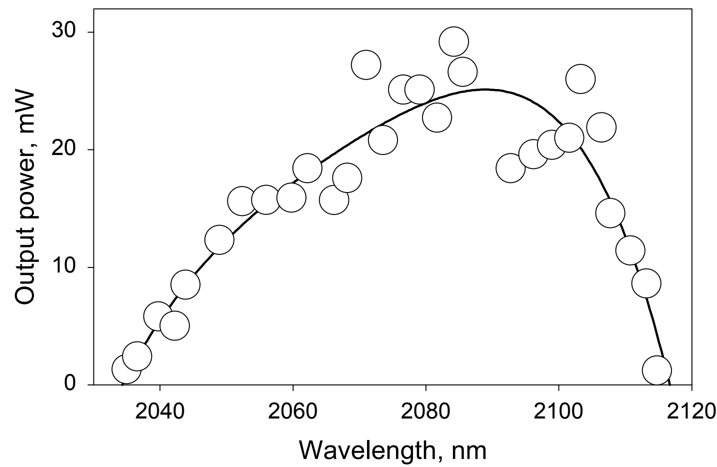

Fig. 3: Tuning curve of the diode-pumped Cr,Tm,Ho:YSGG:GSAG laser.

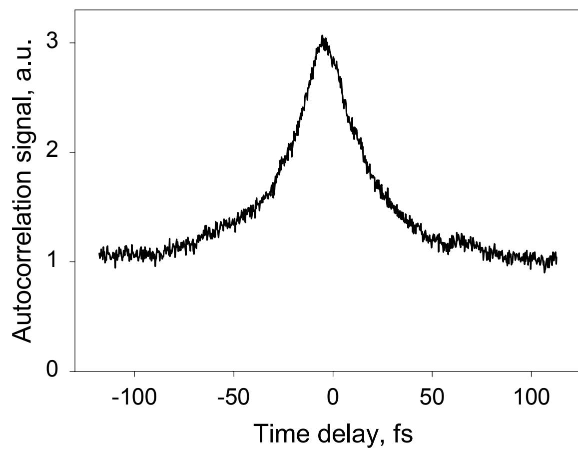

Fig. 4: Collinear autocorrelation of a modelocked Cr,Tm,Ho:YSGG:GSAG laser. Pulsewidth is 25 ± 2 ps, assuming the Gaussian pulseform.

Modelocking was obtained by means of an acousto-optic modulator and resulted in pulsewidths of 25 ± 3 ps at 100 mW of average output power at 100 MHz repetition rate.

The corresponding autocorrelation trace is shown in Fig. 4. The obtained pulse duration agrees with the theoretical prediction [13] for the parameters of our laser, assuming an effective gain bandwidth of 40 nm.

These first mode-locking results are quite promising. The achieved broad tunability along with good efficiency and smooth tuning curve allow to hope for successful passive mode-locking of this crystal and consequently shortening of the pulse duration down into the femtosecond regime (theoretically down to 25 fs). However, analysis and optimization of the cavity dispersion is necessary.

2.2 Cr^{4+}:YAG Laser

The basic experimental setup is shown in Fig. 5. The Cr^{4+}:YAG crystal was pumped through the flat dichroic (HR at 1.5 µm, AR at 970 nm) mirror and absorbed over 90% of pump radiation at 6 mm length. A 1.5 W (up to 2 W pulsed) diode was focused into a ~60 x 100 μm^2 spot. The laser was operated in a stable cw regime for the first time. With all mirrors highly reflecting we measured 0.26 % of losses through the mirrors and 1.1 % crystal internal losses. In this configuration, although using two diode arrays the lasing threshold was 1.6 W at room temperature and total output power reached 20 mW. For comparison, Nd:YLF pumping of the same cavity through the curved mirror yielded 0.7 W threshold.

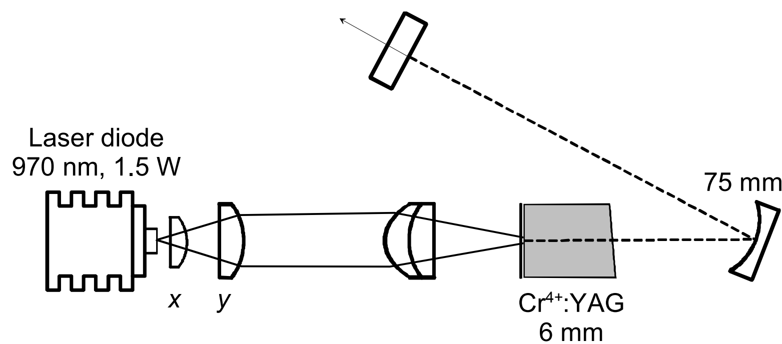

Fig. 5: Experimental setup of a diode pumped Cr^{4+}:YAG laser.

3. Conclusion

In conclusion, diode- and Ti:sapphire-pumped cw broadly tunable (80 nm) and efficient (16% of slope efficiency) laser action of a Cr,Tm,Ho:YSGG:GSAG laser was obtained at room temperature and compared with other common Tm,Ho-doped crystals. In the mode-locked regime, 25 ps pulses at 100 mW of average output power and 100 MHz repetition rate have been obtained by active modelocking. Preliminary results show a large potential of this laser for mode-locking over the entire tuning range of 80 nm and for obtaining much shorter pulse durations using appropriate passive mode-locking techniques.

In case of the diode-pumped Cr^{4+}:YAG laser, we believe that the reported results show good feasibility of cw lasing by direct pumping with diode arrays at 970 – 980 nm. We are currently optimizing the setup parameters to obtain higher output levels at room temperature.

Acknowledgments

This work was supported by the Austrian National Science Foundation Projects P 10733, P 12756, and the Austrian National Bank Project No. 6727.

References

[1] R.G. Stoneman and L. Esterowitz, *Opt. Lett.,* 15, 486, 1990

[2] J.E. Pinto et al., L. Esterowitz and G.H. Rosenblatt, *Opt. Lett.,* 17, 731, 1992

[3] F. Heine et al., E. Heumann, G. Huber and J. Koetke, *OSA Proceedings on Advanced Solid-State Lasers,* 15, 403, 1993

[4] E.V. Zharikov, A.I. Zagumennyi, G.B. Lutts, V.A. Smirnov, I.T. Sorokina, I.A. Shcherbakov, *Las. Phys.* 1, 216, 1991

[5] E. Sorokin, M.H. Ober, I.T. Sorokina, E. Wintner, A.J. Schmidt, A.I. Zagumennyi, G.B. Lutts, E.V. Zharikov, I.A. Shcherbakov, *J. Opt. Soc. Am. B.* 10, 1436, 1993

[6] M.H. Ober, E. Sorokin, I.T. Sorokina, F. Krausz, E. Wintner, *Opt. Lett.,* 17, 1364, 1992

[7] A.I. Zagumennyi, G.B. Lutts, P.A. Popov, N.N. Sirota, I.A. Shcherbakov, *Las. Phys.* 3, 1064, 1993

[8] N.B. Angert et al., *Sov. J. Quantum Electron.,* 18, 73, 1988

[9] N.I. Borodin, V.A. Zhitnyuk, A.G. Okhrimchuk, A.V. Shestakov et al., *Sov. Phys. Izvestiya,* 54, 1500, 1990

[10] J.M. Evans, V. Petricevic, A.B. Bykov, A. Delgado, R.R. Altano et al., *Opt. Lett.,* 22, 1171, 1997

[11] S. Kueck et al., *OSA Proc. on Adv. Solid- State Lasers,* 10, 92, 1991

[12] A.G. Okhrimchuk and A.V. Shestakov, *Opt. Materials,* 3, 1, 1994

[13] D.J. Kuizenga and A.E. Siegman, *IEEE JQE,* QE-6, 694, 1970

Project Information

Project Manager

Univ. Prof. Dr. Ernst WINTNER

Institut für Allgemeine Elektrotechnik und Elektronik, TU Wien

Project Group

Last Name	First Name	Status	Remarks
Carozza	Valentina	diploma	
Naoumov	Sergej	student	
Sorokin	Evgeni	postdoc	
Sorokina	Irina	postdoc	
Unterhuber	Angelika	student	
Wintner	Ernst	university professor	

Books and Contributions to Books

1. E. Wintner: "*Semiconductor Lasers*", Chapter 6, Handbook of the Eurolaser Academy,Vol. I. p267 – 323. Thomson Scientific Publishers (Chapman & Hall) 1998.

Publications in Reviewed Journals

1. I.T. Sorokina, E. Sorokin, E. Wintner, A. Cassanho, H.P. Jenssen, R. Szipöcz: "In situ measurement of ESA, upconversion, and thermal quenching in Cr:LiSAF and Cr:LiSGaF lasers", OSA Trends in Opt. and Photonics (ASSL 1997, Orlando, paper MB 12-1) ,1997.
2. I.T. Sorokina, E. Sorokin, E. Witner, M.A. Noginov, R. Szipöcs, A. Cassanho, H.P. Jenssen: "Femtosecond pulses from the novel solid-state laser source Cr:LiSGaF", Laser Physics 7, pp 187 – 195 ,1997.
3. I.T. Sorokina, E. Sorokin, E. Wintner, A. Cassanho, H.P. Jenssen, R. Szipöcs: "Sub-20 fs pulse generation from the mirror dispersion controlled Cr:LiSGaF and Cr:LiSAF lasers", invited paper, Special issue on ultrashort pulse generation, Appl. Phys. B 65, 245, 1997.
4. I.T. Sorokina, E. Sorokin, E. Wintner, A. Cassanho, H.P. Jenssen, R. Szipöcs: "14-fs pulse generation in KLM prismless Cr:LiSGaF and Cr:LiSAF lasers: observation of pulse self-frequency shift", 22, Optics Lett., 1716 – 18, 1997.

5. I.T. Sorokina, E. Sorokin, E. Wintner: “On the way towards the pulse duration limits in prismless KLM Cr:LiSGaF and Cr:LiSAF lasers”, Proceedings International Workshop on Laser Physics LPHYS’97, Prague (1997) Laser Physics, Vol. 8, No 3, 1998.
6. Q. Lin, E. Wintner: “3-Dimensional Evolution of Ultrashort Pulses in Dispersive Media beyond slowly varying envelope approximation”, to be published in Optics Comm., 1998.
7. E. Sorokin, IlT. Sorokina, A. Unterhuber, E. Wintner, A.I. Zagumennyi, I.A. Shcherbakov, V. Carozza, M. Tonelli: “A novel mode-locked 2 µm Cr, Tm, Ho:YSGG:GSAG laser”, OSA Trends in Opt. and Photonics (ASSL 98, Coeur d’Alene, paper AWC5), 1998.
8. I.T. Sorokina, Q. Lin, E. Sorokin, E. Wintner: “Minimization of adverse effects of dispersive waves in ultrashort-pulses solitary lasers”, OSA Trends in Opt. and Photonics (ASSL 98, Coeur d’Alene, paper Atu B10), 1998.
9. I.T. Sorokina, E. Sorokin, E. Wintner: “Raman induced pulse self-frequency shift in the sub-20 fs Kerr-lens mode-locked Cr:LiSGaF and Cr:LiSAF lasers”, OSA Trends in Opt. and Photonics (ASSL 98, Coeur d’Alene, paper AW E5), 1998.

Presentations

1. I.T. Sorokina, E. Sorokin, E. Wintner, A Cassanho, H.P. Jenssen, R. Szipöcs: “Femtosecond pulse generation from the novel low-loss chirped-mirror dispersion controlled Cr:LiSAF and Cr:LiSGaF lasers”, *Advanced Solid-State Laser Conference* (paper MF2), Orlando, Fl., USA, February 1997.
2. I.T. Sorokina, E. Sorokin, E. Wintner, A. Cassanho, H.P.Jenssen, R. Szipöcs: “In situ measurement of ESA, upconversion and thermal quenching in Cr:LiSAF and Cr:LiSGaF lasers”, *Advanded Solid-State Laser Conference* (paper MB 12-1), Orlando, Februar 1997.
3. I.T. Sorokina, E. Sorokin, E. Wintner, R. Szipöcs: “Passive Modenverkopplung von Cr:LiSAF und Cr:LiSGaf in einen durch neue verlustarme “gechirpte” Spiegel kontrollierten Laserresonator*”, DPG-Frühjahrstagung Quantenoptik*, Vortrag Q 35.4, Mainz, BRD, March 1997.
4. I.T. Sorokina, E. Sorokin, E. Wintner: “Neueste Fortschritte auf dem Gebiet von Cr- und Yb-dotierten Femtosekunden-Festkörperlasern”, *Laserseminar Mauterndorf*, Mauterndorf, Salzburg, March 1997.
5. M. Lenzner, S. Sartania, Z. Cheng, L. Xu, A. Poppe, Ch. Spielmann, F. Krausz, I.T. Sorokina, E. Sorokin, E. Wintner: “Recent Developments in Femtosecond Technology”, *Seminar “Grundlagen und Technologie elektronischer Bauelemente”*, Großarl, Salzburg, March 1997.
6. Q. Lin, T. Brabec, E. Wintner: “3-dimensional evolution of ultrashort pulses in dispersive media”, OSA *Conference on Lasers and Electro-Optics* (CLEO Baltimore 1997), paper Cth 02, May 1997.
7. I.T. Sorokina, E. Sorokin, E. Wintner, A. Cassanho, H.P. Jenssen, R. Szipöcs: “14 fs pulse generation from prismless Cr:LiSAF and Cr:LiSGaF lasers”, invited paper TUF

4, *The Pacific Rim Conference on Lasers and Electro-Optics* (CLEO/Pacific Rim), Chiba, Japan, July 1997.

8. E. Wintner: "Recent developments of semiconductor lasers", invited paper L1, *Second International Austrian-Israeli Technion Symposium*, Graz, June 1997.
9. I.T. Sorokina, E. Sorokin, E. Wintner: "Novel femtosecond solid-state lasers", invited paper, *2nd International Symposium on Modern Problems of Laser Physics*, Novosibirsk, Rußland, July 1997.
10. I.T. Sorokina, E. Sorokin, E. Wintner: "On the way towards the pulse duration limits in prismless KLM Cr:LiSGaF and Cr:LiSAF lasers, *International Workshop on Laser Physics LPHYS'97*, Prag, Tschechien, August 1997.
11. I.T. Sorokina, E. Sorokin, E. Wintner: "Die Grenzen der Impulsdauer in prismenlosen KLM Cr:LiSGaF und Cr:LiSAF-Lasern", *Fachtagung des Ausschusses für Quantenelektronik der ÖPG*, Wien, September 1997.
12. I. T. Sorokina, E. Sorokin, E. Wintner: "Das Phänomen der Seitenbänder in solitären Femtosekundenlasern", *Jahrestagung der Österreichischen Physikalischen Gesellschaft*, Wien, September 1997.
13. E. Sorokin, I.T. Sorokina, A. Unterhuber, E. Wintner, A.I. Zagumennyi, E.V. Zharikov, I.A. Shcherbakov: "Der neue Laserkristall Cr:Tm:Ho:YSGG:GSAG als aktives Medium für durchstimmbare cw 2 µm Laser bei Raumtemperatur", *Jahrestagung der Österreichischen Physikalischen Gesellschaft*, Wien, September 1997.

Patents

1. E. Wintner, E. Sorokin, I.T. Sorokina: "Lasersystem zur Erzeugung ultrakurzer Lichtintensitäten", WI-1727 (Austria).

Cooperations

1. Forschungsinstitut für Festkörperphysik der ungarischen Akademie der Wissenschaften, Budapest (Dr. R. Szipöcs; dispersive Spiegel).
2. Institut für Strahlwerkzeuge der Universität Stuttgart (Dr. A. Giesen; Scheibenlaseraufbauten).
3. Institut für Allgemeine Physik der russischen Akademie der Wissenschaften, Moskau (Prof. I. Shcherbakov; Laserkristalle, opische Komponenten).
4. CREOL, University of Central Florida (Prof. B. Chai, Prof. H. Jenssen; Laserkristalle).
5. Lightning Corp., Tampa, Florida (Dr. A. Cassanho; Laserkristalle).

Appendix

Basics and Technology of Electronic Devices — Seminar Program

Seminar in Großarl (Salzburg), March 19 – 22, 1997

Wednesday, March 19, 1997 17.00 – 17.20
Welcome; Introduction

Wednesday, March 19, 1997 17.20 – 20.00
Sensors

17.20 – 18.00	P. HEIDE, C. SCHMELZ, T. V. KERSSENBROCK: *Microwave and Millimeterwave Sensors Based on Flip-Chip and SAW Technology* ***(Invited Paper)***
18.00 – 18.20	A. EFANOV, K. LÜBKE, CH. DISKUS, A. SPRINGER, A. STELZER, H.W. THIM: *Entwurf und Herstellung von Mikrosystemen für die Millimeterwellen-sensorik*
18.20 – 18.40	BREAK
18.40 – 19.20	A. FELTZ: *Konzepte der Gassensorik und ihre Umsetzung in neuen Produkten* ***(Invited Paper)***
19.20 – 19.40	F. KOHL, P. SVASEK, A. JACHIMOWICZ, G. JOBST, F. KEPLINGER, G. URBAN: *Mikrotechnische Sensorsysteme*
19.40 – 20.00	A. SCHNEIDER, R. CHABICOVSKY: *Modellbildung für einen optischen Kohlenstoffsensor*

Thursday, March 20, 1997 9.00 – 11.20
Lithography; Modeling

09.00 – 09.20	H. KIRCHAUER, S. SELBERHERR: *Dreidimensionale Photolithographie-Simulation*
09.20 – 09.40	M. HAUSER, J. SMOLINER, C. EDER, G. PLONER, G. STRASSER, E.GORNIK: *Nanostrukturierte STM-Spitzen und THz-Detektoren*
09.40 – 10.00	G. BRUNTHALER, H. STRAUB, A. DARHUBER, T. GRILL, Y. ZHUANG, G. BAUER: *Nanostrukturierung von Halbleitermaterialien*
10.00 – 10.20	BREAK

10.20 – 10.40 A. NEUBAUER, P. HUDEK, G. STANGL, K. RIEDLING, D. PUM, W. FALLMANN, U.B. SLEYTR, H. LÖSCHNER, I. KOSTIC, F. RÜDENAUER: *Nanostrukturierung*

10.40 – 11.00 R. MLEKUS, S. SELBERHERR: *An Object Oriented Approach to the Management of Models*

11.00 – 11.20 M. RADI, S. SELBERHERR: *AMIGOS: Analytical Model Interface & General Object Oriented Solver*

Thursday, March 20, 1997 17.00 – 20.20
Materials and Processes; ASICs

17.00 – 17.40 A.R. PEAKER, J.H. EVANS-FREEMAN: *Point and Extended Defects in Ion Implanted Silicon* ***(Invited Paper)***

17.40 – 18.00 S. LANZERSTORFER, W. HEISS, V. SVRCEK, W. JANTSCH, L. PALMETSHOFER, Y. SUPRUN-BELEVICH: *Dotierungsprobleme in Halbleitern: Erbium in Silizium*

18.00 – 18.20 BREAK

18.20 – 18.40 S. ZERLAUTH, CH. PENN, F. SCHÄFFLER: *Si-Ge-C-Schichten: Wachstum und Charakterisierung*

18.40 – 19.00 H. GOLD, J. LUTZ, F. KUCHAR, H. NOLL, M. PIPPAN: *Strukturelle und topographische Untersuchungen von Phosphor-dotierten LPCVD-Schichten*

19.00 – 19.20 K. PIGLMAYER, H. SCHIECHE, R. CHABICOVSKY: *Laser-induziertes Abscheiden und Ätzen von Wolfram-Mikrostrukturen*

19.20 – 19.40 BREAK

19.40 – 20.00 N. KERÖ, G.R. CADEK, W. KAUSEL, E. KOWARSCH, P.C. THORWARTL, T. SAUTER: *UNICHIP-Wien: Ein Technologie-Transfer-Zentrum für ASIC-Design*

20.00 – 20.20 H. LEOPOLD, W. MEUSBURGER, R. RÖHRER, H. SENN, P. SÖSER: *ASICs für die elektronische Instrumentierung*

Friday, March 21, 1997 9.00 – 10.40
Integrated Circuits and ASICs

09.00 – 09.40 H. JACOBS: *Silizium-Technologie für die nächsten 15 Jahre: Herausforderungen, Risiken, Chancen* ***(Invited Paper)***

09.40 – 10.00 BREAK

10.00 – 10.40 W. PRIBYL: *"Mixed Signal" und "Smart Power" — Kernkompetenzen für den globalen Mikroelektronikmarkt* ***(Invited Paper)***

Friday, March 21, 1997 17.00 – 20.00
Solid State Lasers; Panel Discussion

17.00 – 17.40	H. RIECHERT: *LEDs und Laser auf der Basis von III-V-Nitriden — Grundlagen, Probleme, Realisierung* ***(Invited Paper)***
17.40 – 18.00	A. KÖCK, A. GOLSHANI, R. HAINBERGER, P. O. KELLERMANN, E. GORNIK, L. KORTE: *Oberflächenemittierende Laserdioden für WDM-Anwendungen*
18.00 – 18.20	M. LENZNER, S. SARTANIA, Z. CHENG, L. XU, A. POPPE, CH. SPIELMANN, F. KRAUSZ, I.T. SOROKINA, E. SOROKIN, E. WINTNER: *Neueste Entwicklungen in der Femtosekundentechnologie*
18.20 – 18.40	BREAK
18.40 – 20.00	PANEL DISCUSSION: PROJECT MANAGEMENT INDUSTRY – UNIVERSITIES

Saturday, March 22, 1997 09.00 – 10.40
Analytic Techniques

09.00 – 09.40	R. WIESENDANGER: *Rastersondenmikroskopie und -Spektroskopie an Halbleiteroberflächen und Bauelementen* ***(Invited Paper)***
09.40 – 10.00	Ch. RAUCH, G. STRASSER, K. UNTERRAINER, E. GORNIK: *Ballistische Elektronenspektroskopie an komplexen Halbleiter-Heterostrukturen*
10.00 – 10.20	N. SELIGER, C. FÜRBÖCK, P. HABAS, D. POGANY, E. GORNIK: *Backside-Laserprober für die Charakterisierung von Leistungs-Halbleiter-Bauelementen*
10.20 – 10.40	H. HUTTER, K. PIPLITS: *Hochpräzise Tiefenprofile mit SIMS*

Saturday, March 22, 1997 10.40 – 11.00
Conclusion, Discussion

The Society's Managing Committee and Address

President:

Univ.Prof. Dr. Erich GORNIK
TU Wien, Institut für Festkörperelektronik

First Vice-President:

Dipl.-Ing. Gerhard KRAINZ (up to 31 December 1997)
Wirtschaftskammer Österreich

Mag. Miron PASSWEG (starting with 1 January 1998)
Bundesarbeitskammer

Second Vice-President:

Univ.Prof. Dr. Wolfgang FALLMANN (up to 31 December 1997)
TU Wien, Institut für Allgemeine Elektrotechnik und Elektronik

Univ.Prof. Dr. Günther BAUER (starting with 1 January 1998)
Universität Linz, Institut für Halbleiterphysik

Board:

Dr. Wolfgang ATTWENGER
ÖFZ Seibersdorf

Univ.Prof. Dr. Günther BAUER (up to 31 December 1997)
Universität Linz, Institut für Halbleiterphysik

Univ.Prof. Dr. Wolfgang FALLMANN (starting with 1 January 1998)
TU Wien, Institut für Allgemeine Elektrotechnik und Elektronik

Univ.Prof. Dr. Helmut HEINRICH
Universität Linz, Institut für Experimentalphysik

Dipl.-Ing. Gerhard KRAINZ (starting with 1 January 1998)
Wirtschaftskammer Österreich

Univ.Prof. Dr. Hans LEOPOLD
TU Graz, Institut für Elektronik

Univ.Prof. Dr. Fritz PASCHKE
TU Wien, Institut für Allgemeine Elektrotechnik und Elektronik

Mag. Miron PASSWEG (up to 31 December 1997)
Bundesarbeitskammer

Dr. Robert SCHAWARZ
TU Wien, Institut für Allgemeine Elektrotechnik und Elektronik

Univ.Prof. Dr. Arnold SCHMIDT
TU Wien, Institut für Allgemeine Elektrotechnik und Elektronik

Univ.Prof. Dr. Siegfried SELBERHERR
TU Wien, Institut für Mikroelektronik

Secretary-General:

A.o. Univ.Prof. Dr. Karl RIEDLING
TU Wien, Institut für Allgemeine Elektrotechnik und Elektronik

Administration:

Claudia RITTER

Address:

Gesellschaft für Mikroelektronik
c/o Technische Universität Wien
Institut für Allgemeine Elektrotechnik und Elektronik
Gußhausstraße 27-29/359, A-1040 Wien

Phone: +43-1-588 01-5223

Fax: +43-1-505 2666

Mail: gme@iaee.tuwien.ac.at

WWW: http://www.iaee.tuwien.ac.at/gme/